Microbial Transformation of Organic and Inorganic Halogen Compounds

Peng Peng

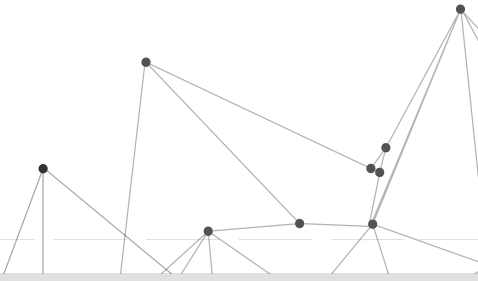

Propositions

1. Genome-guided experiments unveiled novel metabolic features of *Pseudomonas* and *Desulfoluna* strains in transforming halogen compounds.
   (This thesis)

2. Bioremediation efforts can benefit from natural halogen cycling in pristine environments.
   (This thesis)

3. Horizontal gene transfer that endows novel metabolic potential among different microorganisms is significant for bioremediation.

4. Verification of scientific findings using different approaches is necessary to avoid method bias and irreproducible results.

5. Critical thinking helps to avoid unnecessary work.

6. Learning “how to learn” is more important than what needs to be learned.

Propositions belonging to the PhD thesis entitled

Microbial Transformation of Organic and Inorganic Halogen Compounds

Peng Peng

Wageningen, 6 September 2019

Microbial Transformation of Organic and Inorganic Halogen Compounds

Peng Peng

Thesis committee

Promotor

Prof. Dr H. Smidt
Personal chair at the Laboratory of Microbiology
Wageningen University & Research

Co-promotor

Dr S. Atashgahi
Post-Doctoral researcher at the Laboratory of Microbiology
Wageningen University & Research,
Radboud University, Nijmegen

Other members

Prof. Dr H.H.M. Rijnaarts, Wageningen University & Research
Prof. Dr D.B. Janssen, University of Groningen
Prof. Dr S. Vuilleumier, University of Strasbourg, France
Dr I.P.G. Marshall, Aarhus University, Denmark

This research was conducted under the auspices of the Graduate School for Socio-Economic and Natural Sciences of the Environment (SENSE).

Microbial Transformation of Organic and Inorganic Halogen Compounds

Peng Peng

Thesis

submitted in fulfilment of the requirement for the degree of doctor
at Wageningen University
by the authority of the Rector Magnificus
Prof. Dr A.P.J. Mol,
in the presence of the
Thesis Committee appointed by the Academic Board
to be defended in public
on Friday 6 September 2019
at 4 p.m. in the Aula.

Peng Peng
Microbial Transformation of Organic and Inorganic Halogen Compounds
192 pages

PhD thesis, Wageningen University, Wageningen, The Netherlands (2019)
With references, with summary in English

ISBN: 978-94-6395-019-0
DOI: https://doi.org/10.18174/494863

Table of contents

Chapter 1

General introduction and thesis outline

Organic and inorganic halogen compounds

Organic halogenated compounds, organohalogens, contain one or more carbon-halogen (e.g. fluorine, chlorine, bromine, iodine) bond in their structures. Organohalogens are remarkably diverse, ranging from singly halogenated alkanes, alkenes, alkanoates and aromatics to more complex (poly)halogenated (poly)aromatic hydrocarbons (Kennish 2017). In contrast, inorganic halogen compounds are much less diverse. The commonly known inorganic halogen compounds include chlorine dioxide, hypochlorite, chlorite and (per)chlorate (Prince 1964). The organic and inorganic halogen compounds studied in this thesis include haloalkanoates (Fig. 1.1A), haloaromatics (Fig. 1.1B), chloroalkanes (Fig. 1.1C), chloroethenes (Fig. 1.1D), and inorganic chlorate (Fig. 1.1E).

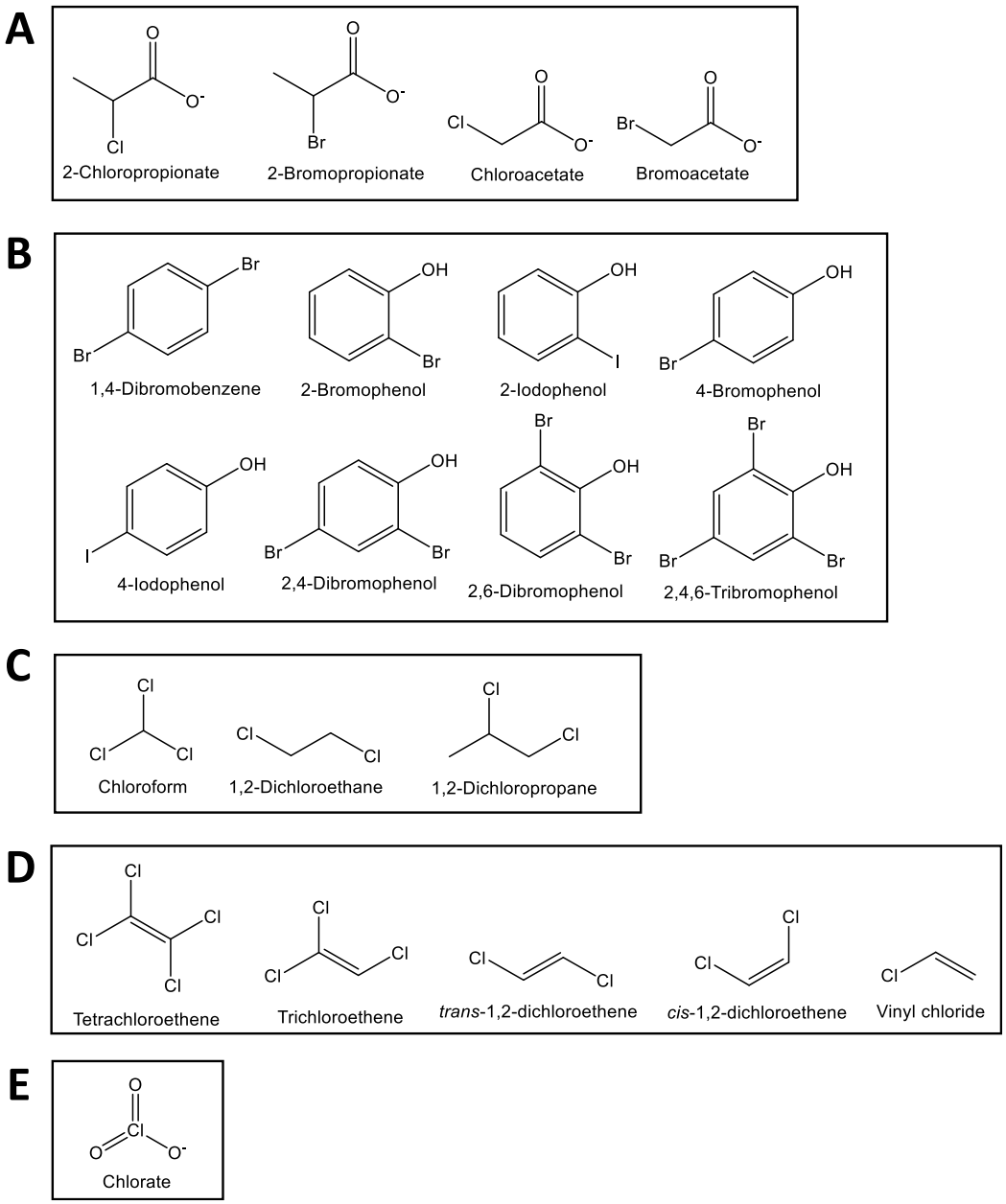

Fig. 1.1 Structure of the haloalkanoates (A), haloaromatics (B), chloroalkanes (C), chloroethenes (D), and inorganic chlorate (E) studied in this thesis. Hydrogen atoms were omitted for structural clarity.

Occurrence of organic and inorganic halogen compounds

Organic and inorganic halogen compounds are usually manufactured in large volumes for a broad range of industrial and agricultural applications due to their extensive structural, chemical-physical varieties, and desirable properties. For example, carbon tetrachloride is manufactured as fire extinguishant (Langford 2005), chloroethenes as solvents (Stringer and Johnston 2001), chlorofluorocarbon as refrigerant (Watanabe and Tsuru 2008), chloropropionates and chlorate as pesticides (Kettlitz *et al.* 2016, Lin *et al.* 2011), and chloramphenicol and vancomycin as drugs (Eliopoulos and Wennersten 2002, Piontek *et al.*

2018). As a result of the massive anthropogenic production of organohalogens and inorganic halogen compounds, each year large quantities of these compounds are accidentally and/or deliberately released into the environment. This has caused great environmental concerns because of the adverse effects of these compounds on human, animal and environmental health (Ni *et al.* 2010, Safe 1990, Weisburger 1977).

Besides their anthropogenic origin, organohalogens and inorganic halogen compounds can also be formed naturally. A comprehensive review of naturally produced organohalogens in 2010 listed more than 5000 compounds (Gribble 2010). These organohalogens are produced through abiotic and biotic halogenation processes. The known abiotic halogenation mechanisms include Fenton-like reactions (Leri *et al.* 2015), photochemical reactions, and combustion events such as forest fire and volcanic activities (Méndez-Díaz *et al.* 2014). Biotic halogenation is performed by a broad range of (micro)organisms, plants and animals (Agarwal *et al.* 2017, Atashgahi *et al.* 2018b, Gribble 2015). The organohalogens produced by these organisms were proposed to play a role in chemical defense against predators or as regulatory hormones (Gribble 1998, Weiss *et al.* 1996). Inorganic chlorine compounds such as (per)chlorate can also be naturally produced through atmospheric processes e.g. by ozone oxidation of chloride (Kang *et al.* 2008), and large natural deposits of (per)chlorate have been found in the hyper-arid regions e.g. in the Atacama desert of Chile (Orris *et al.* 2003).

Microbial transformation of organic and inorganic halogen compounds

Naturally produced organic and inorganic halogen compounds have a long history on earth (Atashgahi *et al.* 2018a, Gribble 1998, Rao *et al.* 2007). The natural and ancient origin of these compounds has been proposed to have primed the development of biochemical pathways for their transformations (Atashgahi *et al.* 2018a, Harper 2000, Smidt and de Vos 2004). Accordingly, various microbes from contaminated as well as pristine environments have been reported capable of metabolic or co-metabolic transformation of organohalogens and inorganic chlorine compounds. Such microbes play an important role in the transformation/detoxification of these compounds, and thereby contribute to i) the natural attenuation or engineered bioremediation of contaminated sites, ii) the halogen cycling in nature.

Organohalogen dehalogenation

The first step for microbial transformation of organohalogens is often dehalogenation. During this process, the halogen substituents that are usually responsible for toxicity of the compounds are removed (Janssen *et al.* 2001). The dehalogenation products are usually more readily accessible for mineralization due to e.g. reduced toxicity, electronegativity and/or spatial hindrance (Janssen *et al.* 2001, Kunze *et al.* 2017, Mohn and Tiedje 1992). Different

dehalogenation mechanisms including hydrolytic dehalogenation, reductive as well as oxidative dehalogenation have been reported in various aerobic and anaerobic microorganisms (Agarwal *et al.* 2017, Atashgahi *et al.* 2016, Janssen *et al.* 2001, Takagi *et al.* 2009).

Hydrolytic dehalogenation

Hydrolytic dehalogenation, often observed during microbial transformation of haloalkanoates as carbon source, cleaves the carbon-halogen bonds of an organohalogen through nucleophilic substitution by a water molecule, yielding hydroxyl alkanoates (Van der Ploeg *et al.* 1991). Halopropionates and haloacetates are water soluble molecules and are degradable by various aerobic microbes. Known strains that can use haloalkanoates as carbon and energy sources belong to bacterial genera of *Pseudomonas* (Hasan *et al.* 1994, Jones *et al.* 1992, Mesri *et al.* 2009, Motosugi *et al.* 1982a, Motosugi *et al.* 1982b, Peng *et al.* 2017, Senior *et al.* 1976), *Xanthobacter* (Janssen *et al.* 1985), *Methylobacterium* (Omi *et al.* 2007), *Arthrobacter* (Bagherbaigi *et al.* 2013) and *Bacillus* (Lin *et al.* 2011).

The responsible enzymes for the dehalogenation of haloalkanoates are haloacid dehalogenases. One of the most well-characterized haloacid dehalogenases is 2-haloacid dehalogenase, which specifically acts on haloalkanoates with a halogen substitute at the α-carbon, and produces the corresponding hydroxyl alkanoates (Kurihara *et al.* 2000). Based on their substrate and stereochemical specificities, three groups of 2-haloacid dehalogenase have been identified: L- and D-2-haloacid dehalogenases (L-, D-DEX) that catalyse dehalogenation of L-2-haloalkanoates and D-2-haloalkanoates, respectively, and the D,L-2-haloacid dehalogenases (D,L-DEX) that act on both enantiomers (Kurihara *et al.* 2000). The reaction mechanisms of D-DEX and DL-DEX are similar and include a nucleophilic attack of the α-carbon of the haloalkanoate substrate by an activated water molecule produced by the carboxyl group of the catalytic base (Asp) of the enzyme, resulting in production of hydroxyl alkanoate (Fig. 1.2A) (Nardi-Dei *et al.* 1999). The catalytic amino acid residues (Asn and Asp) of the active site of D-DEX and D,L-DEX are conserved (Schmidberger *et al.* 2008). In comparison, in L-DEX, the carboxyl group of the catalytic residue (aspartate) directly attacks the α-carbon of the haloalkanoate, producing an ester intermediate, which is subsequently hydrolyzed using a water molecule to hydroxyl alkanoate (Fig. 1.2B) (Hisano *et al.* 1996b, Li *et al.* 1998b). The amino acid sequences of L-DEX and D/D,L-DEX enzymes share no similarity, and phylogenetic studies have shown that they are evolutionarily unrelated (Hill *et al.* 1999, Kurihara *et al.* 2000, Nardi-Dei *et al.* 1999).

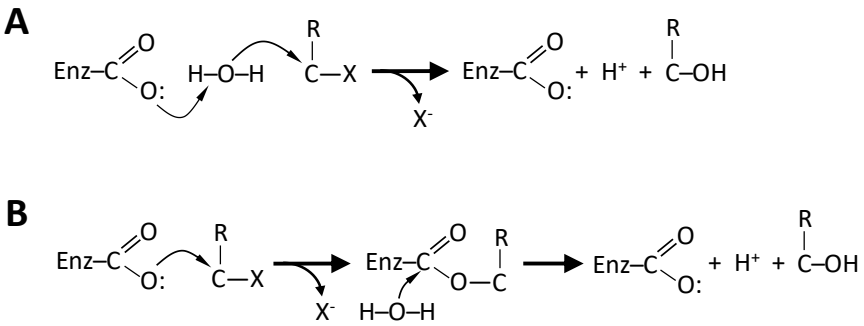

Fig. 1.2 Reaction mechanisms of D- and D,L-2-haloacid dehalogenases (A) and L-2-haloacid dehalogenase (B).

2-haloacid dehalogenase is encoded by 2-haloacid dehalogenase gene, the expression of which is either constitutive or regulated. For example, expression of the D-haloacid dehalogenase gene of *Xanthobacter autotrophicus* GJ10 (van der Ploeg and Janssen 1995) and *Pseudomonas chloritidismutans* AW-1^T (Chapter 6 of this thesis) are likely controlled by a sigma factor 54 dependent transcriptional activator. In contrast, the L-haloacid dehalogenase gene of *P. chloritidismutans* AW-1^T is constitutively expressed (Peng *et al.* 2017).

Reductive dehalogenation

Polyhalogenated organohalogens usually have low solubility in water and persistent under oxic conditions (Field and Sierra-Alvarez 2008, Nikel *et al.* 2013). Reductive dehalogenation is the only documented microbial process for dehalogenation of these organohalogens that has been observed in suboxic and anoxic environments such as subsurface soil, groundwater and marine environments (Atashgahi *et al.* 2016). In reductive dehalogenation, the halogen substituent of an organohalogen is removed with concurrent addition of hydrogen and electrons to the molecule (Mohn and Tiedje 1992). Reductive dehalogenation is mainly mediated by organohalide-respiring bacteria (OHRB) that can use the organohalogens as the terminal electron acceptors and couple dehalogenation of organohalogens to growth, a process known as organohalide respiration (OHR) (Atashgahi *et al.* 2016, DeWeerd *et al.* 1990, Fincker and Spormann 2017, Schubert *et al.* 2018). The known OHRB isolates are divided into two groups, obligate and facultative OHRB, based on whether OHR is their only energy-gaining metabolism (Atashgahi *et al.* 2016, Fincker and Spormann 2017). The first isolated organohalide-respiring bacterium was *Desulfomonile tiedjei* DCB1 that was shown to use 3-chlorobenzoate as the electron acceptor for growth (DeWeerd *et al.* 1990). Since then, numerous OHRB have been isolated and characterized. OHRB are spread among several bacterial phyla including *Chloroflexi*, *Firmicutes* and *Proteobacteria*, and have been

shown to use various organohalogens for growth, such as tetra- and trichloromethanes, chloroethanes, chloroethenes, chlorinated/brominated aromatics, polychlorinated biphenyls, dibenzo-*p*-dioxin and polybrominated diphenyl ethers (Atashgahi *et al.* 2016).

The responsible enzymes for reductive dehalogenation are reductive dehalogenases (RDases) that are membrane-associated and corrinoid-dependent proteins. In most cases, vitamin B_{12} (cob(I)alamin) serves as the corrinoid-cofactor. Amino acid sequence comparison of RDases from phylogenetically distinct bacteria has revealed several conserved motifs, including two iron-sulfur (Fe-S) binding motifs and one twin arginine (TAT) motif that is likely involved in maturation and transport of RDases to the outer side of the membrane (Smidt and de Vos 2004). Due to difficulties in cultivation of OHRB and obtaining functional RDases in model host microbes such as *Escherichia coli*, enzymology of RDases such as the reaction mechanism is not as well-understood as for the well-characterized 2-haloacid dehalogenases. Based on structural and biochemical analyses of the tetrachloroethene (PCE) RDase (PceA) in *Sulfurospirillum multivorans* (Bommer *et al.* 2014) and ortho-dibromophenol RDase (NpRdhA) in *Nitratireductor pacificus* pht-3B (Payne *et al.* 2015), three different reactions and electron transfer mechanisms have been proposed (Fincker and Spormann 2017). The first one is proposed to start with nucleophilic attack of Co(I) to the halogenated carbon of the organohalogen substrate, producing an organocobalt adduct (substrate-Co(III) corrinoid) with elimination of the halogen (Fig. 1.3A). This step is similar to the L-2-haloacid dehalogenase mechanism shown in Fig. 1.2B. Then the organocobalt adduct accepts two electrons delivered from the Fe-S clusters to generate the dehalogenation product and to regenerate Co(I) (Fig. 1.3A). The second mechanism is proposed to be initiated by the transfer of a single electron from Co(I) to the substrate, producing a transient substrate radical anion intermediate. The radical anion intermediate then accepts two electrons delivered from the Fe-S clusters to generate the dehalogenation product and to regenerate Co(I) (Fig. 1.3B) (Fincker and Spormann 2017). The third mechanism is proposed to be initiated by the attack of Co(I) to the halogen substitute of the substrate, resulting in the formation of an intermediate containing a cobalt-halogen bond. The carbon-halogen bond of the intermediate is then cleaved yielding a transient Co(III)-halogen adduct and the dehalogenation product. The transient Co(III)-halogen adduct subsequently accepts two electrons from the Fe-S clusters to eliminate the halogen and to regenerate Co(I) (Fig. 1.3C) (Fincker and Spormann 2017, Payne *et al.* 2015).

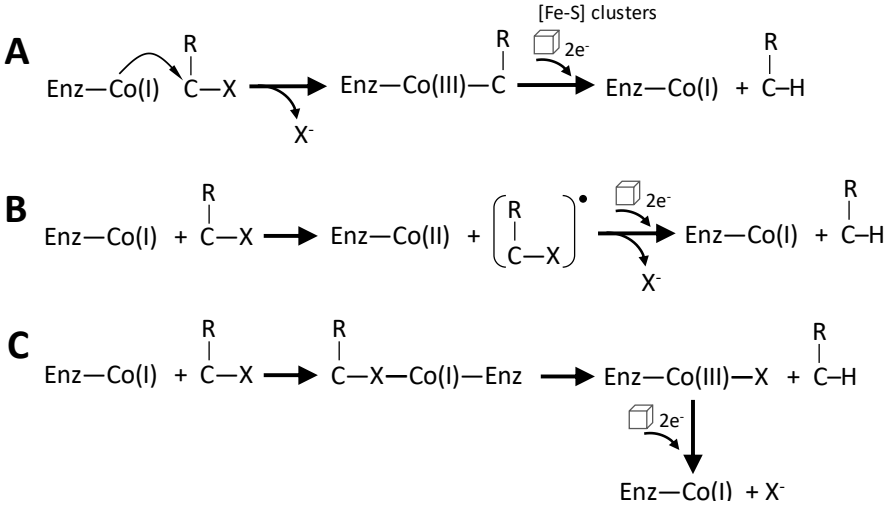

Fig. 1.3 Reaction mechanisms of RDases.

The catabolic subunit of the RDases is encoded by reductive dehalogenase genes known as *rdhA*. The published genomes of OHRB usually contain one or more *rdhA* genes (Kruse *et al.* 2016, Lu *et al.* 2015) that are commonly found next to a small gene (*rdhB*) encoding a putative membrane anchor protein for the RdhA (Neumann *et al.* 1998). The *rdhAB* gene clusters are frequently accompanied by a variable set of accessory genes, and some of the genes have been shown to encode proteins that regulate *rdhAB* gene expression (Pop *et al.* 2004). Three types of regulation systems have been proposed to regulate the expression of *rdhAB*. The first one is the antibiotic resistance regulator MarR-type or two-component (TCS) regulatory systems that are frequently observed in strains of *Dehalococcoides mccartyi* (Fig. 1.4A) (Wagner *et al.* 2013). The second type includes cAMP receptor protein/fumarate and nitrate reduction (CRP/FNR) regulators. An example of such a regulator is CprK in *Desulfitobacterium hafniense* DCB-2^{T} that induces the expression of the chlorophenol *rdh* gene (*cprA*) in the presence of its substrate 3-chloro-4-hydroxyphenylacetate (Cl-OHPA) (Fig. 1.4B) (Gábor *et al.* 2006, Kemp *et al.* 2013). The third system is a post-translational regulation system which has been described for regulating the *rdh* gene responsible for PCE dechlorination (*pceA*) in *Desulfitobacterium hafniense* strains Y51 and TCE-1 (Reinhold *et al.* 2012) (Fig. 1.4C). The *pceA* of strains Y51 and TCE-1 is constitutively expressed, and the gene product, PceA, was only found to be translocated across the cell membrane when PCE was present in the growth medium (Reinhold *et al.* 2012). Besides, the NosR/NirI like protein (RdhC) encoded by *rdhC* was also speculated as a transcriptional regulatory protein for *cprBA* in the chlorophenol dehalogenating *Desulfitobacterium dehalogenans* (Smidt *et al.* 2000). In turn, recent studies using *Dehalobacter restrictus* have proposed that RdhC may play a role in electron transfer during OHR (Buttet *et al.* 2018).

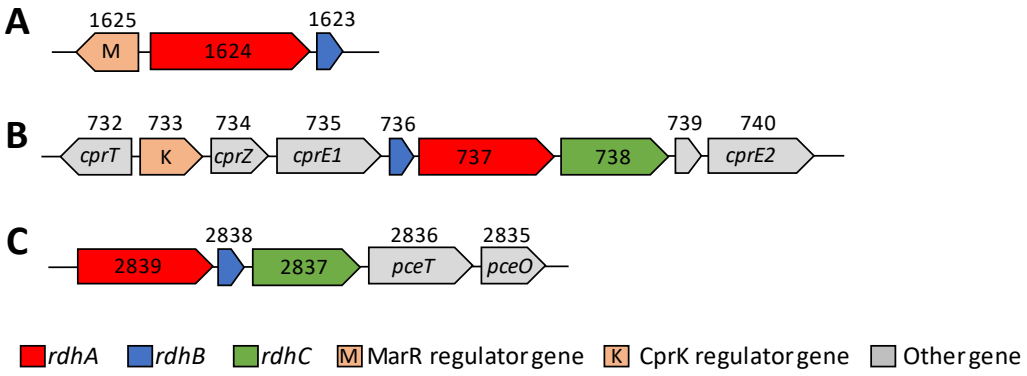

Fig. 1.4 Genetic organization of *rdh* gene clusters from *Dehalococcoides mccartyi* CBDB1 (A), *Desulfitobacterium hafniense* DCB-2^{T} (B), and *Desulfitobacterium hafniense* Y51 (C). Numbers indicate the locus tags of the respective genes in the genomes of the respective OHRB.

Electron transport chain for OHR

The electron transport chain for OHR has been classified into quinone-dependent and quinone-independent categories (Fincker and Spormann 2017). The former one needs quinone as an electron shuttle to carry electrons from the electron donor (e.g. hydrogen) to the catalytic domain of the RDase (RdhA) (Fig. 1.5A) and has been found in many facultative OHRB that are not restricted to OHR as the sole metabolism (Schubert *et al.* 2018). The electron transport pathway in quinone-dependent electron transport chains has not been fully characterized. The redox potential of menaquinone ($E^{o'}$ (MK/MK2) = -74 mV) is much higher than that of the Co(II)/Co(I) redox couple ($E^{o'}$ = ~ -370 mV) of the RdhA-bound corrinoid cofactor (Fig. 1.5A) and hence, electron transport from quinone to RdhA is thermodynamically unfavorable (Schubert *et al.* 2018). The proteins or processes involved to overcome this energy barrier have not been determined.

In quinone-independent electron transport chains, electrons are transferred from the electron donor (hydrogen) to RdhA via a protein complex containing Hup hydrogenases (encoded by *hupL*, *hupS*, *hupX*), and OmeAB, an iron–sulfur molybdoenzyme complex that interacts with Hup hydrogenase and RdhA to facilitate electron transport from Hup hydrogenases to RdhA (Fig. 1.5B) (Kublik *et al.* 2016, Schubert *et al.* 2018). The quinone-independent electron transport chain has only been found in obligate organohalide-respiring strains of *D. mccartyi*, which use OHR as the sole metabolism for energy conservation (Kublik *et al.* 2016).

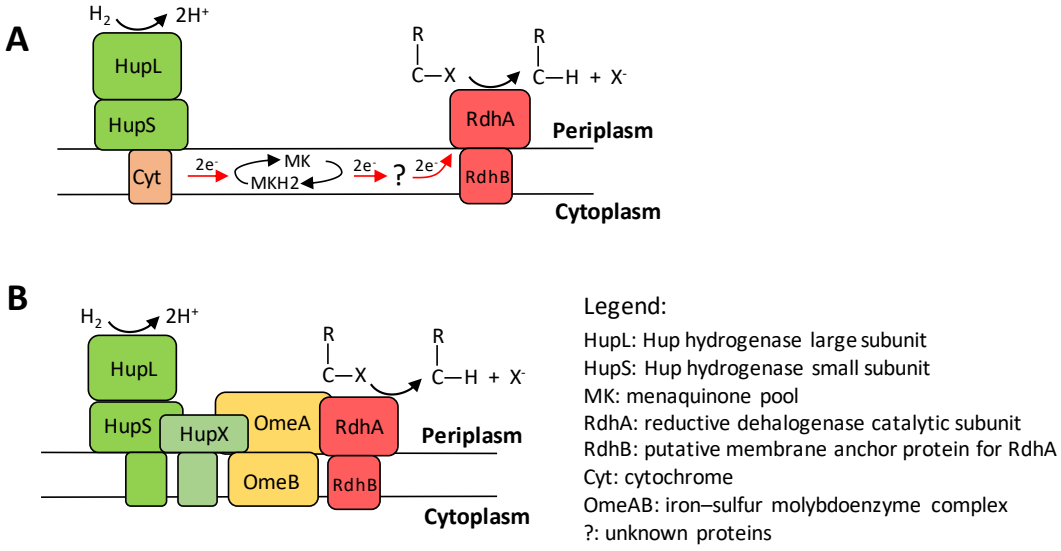

Fig. 1.5 Quinone-dependent (A) and quinone-independent (B) electron transport chains during OHR. Probable electron flow path is shown by red arrows.

Co-metabolic reductive dehalogenation

Anaerobic reductive dehalogenation of organohalogens can also be achieved through fortuitous transformations known as co-metabolic processes that have been reported in acetogens and methanogens. For example, acetogenic bacteria *Clostridium* sp. (Gälli and McCARTY 1989) and *Acetobacterium woodii* (Egli *et al.* 1988), and methanogenic *Methanosarcina* spp. (Bagley and Gossett 1995, Mikesell and Boyd 1990) are able to co-metabolically transform chloroform (CF) to dichloromethane (DCM) and CO_2 likely using enzymes involved in acetogenesis and methanogenesis (Egli *et al.* 1988, Holliger *et al.* 1992). Moreover, transition-metal co-factors, e.g. cob(I)/cob(II)alamins and F_{430} (nickel(I)-porphinoid), that facilitate key enzymes of acetogenesis (5-methyltetrahydrofolate corrinoid/iron-sulfur protein methyltransferase) and methanogenesis (methyl-coenzyme M reductase) can act as reductants and nucleophilic reagents catalyzing nonspecific reductive dechlorination (Gantzer and Wackett 1991, Krone *et al.* 1989a, Krone *et al.* 1989b). The reaction kinetics and mechanisms for transition-metal cofactor catalyzed reductive dehalogenation are complicated, and are influenced by type and concentration of the cofactors, redox condition, and the pH of the reaction system (Assaf-Anid *et al.* 1994, Chiu and Reinhard 1995, Krone *et al.* 1989a, Lewis *et al.* 1995). In general, transition-metal cofactor-catalyzed dehalogenation follows first order kinetics with higher dehalogenation rate for polyhalogenated organohalogens. For example, in the sequential reductive dechlorination of PCE to ethene through trichloroethene (TCE), dichloroethene (DCE) and vinyl chloride (VC), each step was first-order, and each succeeding reaction was over 10-fold slower than the preceding reaction (Tandoi *et al.* 1994).

Hence, the dechlorination rate of VC to ethene was 10,000-fold slower than that of PCE to TCE at equivalent concentrations using either corrinoid or F_{430} cofactors as a catalyst (Tandoi *et al.* 1994). Similar kinetics were also observed in carbon tetrachloride dechlorination to methane by corrinoid or F_{430} cofactors (Krone *et al.* 1989a).

Oxidative dehalogenation

Organohalogen dehalogenation can also be catalyzed by oxygenases under oxic conditions. Oxidative dehalogenation involves replacement of a halogen substitute with a hydroxyl group derived from molecular oxygen (Agarwal *et al.* 2017). Unlike hydrolytic dehalogenation that involves redox neutral substitution of a halogen by a hydroxyl derived from a water molecule, the oxygenase-catalyzed dehalogenation needs NAD(P)H as the source of electron and hydrogen to reduce oxygen. Examples of monooxygenases mediating dehalogenation are the pentachlorophenol 4-monooxygenase from *Sphingobium chlorophenolicum* converting pentachlorophenol to tetrachloroquinone (Crawford *et al.* 2007, Orser *et al.* 1993), and the monooxygenase from *Pseudomonas* sp. strain DCA1 that converts 1,2-dichloroethane (1,2-DCA) to 1,2-dichloroethanol (Hage and Hartmans 1999). Besides monooxygenases, dioxygenases, such as the 2-halobenzoate 1,2-dioxygenase from *Pseudomonas cepacia* 2CBS, can catalyze dechlorination of 2-chlorobenzoate to catechol (Fetzner *et al.* 1992). A remarkable difference between oxidative dehalogenation and hydrolytic and reductive dehalogenation is that most oxidative dehalogenases (including the monooxygenases and dioxygenase described above) are unspecific enzymes that can also convert substrates with substituents (other than halogen) at the same position of the halogen. It is not clear whether these enzymes have a specific interaction with the halogen substitute for catalysis and dehalogenation (Janssen *et al.* 1994).

Microbial reduction of (per)chlorate

(Per)chlorate reduction to chloride and oxygen has been found in (per)chlorate-reducing bacterial genera belong to *Firmicutes* and *Proteobacteria* isolated from both pristine and contaminated environments. Examples include members of *Moorella* (Balk *et al.* 2008), *Magnetospirillum* (Thrash *et al.* 2010), *Dechloromonas* (Achenbach *et al.* 2001), *Pseudomonas* (Wolterink *et al.* 2002) and *Arcobacter* (Carlström *et al.* 2013). The responsible enzymes for perchlorate and chlorate reduction are perchlorate and chlorate reductases, respectively. Perchlorate reductase catalyzes perchlorate reduction to chlorate, which can be further reduced to chlorite by chlorate reductase. Chlorite dismutase catalyzes chlorite dismutation to chloride and oxygen (Fig. 1.6) (Van Ginkel *et al.* 1996). The genes encoding (per)chlorate reductase are *clrABDC*, which encode the corresponding α, β, γ and δ subunits of (per)chlorate reductase. The *cld* gene encodes chlorite dismutase. Regulation of *clrABDC* and *cld*

expression is not well-understood due to lack of the regulatory genes in many chlorate-reducing bacteria such as *P. chloritidismutans* AW-1^T. Previous studies showed that regulation of *clrABDC* and *cld* might be absent, or regulated chromosomally like the nutrient cation and anion uptake systems in many bacteria (Clark *et al.* 2013, Silver and Walderhaug 1992).

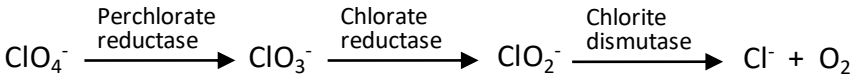

Fig. 1.6 (Per)chlorate reduction pathway.

Thesis outline

Microbes capable of detoxification and/or complete degradation of organohalogens and inorganic chlorine compounds are important for bioremediation. However, efficient bioremediation is often hampered by a lack of knowledge of the responsible microbes and metabolic processes. On the other hand, most of the microbes capable of transformation of organohalogens and inorganic chlorine compounds have been derived from contaminated environments. Accordingly, there is lack of knowledge of such microbes from pristine habitats where natural production of organohalogens and inorganic chlorine compounds has been documented (Atashgahi *et al.* 2018a, Orris *et al.* 2003). This thesis describes microbial transformation of organohalogens and inorganic chlorate by microbes ranging from pure cultures to complex consortia obtained from different environments such as contaminated wetland, pristine marine environments and hypersaline lakes. The responsible microbes, their ecophysiology and genetics were studied using a wide range of complementary approaches including (enrichment) cultivation, physiological, biochemical and stable isotope-based analyses, molecular biology, (meta)genomics and proteomics.

Chapter 2 reports microbial transformation of haloalkanoates with chlorate as the electron acceptor mediated by *P. chloritidismutans* AW-1^T, a facultative anaerobic chlorate-reducing bacterium isolated from a bioreactor inoculated with chlorate and bromate polluted wastewater (Wolterink *et al.* 2002). Genomic analysis of strain AW-1^T showed co-existence of chlorate reduction genes (*clrABDC*, *cld*) and D/L-2-haloacid dehalogenase genes (*dehI* and L-DEX gene). This chapter, for the first time, verified concurrent transformation of haloalkanoates and chlorate by a single bacterium.

Chapter 3 reports isolation and characterization of a new sulfate-reducing organohalide-respiring bacterium, *Desulfoluna spongiiphila* strain DBB, from pristine marine intertidal sediment samples. This chapter describes comparative physiology and genomics of strain DBB and two previous reported *Desulfoluna* species isolated from marine environments. Genomic analysis revealed similar potential for OHR, corrinoid biosynthesis, and resistance to

oxygen among the three strains, and physiological experiments showed their specific preference for brominated/iodinated compounds rather than chlorinated compounds, and stimulation of OHR during concurrent sulfate reduction.

Chapter 4 reports CF microbial transformation in sediment samples obtained from hypersaline lake Strawbridge in Western Australia, where biotic formation of CF was previously reported (Ruecker *et al.* 2014). CF in the sediment- and sediment-free enrichment cultures was transformed to DCM and CO_2. Known OHRB and *rdhA* genes were not present in the sediment free enrichment cultures. Rather, acetogenic *Clostridium* and genes involved in acetogenesis were enriched and likely mediated fortuitous (co-metabolic) transformation of CF to DCM and CO_2. This study for the first time shows transformation of CF in pristine hypersaline environment that is a natural source of CF, indicating that microbiota may act as a filter to reduce CF emission from hypersaline lakes to the atmosphere.

Chapter 5 investigates OHRB and kinetics of 1,2-DCA reductive dechlorination in the presence of chloroethenes and 1,2-dichloropropane (1,2-DCP) as co-contaminants. Dechlorination rates of 1,2-DCA were strongly decreased in the presence of a single chlorinated co-contaminant in enrichment cultures obtained from a contaminated wetland. This study contributes to better understand the underlying mechanisms of 1,2-DCA persistence in environments in relation to specific 1,2-DCA dechlorinating microbial populations.

Finally, **Chapter 6** provides a general discussion of the findings described in this thesis and future perspectives.

Chapter 2

Concurrent haloalkanoate degradation and chlorate reduction by *Pseudomonas chloritidismutans* AW-1^T

Peng Peng, Ying Zheng, Jasper J. Koehorst, Peter J Schaap, Alfons J.M. Stams, Hauke Smidt, Siavash Atashgahi

Published in *Applied and Environmental Microbiology*

Abstract

Haloalkanoates are environmental pollutants that can be degraded aerobically by microorganisms producing hydrolytic dehalogenases. However, there is lack of information about anaerobic degradation of haloalkanoates. Genome analysis of *Pseudomonas chloritidismutans* AW-1^T, a facultative anaerobic chlorate-reducing bacterium, showed presence of two putative haloacid dehalogenase genes, the L-DEX gene and *dehI*, encoding an L-2-haloacid dehalogenase (L-DEX) and a halocarboxylic acid dehydrogenase (DehI). Hence, we studied concurrent degradation of haloalkanoates and chlorate as a yet unexplored trait of strain AW-1^T. The deduced amino acid sequences of L-DEX and DehI revealed 33−37% and 26−86% similarities with biochemically/structurally characterized L-DEX and D-, DL-2-haloacid dehalogenase enzymes, respectively. Physiological experiments confirmed that strain AW-1^T can grow on chloroacetate, bromoacetate and both L- and D- α-halogenated propionates with chlorate as an electron acceptor. Interestingly, growth and haloalkanoates degradation were generally faster with chlorate as an electron acceptor than with oxygen. In line with this, analyses of L-DEX and DehI dehalogenase activities using cell free extract (CFE) of strain AW-1^T grown on DL-2-chloropropionate under chlorate-reducing condition showed up to 3.5-fold higher dehalogenase activity than the CFE obtained from cells grown on DL-2-chloropropionate under aerobic condition. Reverse transcription quantitative PCR showed that the L-DEX gene was expressed constitutively independent of the electron donor (haloalkanoates or acetate) or acceptor (chlorate or oxygen), whereas expression of *dehI* was induced by haloalkanoates. Concurrent degradation of organic and inorganic halogenated compounds by strain AW-1^T represents a unique metabolic capacity in a single bacterium, providing a new piece in the puzzle of the microbial halogen cycle.

Introduction

Haloalkanoates are widely used as intermediates and raw materials for production of pesticides, pharmaceuticals and other organic compounds (Lin *et al.* 2011). Each year large amounts of these compounds are introduced into the environment causing serious concerns due to their environmental toxicity as well as their carcinogenic and genotoxic effects on animals and humans (Plewa *et al.* 2010). Microbial degradation plays an important role in detoxification and mineralization of haloalkanoates. Dehalogenation is often one of the first reactions during the degradation process, through which the halogen substituents, usually responsible for toxicity of these compounds, are removed (Janssen *et al.* 2001). Bacterial strains capable of using haloalkanoates as the sole source of carbon and energy have been isolated and characterized from different genera, including *Pseudomonas* (Hasan *et al.* 1994, Jones *et al.* 1992, Motosugi *et al.* 1982a, Motosugi *et al.* 1982b, Senior *et al.* 1976), *Xanthobacter* (Janssen *et al.* 1985) and *Methylobacterium* (Omi *et al.* 2007).

Enzymes involved in dehalogenation of haloalkanoates are known as haloacid dehalogenases, which catalyze the hydrolytic dehalogenation of haloalkanoates and produce the corresponding hydroxyl alkanoates. Bacterial 2-haloacid dehalogenases that specifically act on α-substituted haloalkanoates are classified into three groups based on their substrate and stereochemical specificities. L-2-haloacid dehalogenase (L-DEX) catalyzes the dehalogenation of L-2-haloacids, D-2-haloacid dehalogenase (D-DEX) acts on D-2-haloacids and DL-2-haloacid dehalogenase (DL-DEX) acts on both enantiomers (Kurihara *et al.* 2000). For example, 2-haloacid dehalogenases catalyze dehalogenation of D or L-2-chloropropionate (D- or L-2CP) to L- or D-lactate, respectively, which is channeled to the TCA cycle by further degradation to pyruvate and acetyl CoA. The known haloalkanoate dehalogenating bacteria degrade D- and L-2CP with molecular oxygen as a terminal electron acceptor. To our knowledge, no other terminal electron acceptors such as chlorate, nitrate, Fe(III) or sulfate have been reported to be used for bacterial growth on haloalkanoates, however, oxidation of L-2CP as a model compound coupled to reduction of these electron acceptors is thermodynamically feasible, with chlorate being the most favorable electron acceptor (Table 2.1). Oxidation of haloalkanoates coupled to chlorate reduction is of particular interest due to concurrent removal of these two environmentally problematic compounds that could potentially co-occur in environments as herbicides (Ali *et al.* 2016, Bodnár *et al.* 1990) or as disinfection by-products (Righi *et al.* 2014). Chlorate-reducing bacteria generally reduce chlorate first to chlorite by chlorate reductase (encoded by the *clr* gene), and chlorite is then split into chloride and oxygen by chlorite dismutase (encoded by *cld)* (Rikken *et al.* 1996, Wolterink *et al.* 2002, Youngblut *et al.* 2016). The molecular oxygen released from chlorite dismutation can be utilized as terminal electron acceptor for final mineralization of haloalkanoates.

In this study, *Pseudomonas chloritidismutans* AW-1^T was selected as a potential degrader of haloalkanoates coupled to chlorate reduction. This bacterium was previously isolated from an anoxic bioreactor (Wolterink *et al.* 2002) and is able to degrade a wide variety of electron donors including *n*-alkanes with chlorate as electron acceptor (Mehboob *et al.* 2009a, Mehboob *et al.* 2015). Genome analysis of strain AW-1^T showed the presence of two putative haloacid dehalogenase genes e.g. the L-DEX gene and *dehI* predicted to encode L-DEX and halocarboxylic acid dehydrogenase (DehI), respectively. Hence, growth on haloalkanoates with chlorate as an alternative electron acceptor might represent a unique metabolic capacity in this bacterium. To test this hypothesis, different haloalkanoates were tested as electron donor and carbon source with either chlorate or oxygen as electron acceptor. Functionality of the two putative 2-haloacid dehalogenases was determined by gene expression studies using reverse transcription quantitative PCR (RT-qPCR) and *in vitro* dehalogenase activity measurements.

Table 2.1 Stoichiometric equations and standard Gibbs free energy changes for L-2-chloropropionate oxidation coupled to reduction of various electron acceptors.

Electron acceptor (ox/red)	Stoichiometric equation	ΔG°′ (kJ/mol)
O_2/H_2O	$C_3H_4O_2Cl^- + 3O_2 + H_2O \rightarrow 3HCO_3^- + Cl^- + 3H^+$	-1284
ClO_3^-/Cl^-	$C_3H_4O_2Cl^- + 2ClO_3^- + H_2O \rightarrow 3HCO_3^- + 3Cl^- + 3H^+$	-1533
NO_3^-/N_2	$C_3H_4O_2Cl^- + 2.4NO_3^- \rightarrow 3\ HCO_3^- + 1.2N_2 + Cl^- + 0.6H^+ + 0.2H_2O$	-1309
Fe^{3+}/Fe^{2+}	$C_3H_4O_2Cl^- + 36Fe(OH)_{3\ (s)} \rightarrow 3HCO_3^- + 12Fe_3O_{4\ (s)} + Cl^- + 53H_2O + 3H^+$	-1207
SO_4^{2-}/H_2S	$C_3H_4O_2Cl^- + 1.5SO_4^{2-} + H_2O \rightarrow 3HCO_3^- + 1.5HS^- + Cl^- + 1.5H^+$	-149
CO_2/CH_4	$C_3H_4O_2Cl^- + 2.5H_2O \rightarrow 1.5HCO_3^- + 1.5CH_4 + Cl^- + 1.5H^+$	-124

Standard Gibbs free energy formation of the inorganic compounds were taken from Oelkers et al.(Oelkers *et al.* 1995) and http://www2.ucdsb.on.ca/tiss/stretton/database/inorganic_thermo.htm. Standard Gibbs free energy formation of 2-chloropropionate was taken from Dolfing and Janssen (Dolfing and Janssen 1994).

Materials and Methods

Chemicals

Chloroacetate, bromoacetic acid, 2-chloropropionic acid, L-2-chloropropionic acid, L-2-bromopropionic acid, D-2-chloropropionic acid, D-2-bromopropionic acid, 3-chloropropionic acid, 3-bromopropionic acid, 3-iodopropionic acid, 2,3-dichloropropionic acid, 2-chlorobutyric acid and 4-chlorobutyric acid were all purchased from Sigma-Aldrich. All inorganic salts used in this study were of analytical grade.

Bacterial strain and growth conditions

P. chloritidismutans AW-1^T was cultivated in 120 ml bottles containing 50 ml of anoxic medium as previously described (Wolterink *et al.* 2002) with nitrogen or air (140 kPa) as the headspace and incubated statically in the dark at 30°C. Vitamins and trace elements were added as described by Holliger et al. (Holliger *et al.* 1993) except that the trace elements were supplemented with (per liter of trace elements solution) Na_2SeO_3, 0.06 g; $NaWO_4 \cdot 2H_2O$, 0.0184 g. To obtain a pre-culture, 10 mM acetate and 10 mM chlorate were used as the electron donor and acceptor, respectively. When all acetate was consumed and the optical density at 600 nm (OD_{600}) reached ~0.5, the pre-culture was transferred (5%, v/v) into fresh media with different haloalkanoates as electron donor instead of acetate and either chlorate or oxygen as electron acceptor. Haloalkanoic acids were neutralized with an equimolar amount of NaOH to produce the corresponding haloalkanoates and filter-sterilized through a 0.2 μm filter (Advanced Microdevices, Ambala, India) before adding to the medium at 3−10 mM final concentration. For transcription analysis, degradation of D-2CP, L-2CP and chloroacetate with chlorate, acetate with chlorate, and acetate with oxygen were tested. To ensure sufficient biomass for transcription analysis, 10 replicate microcosms were prepared for each condition, and for each sampling occasion, two microcosms were randomly selected and sacrificed for RNA extraction after taking samples for HPLC analysis of metabolites and OD_{600} measurements. Specific growth rate was calculated according to the equation:

$$\ln(OD_{600(t2)} / OD_{600(t1)}) = k(t_2 - t_1)$$

Where k is the specific growth rate; $OD_{600(t1)}$ and $OD_{600(t2)}$ are the optical densities of liquid cultures measured at 600nm at the start and end of exponential growth phase, respectively; t_1 and t_2 are the start and end points (h) of exponential growth phases, respectively.

RNA extraction and cDNA synthesis

RNA was extracted from strain AW-1^T at different time points during growth on L-2CP (0, 12, 18, 24, 36 h), D-2CP (0, 48, 96, 144, 168 h), chloroacetate (0, 24, 30, 36, 48 h), acetate (0, 4.5, 9, 14, 24 h) with chlorate, and acetate (0, 9, 24, 39, 48 h) with oxygen. RNA extraction

was performed with a bead-beating procedure as described earlier (Egert *et al.* 2007). RNA was purified using RNeasy columns (Qiagen, Venlo, The Netherlands) with DNase I (Roche, Almere, The Netherlands) treatment according to the manufacturers' protocols. cDNA was synthesized from 500 ng total RNA using the Maxima H Minus First Strand cDNA Synthesis Kit (Thermo Scientific, Vilnius, Lithuania) according to the manufacturer's protocols. Absence of genomic DNA was confirmed by 16S rRNA gene targeted PCR with extracted RNA samples as templates.

qPCR assays

Primers for amplification of *cld*, the L-DEX gene, and *dehI* genes were designed using the primer 3 online program (http://primer3.ut.ee/software) or the NCBI online primer design tool (http://www.ncbi.nlm.nih.gov/tools/primer-blast/) (Table 2.2). Primers were tested in silico using OligoAnalyzer 3.1 (http://eu.idtdna.com/analyzer/Applications/OligoAnalyzer/). The *cld*, L-DEX, and *dehI* genes were PCR amplified using the following program: 95°C for 3 min, followed by 30 cycles of 95°C for 30 s, 55°C for 30 s and 72°C for 30 s, followed by a final extension at 72°C for 10 min. The PCR products were purified using the GeneJET PCR Purification Kit (Thermo Scientific, Vilnius, Lithuania) and cloned into pGEM®-T Easy Vector (Promega, WI, USA). The plasmid was introduced into *E. coli* JM109 competent cells (Promega, WI, USA). Primer specificity and efficiency of amplification were tested by temperature-gradient PCRs on the iQ5 iCycler (Bio-Rad, Veenendaal, the Netherlands) using plasmid or PCR product amplified with T7/SP6 primers from the plasmid containing target gene inserts. The same T7/SP6 PCR products were subsequently used to obtain qPCR calibration curves. qPCRs were performed using the iQ SYBR Green supermix (Bio-Rad, CA, USA) as described earlier (Atashgahi *et al.* 2013). The program for qPCR assays of *cld*, L-DEX and *dehI* genes was: 95°C for 10 min, followed by 40 cycles of 95°C for 15 s, 60°C for 30 s and 72°C for 30 s. Melting curves were measured from 65°C to 95°C with increments of 0.5°C and 10 s at each step. Transcript levels of the *cld*, L-DEX and *dehI* genes were calculated by relative quantification using the $2^{-\Delta\Delta Cq}$ method (Pfaffl 2001). The 16S rRNA gene was used as the reference gene (Kirk *et al.* 2014) and quantified as described previously (Atashgahi *et al.* 2013). Gene expression over time was calibrated to the 0 hour time point (Kirk *et al.* 2014). A relative expression higher than 10 was arbitrarily set as representing significant induction (Bisaillon *et al.* 2011).

Table 2.2 Overview of qPCR primers used in this study.

Gene name	Primer name and sequence (5′−3′)
cld	CldF (ACACGACACCTACCTTAGCC) CldR (CCCCAACGAACGTGGAATTT)
L-DEX gene	L-DEXF (CTTTATCGGCGTGGTGAGTG) L-DEXR (CCCACGGATCGAATAATGCC)
dehI	DehIF (CTACCGGCCTTTCTTTGTCG) DehIR (CTGATCAATCTCACGCACCG)

Preparation of cell-free extract (CFE) and dehalogenase assay

CFEs were prepared from 50 ml cultures of strain AW-1^T at early stationary phase grown with DL-2CP under either chlorate-reducing or aerobic condition. Cells were harvested by centrifugation at 4,700 × *g* for 15 min at 4°C. The cell pellets were washed twice with 100 mM Tris-sulfate buffer (pH 7.5) and re-suspended in 1 ml of the same buffer supplied with 10% glycerol. Cells were lysed by sonication using a Branson sonifier (Branson, CT, USA) equipped with a 3 mm tip by six pulses of 30 s with 30 s rest in between of each pulse. Intact cells and cell debris were removed by centrifugation at 15,000 × *g* for 15 min at 4°C. Protein concentration of the supernatant was determined with the Qubit protein assay kit (Invitrogen, OR, USA) following the manufacturer's instructions. Dehalogenase activity of the freshly prepared CFEs was measured by determining the release of halide ions under aerobic condition without chlorate. The optimum pH and temperature for the dehalogenase activity were determined using two buffer types with distinct, yet overlapping pH ranges (100 mM Tris-sulfate, pH 7.5, 8.0, 8.5, 9.0; 100 mM glycine-NaOH, pH 9.0, 9.5, 10.0, 10.5, 11.0, 11.5, 12.0) and different temperatures (20, 25, 30, 35, 40°C). A control reaction lacking CFEs was included in each set of assays to detect any spontaneous release of halide ions. The dehalogenase assay system contained 400 µl of the buffer solutions, 20 mM haloalkanoates and 50 µl of CFE. All reaction components except the CFE were combined and allowed to equilibrate for 5 min at a given temperature, after which the reaction was initiated by adding 50 µl CFE. The reaction was performed under aerobic conditions and terminated after 10 min by adding 75 µl of 2 N H_2SO_4. The release of halide ions was measured by ion chromatography. One unit of dehalogenase activity was defined as the amount of protein that catalyzes the dehalogenation of 1 µmol of a substrate per minute of the reaction time.

Analytical methods

Chlorate and halide ions were analyzed using the ThermoFisher Scientific Dionex™ ICS-2100 Ion Chromatography System and a Dionex Ionpac analytical column (AS19, 2 × 250 mm) equipped with a suppressed conductivity detector. The ions were analyzed under a three step gradient profile consisting of 10 mM KOH for 4 min, 10−40 mM KOH for 16 min, followed

by 40−10 mM KOH for 1.5 min. Haloalkanoates were analyzed on a ThermoFisher Scientific SpectraSYSTEM™ HPLC equipped with an Agilent column (Metacarb 67H, 300 × 6.5 mm) and an RI detector. The mobile phase was 0.01 N H_2SO_4. Oxygen was measured by taking 0.5 ml headspace samples and analyzed using a gas chromatograph equipped with thermal conductivity detector (GC-TCD, Shimadzu 2014) and a Restek column (Molsieve 13X, 200 × 3 mm). The column temperature was 60°C and held for 2.75 min. Cell growth was determined by measuring OD_{600} using a WPA CO8000 cell density meter (Biochrom, Cambridge, UK).

Genome annotation

Bacterial genomes with a high quality genome sequence available in the European Nucleotide Archive (ENA) version 121 were scanned for co-occurrence of L-DEX and chlorite dismutase (Cld) using protein domains (IPR006439, IPR006328, IPR023214, IPR010644). The DehI in AW-1^T genome was found using the conserved regions of D- and DL-DEX from *Pseudomonas putida* PP3 (Weightman *et al.* 2002), *Pseudomonas* sp. 113 (Nardi-Dei *et al.* 1997), *Methylobacterium* sp. CPA1 (Omi *et al.* 2007) and *Pseudomonas putida* AJ1(Barth *et al.* 1992). To avoid potential miss-annotations, the selected genomes were *de novo* re-annotated using the SAPP framework (Koehorst *et al.* 2016a, Koehorst *et al.* 2016b). Genes were identified using Prodigal (2.6.3) (Hyatt *et al.* 2010a), and protein annotation was performed though protein domains using InterProscan (5.19−58.0) (Mitchell *et al.* 2014).

Results and discussion

Bioinformatic analysis

The genome of strain AW-1^T (Mehboob *et al.* 2015) (GenBank accession no. AOFQ01000000) harbors two haloacid dehalogenase genes (L-DEX gene and *dehI*) predicted to encode L-DEX and DehI with 228 and 301 amino acid residues, respectively (Fig. 2.1). The amino acid sequence of L-DEX of strain AW-1^T shares 33%, 34%, 34% and 37% identities with the L-DEX of *Pseudomonas putida* 109 (Kawasaki *et al.* 1994), *Pseudomonas putida* AJ1 (Jones *et al.* 1992), *Pseudomonas* sp. YL (Nardi-Dei *et al.* 1994) and of *Xanthobacter autotrophicus* GJ10 (Van der Ploeg *et al.* 1991), respectively. The amino acid sequence of DehI of strain AW-1^T shares 86%, 29%, 28% and 26% identities with the D-DEX of *Pseudomonas putida* AJ1(Barth *et al.* 1992), DL-DEX of *Pseudomonas putida* PP3 (Weightman *et al.* 2002), DL-DEX of *Pseudomonas* sp. 113 (Nardi-Dei *et al.* 1997) and DL-DEX of *Methylobacterium* sp. CPA1 (Omi *et al.* 2007), respectively.

The proposed substrate binding and catalytic residues of the active site of the structurally characterized L-DEX of *Pseudomonas* sp. YL (Hisano *et al.* 1996a, Li *et al.* 1998a) are identical in the L-DEX of strain AW-1^T (Fig. 2.1A), indicating dehalogenation of L-2-

halopropionates and haloacetates by this enzyme. In contrast, only the catalytic residues of the active site of the structurally characterized DL-DEX of *Pseudomonas putida* PP3 (Schmidberger *et al.* 2008) are identical in the DehI of strain AW-1^T and D-DEX of *Pseudomonas putida* AJ1 (Barth *et al.* 1992) (Fig. 2.1B). The halide-binding residues for L- and D-form halopropionates are only identical in the DL-DEX of *Pseudomonas* sp. 113 (Nardi-Dei *et al.* 1997) and *Methylobacterium* sp. CPA1 (Omi *et al.* 2007), but not in the DehI of strain AW-1^T and D-DEX of *Pseudomonas putida* AJ1 (Barth *et al.* 1992). Moreover, the key residue for dictating stereoselectivity, Ala 207, in the DL-DEX (Schmidberger *et al.* 2008) is replaced by Asn in the D-DEX and DehI (Fig. 2.1B). These indicate that the DehI of strain AW-1^T is a D-DEX and mediates dehalogenation of D-2-halopropionates and haloacetates. The DehI and L-DEX of strain AW-1^T share no sequence identity with each other. This is in agreement with previous studies showing that D-DEX (and DL-DEX) and L-DEX are evolutionarily unrelated and have different reaction mechanisms (Hill *et al.* 1999, Nardi-Dei *et al.* 1999).

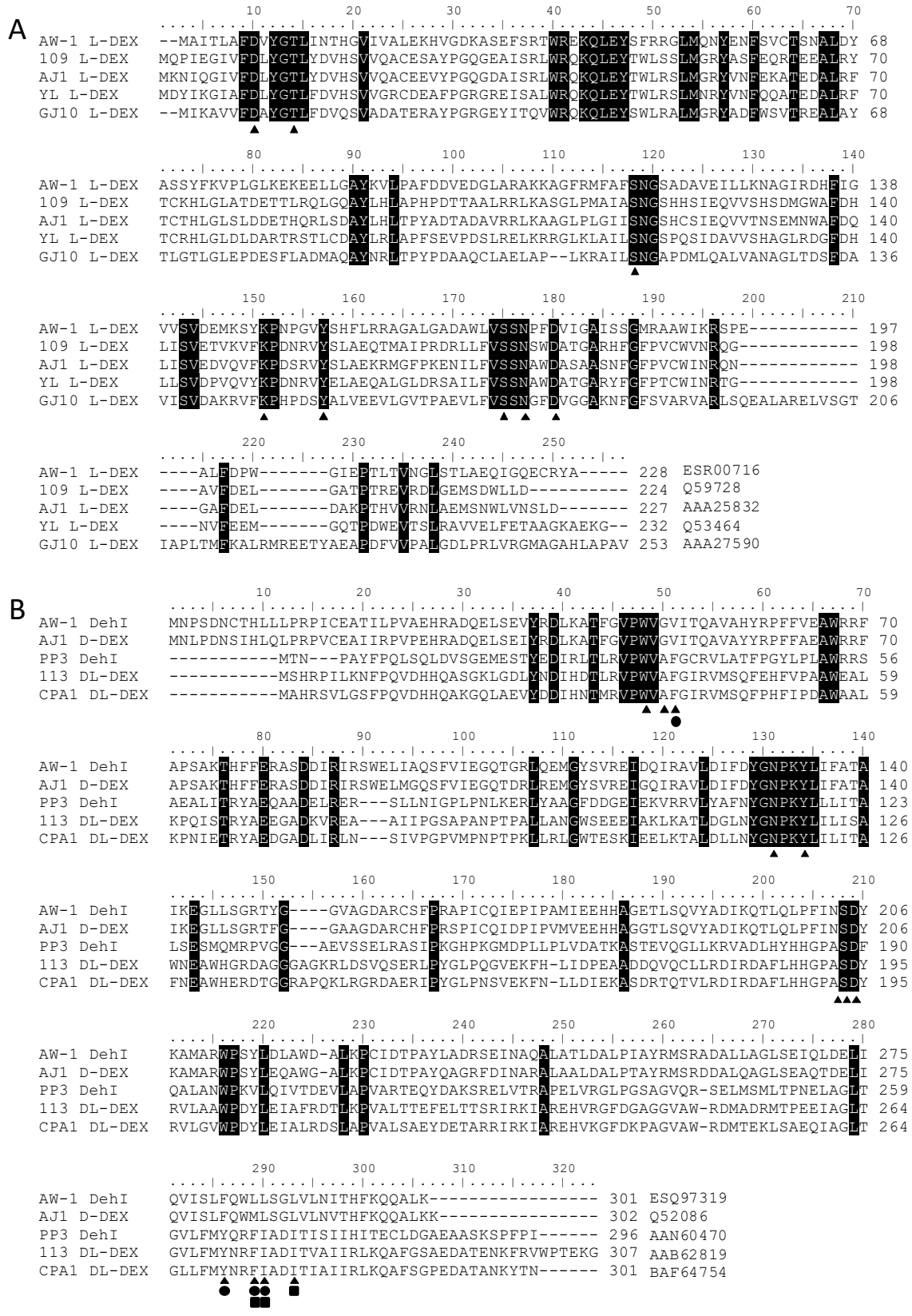

Fig. 2.1 Multiple sequence alignments of (A) L-DEX and (B) D-, DL-DEX and DehI. White letters on a black background indicate amino acids that are identical in all sequences. Active site residues are indicated with triangles. The D-and L-form halide binding residues are indicated with squares and circles,

respectively. The catalytic residues are indicated with stars. The source bacterial abbreviations are: AW-1, *Pseudomonas chloritidismutans* AW-1^T; 109, *Pseudomonas putida* 109; AJ1, *Pseudomonas putida* AJ1; YL, *Pseudomonas* sp. YL; GJ10, *Xanthobacter autotrophicus* GJ10; PP3, *Pseudomonas putida* PP3; 113, *Pseudomonas* sp. 113; CPA1, *Methylobacterium* sp. CPA1. GenBank accession numbers are indicated at the C-terminal end. ClustalW multiple sequence alignment was conducted using BioEdit version 7.2.5 (http://bioedit.software.informer.com/).

Degradation of haloalkanoates by strain AW-1^T with either chlorate or oxygen as electron acceptor

Strain AW-1^T can utilize DL-2CP, L-2CP, D-2CP, L-2-bromopropionate (L-2BP), D-2-bromopropionate (D-2BP), chloroacetate and bromoacetate as sole carbon and energy sources with chlorate or oxygen as electron acceptor (Fig. 2.2 and 2.3, Fig. S2.1). Under chlorate-reducing conditions, the fastest degradation of haloalkanoates by strain AW-1^T was observed with L-2CP (Fig. 2.2A), DL-2CP (Fig. S2.1A), L-2BP (Fig. 2.3A) and D-2BP (Fig. 2.3B) with specific growth rates of 0.17, 0.12, 0.081, and 0.10 h^{-1}, respectively. Chloroacetate (Fig. 2.2E), bromoacetate (Fig. 2.3C), were less favorable substrates resulting in specific growth rates of 0.047 and 0.052 h^{-1}, respectively. D-2CP was the least favorable substrate, with the lowest specific growth rate (0.025 h^{-1}) among all substrates tested in this study (Fig. 2.2C). The chemical instability of D(L)-2BP in aqueous solution that could be spontaneously hydrolyzed to L(D)-lactate (Kurihara *et al.* 2000), might facilitate the dehalogenation of D-2BP to L-lactate and contribute to the higher specific growth rate of the strain AW-1^T with D-2BP (Fig. 2.3B) as compared to D-2CP (Fig. 2.2C). However, the uninoculated control experiment did not show any concentration decrease of D- and L-2BP within 36 h, indicating lack of abiotic D- and L-2BP dehalogenation (data not shown). Oxygen concentration in the cultures of strain AW-1^T grown on chlorate with either DL-2CP or chloroacetate did not surpass 0.009 mM dissolved oxygen (Fig. S2.2) indicating that oxygen produced from chlorate reduction was continuously consumed for mineralization of the haloalkanoates by strain AW-1^T. Interestingly, degradation of some haloalkanoates was faster with chlorate as an electron acceptor than with oxygen. For example, the specific growth rates of DL-2CP (Fig. S2.1B), L-2CP (Fig. S2.1D) and chloroacetate (Fig. S2.1H) by strain AW-1^T under aerobic conditions were 6.5, 5.8 and 3.9-fold lower, respectively, than the corresponding specific growth rates of these substrates under chlorate-reducing conditions. No growth was observed using β-substituted haloalkanoates such as 3-chloropropionate, 3-bromopropionate, 3-iodopropionate and 4-chlorobutyrate, nor with 2,3-dichloropropionate or 2-chlorobutyrate as substrates with chlorate as electron acceptor (data not shown). Therefore, degradation of these substrates with oxygen as electron acceptor was not tested in this study. Compared to the common degradation of α-substituted haloalkanoates, degradation of β-substituted haloalkanoates was reported less frequently and the responsible dehalogenase genes and enzymes have not been verified experimentally (Bagherbaigi *et al.* 2013, Lin *et al.* 2011, Mesri *et al.* 2009).

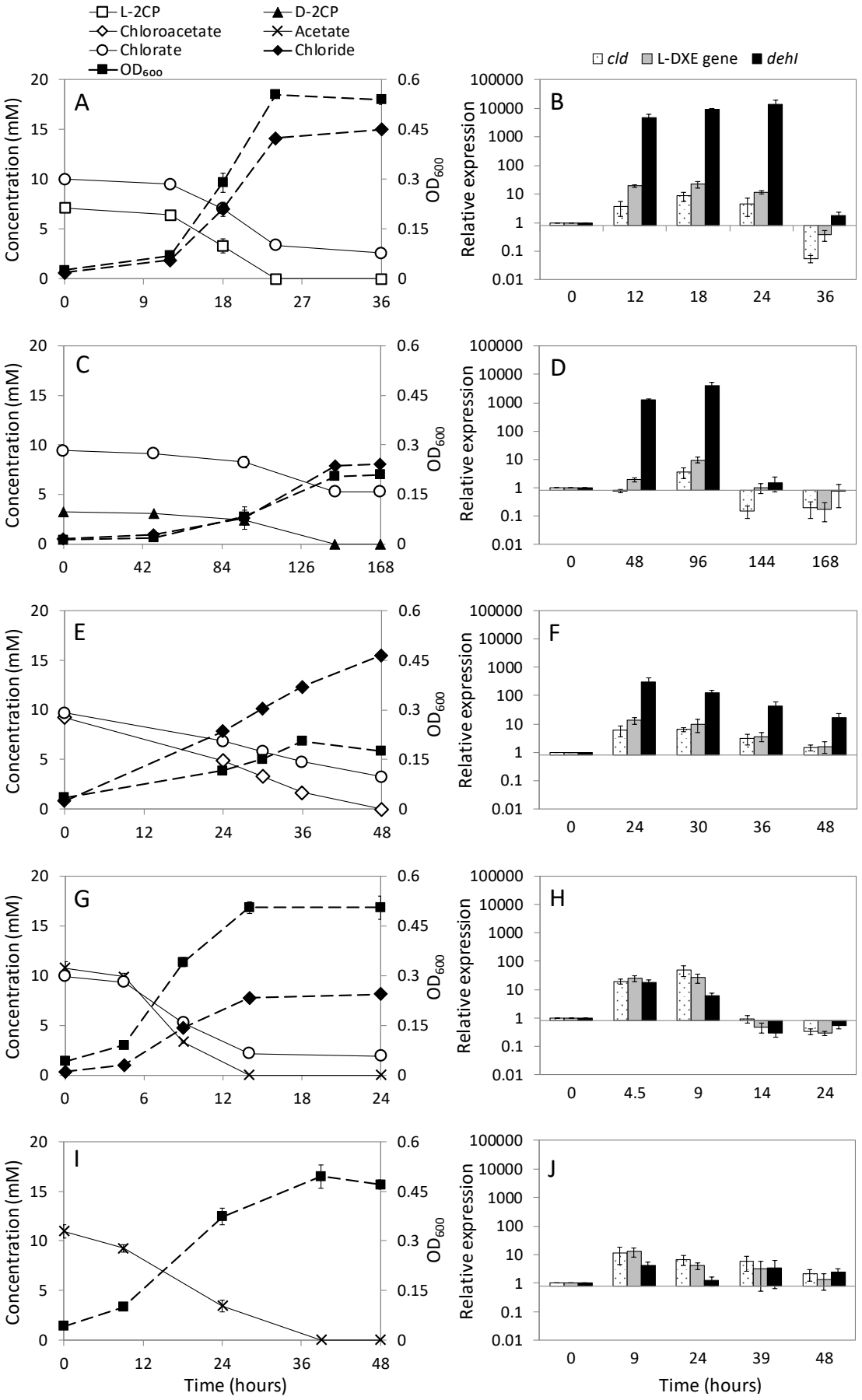
L-2CP
D-2CP
Chloroacetate
Acetate
Chlorate
Chloride
OD600
cld
L-DXE gene
dehI
A
B
C
D
E
F
G
H
I
J
Concentration (mM)
Relative expression
Time (hours)

Fig. 2.2 Growth of *P. chloritidismutans* AW-1^T on L-2CP (A), D-2CP (C), chloroacetate (E) and acetate (G) with chlorate and on acetate (I) with oxygen as electron acceptor, and relative expression of the L-2-haloacid dehalogenase gene (L-DEX gene), halocarboxylic acid dehydrogenase gene (*dehI*) and chlorate dismutase gene (*cld*) during growth on L-2CP (B), D-2CP (D), chloroacetate (F) and acetate (H) with chlorate and on acetate with oxygen (J) as an electron acceptor. Two random cultures out of 10 replicates for each growth condition were sacrificed at each sampling point for growth, HPLC and RT-qPCR analyses. Triplicate qPCRs were performed on samples withdrawn from two random replicate microcosms (n = 2×3).

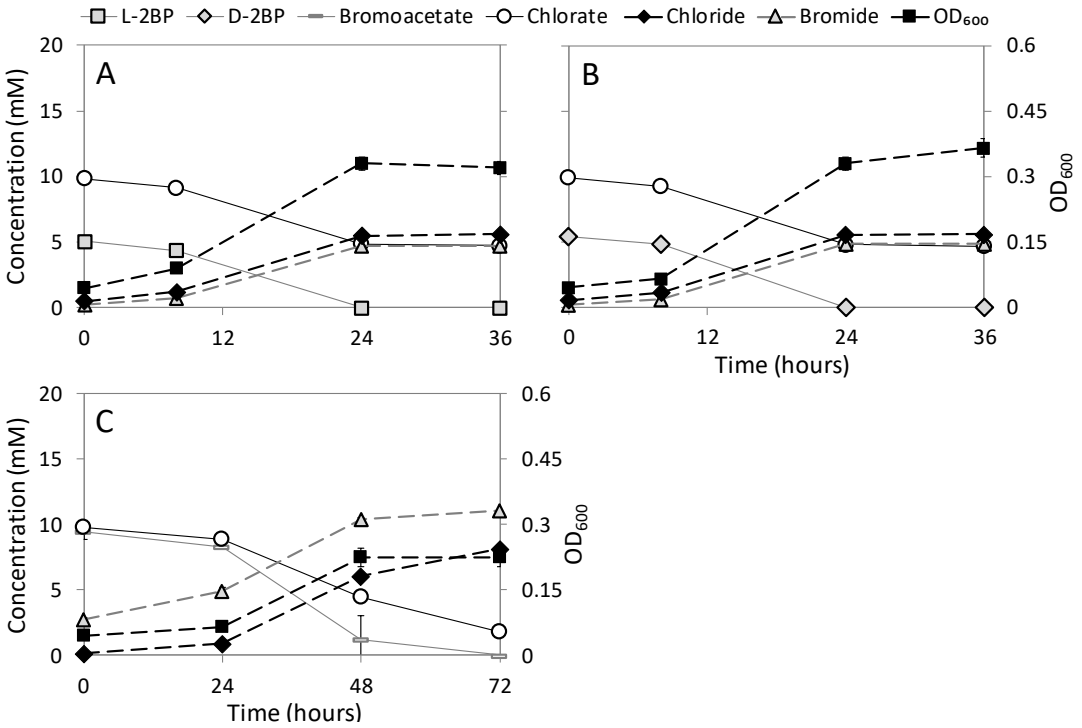

Fig. 2.3 Growth of *P. chloritidismutans* AW-1^T on L-2BP (A), D-2BP (B) and bromoacetate (C) with chlorate as electron acceptor. Points and error bars represent the average and standard deviation of samples taken from duplicate cultures.

Dehalogenase activity assays

The dehalogenase activity was determined in cell free extracts (CFEs) of strain AW-1^T. The optimal pH for dehalogenase activity of the CFE from AW-1^T cells grown on DL-2CP and chlorate at 30°C for 24 hours was 10.5 (Fig. 2.4). The optimal growth temperature of 30°C (Wolterink *et al.* 2002) was selected for further dehalogenase activity assays. Although higher dehalogenase activities were observed at higher temperatures, spontaneous release of bromide was detected in dehalogenase activity assays with D- and L-2BP as substrates. This also confirmed the chemical instability of D(L)-2BP in aqueous solution, which might lead to the faster apparent degradation of D-2BP than D-2CP by strain AW-1^T.

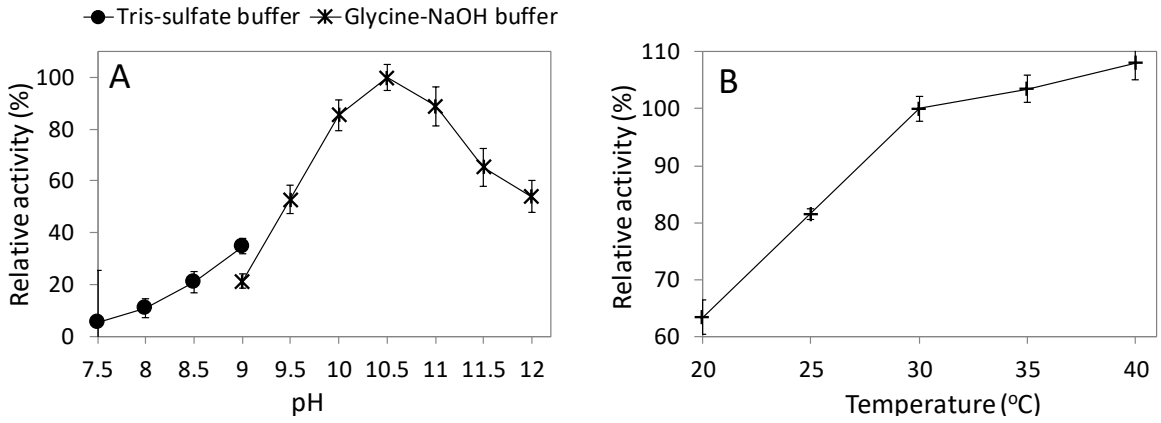

Fig. 2.4 Effect of pH (A) and temperature (B) on dehalogenase activity of the CFE prepared from *P. chloritidismutans* AW-1^T cells grown on DL-2CP and chlorate at 30°C for 24 hours. The pH (A) and temperature (B) yielding the highest dehalogenase activity was set as 100% and activities were shown as percentage against the highest activity. The points are average of two technical replicates and the error bars represent the standard deviations.

The CFEs prepared from both chlorate- and oxygen-grown cultures of strain AW-1^T showed dehalogenase activities with all the growth-supporting haloalkanoates tested in this study (Table 2.3). In addition, enzyme activity was also noted with 2-chlorobutyrate while it was not used as growth substrate. No activity was observed with 4-chlorobutyrate, 3-chloropropionate, 3-bromopropionate, 3-iodopropionate or 2,3-dichloropropionate (Table 2.3). The dehalogenase activity of the CFE from AW-1^T cells grown in presence of chlorate was up to 3.5-fold higher than the CFE obtained from AW-1^T cells grown in the presence of oxygen (Table 2.3). This is in line with the growth experiments that showed faster growth when chlorate was used as an electron acceptor as compared to aerobic cultures (Fig. S2.1). Chlorite dismutase is a periplasmic enzyme (Carlström *et al.* 2015, Mehboob *et al.* 2015, Mehboob *et al.* 2009b, Stenklo *et al.* 2001) and hence utilization of the molecular oxygen derived from chlorite dismutation by oxygenases involved in the further oxidation of the dehalogenated

haloalkanoates could be more efficient than using the oxygen from the extra-cellular environment. To this end, it should be noted that the solubility of chlorate in water (9.93 M at 25°C) is much higher than that of oxygen (0.000269 M at 25°C, under air), suggesting that exponentially growing cells of strain AW-1^T might be oxygen-diffusion limited in case of aerobic cultivation. Finally, thermodynamic analysis shows that chlorate is a more favorable electron acceptor than oxygen for complete oxidation of L-2CP (Table 2.1).

Table 2.3 Dehalogenase activity of the CFEs of *P. chloritidismutans* AW-1^T on various haloalkanoate substrates.

	Dehalogenase activity (U/mg of protein) [a]	
Substrate	DL-2CP + Chlorate [b]	DL-2CP + Oxygen [c]
L-2-Chloropropionate	1.58 ± 0.19	0.46 ± 0.05
D-2-Chloropropionate	0.09 ± 0.021	0.11 ± 0.35
DL-2-Chloropropionate	1.50 ± 0.04	0.59 ± 0.01
L-2-Bromopropionate	1.54 ± 0.02	0.89 ± 0.26
D-2-Bromopropionate	1.48 ± 0.26	0.42 ± 0.10
Chloroacetate	1.43 ± 0.09	1.33 ± 0.01
Bromoacetate	2.10 ± 0.03	1.71 ± 0.26
2-Chlorobutyrate	0.39 ± 0.13	0.09 ± 0.03
4-Chlorobutyrate	ND [c]	ND
3-Chloropropionate	ND	ND
3-Bromopropionate	ND	ND
3-Iodopropionate	ND	ND
2,3-Dichloropropionate	ND	ND

[a] Values of dehalogenase activity are the mean ± standard error of technical duplicate analysis. ND: Not detected
[b] CFE was prepared from cells grown on DL-2CP and chlorate for 24 hours
[c] CFE was prepared from cells grown on DL-2CP and oxygen for 90 hours

Transcription analysis

Under all tested conditions, the time 0 expression of *cld*, the L-DEX gene and *dehI* was comparable for all cultures, and the 16S rRNA gene was stably expressed throughout growth phases of strain AW-1^T (Fig. S2.3). Among the three analyzed genes, *dehI* showed the highest induction under chlorate-reducing conditions with L-2CP, D-2CP and chloroacetate as electron donors, which was significant in early- and mid-exponential growth phases (Fig. 2.2B, D and F). Upregulation of *dehI* reached its highest level (~14,000-fold) in L-2CP fed cultures within 24 hours and then decreased (Fig. 2.2B). In contrast, the expression of L-DEX gene was relative stable and the highest upregulation (~22-fold) was observed in the cultures amended

with L-2CP after 18 hours and then decreased (Fig. 2.2B, D and F). Similar to the L-DEX gene, *cld* also showed no significant upregulation in the cultures amended with the chloroalkanoates and chlorate (Fig. 2.2B, D and F). In cultures grown on non-chlorinated substrate (acetate) with either chlorate or oxygen, upregulations of *dehI*, the L-DEX gene, and *cld* did not surpass 18-, 26-, and 49-fold, respectively (Fig. 2.2H and J). These results collectively show the inductive expression of *dehI* by haloalkanoates and high constitutive expression of the L-DEX gene and *cld* independent of electron donor and acceptor (Fig. S2.2). In line with the expression pattern of *cld*, a previous proteomic study showed abundance of chlorite dismutase in strain AW-1^T even when chlorate was replaced by oxygen (Mehboob *et al.* 2015).

Previous research on degradation of organic and inorganic halogenated compounds has mainly focused on their degradation either as electron donor or electron acceptor, but not on concurrent degradation. This study showed for the first time concurrent degradation of halogenated compounds as electron donor and acceptor in a single bacterium, representing a unique and untapped metabolic potential. A survey of available bacterial genomes showed similar co-occurrence of genes involved in degradation of haloalkanoates and chlorate in other bacterial strains belonging to various genera including, but not limited to, *Bacillus, Exiguobacterium, Mycobacterium, Staphylococcus* and *Roseiflexus* (Table S2.1). Although none of these bacteria were experimentally tested for chlorate reduction and (or) haloalkanoates degradation, and thus further experimental verification is needed, this suggests that the potential catabolic machineries to degrade both halogenated organic and inorganic compounds by a single bacterium are widespread. Besides bioremediation prospects, such degradation of different halogenated compounds is of interest for the natural halogen cycle in different aquatic and terrestrial ecosystems where ample natural production of halogenated compounds has been documented (Gribble 2000, Gribble 2003, Rajagopalan *et al.* 2008, Rao *et al.* 2010).

Acknowledgement

This project is financially supported by the BE-Basic Foundation through project MicroControl (8.004.01). PP and YZ are sponsored by China Scholarship Council. Research of AJMS is supported by ERC Grant (project 323009) and the Gravitation grant (project 024.002.002) of the Netherlands Ministry of Education, Culture and Science.

Supplementary Information

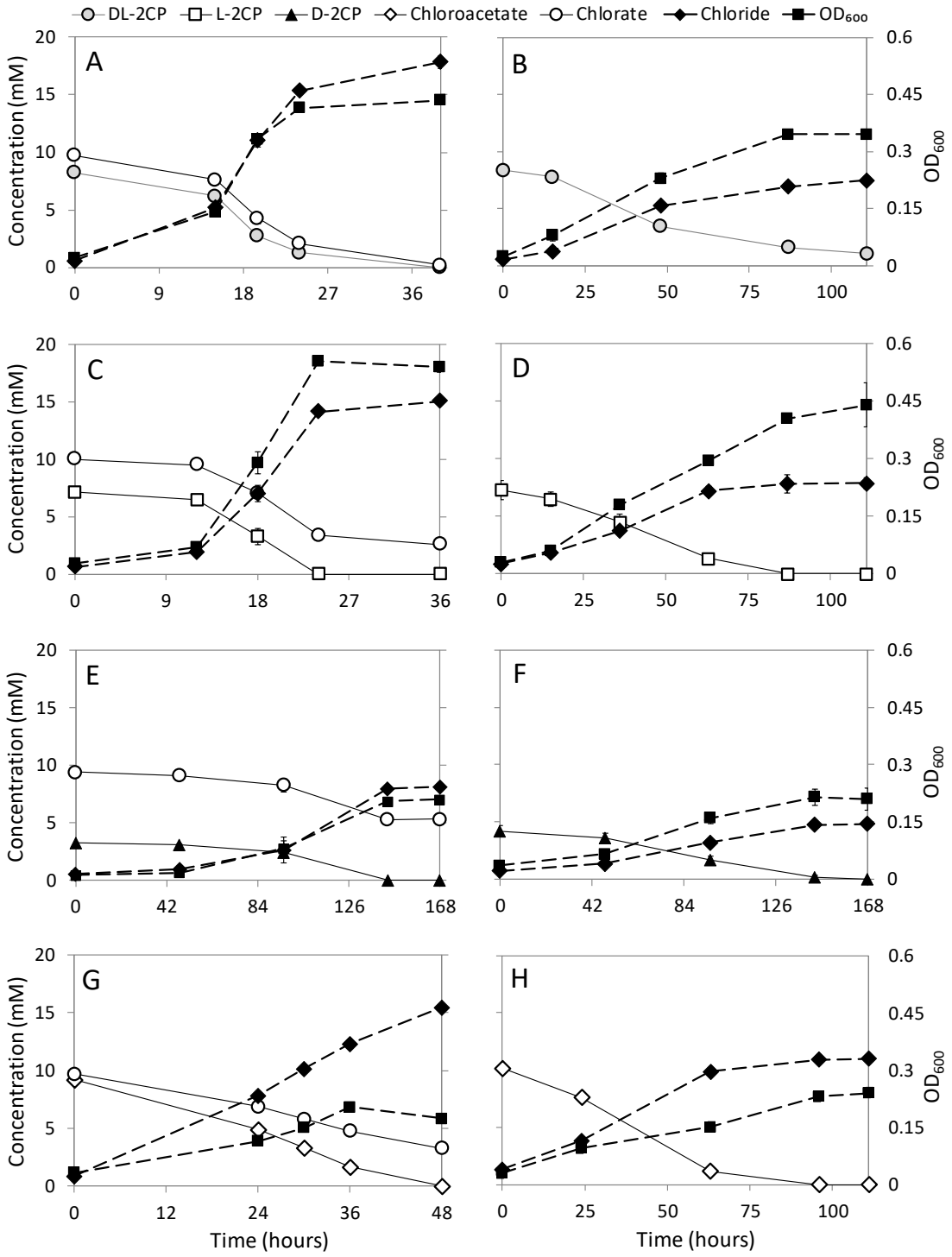

Fig. S2.1 Growth of *P. chloritidismutans* AW-1^T on DL-2-chloropropionate (DL-2CP, A, B), L-2-chloropropionate (L-2CP, C, D), D-2-chloropropionate (D-2CP, E, F), chloroacetate (G, H) with chlorate (left panels) and oxygen (right panels) as terminal electron acceptor. Note that panel C, E and G are the same as panel A, C and E in Fig 2.2 and presented here to facilitate comparison with aerobic conditions. Points and error bars in the remaining panels represent the average and standard deviation of samples taken from duplicate cultures.

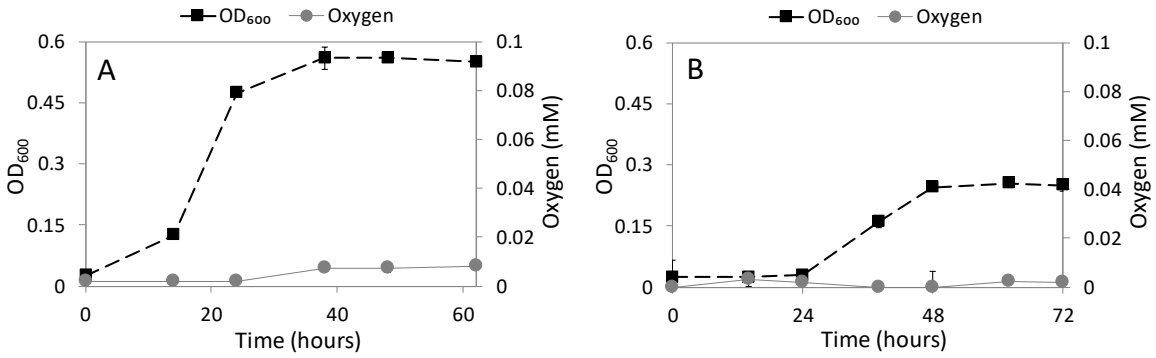

Fig. S2.2 Oxygen formation during growth of *P. chloritidismutans* AW-1^T on DL-2CP (A) and chloroacetate (B) under chlorate-reducing condition. Points and error bars represent the average and standard deviation of samples taken from duplicate cultures.

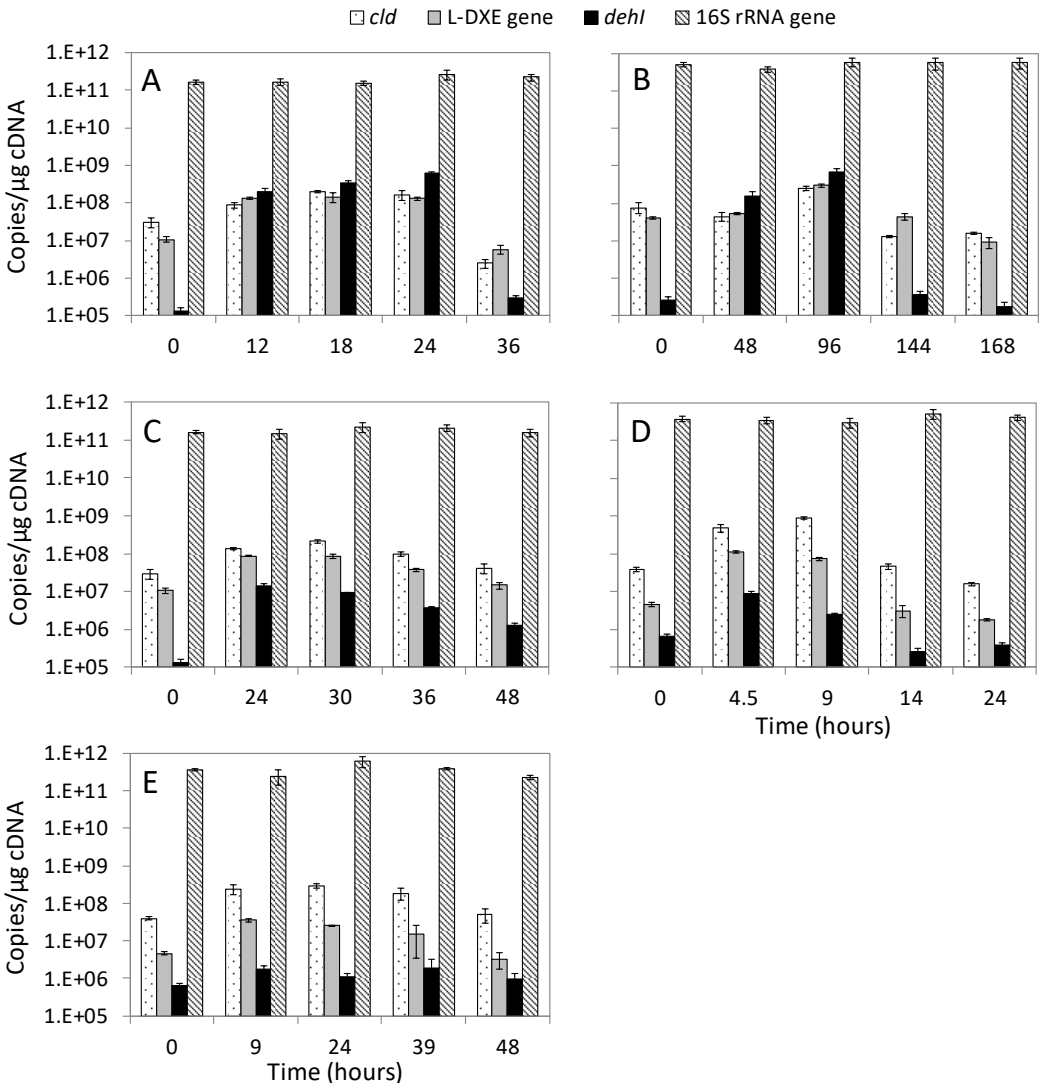

Fig. S2.3 Expression profiles of the L-2-haloacid dehalogenase gene (L-DEX gene), halocarboxylic acid dehydrogenase gene (*dehI*), chlorate dismutase gene (*cld*) and 16S rRNA gene of *P. chloritidismutans* AW-1^T during growth on L-2CP (A), D-2CP (B), chloroacetate (C) and acetate (D) with chlorate and on acetate (E) with oxygen as terminal electron acceptor.

Table S2.1 Co-occurrence of 2-haloacid dehalogenase and chlorite dismutase genes in available bacterial genomes.

Strain	Protein	Protein ID
Bacillus megaterium DSM 319	2-haloacid dehalogenase	WP_013082018.1
	chlorite dismutase (heme-binding protein)	WP_013085502.1
Bacillus megaterium QM B1551	2-haloacid dehalogenase	WP_013055715.1
	chlorite dismutase (heme-binding protein)	WP_013059854.1
Bacillus megaterium WSH-002	2-haloacid dehalogenase	WP_014461303.1
	chlorite dismutase (heme-binding protein)	WP_014457727.1
Bradyrhizobium sp. S23321	2-haloacid dehalogenase	WP_015688637.1
	chlorite dismutase	WP_015688409.1
Exiguobacterium antarcticum B7	2-haloacid dehalogenase	WP_014971509.1
	chlorite dismutase (heme-binding protein)	WP_014969243.1
Exiguobacterium sp. AT1b	2-haloacid dehalogenase	WP_012727283.1
	chlorite dismutase (heme-binding protein)	WP_012727491.1
Exiguobacterium sp. MH3	2-haloacid dehalogenase	WP_023469611.1
	chlorite dismutase (heme-binding protein)	WP_023466755.1
Exiguobacterium sibiricum 255-15	2-haloacid dehalogenase	WP_012371658.1
	chlorite dismutase (heme-binding protein)	WP_012369128.1
Halobacillus halophilus DSM 2266	2-haloacid dehalogenase	WP_014642685.1
	chlorite dismutase (heme-binding protein)	WP_014644882.1
Marinithermus hydrothermalis DSM 14884	2-haloacid dehalogenase	WP_013703677.1
	chlorite dismutase	WP_013703158.1
Mycobacterium indicus pranii MTCC 9506	2-haloalkanoic acid dehalogenase	WP_014941252.1
	chlorite dismutase	WP_008258510.1
Mycobacterium intracellulare ATCC 13950	2-haloalkanoic acid dehalogenase	WP_014379092.1
	chlorite dismutase	WP_008258510.1
Mycobacterium intracellulare MOTT 02	2-haloalkanoic acid dehalogenase	WP_009951930.1
	chlorite dismutase	WP_014382908.1
Mycobacterium intracellulare MOTT 64	2-haloalkanoic acid dehalogenase	WP_014383798.1
	chlorite dismutase	WP_008258510.1
Mycobacterium sp. MOTT 36Y	chlorite dismutase	WP_008258510.1
	2-haloalkanoic acid dehalogenase	WP_009951930.1
Mycobacterium yongonense 05-1390	2-haloacid dehalogenase	WP_008263884.1
	chlorite dismutase	WP_008258510.1

Pseudonocardia dioxanivorans CB1190	2-haloacid dehalogenase	AEA24138.1
	chlorite dismutase	AEA25096.1
Rhodanobacter denitrificans 2APBS1	2-haloalkanoic acid dehalogenase	WP_015449095.1
	chlorite dismutase	WP_015448156.1
Rhodopirellula baltica SH1	2-haloalkanoic acid dehalogenase	NP_866175.1
	chlorite dismutase (heme peroxidase)	NP_869234.2
Roseiflexus castenholzii DSM 13941	2-haloalkanoic acid dehalogenase	WP_012119159.1
	chlorite dismutase	WP_012120539.1
Roseiflexus sp. RS1	2-haloalkanoic acid dehalogenase	WP_011958215.1
	chlorite dismutase	WP_011956484.1
Rubrobacter xylanophilus DSM 9941	2-haloalkanoic acid dehalogenase	WP_011564651.1
	chlorite dismutase	WP_011563733.1
Sphaerobacter thermophilus DSM 20745	2-haloalkanoic acid dehalogenase	WP_012873678.1
	chlorite dismutase	WP_012873220.1
Staphylococcus carnosus TM300	2-haloalkanoic acid dehalogenase	WP_015901332.1
	chlorite dismutase (heme-binding protein)	WP_012664269.1
Thermomicrobium roseum DSM 5159	2-haloalkanoic acid dehalogenase	WP_012643089.1
	chlorite dismutase	WP_012643117.1

Chapter 3

Organohalide-respiring *Desulfoluna* species isolated from marine environments

Peng Peng, Tobias Goris, Yue Lu, Bart Nijsse, Anna Burrichter, David Schleheck, Jasper J. Koehorst, Jie Liu, Detmer Sipkema, Jaap S. Sinninghe Damste, Alfons J. M. Stams, Max M. Häggblom, Hauke Smidt, Siavash Atashgahi

Under review in *The ISME Journal*

Abstract

The genus *Desulfoluna* comprises two anaerobic sulfate-reducing strains, *D. spongiiphila* AA1^T and *D. butyratoxydans* MSL71^T, of which only the former was shown to perform organohalide respiration (OHR). Here we isolated a third member of this genus from marine intertidal sediment, designated *D. spongiiphila* strain DBB. Each of the three *Desulfoluna* strains harbours three reductive dehalogenase gene clusters (*rdhABC*) and corrinoid biosynthesis genes in their genomes. Brominated but not chlorinated aromatic compounds were dehalogenated by all three strains. The *Desulfoluna* strains maintained OHR in the presence of 20 mM sulfate or 20 mM sulfide, which often negatively affect OHR. Strain DBB sustained OHR with 2% oxygen in the gas phase, in line with its genetic potential for reactive oxygen species detoxification. Reverse transcription-quantitative PCR (RT-qPCR) revealed differential induction of *rdhA* genes in strain DBB in response to 1,4-dibromobenzene or 2,6-dibromophenol. Proteomic analysis confirmed differential expression of *rdhA1* with 1,4-dibromobenzene, and revealed a possible electron transport chain from lactate dehydrogenases and pyruvate oxidoreductase to RdhA1 via menaquinones and either RdhC, or Fix complex (electron transfer flavoproteins), or Qrc complex (Type-1 cytochrome c3:menaquinone oxidoreductase). This study indicates an important role of marine organohalide-respiring *Deltaproteobacteria* in halogen, sulfur and carbon cycling.

Introduction

More than 5,000 naturally produced organohalides have been identified, some of which have already been present in a variety of environments for millions of years (Gribble 2010). In particular, marine environments are a rich source of chlorinated, brominated and iodinated organohalides produced by marine algae, seaweeds, sponges, and bacteria (Gribble 2015), Fenton-like (Leri *et al.* 2015) and photochemical reactions, as well as volcanic activities (Lavric *et al.* 2004, Méndez-Díaz *et al.* 2014). Such a natural and ancient presence of organohalogens in marine environments may have primed development of various microbial dehalogenation metabolisms (Atashgahi *et al.* 2018a). Furthermore, marine environments and coastal regions in particular are also commonly reported to be contaminated with organohalogens from anthropogenic sources (Lu *et al.* 2017).

During organohalide respiration (OHR) organohalogens are used as electron acceptors, and their reductive dehalogenation is coupled to energy conservation (Fincker and Spormann 2017, Mohn and Tiedje 1992, Schubert *et al.* 2018). This process is mediated by reductive dehalogenases (RDases), which are membrane-associated, corrinoid-dependent, and oxygen sensitive proteins (Fincker and Spormann 2017, Gadkari *et al.* 2018, Schubert *et al.* 2018). The corresponding *rdh* gene clusters usually consists of *rdhA* encoding the catalytic subunit, *rdhB* encoding a putative membrane anchor protein (Schubert *et al.* 2018), and a variable set of accessory genes encoding RdhC and other proteins likely involved in regulation, maturation and/or electron transport (Kruse *et al.* 2016, Türkowsky *et al.* 2018). The electron transport chain from electron donors to RDases has been classified into quinone-dependent (that rely on menaquinones as electron shuttles between electron donors and RDases) and quinone-independent pathways (Fincker and Spormann 2017, Kublik *et al.* 2016, Schubert *et al.* 2018). Recent studies suggested that RdhC may serve as electron carrier during OHR in *Firmicutes* (Buttet *et al.* 2018, Futagami *et al.* 2014).

OHR is mediated by organohalide-respiring bacteria (OHRB), which belong to a broad range of phylogenetically distinct bacterial genera. OHRB belonging to *Chloroflexi* and the genus *Dehalobacter* (*Firmicutes*, e.g. *Dehalobacter restrictus*) are specialists restricted to OHR, whereas proteobacterial OHRB and members of the genus *Desulfitobacterium* (*Firmicutes*, e.g. *Desulfitobacterium hafniense*) are generalists with a versatile metabolism (Atashgahi *et al.* 2016, Hug *et al.* 2013). Numerous studies have reported OHR activity and occurrence of OHRB and *rdhA* genes in marine environments (Ahn *et al.* 2009, Atashgahi *et al.* 2018a, Futagami *et al.* 2009, Liu *et al.* 2017). Recent genomic (Atashgahi 2019, Liu and Häggblom 2018, Sanford *et al.* 2016) and single-cell genomic (Jochum *et al.* 2018) analyses revealed widespread occurrence of *rdh* gene clusters in marine *Deltaproteobacteria*, indicting untapped potential for OHR. Accordingly, OHR metabolism was experimentally verified in three *Deltaproteobacteria* strains, not previously known as OHRB (Liu and Häggblom 2018).

OHRB, and in particular members of the *Chloroflexi*, are fastidious microbes, and are susceptible to inhibition by oxygen (Adrian *et al.* 2007), sulfate (May *et al.* 2008) or sulfide (He *et al.* 2005, Mao *et al.* 2017). In the presence of both 3-chlorobenzoate and either sulfate, sulfite or thiosulfate, *Desulfomonile tiedjei* isolated from sewage sludge preferentially performed sulfur oxyanion reduction (Townsend and Suflita 1997), and OHR inhibition was suggested to be caused by downregulation of *rdh* gene expression (Townsend and Suflita 1997). In contrast, concurrent sulfate reduction and OHR was observed in *Desulfoluna spongiiphila* AA1^T isolated from the marine sponge *Aplysina aerophoba* (Ahn *et al.* 2009), and three newly characterized organohalide-respiring marine deltaproteobacterial strains (Liu and Häggblom 2018). Sulfate- and sulfide-rich marine environments may have exerted a selective pressure resulting in development of sulfate- and sulfide-tolerant OHRB.

The genus *Desulfoluna* comprises two anaerobic sulfate-reducing strains, *D. spongiiphila* AA1^T isolated from the bromophenol-producing marine sponge *Aplysina aerophoba* (Ahn *et al.* 2009, Ahn *et al.* 2003), and *D. butyratoxydans* MSL71^T isolated from estuarine sediments (Suzuki *et al.* 2008). Strain AA1^T can reductively dehalogenate various bromophenols but not chlorophenols. The genome of strain AA1^T harbours three *rdhA* genes, one of which was shown to be induced by 2,6-dibromophenol (Liu *et al.* 2017). The OHR potential and the genome of strain MSL71^T have not been studied before. In this study, a third member of the genus *Desulfoluna*, designated *D. spongiiphila* strain DBB, was isolated from a marine intertidal sediment. The OHR metabolism of strain DBB and of strain MSL71^T was verified in this study. In line with former reports (Atashgahi 2019, Jochum *et al.* 2018, Liu and Häggblom 2018, Sanford *et al.* 2016), this study further reinforces an important role of marine organohalide-respiring *Deltaproteobacteria* in halogen, sulfur and carbon cycling.

Materials and Methods

Chemicals

Brominated, iodinated and chlorinated benzenes and phenols were purchased from Sigma-Aldrich. Other organic and inorganic chemicals used in this study were of analytical grade.

Bacterial strains

D. spongiiphila AA1^T (DSM 17682^T) and *D. butyratoxydans* MSL71^T (DSM 19427^T) were obtained from the German Collection of Microorganisms and Cell Cultures (DSMZ, Braunschweig, Germany), and were cultivated as described previously (Ahn *et al.* 2009, Suzuki *et al.* 2008).

Enrichment, isolation and cultivation of strain DBB

Surface sediment of an intertidal zone, predominantly composed of shore sediment, was collected at the shore in L'Escala, Spain (42°7'35.27"N, 3°8'6.99"E). Five grams of sediment were

transferred into 120-ml bottles containing 50 ml of anoxic medium (Monserrate and Häggblom 1997) with lactate and 1,4-dibromobenzene (1,4-DBB) as the electron donor and acceptor, respectively. Sediment-free cultures were obtained by transferring the suspensions of the enrichment culture to fresh medium. A pure culture of a 1,4-DBB debrominating strain, designated as *D. spongiiphila* strain DBB, was obtained from a dilution series on solid medium with 0.8% low-melting point agarose (Sigma-Aldrich). A detailed description of enrichment, isolation and physiological characterization of strain DBB is provided in the Supplementary Information.

Cell morphology and cellular fatty acids analyses

Cell morphology and motility were observed using a LEICA DM 2000 Microscope and a JEOL-6480LV Scanning Electron Microscope (SEM). Actively growing cells were directly observed under the 100x magnification objective of the LEICA DM 2000 Microscope. Sample fixation and dehydration for SEM were performed as described previously (Bui *et al.* 2014). The cellular fatty acid composition was analysed from 500 ml cultures of AA1^T, DBB and MSL71^T, which were grown with 20 mM lactate and 10 mM sulfate. Fatty acids in the cell were analysed by acid hydrolysis of total cell material following a method previously described (Damsté *et al.* 2011).

DNA extraction and bacterial community analysis

DNA of the intertidal sediment (5 g) and the 1,4-DBB-respiring enrichment culture (10 ml) was extracted using the DNeasy PowerSoil Kit (MO-BIO, CA, USA). A 2-step PCR strategy was applied to generate barcoded amplicons from the V1–V2 region of bacterial 16S rRNA genes as described previously (Atashgahi *et al.* 2017). Primers for PCR amplification of the 16S rRNA genes were listed in Table S3.1. Sequence analysis was performed using NG-Tax (Ramiro-Garcia *et al.* 2016). Operational taxonomic units (OTUs) were assigned taxonomy using uclust (Edgar 2010) in an open reference approach against the SILVA 16S rRNA gene reference database (LTPs128_SSU) (Quast *et al.* 2012). Finally, a biological observation matrix (biom) file was generated and sequence data were further analyzed using Quantitative Insights Into Microbial Ecology (QIIME) v1.2 (Caporaso *et al.* 2010).

Genome sequencing and annotation

DNA of DBB and MSL71^T cells was extracted using the MasterPure™ Gram Positive DNA Purification Kit (Epicentre, WI, USA). The genomes were sequenced using the Illumina HiSeq2000 paired-end sequencing platform (GATC Biotech, Konstanz, Germany). The genome of strain DBB was further sequenced by PacBio sequencing (PacBio RS) to obtain longer read lengths. Optimal assembly kmer size for strain DBB was detected using kmergenie (v.1.7039) (Chikhi and Medvedev 2013). A *de novo* assembly with Illumina HiSeq2000 paired-reads was made with assembler Ray (v2.3.1) (Chikhi and Medvedev 2013) using a kmer size of 81. A hybrid assembly

for strain DBB with both the PacBio and the Illumina HiSeq reads was performed with SPAdes (v3.7.1, kmer size: 81) (Bankevich *et al.* 2012). The two assemblies were merged using the tool QuickMerge (v1) (Chakraborty *et al.* 2016). Duplicated scaffolds were identified with BLASTN (Camacho *et al.* 2009) and removed from the assembly. Assembly polishing was performed with Pilon (v1.21) (Walker *et al.* 2014) using the Illumina HiSeq reads. Optimal assembly kmer size for strain MSL71^T was also identified using kmergenie (v.1.7039), and a *de novo* assembly with Illumina HiSeq2000 paired-end reads was performed with SPAdes (v3.11.1) with a kmer-size setting of 79,101,117. FastQC and Trimmomatic (v0.36) (Bolger *et al.* 2014) was used for read inspection and trimming using the trimmomatic parameters: TRAILING:20 LEADING:20 SLIDINGWINDOW:4:20 MINLEN:50. Trimmed reads were mapped with Bowtie2 v2.3.3.1 (Langmead and Salzberg 2012). Samtools (v1.3.1) (Li *et al.* 2009) was used for converting the bowtie output to a sorted and indexed bam file. The assembly was polished with Pilon (v1.21).

Transcriptional analysis of the *rdhA* genes of *D. spongiiphila* DBB

Transcriptional analysis was performed using DBB cells grown with lactate (20 mM), sulfate (10 mM) and either 1,4-DBB (1 mM) or 2,6-DBP (0.2 mM). DBB cells grown with lactate and sulfate but without any organohalogens were used as control. Ten replicate microcosms were prepared for each experimental condition, and at each sampling time point, two microcosms were randomly selected and sacrificed for RNA isolation as described previously (Peng *et al.* 2017). RNA was purified using RNeasy columns (Qiagen, Venlo, The Netherlands) followed by DNase I (Roche, Almere, The Netherlands) treatment. cDNA was synthesized from 200 ng total RNA using SuperScript™ III Reverse Transcriptase (Invitrogen, CA, USA) following manufacturer's instructions. Primers for RT-qPCR assays were listed in Table S3.1. RT-qPCR assays were performed as outlined in Supplementary Information.

Protein extraction and proteomic analysis

Triplicate cultures of strain DBB grown with lactate/sulfate (LS condition) or lactate/sulfate/1,4-DBB (LSD condition) were used for proteomic analysis. Preparation of cell-free extracts (CFE), determination of protein concentration, SDS-PAGE purification of total proteins in CFE and of proteins in membrane fragments, and the peptide fingerprinting-mass spectrometry (PF-MS) analysis, were performed as outlined in Supplementary Information. Statistical analysis was performed using prostar proteomics (Wieczorek *et al.* 2017). Top three peptide area values were normalized against all columns. The values of proteins detected in at least two of the three replicates were differentially compared and tested for statistical significance. Missing values were imputed using the SLSA function of prostar, and hypothesis testing with a student's t-test was performed for LSD vs LS growth conditions. The *p*-values were Benjamini-Hochberg corrected and

proteins with p-values below 0.05 and a log2 value of 1 or larger were considered statistically significantly up- or downregulated.

Analytical methods

Halogenated benzenes and benzene were analyzed on a GC equipped with an Rxi-5Sil capillary column (Retek, PA, USA) and a flame ionization detector (GC-FID, Shimadzu 2010). Halogenated phenols and phenol were analyzed on a Thermo Scientific Accela HPLC System equipped with an Agilent Poroshell 120 EC-C18 column and a UV/Vis detector. Organic acids and sugars were analyzed using a ThermoFisher Scientific SpectraSYSTEM™ HPLC equipped with an Agilent Metacarb 67H column and RI/UV detectors. Sulfate, sulfite and thiosulfate were analyzed using a ThermoFisher Scientific Dionex™ ICS-2100 Ion Chromatography System equipped with a Dionex Ionpac analytical column and a suppressed conductivity detector. Cell growth was determined by measuring OD_{600} using a WPA CO8000 cell density meter (Biochrom, Cambridge, UK). Sulfide was measured by a photometric method using methylene blue as described previously (Cline 1969).

Strain and data availability

D. spongiiphila strain DBB was deposited in DSMZ under accession number DSM 104433. The 16S rRNA gene sequences of strain DBB were deposited in GenBank (accession numbers: MK881098–MK881099). The genome sequences of strains DBB and MSL71 were deposited in the European Bioinformatics Institute (EBI, Project ID: PRJEB31368). A list of proteins detected from strain DBB under LS and LSD growth conditions is available in Supplementary Datasets S3.1 (Soluble fraction) and S3.2 (Membrane fraction).

Results and discussion

Enrichment of 1,4-DBB debrominating cultures and isolation of strain DBB

Reductive debromination of 1,4-DBB to bromobenzene (BB) and benzene was observed in the original cultures containing intertidal sediment (Fig. 3.1A, B). Debromination of 1,4-DBB was maintained in the subsequent sediment-free transfer cultures (Fig. 3.1C). However, benzene was no longer detected and BB was the only debromination product, indicating loss of the BB-debrominating population. Up to date, the only known OHRB that can debrominate BB to benzene is *Dehalococcoides mccartyi* strain CBDB1 (Wagner *et al.* 2012). 1,4-DBB debromination to BB was stably maintained during subsequent transfers (data not shown) and after serial dilution (Fig. 3.1D). Bacterial community analysis showed an increase in the relative abundance of *Deltaproteobacteria* from ~2% in the intertidal sediment at time zero to ~13% after 104 days of enrichment (Fig. 3.1E). The genus *Desulfoluna* was highly enriched and comprised more than 80% relative abundance in the most diluted culture (10^7 dilution) (Fig. 3.1E).

Single colonies were observed in roll tubes with 0.8% low-melting agarose after 15 days of incubation. Among the six single colonies randomly selected and transferred to liquid media, one showed 1,4-DBB debromination (Fig. 3.1F) which was again subjected to the roll tube isolation procedure to ensure purity. The final isolated strain was designated DBB.

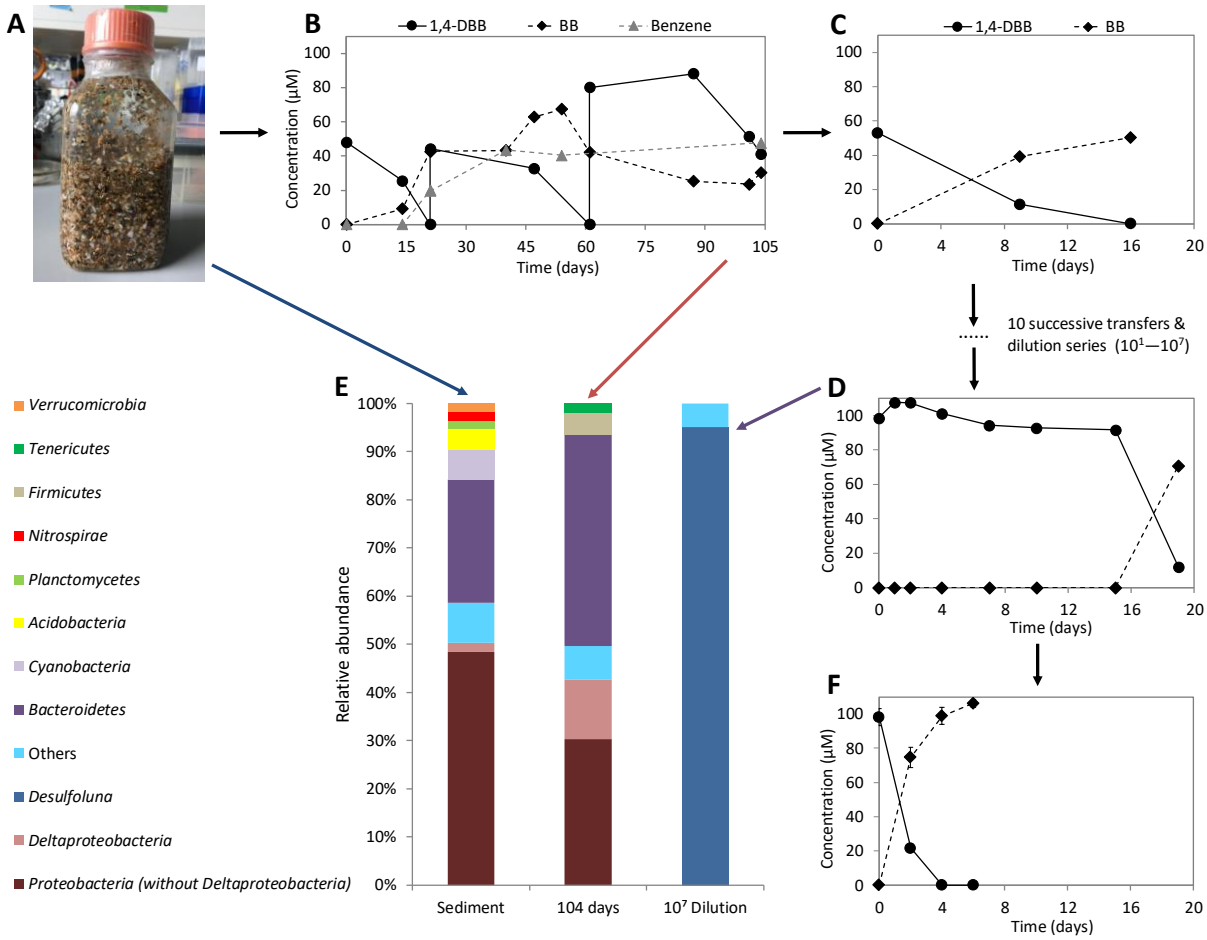

Fig. 3.1 Enrichment and isolation of *D. spongiiphila* DBB. Intertidal sediment mainly composed of shore sediment used for isolation (A). Reductive debromination of 1,4-DBB by: the original microcosms containing intertidal sediment (B), the sediment-free enrichment cultures (C), the most diluted culture (10^7) in the dilution series (D). Phylogenetic analysis of bacterial communities in the microcosms from the shore sediment at time zero (left), the original 1,4-DBB debrominating enrichment culture after 104 days incubation (middle) and the 10^7 dilution series culture (right) (E). Reductive debromination of 1,4-DBB by the isolated pure culture (F). Sediment enrichment culture and sediment-free transfer cultures (B–D) were prepared in single bottles. Pure cultures (F) were prepared in duplicate bottles. Points and error bars represent the average and standard deviation of samples taken from the duplicate cultures. Phylogenetic data are shown at phylum level, except *Deltaproteobacteria* shown at class level and *Desulfoluna* at genus level. Taxa comprising less than 1% of the total bacterial community are categorized as 'Others'.

Characterization of the *Desulfoluna* strains

Cells of strain DBB were slightly curved rods with a length of 1.5 to 3 µm and a diameter of 0.5 µm as revealed by SEM (Fig. S3.1A, B), which was similar to strain AA1^T (Fig. S3.1C) and MSL71^T (Fig. S3.1D). In contrast to strain AA1^T (Ahn *et al.* 2009), but similar to strain MSL71^T (Suzuki *et al.* 2008), strain DBB was motile when observed by light microscopy, with evident flagella being observed by SEM (Fig. S3.1A, B).

The cellular fatty acid profiles of the three strains consisted mainly of even-numbered saturated and mono-unsaturated fatty acids (Table S3.2).

Strain DBB used lactate, pyruvate, formate, malate and butyrate as electron donors for sulfate reduction (Table 3.1). Lactate was degraded to acetate, which accumulated without further degradation, and sulfate was reduced to sulfide (Fig. S3.2A). In addition, sulfite and thiosulfate were utilized as electron acceptors with lactate as the electron donor (Table 3.1). Sulfate and 1,4-DBB could be concurrently utilized as electron acceptors by strain DBB (Fig. S3.2). Independent of the presence of sulfate in the medium, strain DBB stoichiometrically debrominated 1,4-DBB to bromobenzene (BB), and 2-bromophenol (2-BP), 4-bromophenol (4-BP), 2,4-bromophenol (2,4-DBP), 2,6-DBP, 2,4,6-tribromophenol (2,4,6-TBP), 2-iodophenol (2-IP) and 4-iodophenol (4-IP) to phenol (Table 3.1) using lactate as the electron donor. Hydrogen was not used as an electron donor for 1,4-DBB debromination (data not shown). Strain DBB was unable to dehalogenate the tested chlorinated aromatic compounds and several other bromobenzenes listed in Table 3.1. This is in accordance with the dehalogenating activity reported for strain AA1^T that was unable to use chlorinated aromatic compounds as electron acceptors (Ahn *et al.* 2009). The majority of the known organohalogens from marine environments are brominated (Gribble 2010) and hence marine OHRB may be less exposed to organochlorine compounds in their natural habitats. For instance, strain AA1^T was isolated from the sponge *Aplysina aerophoba* (Ahn *et al.* 2009) in which organobromine metabolites can account for over 10% of the sponge dry weight (Turon *et al.* 2000).

Table 3.1 Physiological and genomic properties of *Desulfoluna* strains

Strain	DBB	AA1^{T} [a]	MSL71^{T} [b]
Isolation source	Marine intertidal sediment	Marine sponge	Estuarine sediment
Cell morphology	Curved rods	Curved rods	Curved rods
Optimum NaCl concentration (%)	2.0	2.5	2.0
Temperature optimum/range (°C)	30/10–30	28/10–36	30/ND [c]
Utilization of electron donors			
Lactate	+	+	+
Butyrate	+	-	+
Formate	+	+	+
Acetate	-	-	-
Fumarate	-	-	-
Citrate	-	+	-
Glucose	-	+	-
Malate	+	+	+
Pyruvate	+	+	+
Hydrogen	- [d]	ND	+
Propionate	-	-	-
Succinate	-	-	-
Utilization of electron acceptors			
Sulfate	+	+	+
Sulfite	+	+	+
Thiosulfate	+	+	+
1,4-Dibromobenzene	+	+ [e]	- [e]
1,2-Dibromobenzene	-	ND	ND
1,3-Dibromobenzene	-	ND	ND
1,2,4-Tribromobenzene	-	ND	ND
Bromobenzene	-	ND	ND
1,2-Dichlorobenzene	-	ND	ND
1,3-Dichlorobenzene	-	ND	ND
1,4-Dichlorobenzene	-	ND	ND
1,2,4-Trichlorobenzene	-	ND	ND
2-Bromophenol	+	+	+ [e]
4-Bromophenol	+	+	- [e]
2,4-Dibromophenol	+	+	+ [e, f]
2,6-Dibromophenol	+	+	+ [e]
2,4,6-Tribromophenol	+	+	+ [e, f]
2-Iodophenol	+	+ [e]	- [e]
4-Iodophenol	+	+ [e]	- [e]
2,4-Dichlorophenol	-	-	- [e]

2,6-Dichlorophenol	-	-	- [e]
2,4,6-Trichlorophenol	-	-	- [e]
Genomic information			
Genome size (Mb)	6.68	6.53 [g]	6.05 [h]
G+C content (%)	57.1	57.9 [g]	57.2 [h]
Total genes	5497	5356 [g]	4894 [h]
Total proteins	5301	5203 [g]	4186 [h]

[a] Data from Ahn et al. (Ahn *et al.* 2009)
[b] Data from Suzuki et al. (Suzuki *et al.* 2008)
[c] ND, not determined
[d] Tested with 1,4-dibromobenzene as the electron acceptor
[e] Data from this study
[f] 4-Bromophenol rather than phenol was the debromination product
[g] Data from GenBank (accession number: NZ_FMUX01000001.1)
[h] Predicted based on draft genome

Genomic and phylogenetic characterization of the *Desulfoluna* strains

The genome of strain DBB is closed and consists of a single chromosome with a size of 6.68 Mbp (Fig. S3.3). The genome of strain AA1^T (GenBank accession number: NZ_FMUX01000001.1) and strain MSL71T (sequenced in this study) are draft genomes with similar G+C content (Table 3.1). The average nucleotide identity (ANI) of the DBB genome to AA1^T and MSL71^T genomes was 98.5% and 85.9%, respectively. This indicates that DBB and AA1^T strains belong to the same species of *D. spongiiphila* (Richter and Rosselló-Móra 2009). 16S rRNA gene and protein domain-based phylogenetic analyses with other genera of the *Desulfobacteraceae* placed *Desulfoluna* strains in a separate branch of the corresponding phylogenetic trees (Fig. 3.2). Whole genome alignment of strains DBB, AA1^T and MSL71^T revealed the presence of 11 locally colinear blocks (LCBs) with several small regions of inversion and rearrangement (Fig. S3.4). A site-specific recombinase gene (DBB_14420) was found in one of the LCBs. The same gene was also found in the corresponding inversed and rearranged LCBs in AA1^T (AA1_11599) and MSL71^T (MSL71_ 48620), suggesting a role of the encoded recombinase in genomic rearrangement in the *Desulfoluna* strains.

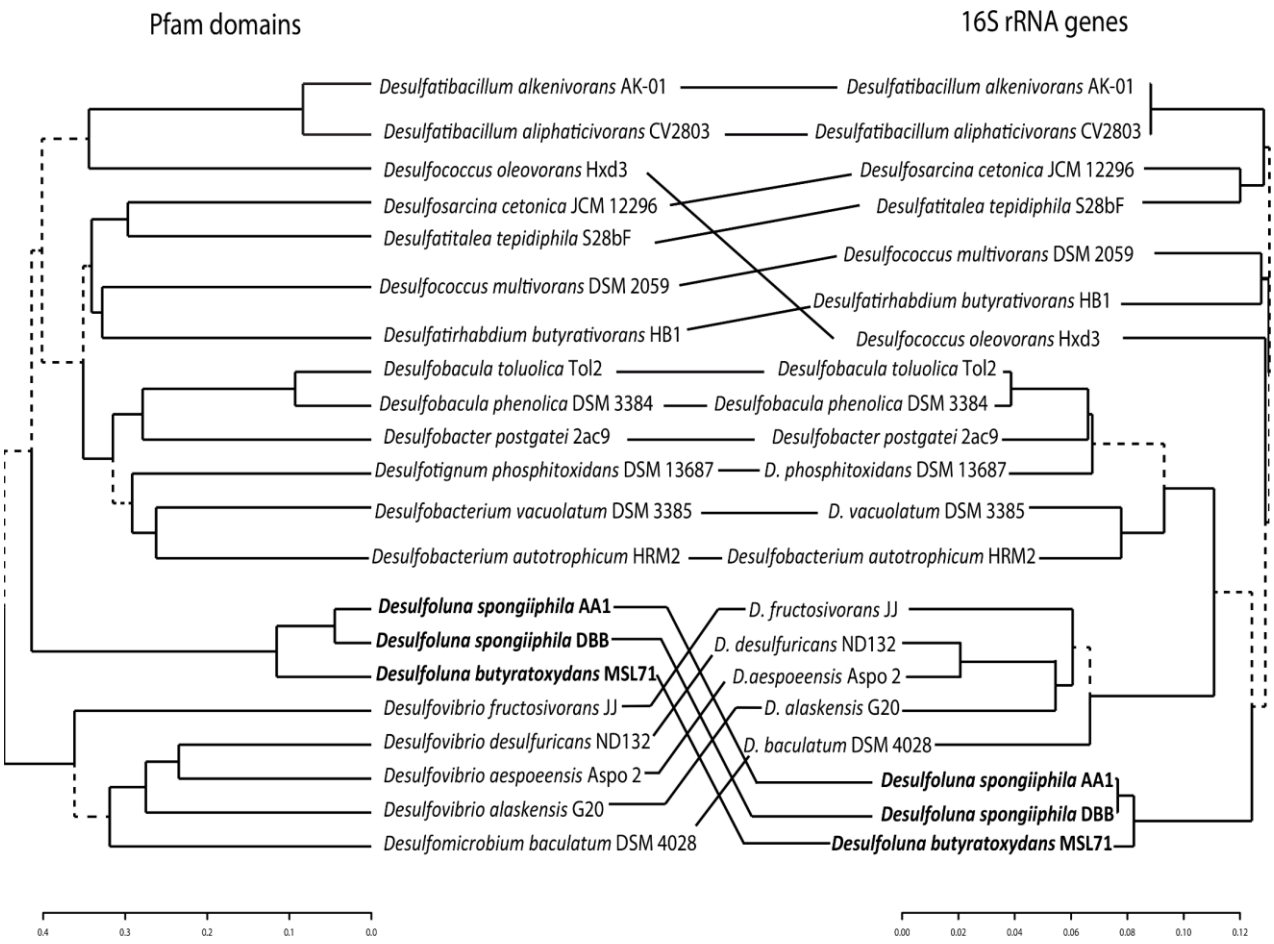

Fig. 3.2 Phylogenetic tree based on 16S rRNA gene sequence and protein domain analyses. A comparison is included as horizontal lines between the two trees, showing the position of strain DBB relative to other strains belonging to the family *Desulfobacteraceae* as well as several *Desulfovibrio* strains. The "unique" nodes between the 16S rRNA gene- and domain-based tree are indicated with dashed lines. Genomes (Table S3.3) were selected based on the phylogenetic tree of the family *Desulfobacteraceae* (Kuever 2014).

Comparison of the *rdh* gene region of the *Desulfoluna* strains

Similar to strain AA1^T (Liu *et al.* 2017), the genomes of strains DBB and MSL71^T also harbor three *rdhA* genes. The amino acid sequences of the RdhA homologs in DBB share >99% identity to the corresponding RdhAs in AA1^T, and 80–97% identity with the corresponding RdhAs in MSL71^T (Fig. 3.3). However, the three distinct RdhA homologs in the *Desulfoluna* strains share low identity (20–30%) with each other and form three distant branches in the phylogenetic tree of RdhAs (Hug *et al.* 2013), and cannot be grouped with any of the currently known RdhA groups (Fig. S3.5). Therefore, we propose three new RdhA homolog groups, RdhA1 including DBB_38400, AA1_07176 and MSL71_22580; RdhA2 including DBB_36010, AA1_02299 and MSL71_20560; RdhA3 including DBB_45880, AA1_11632 and MSL71_30900 (Fig. 3.3, Fig. S3.5).

The *rdh* gene clusters in DBB and MSL71^T show a similar gene order to the corresponding *rdh* gene clusters in AA1^T (Fig. 3.3), except that the *rdhA1* gene cluster of MSL71^T lacks *rdhB* and *rdhC*. Genes encoding sigma-54-dependent transcriptional regulators in the *rdhA1* and *rdhA3* gene

clusters of AA1^T (Liu *et al.* 2017), were also present in the corresponding gene clusters of DBB and MSL71^T (Fig. 3.3). Likewise, genes encoding the LuxR and MarR-type regulators are present up- and downstream of the *rdhA2* gene clusters of DBB and MSL71^T, in line with the organization of the *rdhA2* gene cluster of AA1^T (Fig. 3.3). This may indicate similar regulation systems of the *rdh* genes in the *Desulfoluna* strains studied here. The conserved motifs from known RDases (RR, C1−C5, FeS1, and FeS2) (Lu *et al.* 2015, Smidt and de Vos 2004) are also conserved among all the RdhAs of the *Desulfoluna* strains, except for RdhA1 of MSL71^T which lacks the RR motif (Fig. S3.6). This may indicate a cytoplasmic localization and a non-respiratory role of the RdhA1 in strain MSL71^T (Atashgahi *et al.* 2018a).

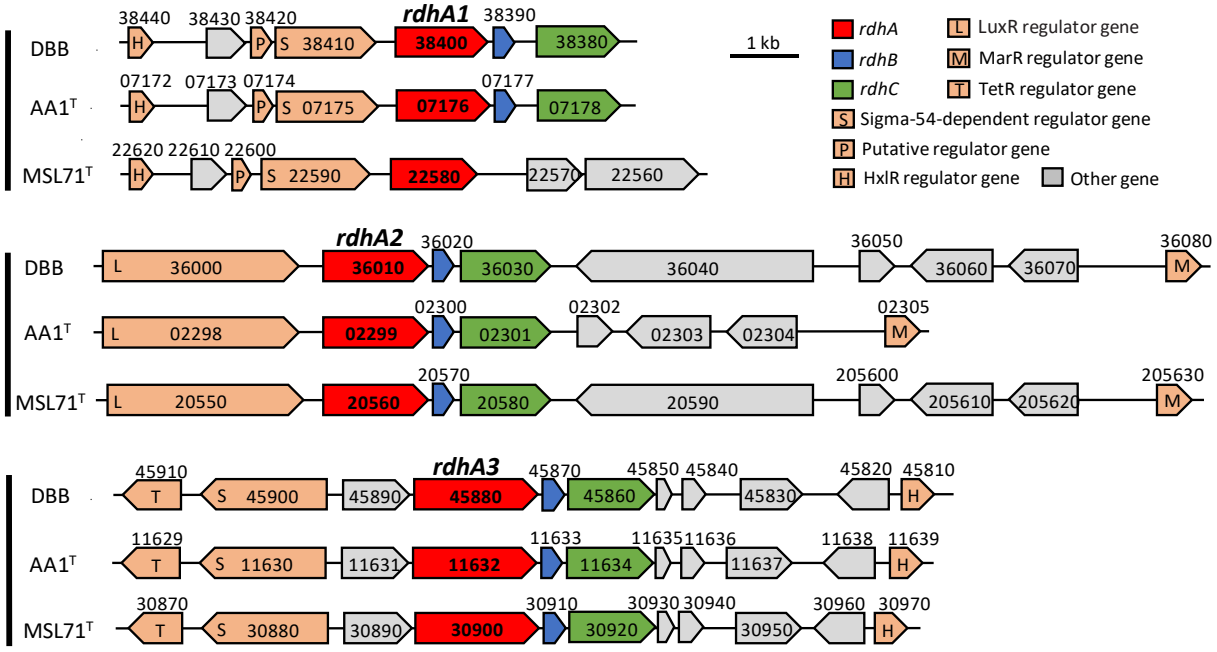

Fig. 3.3 Comparison of the *rdh* gene clusters in *D. spongiiphila* DBB, *D. spongiiphila* AA1^T and *D. butyratoxydans* MSL71^T. Numbers indicate the locus tags of the respective genes.

OHR metabolism of *D. butyratoxydans* MSL71^T

Guided by the genomic potential of strain MSL71^T for OHR, physiological experiments in this study indeed confirmed that strain MSL71^T is capable of using 2-BP, 2,4-DBP, 2,6-DBP and 2,4,6-TBP as electron acceptors with lactate as the electron donor. Similar to DBB and AA1^T, chlorophenols such as 2,4-DCP, 2,6-DCP and 2,4,6-TCP were not dehalogenated by strain MSL71^T (Table 3.1). In contrast to strains DBB and AA1^T, strain MSL71^T was unable to debrominate 1,4-DBB and 4-BP. Hence, debromination of 2,4-DBP and 2,4,6-TBP was incomplete with 4-BP as the final product rather than phenol (Table 3.1). Moreover, strain MSL71^T was unable to deiodinate 2-IP and 4-IP, again in contrast to strains DBB and AA1^T (Fig. S3.7, Table 3.1).

Induction of *rdhA* genes during OHR by strain DBB

When strain DBB was grown with sulfate and 1,4-DBB with concomitant production of BB (Fig. 3.4A), its *rdhA1* gene showed significant up-regulation (60-fold) at 24 h, reached its highest level (120-fold) at 48 to 72 h, and then decreased (Fig. 3.4B). In contrast, no significant up-regulation of *rdhA2* or *rdhA3* was noted, suggesting that RdhA1 mediates 1,4-DBB debromination. Accordingly, RdhA1 was found in the proteome of the LSD growth condition but not in that of the LS condition (Table S3.4, Dataset S3.1 and S3.2). When strain DBB was grown with sulfate and 2,6-DBP, both *rdhA1* and *rdhA3* were significantly up-regulated and reached their highest level at 4 h (65- and 2000-fold, respectively, Fig. 3.4D). However, *rdhA3* was the dominant gene at 8 h (Fig. 3.4D), after which 2-BP was debrominated to phenol (Fig. 3.4C) indicating a role of RdhA3 in 2,6-DBP and 2-BP debromination by strain DBB. A previous transcriptional study of the *rdhA* genes in strain AA1^T during 2,6-DBP debromination also showed a similar induction of its *rdhA3* (Liu *et al.* 2017).

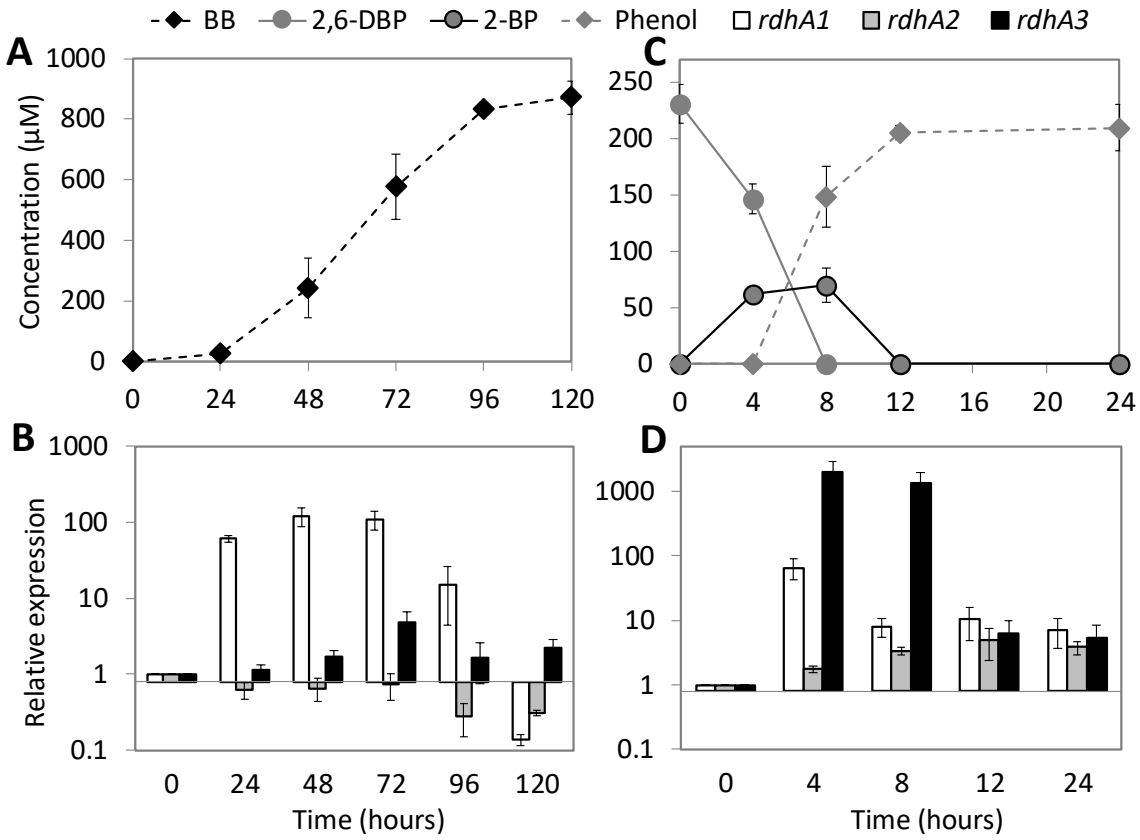

Fig. 3.4 Debromination of 1,4-DBB (A) and 2,6-DBP (C) by *D. spongiiphila* DBB and relative induction of its three *rdhA* genes during debromination of 1,4-DBB (B) and 2,6-DBP (D). Error bars in panels A and C indicate the standard deviation of two random cultures analyzed out of 10 replicates. The concentration of 1,4-DBB (> 0.1 mM) could not be accurately measured due to large amount of undissolved compound and hence was not plotted. Error bars in panels B and D indicate standard deviation of triplicate RT-qPCRs performed on samples withdrawn from duplicate cultures at each time point (n = 2 × 3).

Corrinoid biosynthesis in *Desulfoluna* strains

Most known RDases depend on corrinoid cofactors such as cyanocobalamin for dehalogenation activity (Schubert *et al.* 2018). Both strains DBB (this study) and AA1^T (Liu *et al.* 2017) were capable of OHR in the absence of externally added cobalamin. With one exception (*cbiJ*), the genomes of the *Desulfoluna* strains studied here harbor all genes necessary for *de novo* anaerobic corrinoid biosynthesis starting from glutamate (Table S3.5). The genes for cobalamin biosynthesis from precorrin-2 are arranged in one cluster (DBB_3730–3920, AA1_12810–12829, MSL71_49290–49480) including an ABC transporter (*btuCDF*) for cobalamin import (Fig. 3.5). Another small cobalamin-related gene cluster was detected in the *Desulfoluna* genomes (DBB_52170–52260, AA1_10815–10826, MSL71_44540–44630), which includes genes coding for the outer membrane corrinoid receptor BtuB and a second copy of the corrinoid-transporter BtuCDF plus another BtuF. Additionally, cobaltochelatase CbiK as well as a putative cobaltochelatase CobN are encoded in this gene cluster. The latter is usually involved only in the aerobic cobalamin biosynthesis pathway, and its function in *Desulfoluna* strains is unknown. Three of the proteins encoded by DBB_3730–3920 (Cbik: 3730, CbiL: 3790, CbiH: 3850) were detected in the proteome of cells grown under both the LS and LSD conditions (Table S3.4, Dataset S3.1). The abundance of the cobalamin biosynthesis proteins was not significantly different between LS and LSD conditions (Table S3.4, Dataset S3.1 and S3.2), except for the tetrapyrrole methylase CbiH encoded by DBB_3850 that was significantly more abundant in LSD cells (Table S3.4, Dataset S3.1). The detection of cobalamin biosynthesis proteins in the absence of 1,4-DBB in LS condition could be due to the synthesis of corrinoid-dependent enzymes in the absence of an organohalogen. Accordingly, three corrinoid-dependent methyltransferase genes (encoded by DBB_7090, 43520, 16050) were detected in the proteomes, which might be involved in methionine, methylamine or o-demethylation metabolism. This might also indicate a constitutive expression of the corresponding genes, in contrast to the organohalide-induced cobalamin biosynthesis in *Sulfurospirillum multivorans* (Goris *et al.* 2015).

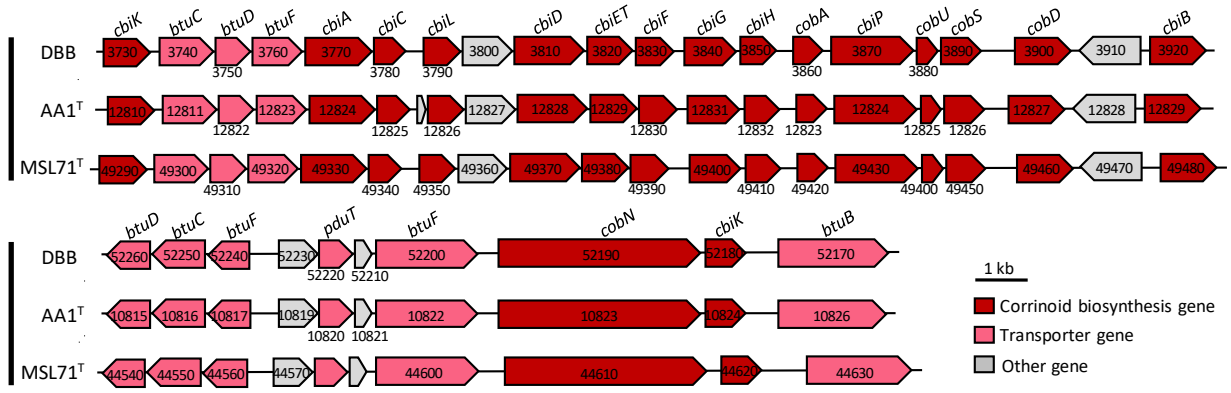

Fig. 3.5 Corrinoid biosynthesis and transporter gene clusters of *Desulfoluna* strains. Numbers indicate the locus tags of the respective genes. The corresponding enzymes encoded by the genes and their functions in corrinoid biosynthesis are indicated in Table S3.4.

Sulfur metabolism and impact of sulfate and sulfide on debromination by *Desulfoluna* strains

All three strains were capable of using sulfate, sulfite, and thiosulfate as the terminal electron acceptors (Table 3.1). Four sulfate permease genes are present in the genomes of the *Desulfoluna* strains (Table S3.6), and one of the sulfate permeases (DBB_22290) was detected in DBB cells grown under LS and LSD conditions (Table S3.4, Dataset S3.2). The genes involved in sulfate reduction, including those encoding sulfate adenylyltransferase (Sat), APS reductase (AprBA) and dissimilatory sulfite reductase (DsrAB), were identified in the genomes of all three strains (Table S3.6). The corresponding proteins were detected in DBB cells grown under both LS and LSD conditions (Fig. 3.6, Table S3.4) with AprBA, disulfite reductase (DsrMKJOP) and Sat among the most abundant proteins in both, soluble and membrane fractions (Dataset S3.1 and S3.2). Tetrathionate reductase encoding genes (*ttrA*) were found only in the genomes of strains DBB and AA1^T. Interestingly, thiosulfate reductase genes were not found in any of the three genomes, whereas all strains can use thiosulfate as the electron acceptor (Table 3.1). *Desulfitobacterium metallireducens* was also reported to reduce thiosulfate despite lacking a known thiosulfate reductase gene (Finneran *et al.* 2002, Kruse *et al.* 2017), suggesting the existence of a not-yet-identified gene encoding a thiosulfate reductase (Kruse *et al.* 2017). Possible alternatives are genes encoding rhodanese-like protein (RdlA) (Table S3.6) (Ravot *et al.* 2005) or the three-subunit, periplasmic molybdopterin oxidoreductase (Table S3.6), as a putative polysulfide reductase (Psr) (Burns and DiChristina 2009).

Sulfate and sulfide are known inhibitors of many OHRB (Townsend and Suflita 1997, Weatherill *et al.* 2018, Zanaroli *et al.* 2015). However, debromination of 2,6-DBP was not affected in *Desulfoluna* strains in the presence of up to 20 mM sulfate (Fig. S3.8B, D, F), and sulfate and 2,6-DBP were reduced concurrently (Fig. S3.8). This is similar to some other *Deltaproteobacteria*

(Liu and Häggblom 2018), but in contrast to *D. tiedjei* which preferentially performs sulfate reduction over OHR with concomitant down-regulation of *rdh* gene expression (Townsend and Suflita 1997). Moreover, sulfide, an RDase inhibitor in *D. tiedjei* (DeWeerd and Suflita 1990) and *Dehalococcoides mccartyi* strains (He *et al.* 2005, Mao *et al.* 2017), did not impact 2,6-DBP debromination by *Desulfoluna* strains at a concentration of 10 mM (Fig. S3.9A–F). However, debromination was delayed in the presence of 20 mM sulfide, and no debromination was noted in the presence of 30 mM sulfide (Fig. S3.9G–L). This high resistance to sulfide was not reported before for the known OHRB, and is also rare among sulfate-reducing bacteria (Caffrey and Voordouw 2010), and may confer an ecological advantage to these sulfate-reducing OHRB. Although hydrogen sulfide can be oxidized abiotically or serve as electron donor for sulfide-oxidizing microorganisms (Wasmund *et al.* 2017), naturally sustained and high concentrations of hydrogen sulfide are found in some marine environments (Tobler *et al.* 2016).

Electron transport chains of strain DBB

Two lactate dehydrogenases (LdhA-1/2, DBB_24880/24970) with HdrD-like putative iron-sulfur subunits (LdhB-1/2, DBB_24870/24960) were found in the proteome of DBB cells grown under LS and LSD conditions. Similar Ldhs were reported to be essential for the growth of *Desulfovibrio alaskensis* G20 with lactate and sulfate (Meyer *et al.* 2013). Similar to *D. alaskensis* G20 and *D. vulgaris* strain Hildenborough (Meyer *et al.* 2013, Vita *et al.* 2015), the two Ldhs were encoded by an organic acid oxidation gene cluster (DBB_24870–24970) including genes encoding lactate permease (DBB_24890), the Ldhs and pyruvate oxidoreductase (Por, DBB_24940). Based on previous studies with *D. vulgaris* Hildenborough (Keller and Wall 2011), the electron transport pathway in strain DBB with lactate and sulfate could take one of the following routes: the Ldh's either reduce menaquinone directly (Keller and Wall 2011), or transfer electrons via the HdrD-like subunit (Pereira *et al.* 2011) and DsrC (DBB_370, a high redox potential electron carrier with disulfide/dithiol (RSS/R(SH)2)) to QmoA (Flowers *et al.* 2018). The pyruvate produced by lactate oxidation is further oxidized by Por (DBB_310/24940), and the released electrons are carried/transferred by a flavodoxin (DBB_37290). From there, the electrons from the low-potential ferredoxin and the electrons from the high-potential (disulfide bond) DsrC could be confurcated to QmoABC, which reduces menaquinone (Fig. 3.6A, B). The electrons are then transferred from menaquinol to the APS reductase (AprBA, DBB_23880–890) which is, together with three other enzyme complexes (Sat, encoded by DBB_23930, DsrABD, DBB_25620–640, and DsrMKJOP, DBB_27290–330), responsible for the sulfate reduction cascade (Santos *et al.* 2015).

The electron transport chain from Ldh to menaquinones or QmoABC during OHR is likely shared with sulfate reduction. Electron transport from menaquinol ($E^{0'}$ = -75 mV) to the RDase ($E^{0'}$ (CoII/CoI) ≈ -360 mV) is thermodynamically unfavorable (Schubert *et al.* 2018), and the proteins involved to overcome this barrier have not been identified and most likely are not the same in

different organohalide-respiring bacterial genera. Based on the genomic and proteomic analyses of strain DBB, we identified several possible electron transfer proteins connecting the menaquinone pool and RdhA1. The first is the membrane-integral protein RdhC1 (encoded by DBB_38380, Fig. 3.3), a homolog of proteins previously proposed to function as transcriptional regulator for *rdhAB* gene expression in *Desulfitobacterium dehalogenans* (Smidt *et al.* 2000). However, a recent study on PceC from *Dehalobacter restrictus* proposed a possible role for RdhC in electron transfer from menaquinones to PceA via its exocytoplasmically-facing flavin mononucleotide (FMN) co-factor (Buttet *et al.* 2018). RdhC in *Desulfoluna* strains also showed the conserved FMN binding motif (in particular the fully conserved threonine residue) and two CX_3CP motifs predicted to have a role in electron transfer (Buttet *et al.* 2018) (Fig. S3.10). Moreover, the five transmembrane helices of RdhC in DBB were also conserved (Fig. S3.11), indicating a possible function of RdhC1 in electron transfer from menaquinones to RdhA1 (Fig. 3.6A). However, RdhC1 was not found in our proteomic analysis, probably due to tight interaction with the membrane.

A second link between menaquinol/QmoABC and RdhA1 could be the Fix complex homolog, an electron transfer flavoprotein complex found in nitrogen-fixing microorganisms such as *Azotobacter vinelandii* and *Rhodospirillum rubrum* (Edgren and Nordlund 2004, Ledbetter *et al.* 2017). The Fix complex is capable of using electron bifurcation to generate low-potential reducing equivalents for nitrogenase (Ledbetter *et al.* 2017). Strain DBB does not encode the minimum genes necessary for nitrogen fixation (Dos Santos *et al.* 2012). Hence, the Fix complex in DBB cells is likely linked to other cellular processes. Induction of the *fix* genes under OHR conditions was reported in other OHRB such as *Desulfitobacterium hafniense* TCE1 (Prat *et al.* 2011), and the corresponding Fix complex was suggested to provide low-redox-potential electrons for OHR. However, the obligate organohalide-respiring *Dehalobacter* spp., which are phylogenetically related to *Desulfitobacterium* spp., do not encode FixABC, questioning a general role of Fix complex in OHR (Türkowsky *et al.* 2018). In strain DBB, the abundance of FixABC (encoded by DBB_25970–990) was not higher in the cells grown under LSD as opposed to LS condition, but FixAB were among the most abundant 10% proteins in the soluble fraction (Dataset S3.1), indicating a potential role in electron transfer in both sulfate reduction and OHR. In this scenario, FixABC accepts two electrons from menaquinol, subsequently bifurcating them to unidentified high- and low-potential electron acceptors (Fig. 3.6B). The low-potential electron acceptor may also serve as an electron carrier that transfers electrons from cytoplasm-facing FixABC to the exoplasm-facing RdhA1 via an as-yet-unidentified electron carrier across the membrane (Kruse *et al.* 2015) (Fig. 3.6B).

A third scenario is the involvement of QmoABC- and QrcABCD-mediated reverse electron transport (Fig. 3.6C), similar to the electron transport system of *D. alaskensis* G20 cultivated in syntrophic interaction with *Methanococcus maripaludis* (Meyer *et al.* 2013). The electron transport from menaquinol to the periplasmic hydrogenase or formate dehydrogenase in strain G20 also

needs to overcome an energy barrier similar to that of OHR (redox potential of H_2/H^+ and formate/CO_2 are −414 mV and −432 mV, respectively) (Meyer *et al.* 2013). In this scenario, lactate is oxidized to pyruvate as described above, transferring electrons to a thiol-disulfide redox pair. Pyruvate is oxidized by Por and the electrons are accepted by the flavodoxin. QmoABC then confurcates electrons from the low-potential ferredoxin and the high-potential thiol-disulfide redox pair to drive reduction of menaquinones. Electrons are transferred from menaquinol to RdhA1 via QrcABCD by reverse electron transport (Fig. 3.6C). The energy required for reverse electron transport is likely derived from the proton motive force mediated by QrcABCD (Duarte *et al.* 2018). In this scenario, QmoABC plays a key role in the metabolism of strain DBB as a link between sulfate reduction and OHR. This electron transport pathway provides a possible explanation for the increased 1,4-DBB debromination rate by DBB when sulfate is concurrently present (Fig. 3.1E, Fig. S3.1B). Hence, sulfate reduction may stimulate the electron confurcation process that is also used for OHR. Moreover, sulfate reduction can generate the proton motive force required for the reverse electron transport from QmoABC to RdhA1. Qmo and Qrc complexes are frequently found in sulfate-reducing *Deltaproteobacteria* and were proposed to be involved in energy conservation (Pereira *et al.* 2011, Venceslau *et al.* 2010, Zane *et al.* 2010). However, biochemical studies with sulfate-reducing OHRB are necessary to further corroborate such a reverse electron flow and the intricate relationship of electron transfer in sulfate reduction and OHR.

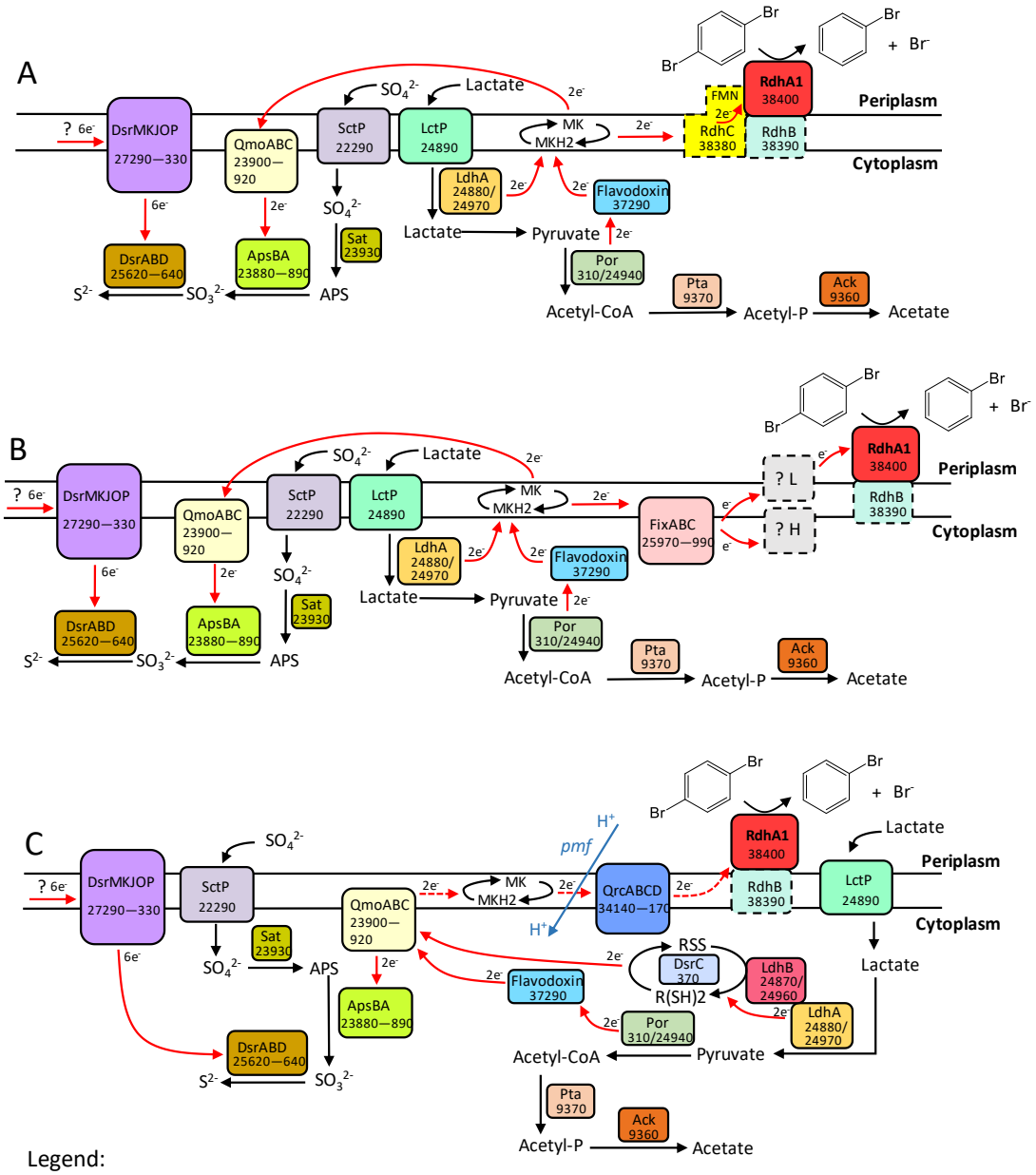

Legend:

Ack: acetate kinase
ApsBA: APS reductase
DsrABD: dissimilatory sulfite reductase
DsrC: Dissimilatorysulfitereductase gamma subunit
DsrMKJOP: electron transport complex function with DsrABD
FixABC: electron transfer flavoproteins
H: high potential electron acceptor
L: low potential electron acceptor
LdhA: lactate dehydrogenases
LdhB: HdrD-like putative subunits for LdhA
LctP: lactate permease
MK: menaquinone pool
Por: pyruvate oxidoreductase
Pta: phosphate acetyltransferase
pmf: proton motive force
QmoABC: electron transport complex
QrcABCD: electron transport complex
RdhA1: reductive dehalogenase catalytic subunit
RdhB: putative membrane anchor protein for RdhA1
RdhC: putative electron transport protein for RdhA1
R(SH)2 and RSS, reduced and oxidized forms of thiol-disulfide redox pair
SctP: sulfate permease
Sat: sulfate adenylyltransferase
?: unknown processes or proteins

Fig. 3.6 Proposed electron transport pathways with OHR mediated by RdhC (A), Fix complex (B), Qmo/Qrc complexes (C) in *D. spongiiphila* DBB grown on lactate and sulfate (LS) and lactate, sulfate and 1,4-DBB (LSD). Corresponding gene locus tags are given for each protein. Log protein abundance ratios between LSD and LS grown cells are indicated next to the gene locus tag. Proteins shown in dashed line square were not detected under the tested conditions. Probable electron flow path is shown in red arrows, and the dashed red arrows indicate reverse electron transport.

Potential oxygen defense in *Desulfoluna* strains

Sulfate reducers, which have been assumed to be strictly anaerobic bacteria, not only survive oxygen exposure but also can utilize it as an electron acceptor (Dolla *et al.* 2006, Fournier *et al.* 2003). However, the response of organohalide-respiring sulfate reducers to oxygen exposure is not known. Most of the described OHRB are strict anaerobes isolated from anoxic and usually organic matter-rich subsurface environments (Atashgahi *et al.* 2016). In contrast, strain DBB was isolated from marine intertidal sediment mainly composed of shore sand (Fig. 3.1A), where regular exposure to oxic seawater or air can be envisaged. The genomes of the *Desulfoluna* strains studied here harbor genes encoding enzymes for oxygen reduction and reactive oxygen species (ROS) detoxification (Table S3.7). Particularly, the presence of a cytochrome *c* oxidase is intriguing and may indicate the potential for oxygen respiration. Accordingly, in the presence of 2% oxygen in the headspace of DBB cultures, the redox indicator resazurin in the medium turned from pink to colorless within two hours, indicating consumption/reduction of oxygen by strain DBB. Growth of strain DBB on lactate and sulfate was retarded in the presence of 2% oxygen (Fig. S3.12C). However, in both the presence (Fig. S3.12C) and absence of sulfate (Fig. S3.12D), slower but complete debromination of 2,6-DBP to phenol was achieved with 2% oxygen in the headspace. Neither growth nor 2,6-DBP debromination was observed with an initial oxygen concentration of 5% in the headspace (Fig. S3.12E, F). Such resistance of marine OHRB to oxygen may enable them to occupy niches close to halogenating organisms/enzymes that nearly all use oxygen or peroxides as reactants (Field 2016). For instance, the marine sponge *A. aerophoba* from which *D. spongiiphila* AA1^T was isolated (Ahn *et al.* 2009) harbors bacteria with a variety of $FADH_2$-dependent halogenases (Bayer *et al.* 2013), and produces a variety of brominated secondary metabolites (Turon *et al.* 2000). Testing survival and OHR of *Desulfoluna* strains under continuous oxygen exposure and studying the mechanisms of oxygen defense as studied in *Sulfurospirillum multivorans* (Gadkari *et al.* 2018) are necessary to further unravel oxygen resistance/metabolism mechanisms in *Desulfoluna* strains.

Conclusions

Widespread environmental contamination with organohalogen compounds and their harmful impacts to human and environmental health has been the driver of chasing OHRB since the 1970s. In addition, the environment itself is an ample and ancient source of natural organohalogens, and accumulating evidence shows widespread occurrence of *rdhA* in marine environments (Atashgahi *et al.* 2018a). The previous isolation and description of strain AA1^T from a marine sponge, the isolation of strain DBB from intertidal sediment samples, and verification of the OHR potential of strain MSL71^T in this study indicate niche specialization of the members of the genus *Desulfoluna* as chemoorganotrophic facultative OHRB in marine environments rich in sulfate and organohalogens. As such, *de novo* corrinoid biosynthesis, resistance to sulfate, sulfide

and oxygen, versatility in using electron donors, and the capacity for concurrent sulfate and organohalogen respiration confer an advantage to *Desulfoluna* strains in marine environments. Interestingly, approximately 10% of the sequenced deltaproteobacterial genomes, that have mostly been obtained from marine environments, contain one or multiple *rdh* genes (Liu and Häggblom 2018, Sanford *et al.* 2016), and OHR metabolism was experimentally verified in three strains not previously known as OHRB (Liu and Häggblom 2018). These findings reinforce an important ecological role of sulfate-reducing organohalide-respiring *Deltaproteobacteria* in sulfur, halogen and carbon cycling in a range of marine environments.

Acknowledgements

We thank Johanna Gutleben and Maryam Chaib de Mares for sediment sampling, W. Irene C. Rijpstra for fatty acid analysis, and Andreas Marquardt (Proteomics Centre of the University of Konstanz) for proteomic analyses. We acknowledge the China Scholarship Council (CSC) for the support to PP and YL. The authors thank BE-BASIC funds (grants F07.001.05 and F08.004.01) from the Dutch Ministry of Economic Affairs, ERC grant (project 323009), the Gravitation grant (project 024.002.002) of the Netherlands Ministry of Education, Culture and Science and the Netherlands Science Foundation (NWO), and National Natural Science Foundation of China (project No.51709100) for funding.

Supplementary Information

Enrichment, isolation and cultivation of strain DBB

The sediment sampling bottles were filled with seawater to leave no headspace. For preparation of microcosms, sediment (5 g) was transferred into 120 ml bottles containing 50 ml of anoxic medium (Monserrate and Häggblom 1997) and N_2/CO_2 (80 : 20%, 140 kPa) as the headspace. Vitamins and trace elements were added as described previously (Stams *et al.* 1993) except that cyanocobalamin was omitted. Lactate (5 mM) and 1,4-dibromobenzene (1,4-DBB, 50 µM) were used as the electron donor and acceptor, respectively. 1,4-DBB was added from a 10 mM stock solution dissolved in acetone. The bottles were sealed with viton stoppers and aluminium crimp caps and incubated statically in the dark at 25°C. After debromination of three spikes of 1,4-DBB, sediment-free cultures were obtained by transferring the suspensions of the enrichment culture (10% v/v) to fresh medium using the same growth condition as described above. After ten successive transfers of the sediment-free cultures, a dilution series from 10^1 to 10^7-fold was performed. The most diluted culture showing 1,4-DBB debromination (10^7-fold) was then serially diluted from 10^1- to 10^3-fold in 25 ml roll tubes containing 10 ml medium and 0.8% low-melting point agarose (Sigma-Aldrich) and incubated in the dark at 25°C. Individual colonies were randomly picked and transferred into liquid medium to check for 1,4-DBB debromination. A culture showing debromination activity was re-isolated in roll tubes as described above to ensure the purity.

The optimum NaCl concentration for growth of strain DBB was determined in the range from 10 to 30 g/L. Using the optimal NaCl concentration (20 g/L), the following halogenated aromatic compounds were tested as electron acceptors for strain DBB with lactate (5 mM) as the electron donor and carbon source: 1,2-dibromobenzene (1,2-DBB), 1,3-dibromobenzene (1,3-DBB), 1,2,4-tribromobenzene (1,2,4-TBB), 2-bromophenol (2-BP), 4-bromophenol (4-BP), 2,4-dibromophenol (2,4-DBP), 2,6-dibromophenol (2,6-DBP), 2,4,6-tribromophenol (2,4,6-TBP), 2-iodophenol (2-IP), 4-iodophenol (4-IP), 1,2-dichlorobenzene (1,2-DCB), 1,3-dichlorobenzene (1,3-DCB), 1,4-dichlorobenzene (1,4-DCB), 1,2,4-trichlorobenzene (1,2,4-TCB), 2,4-dichlorophenol (2,4-DCP), 2,6-dichlorophenol (2,6-DCP) and 2,4,6-trichlorophenol (2,4,6-TCP). Brominated and chlorinated benzenes, 2,4,6-TBP and 2,4,6-TCP were added from 10 mM stock solutions dissolved in acetone to nominal concentrations of 100 µM in the medium. The remaining di- and mono-brominated phenols were added from 10 mM stock solutions in 0.1 N NaOH to nominal concentrations of 50−100 µM. Sulfate, sulfite and thiosulfate (5 mM) were tested as electron acceptors with 10 mM lactate as the electron donor. To test the utilization of electron donors, acetate, propionate, fumarate, malate, butyrate, lactate, pyruvate, succinate, glucose and citrate were added separately at 10 mM to the medium containing 10 mM sulfate. Utilization of hydrogen (5 mM) and formate (5 mM) as the electron donors for debromination of 1,4-DBB (100 µM) was tested in presence of acetate (5 mM) as the carbon source. To study the effect of sulfate and sulfide on debromination,

sulfate (10−20 mM) or sulfide (1−30 mM) together with lactate (20−40 mM) were added to the medium containing 100 µM of 1,4-DBB or 2,6-DBP. To test the impact of oxygen on debromination, strain DBB was grown in medium without Na_2S as the reducing agent, in presence or absence of sulfate (10 mM). The medium contained 20 mM lactate, 100 µM 2,6-DBP and 0%, 2% or 5% oxygen in the headspace.

Cellular fatty acids analysis

The cultures were harvested at the early stationary growth phase by centrifugation at 4700 × *g* for 15 min at 4°C. Cellular fatty acids were analysed by acid hydrolysis of total cell material following a method previously described (Damsté *et al.* 2011). The fatty acids were identified by analysis with gas chromatography-mass spectrometry before and after derivatisation of double bonds with dimethyl disulphide to enable localization of the double bond position (Damsté *et al.* 2011).

RT-qPCR assays

Primers for amplification of the three *rdhA* genes in strain DBB were designed using the NCBI online primer design tool (http://www.ncbi.nlm.nih.gov/tools/primer-blast/) (Table S3.1). In order to prepare standards for the qPCR assays, the *rdhA* genes were PCR amplified using the following program: 95°C for 5 min, followed by 30 cycles of 95°C for 30 s, 55°C for 30 s and 72°C for 30 s, followed by a final extension at 72°C for 10 min. The *rdhA* genes were then cloned into pGEM®-T Easy Vector (Promega, WI, USA) and introduced into *E. coli* JM109 competent cells (Promega, WI, USA). Plasmid purification and preparation of the dilution series of the RT-qPCR standards (from 10^1 to 10^8 copies/µl) were done as described earlier (Peng *et al.* 2017). RT-qPCRs were performed using the iQ SYBR Green supermix (Bio-Rad, CA, USA). The RT-qPCR program was: 95°C for 10 min, followed by 40 cycles of 95°C for 15 s, 60°C for 30 s and 72°C for 30 s. Melting curves were measured from 65°C to 95°C with increments of 0.5°C and 10 s at each step. Transcription of the *rdhA* genes was determined using cDNA as the template. The transcript levels were calculated by relative quantification using the $2^{-\Delta\Delta Cq}$ method with the 16S rRNA gene as the reference gene (Kirk *et al.* 2014, Pfaffl 2001). Gene expression data was normalized to values observed at the 0 h time point, at which 1,4-DBB or 2,6-DBP were initially amended (Kirk *et al.* 2014). A relative expression difference higher than 10-fold was arbitrarily set as representing significant induction (Bisaillon *et al.* 2011).

Protein extraction and proteomic analysis

Protein was extracted from 100 ml culture of strain DBB grown with lactate (20 mM)/sulfate (10 mM) and lactate (20 mM)/sulfate (10 mM)/1,4-DBB (100 µM); triplicate samples were prepared for each condition. Cells were collected by centrifugation at 4500 × *g* for 20 min at 4°C. The cells

were then re-suspended in 1 ml 100 mM Tris-HCl buffer (pH 7.5) containing 10 µl protease inhibitor (Halt Protease Inhibitor Cocktail; Thermo Fisher Scientific, Rockford, USA). Cells were lysed by sonication using a Branson sonifier (Branson, CT, USA) equipped with a 3 mm tip by six pulses of 30 s with 30 s rest in between of each pulse. Cell debris was removed by centrifugation at 10,000 *g* for 10 min at 4°C. The protein concentration of the cell-free extracts (CFE) was determined using the Bradford assay (Bradford 1976). The total-proteomics samples were prepared and the analyses were done as described by Burrichter et al. (Burrichter *et al.* 2018). Total protein (200 µg) in CFE was purified through SDS-PAGE until the proteins had entered the stacking gel (without any separation); the Coomassie-stained total-protein bands were excised and then subjected to peptide fingerprinting-mass spectrometry (see below). For analysis of proteins associated to the membrane, the membrane fragments in the CFE were separated by ultracentrifugation at 104,000 × *g* for 35 min at 4°C; the membrane pellet was solubilized in SDS-PAGE loading dye and the proteins were also purified by SDS-PAGE and the Coomassie-stained total-protein bands were excised, as described above. The total-protein bands excised from SDS-PAGE gels were subjected to peptide fingerprinting-mass spectrometry at the Proteomics Facility of the University of Konstanz (www.proteomics-facility.uni-konstanz.de) (Burrichter *et al.* 2018). Each sample was analyzed twice on a Orbitrap Fusion with EASY-nLC 1200 (Thermo Fisher Scientific) and tandem mass spectra were searched against an appropriate protein database of strain DBB using Mascot (Matrix Science) and Proteome Discoverer V1.3 (Thermo Fisher Scientific) with “Trypsin” enzyme cleavage, static cysteine alkylation by chloroacetamide, and variable methionine oxidation (Burrichter *et al.* 2018).

Analytical methods

The column temperature program of the GC-FID was: 40°C hold for 2 min, followed by an increase of 6°C min^{-1} to 100°C and hold for 2 min, followed by further increase at 10°C min^{-1} to 225°C and hold for 2 min. The program for benzene measurement was as described earlier (Lu *et al.* 2017). The wavelength of the UV detector of the HPLCs was 210 nm. The mobile phases for the Thermo Scientific Accela HPLC System were 0.1% formic acid in water (eluent A) and 0.1% formic acid in acetonitrile (eluent B). The mobile phase for the ThermoFisher Scientific SpectraSYSTEM™ HPLC was 0.01 N H_2SO_4. Halogenated phenols and phenol were analyzed using a three-step gradient profile consisting of: i) 90% eluent A and 10% eluent B for 2 min, ii) 90−20% eluent A and 10−80% eluent B for 14 min and hold at 20% eluent A and 80% eluent B for 3 min, iii) followed by 20−90% eluent A and 80−10% eluent B for 1 min. The ions were analyzed using a three-step gradient profile consisting of 1 mM KOH for 1 min, 1−40 mM KOH for 14 min and hold at 40 mM KOH for 4 min, followed by 40−1 mM KOH for 4.5 min.

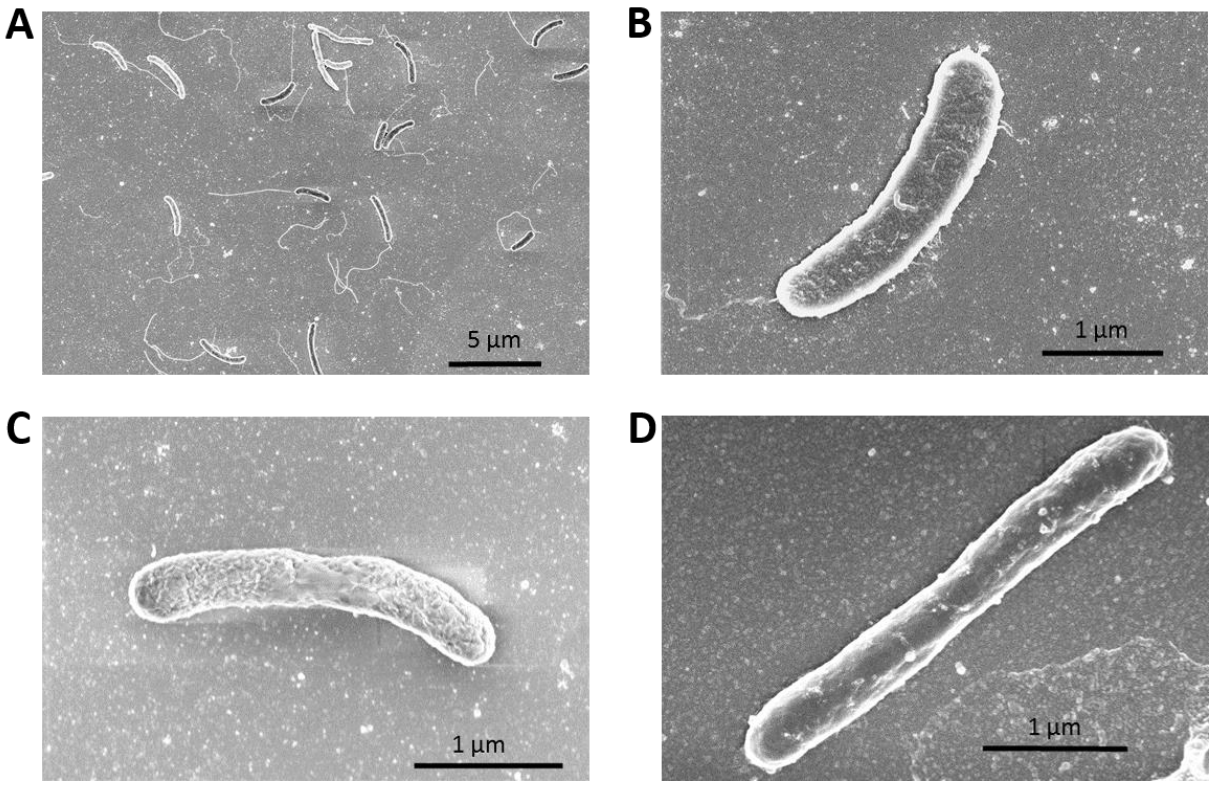

Fig. S3.1 Scanning electron micrograph of *D. spongiiphila* DBB (A and B), *D. spongiiphila* AA1^T (C) and *D. butyratoxydans* MSL71^T (D).

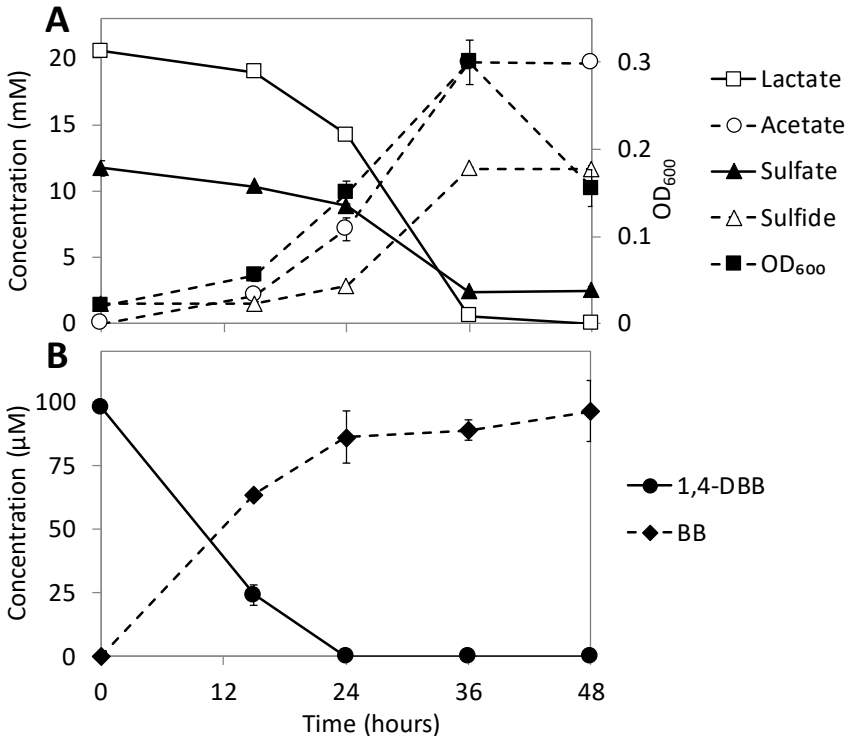

Fig. S3.2 Concurrent 1,4-DBB debromination and sulfate reduction by strain DBB with lactate as the electron donor. Points and error bars represent the average and standard deviation of samples taken from duplicate cultures.

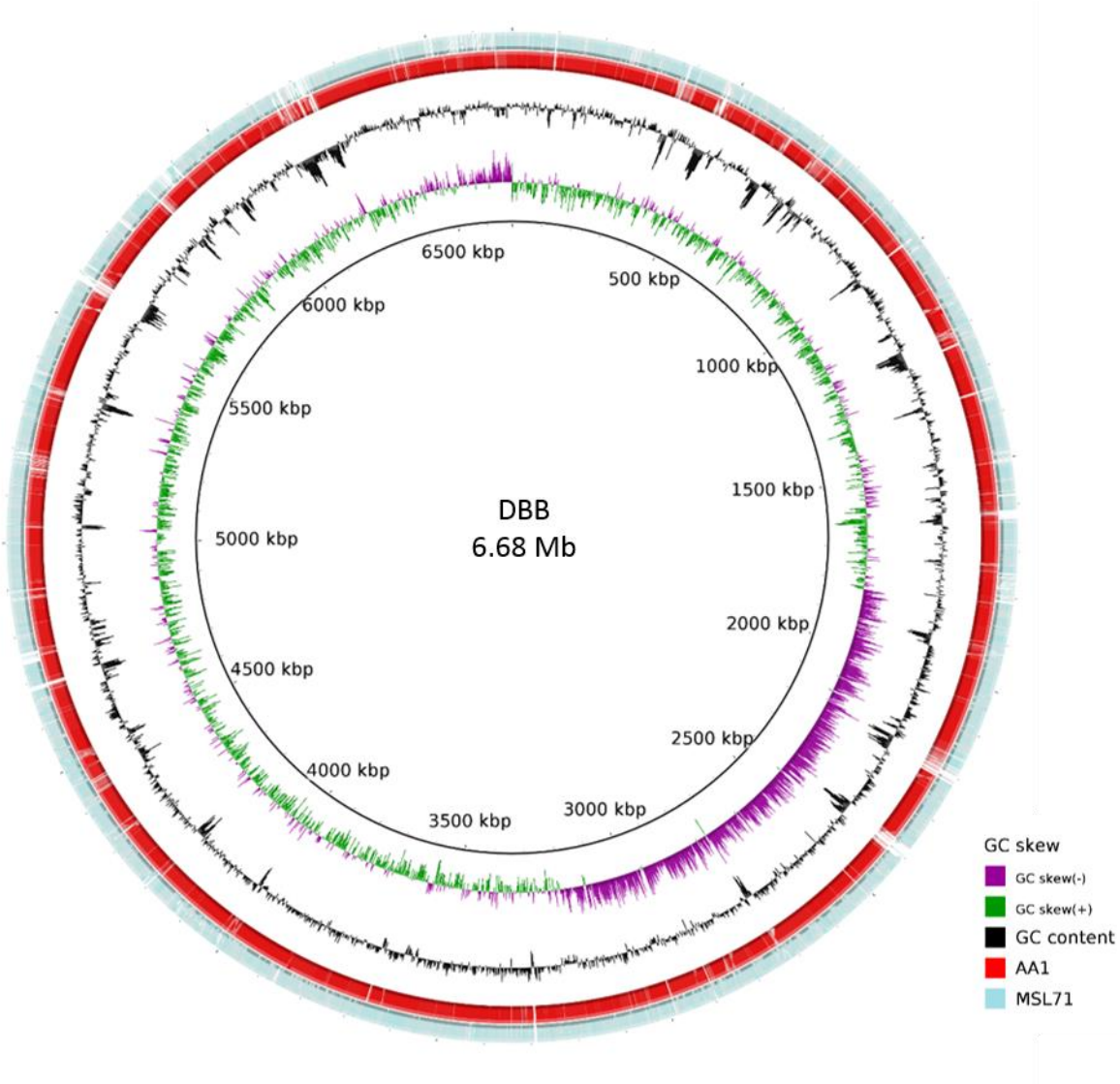

Fig. S3.3 Circular representation of the genome sequence of *D. spongiiphila* DBB in comparison with the genomes of *D. spongiiphila* AA1^{T} and *D. butyratoxydans* MSL71^{T}.

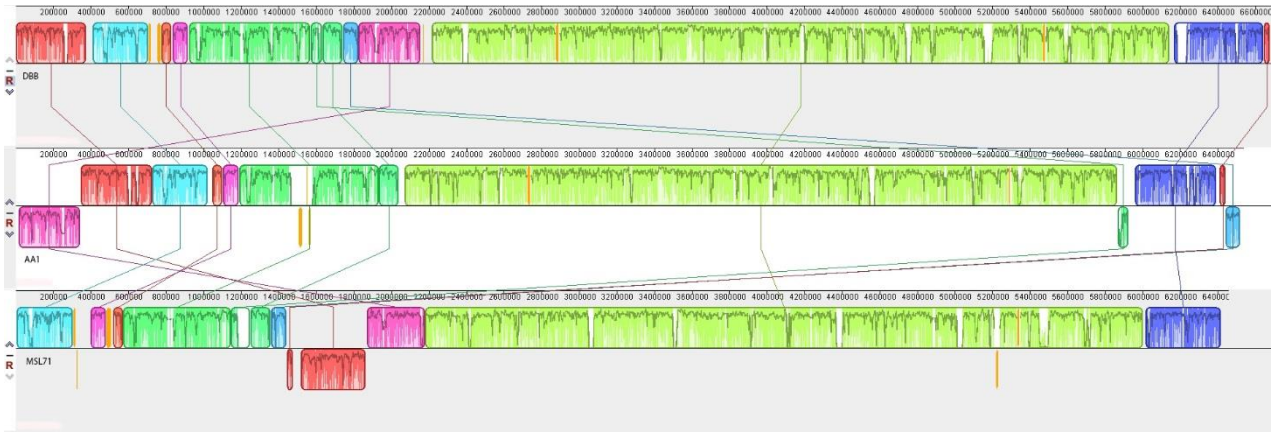

Fig. S3.4 Whole genome alignment of *D. spongiiphila* DBB (Top), *D. spongiiphila* AA1^T (middle) and *D. butyratoxydans* MSL71^T (bottom). The genome of strain DBB was used as reference for global alignment using progressive MAUVE (Darling *et al.* 2010). The locally collinear blocks (LCBs) that were identified in the genomes were outlined in frame. Conserved and highly related regions are coloured, and low-identity unique regions are in white (colorless). LCBs below the mid-line in *D. spongiiphila* AA1^T and *D. butyratoxydans* MSL71^T are inverted relative to *D. spongiiphila* DBB.

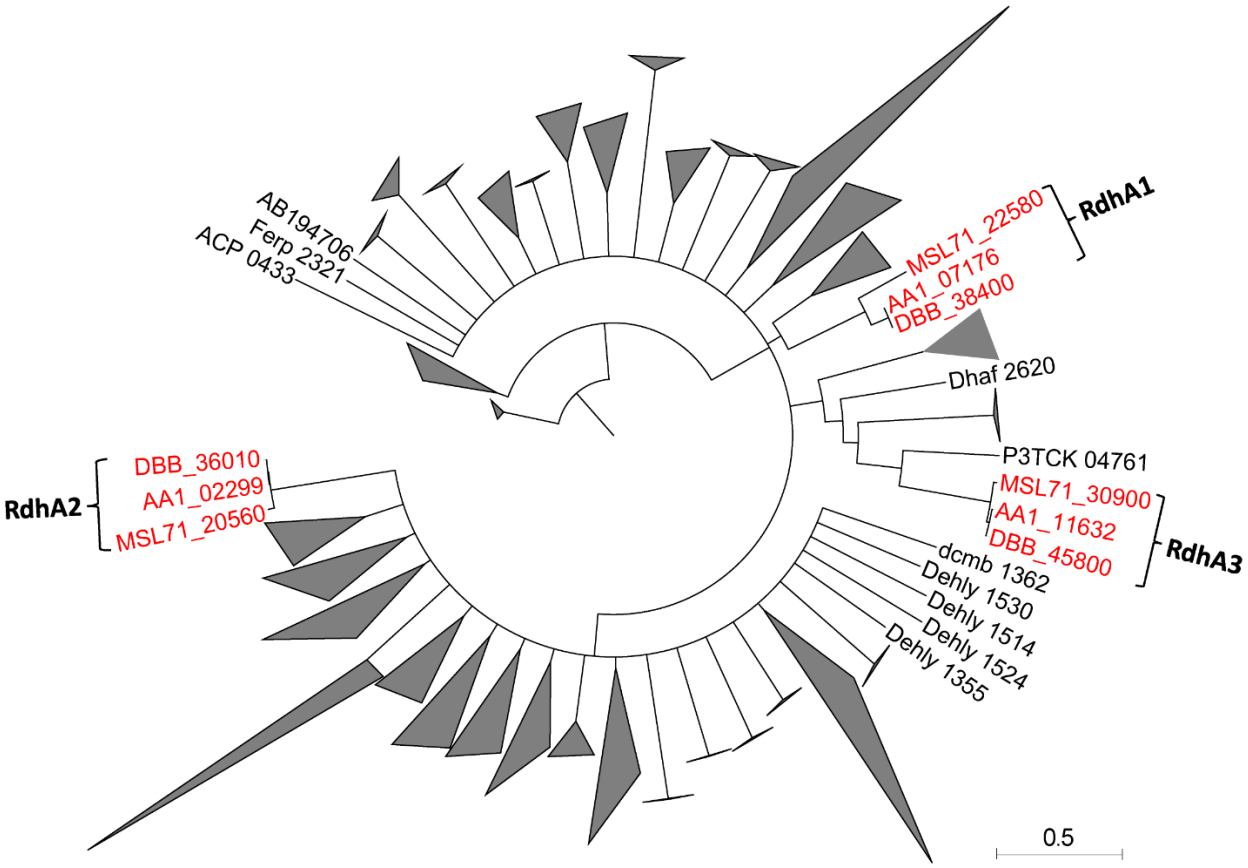

Fig. S3.5 Phylogenetic analysis of the RdhAs of *Desulfoluna* strains and 548 RdhAs reported previously (Hug *et al.* 2013). The RdhA sequences were obtained from the public link: https://drive.google.com/drive/folders/0BwCzK8wzlz8ON1o2Z3FTbHFPYXc. The multiple sequence alignment was processed using Geneious software with the MAFFT algorithm, and the phylogenetic tree was constructed using the same software with default settings. Further polishing of the phylogenetic tree was performed on the Interactive Tree of Life web browser (http://itol.embl.de/) (Letunic and Bork 2011). The RdhAs of *Desulfoluna* strains are shown in red font.

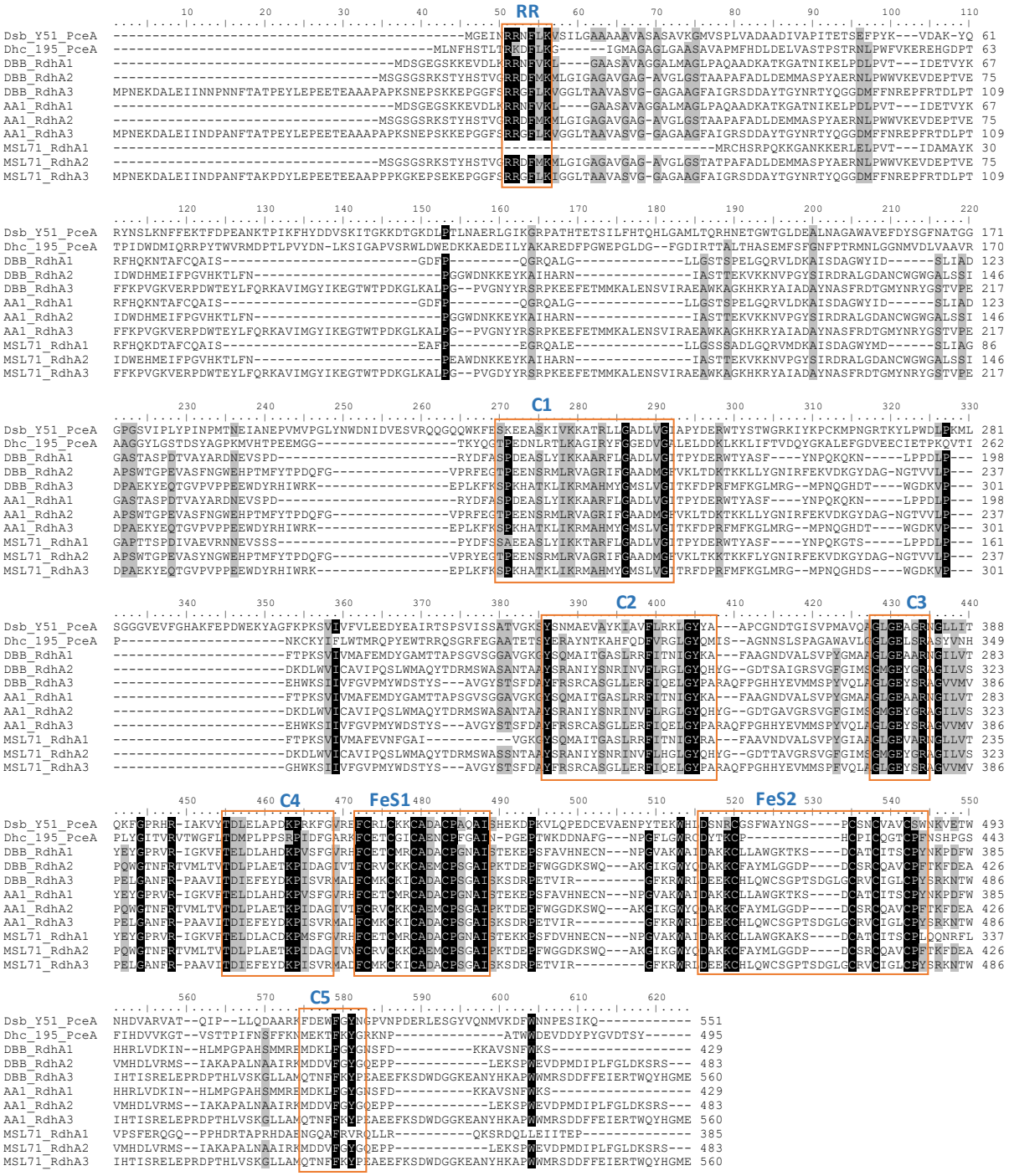

Fig. S3.6 Multiple-sequence alignment of the RdhAs from *D. spongiiphila* DBB, *D. spongiiphila* AA1^T and *D. butyratoxydans* MSL71^T and two functionally characterized RdhAs from *Desulfitobacterium hafniense* Y51, and *Dehalococcoides mccartyi* strain 195. The conserved sequence motifs (RR, C1−C5, FeS1, and FeS2) are enclosed within orange boxes. The selected RdhAs (GenBank accession number or locus number) and corresponding bacteria are: Dsb_Y51_PceA: *D. hafniense* Y51, BAC00915. Dhc_195_PceA: *D. mccartyi* 195, Q3Z9N3. DBB_3755: *D. spongiiphila* DBB. DBB_3984: *D. spongiiphila* DBB. DBB_4749: *D. spongiiphila* DBB. AA1_02299: *D. spongiiphila* AA1^T. AA1_07176: *D. spongiiphila* AA1^T. DBB_11632: *D. spongiiphila* AA1^T. MSL71_1800: *D. butyratoxydans* MSL71^T. MSL71_2003: *D. butyratoxydans* MSL71^T. MSL71_4258: *D. butyratoxydans* MSL71^T

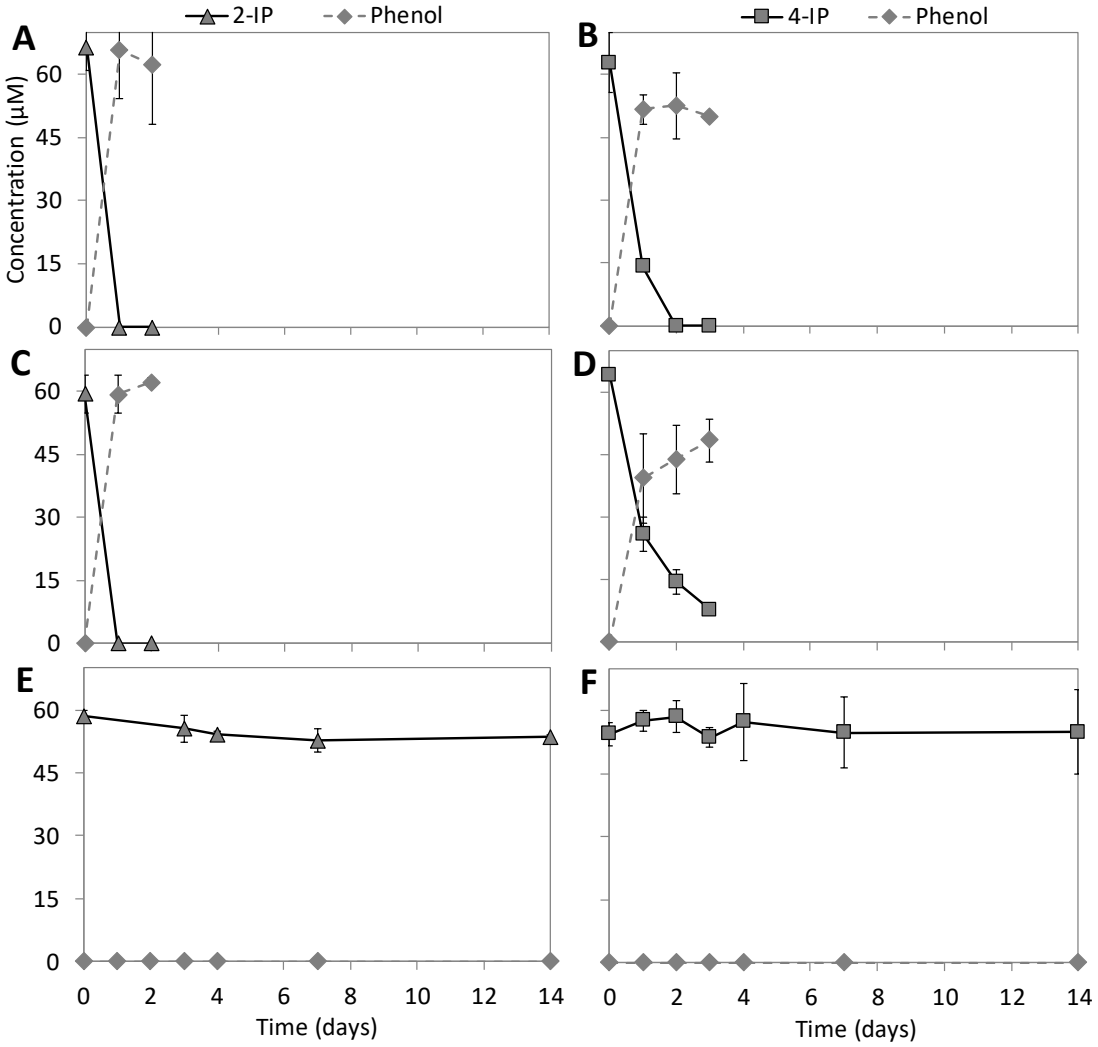

Fig. S3.7 Deiodination of 2-IP and 4-IP by *D. spongiiphila* DBB (A, B), *D. spongiiphila* AA1^T (C, D) and *D. butyratoxydans* MSL71^T (E, F) with lactate (5 mM) as the electron donor. Points and error bars represent the average and standard deviation of samples taken from duplicate cultures.

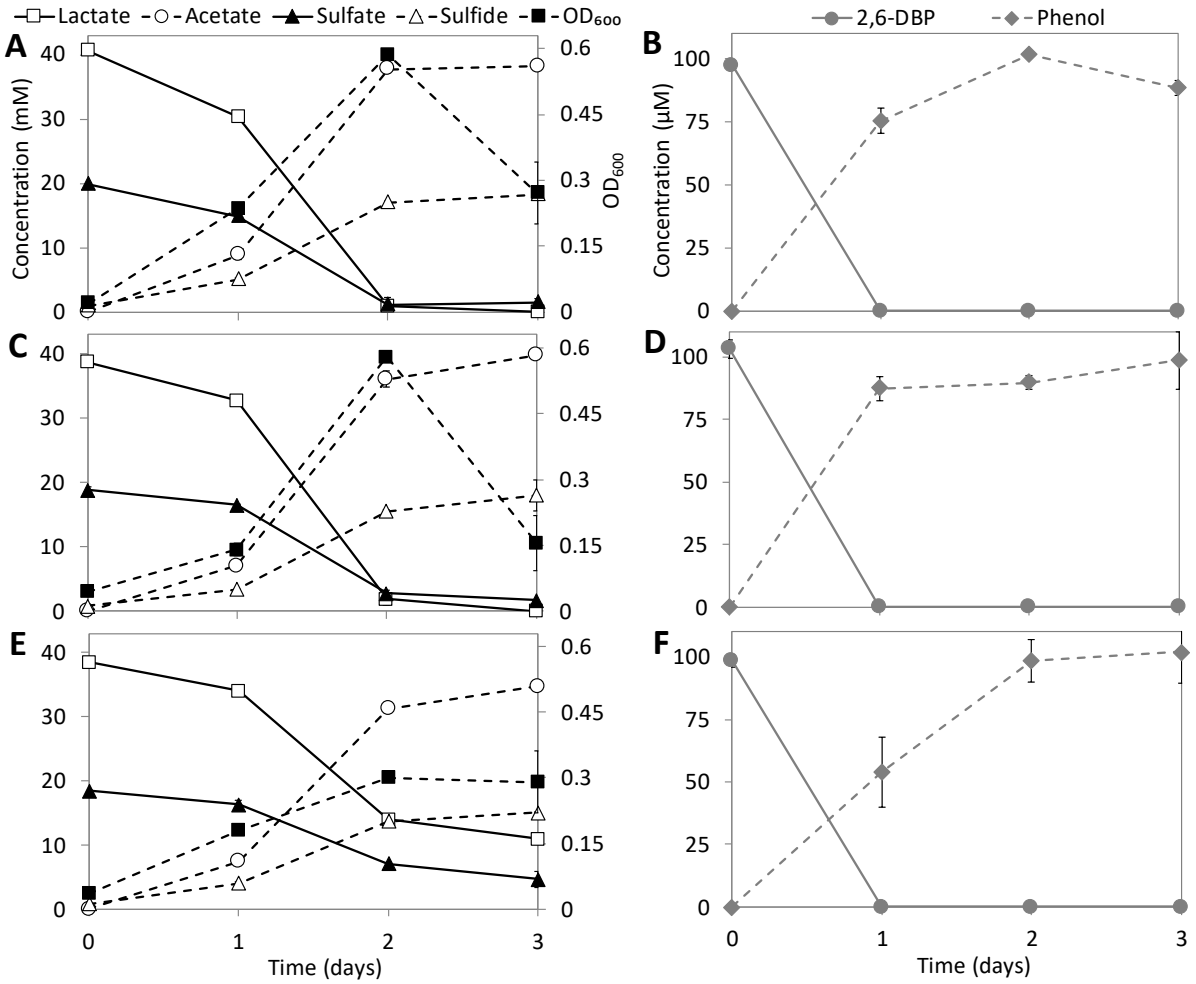

Fig. S3.8 Concurrent debromination of 2,6-DBP (100 µM) and sulfate (20 mM) reduction by *D. spongiiphila* DBB (A, B), *D. spongiiphila* AA1^T (C, D) and *D. butyratoxydans* MSL71^T (E, F) with lactate (40 mM) as the electron donor. Points and error bars represent the average and standard deviation of samples taken from duplicate cultures.

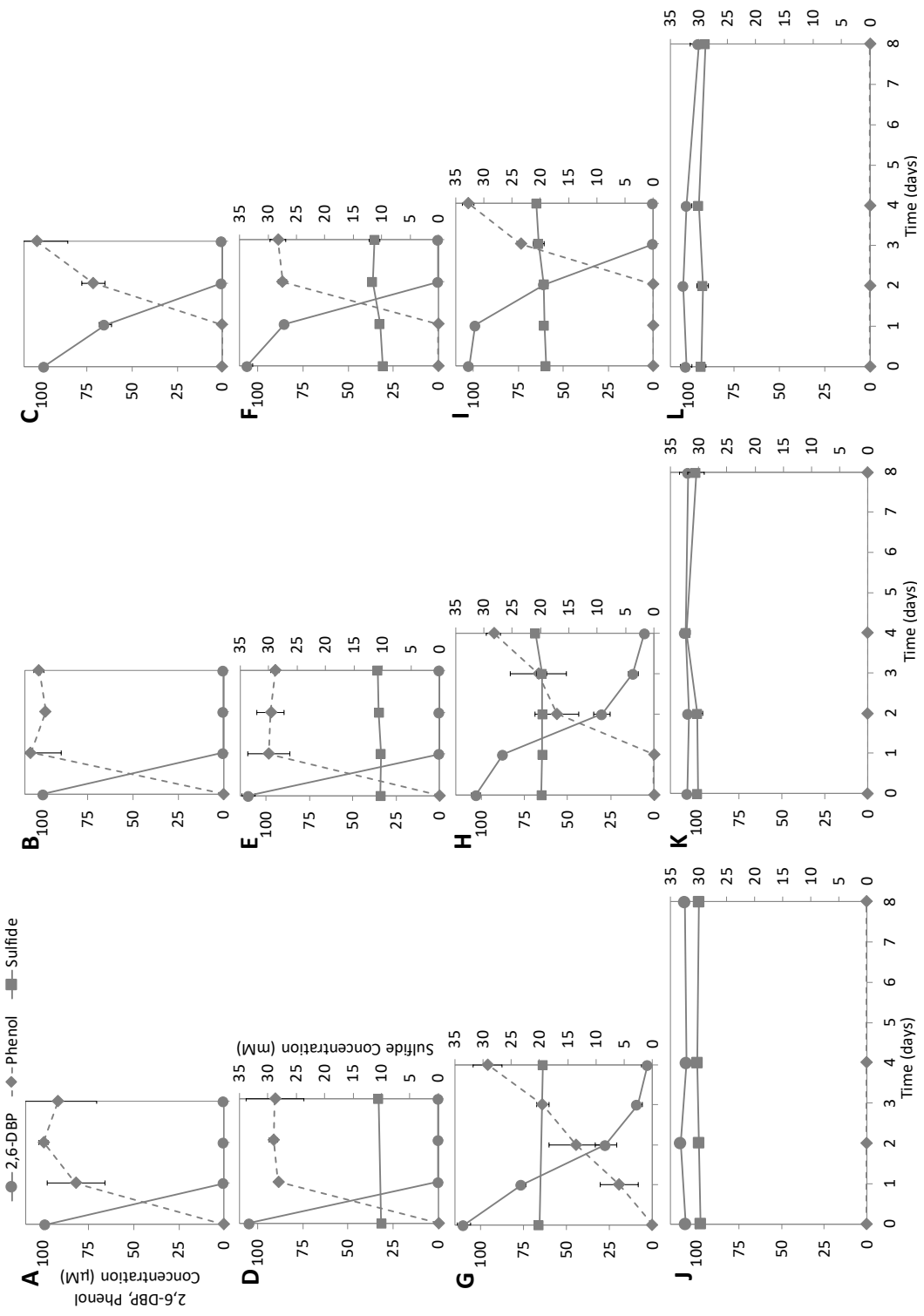

Fig. S3.9 Debromination of 2,6-DBP by *D. spongiiphila* DBB (A, D, G, J), *D. spongiiphila* AA1^T (B, E, H, K) and *D. butyratoxydans* MSL71^T (C, F, I, L) in presence of 1 (A, B, C), 10 (D, E, F), 20 (G, H, I) and 30 mM (J, K, L) sulfide. Points and error bars represent the average and standard deviation of samples taken from duplicate cultures.

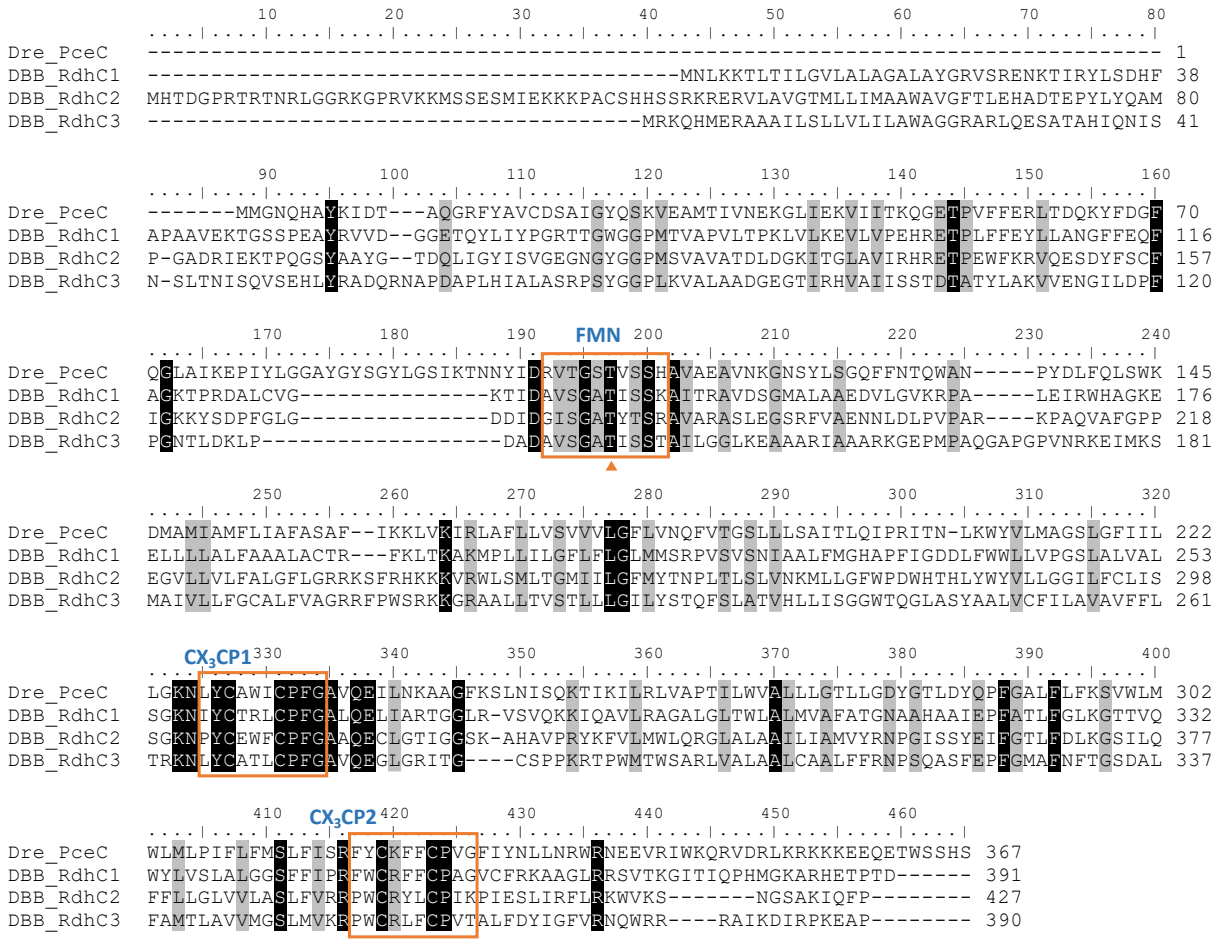

Fig. S3.10 Multiple-sequence alignment of the RdhCs of *Desulfoluna spongiiphila* DBB and *Dehalobacter restrictus* (Dre) (GenBank accession number: CAG70347.1). The conserved FMN binding motifs and two CX_3CP motifs are enclosed within orange boxes. The conserved threonine residue predicted to covalently bind to FMN is indicated with an orange triangle.

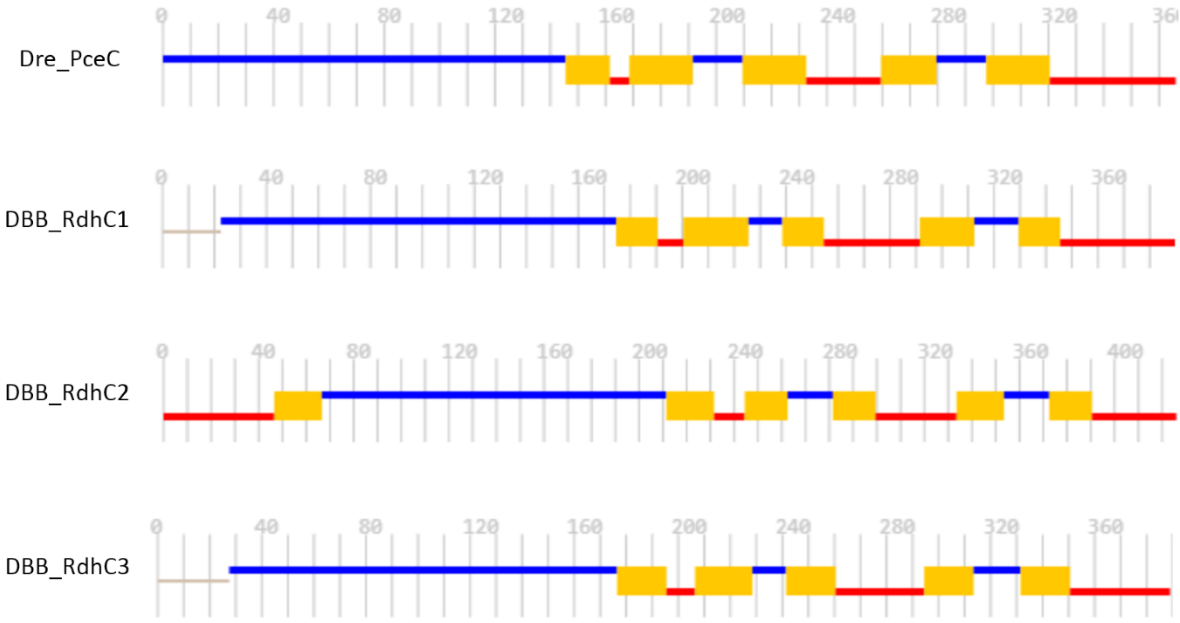

Fig. S3.11 Topology analysis and comparison of the RdhCs in *D. spongiiphila* DBB and PceC of *Dehalobacter restrictus*. The topology was predicted using CCTOP (Dobson *et al.* 2015). Blue lines indicate outside/extra-cytosolic regions. Red lines indicate inside/cytosolic regions. Gray lines indicate regions where topology is not predicted. Yellow rectangles indicate transmembrane regions.

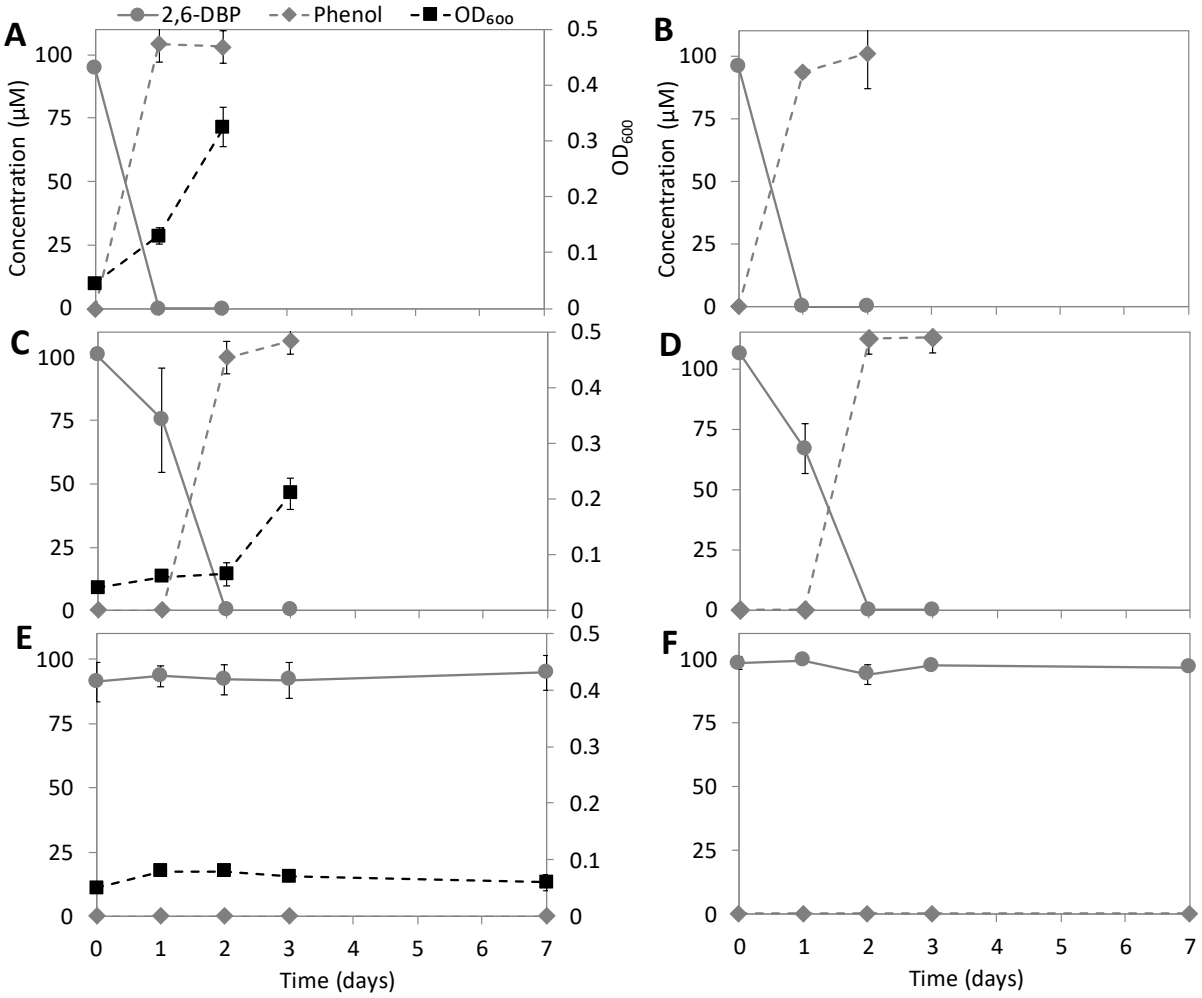

Fig. S3.12 2,6-DBP debromination by *D. spongiiphila* DBB grown in presence (A, C, E) or absence (B, D, F) of sulfate (20 mM) and initial oxygen concentration of 0% (A, B), 2% (C, D), 5% (E, F). Points and error bars represent the average and standard deviation of samples taken from duplicate cultures.

Table S3.1 Primers used in this study

Target	Name	Sequence (5´−3´) [a]	Application	Reference	Reference for PCR/RT-qPCR program
Total bacteria	27F-DegS	GTTYGATYMTGGCTCAG	MiSeq	(van den Bogert *et al.* 2011)	
	338R–I	GCWGCCTCCCGTAGGAGT			
	338R–II	GCWGCCACCCGTAGGTGT	MiSeq	(Daims *et al.* 1999)	(Lu *et al.* 2017)
	Unitag1	GAGCCGTAGCCAGTCTGC			
	Unitag2	GCCGTGACCGTGACATCG	MiSeq	(Tian *et al.* 2016)	(Lu *et al.* 2017)
Total bacteria	Eub341F	CCTACGGGAGGCAGCAG			
	Eub534R	ATTACCGCGGCTGCTGGC	RT-qPCR	(Muyzer *et al.* 1993)	(Atashgahi *et al.* 2013)
rdhA1 [b]	Rdh1F	ACCGCTACGATTTTGCATCC			
	Rdh1R	CCATCTCAAAGGCCATGACG	RT-qPCR	This study	This study
rdhA2 [b]	Rdh2F	CGTTATTCCGCAGTCGTTGT			
	Rdh2R	CACTGGGGACTGACAAGGAT	RT-qPCR	This study	This study
rdhA3 [b]	Rdh3F	TGGCCGACTTTTGCATGAAA			
	Rhd3R	AGGTGTTCTTGCGGGAGTAA	RT-qPCR	This study	This study

[a] M = A or C; R = A or G; W = A or T; Y = C or T

[b] *rdhA* genes of *D. spongiiphila* DBB

Table S3.2 Cellular fatty acid composition (%) of different *Desulfoluna* strains

Fatty acid	*D. spongiiphila* DBB	*D. spongiiphila* AA1^T	*D. butyratoxydans* MSL71^T
C12:0	0.3	0.3	0.8
C14:1ω7	0.9	0.3	1.1
C14:1ω5	0.2	0.1	0.2
C14:0	9.9	6.6	11.5
C16:1ω9	1.4	1.1	1.5
C16:1ω7c	19.4	18.9	22.4
C16:1ω7tr	0.3	0.3	0.3
C16:1ω5	0.6	0.8	0.7
C16:0	28.1	28.4	21.7
C18:1ω9	11.6	11.8	11.3
C18:1ω7	18.6	22.9	19.7
C18:0	2.2	1.1	1.7
β-OH-C12	0.4	0.5	0.4
β-OH-C14	6.2	7.0	6.7

Table S3.3 Selected genomes and their general features that were used for 16S rRNA gene and protein domain based phylogenetic analyses

Strain [a]	Genome size (Mb)	GC (%)	Proteins	GenBank accession number
Desulfoluna spongiiphila DBB	6.68	57.1	5301	PRJEB31368 [b]
Desulfoluna butyratoxydans MSL71^T	6.05	57.9	4186	PRJEB31368 [b]
Desulfoluna spongiiphila AA1^T	6.53	57.2	5203	NZ_FMUX01000001.1
Desulfatibacillum aliphaticivorans CV2803	6.47	54.4	5264	NZ_AUCT00000000.1
Desulfovibrio fructosivorans JJ	4.67	63.9	4046	NZ_AECZ01000001.1
Desulfatibacillum alkenivorans AK-01	6.49	54.7	5277	NC_011768.1
Desulfatirhabdium butyrativorans HB1	4.48	54.9	3852	NZ_KE386985.1
Desulfatitalea tepidiphila S28bF	5.61	56.7	4858	NZ_BCAG01000003.1
Desulfobacter postgatei 2ac9	3.97	47.2	3845	NZ_CM001488.1
Desulfobacterium autotrophicum HRM2	5.65	48.7	4835	NC_012108.1
Desulfobacterium vacuolatum DSM 3385	5.03	46.5	4050	NZ_FWXY01000001.1
Desulfobacula phenolica DSM 3384	4.87	41.4	4181	NZ_FNLL01000001.1
Desulfobacula toluolica Tol2	5.19	41.4	4545	NC_018645.1
Desulfococcus multivorans DSM 2059	4.42	56.8	3783	NZ_CP015381.1
Desulfococcus oleovorans Hxd3	3.94	56.2	3325	NC_009943.1
Desulfomicrobium baculatum DSM 4028	3.94	58.6	3395	NC_013173.1
Desulfosarcina cetonica JCM 12296	7.09	55.7	5582	NZ_BBCC01000001.1
Desulfotignum phosphitoxidans DSM 13687	4.99	51.3	4556	NZ_APJX01000001.1
Desulfovibrio aespoeensis Aspo 2	3.62	62.6	3257	NC_014844.1
Desulfovibrio alaskensis G20	3.64	57.9	3270	NC_007519.1
Desulfovibrio desulfuricans ND132	3.85	65.2	3423	NC_016803.1

[a] Genome information were obtained from GenBank under their respective accession numbers, except *D. spongiiphila* DBB and *D. butyratoxydans* MSL71^T

[b] Project ID of genome sequences deposited in the European Bioinformatics Institute (EBI)

Table S3.4 Abundance of the proteins involved in lactate, sulfate and 1,4-DBB metabolism in cells of *D. spongiiphila* DBB grown in LS and LSD conditions

	Locus tag	LS1 Area	LS2 Area	LS3 Area	LSD1 Area	LSD2 Area	LSD3 Area	log2 fold-change	*p*-value
Proteins involved in lactate metabolism									
Lactate permease	24890	23.64	23.48	24.38	22.96	23.17	24.12	0.42	0.40
LdhA-1	24880	28.72	28.66	29.09	29.09	29.01	28.59	0.08	0.73
LdhA-2	24970	28.03	28.08	28.37	27.89	27.85	27.88	-0.28	0.05
LdhB-1	24870	25.39	25.97	26.61	26.50	25.84	25.93	0.10	0.81
LdhB-2	24960	26.35	26.69	29.20	26.84	25.89	26.12	-1.13	0.29
Por-1	310	31.58	31.55	31.62	30.70	30.64	30.79	-0.87	0.00
Por-2	24940	32.20	32.22	32.18	31.20	31.05	31.25	-1.03	0.00
Pta	9370	27.45	27.31	27.91	27.97	27.56	27.57	0.15	0.55
Ack	9360	28.26	28.72	28.92	29.10	28.35	28.27	-0.06	0.86
Proteins involved in sulfate metabolism									
Sulfate permease	22290	22.35	22.14	22.49	21.25	21.21	22.95	0.52	0.42
Sat	23930	30.04	30.03	29.50	29.71	30.25	29.73	-0.04	0.88
ApsBA	23880	26.33	26.34	25.92	26.22	25.94	26.11	0.11	0.54
	23890	29.22	28.85	28.57	29.21	28.63	29.02	-0.08	0.78
QmoABC	23900	24.36	23.64	24.40	23.92	23.45	24.16	0.29	0.42
	23910	24.88	24.32	24.36	24.18	23.44	24.48	0.48	0.25
	23920	26.22	26.24	26.34	26.10	26.30	26.72	-0.11	0.59
DsrC	370	31.27	31.08	31.57	31.58	30.91	31.38	-0.02	0.95
DsrABD	25620	32.60	32.22	32.75	32.50	32.82	32.47	0.08	0.71
	25630	32.66	32.45	32.50	32.32	32.18	32.31	-0.26	0.03
	25640	29.06	28.67	29.24	29.11	29.04	28.98	0.06	0.77
DsrMKJOP	27290	22.46	21.95	23.37	22.84	22.29	22.87	-0.08	0.87
	27300	24.46	23.24	22.96	22.72	23.43	24.32	0.07	0.92
	27310	ND	ND	ND	ND	ND	ND	-	-
	27320	22.28	19.51	22.20	22.90	22.59	22.90	-1.46	0.18
	27330	22.72	23.09	23.97	22.80	22.52	23.81	0.22	0.70
Electron transport proteins									
FixABC	25970	30.04	29.82	30.06	30.29	30.65	30.11	0.37	0.09
	25980	29.59	29.14	29.98	29.82	30.32	29.85	0.42	0.22
	25990	23.32	22.36	23.48	21.62	20.86	23.02	1.22	0.17
Flavodoxin	37290	33.29	33.59	31.86	32.73	33.16	33.91	0.35	0.61
QrcABCD	34140	ND	ND	ND	ND	ND	ND	-	-
	34150	20.66	21.51	21.22	22.42	21.33	22.31	-0.89	0.11
	34160	22.10	22.60	22.56	22.18	22.28	22.82	-0.01	0.97
	34170	ND	ND	ND	ND	ND	ND	-	-
Reductive dehalogenase									
RdhA1	38400	ND	ND	ND	26.62	25.99	25.39	-	-

Corrinoid biosynthesis proteins									
GltX	24080	25.00	24.89	24.99	24.83	24.45	24.66	-0.31	0.05
HemL	7500	26.66	27.12	26.78	26.39	26.04	24.88	-1.08	0.08
HemB	44050	26.25	26.89	26.29	25.94	25.78	26.45	-0.42	0.22
HemC	18940	27.66	27.70	27.57	27.16	27.31	27.64	-0.27	0.14
HemD	18950	27.94	27.84	27.70	27.71	27.83	26.97	-0.32	0.31
CysG	26600	24.85	25.24	25.21	25.04	25.02	25.05	-0.06	0.63
CbiK	3730	22.33	23.47	22.80	21.70	22.66	22.96	-0.43	0.44
CbiL	3790	24.06	24.62	23.45	24.55	23.59	24.36	0.12	0.79
CbiH	3850	23.81	24.54	24.96	25.56	25.70	26.10	1.35	0.02

The full name of each protein can be found in Fig. 3.6 and Table S3.5
ND: not detected

Table S3.5 Corrinoid biosynthesis pathways and corresponding genes and functions in *Desulfoluna* strains

Biosynthetic pathway	Gene [a]	DBB [b]	AA1^{T} [c]	MSL71^{T} [b]	Function in corrinoid biosynthesis
Glutamate					
↓	*gltX*	**24080**	11166	15970	Glutaminyl-trna synthetase
↓	*hemA*	26620	12922	13190	Glutamyl-trna reductase
↓	*hemL*	**7500**	10673	46530	Glutamate-1-semialdehyde 2,1-aminomutase
↓	*hemB*	**44050**	13043	37790	Porphobilinogen synthase
↓	*hemC*	**18940**	103136	7120	Hydroxymethylbilane synthase
↓	*hemD*	**18950**	103137	7130	Uroporphyrinogen-III synthase
Uroporpyhrinogen III					
↓	*cysG*	**26600**	12920	13210	Uroporphyrin-III C-methyltransferase
Precorrin-2					
↓	*cbiK*	**3730**	12810	49290	Sirohydrochlorin cobaltochelatase
Co(II)- precorrin-2					
↓	*cbiL*	**3790**	12816	49350	Precorrin-2/cobalt-factor-2 C20-methyltransferase
Co(II)- precorrin-3					
↓	*cbiH*	**3850**	12822	49410	Precorrin-3B C17-methyltransferase
Co(II)-precorrin-4					
↓	*cbiF*	3830	12820	49390	Precorrin-4/cobalt-precorrin-4 C11-methyltransferase
Co(II)-precorrin-5A					
↓	*cbiG*	3840	12821	49400	Cobalt-precorrin 5A hydrolase
Co(II)-precorrin-5B					
↓	*cbiD*	3810	12818	49370	Cobalt-precorrin-5B (C1)-methyltransferase
Co(II)-precorrin-6A					
↓	*cbiJ* [d]				Precorrin-6A/cobalt-precorrin-6A reductase
Co(II)-precorrin-6B					
↓	*cbiET*	3820	12819	49380	Cobalt-precorrin-6B (C15)-methyltransferase
Co(II)-precorrin-7,8					
↓	*cbiC*	3780	12815	49340	Precorrin-8X/cobalt-precorrin-8 methylmutase
Cobyrinic acid					
↓	*cbiA*	3770	12814	49330	Cobyrinic acid *a,c*-diamide synthase
Cob(II)yrinic acid *a,c*-diamide					
↓					

Cob(I)yrinic acid *a,c*-diamide					
↓	*cobA*	3860	12823	49420	Cob(I)alamin adenosyltransferase
Ado-cob(I)yrinic acid *a,c*-diamide					
↓	*cbiP*	3870	12824	49430	Adenosylcobyric acid synthase
Adenosyl cobyrinate *a,c*-hexaamide					
↓	*cbiB*	3920	12829	49480	Adenosylcobinamide-phosphate synthase
Ado-cobinamide					
↓	*cobU*	3880	12825	49440	Adenosylcobinamide-phosphate guanylyltransferase
Ado-cobinamide-GDP					
↓	*cobS*	3890	12826	49450	Cobalamin synthase
Cobalamin					

[a] Gene nomenclature for the anaerobic corrinoid biosynthesis pathway was as previously published (Moore and Warren 2012)

[b] Gene Locus numbers are according the genome sequences of *D. spongiiphila* DBB and *D. butyratoxydans* MSL71^T sequenced in this study. The numbers shown in bold are proteins detected in the proteome of strain DBB

[c] Gene Locus numbers are according the genome sequence of *D. spongiiphila* AA1^T in GenBank

[d] Genes that were not found in the *Desulfoluna* genomes

Table S3.6 Sulfur metabolism pathways and corresponding genes in *Desulfoluna* strains

Metabolic pathway	Enzyme	DBB [a]	AA1^{T} [b]	MSL71^{T} [a]
	Sulfate permease	13340, **22290**, 24700, 47100	12364, 11742, 111127, 104190	27680, 17610, 15410, 29700
Tetrathionate				
↓	Tetrathionate reductase	32070, 32080	11084, 11085	ND
Thiosulfate				
↓	Molybdopterin oxidoreductase	8600−8620	106177−106179	41260−41280
	or			
	Rhodanese-like protein[c]	9670, 10640	10968, 10571	51880, 25130
Sulfite				
Sulfate				
↓	Sulfate adenylyltransferase	**23930**	11149	16120
Adenylyl sulfate (APS)				
↓	APS reductase α subunit	**23890**	11145	16160
	APS reductase β subunit	**23880**	11144	16170
Sulfite				
↓	Dissimilatory sulfite reductase α subunit	**25620**	12530	14160
	Dissimilatory sulfite reductase β subunit	**25630**	12529	14150
	Dissimilatory sulfite reductase D	**25640**	12528	14140
Sulfide				

[a] Locus tag numbers are according to the genome of strains DBB and *D. butyratoxydans* MSL71^{T} sequenced in this study. Numbers shown in bold are proteins detected in the proteome of *D. spongiiphila* DBB

[b] Locus tag numbers are according to the genome of *D. spongiiphila* AA1^{T} (NZ_FMUX01000001.1)

[c] Putative function as thiosulfate reductase

ND: not detected

Table S3.7 Enzymes involved in oxygen reduction and ROS detoxification in *Desulfoluna* strains

Enzyme	DBB [a]	AA1^{T} [b]	MSL71^{T} [a]
Rubredoxin–oxygen oxidoreductase	16300	101503	5010
Cytochrome *c* oxidase	43200–43500	11283–11286	36840–36870
Cytochrome *bd* oxygen reductase	15890–15900	101463–101464	4610–4620
Superoxide dismutase	15650	101439	4380
Superoxide reductase	40040	1079	24220
Rubrerythrin	34920	102199	19140
Thiol peroxidase	30870	114122	33350

[a] Locus tag numbers are according to the genomes of *D. spongiiphila* DBB and *D. butyratoxydans* MSL71^{T} sequenced in this study
[b] Locus tag numbers are according to the genome of *D. spongiiphila* stain AA1^{T} (NZ_FMUX01000001.1)

Datasets S3.1 and **S3.2** are available online at https://www.biorxiv.org/content/10.1101/630186v1

Chapter 4

Microbial chloroform transformation in hypersaline sediments as natural sources of chloromethanes

Peng Peng [#], Yue Lu [#], Tom N.P. Bosma, Ivonne Nijenhuis, Bart Nijsse, Alexander Ruecker, Aleksandr Umanetc, Javier Ramiro-Garcia, Andreas Kappler, Detmer Sipkema, Hauke Smidt, Siavash Atashgahi

[#] equal contribution

Manuscript in preparation

Abstract

Chloroform (CF) is an environmental contaminant that can be naturally formed in various environments ranging from forest soils to salt lakes. Here, we investigated CF removal potential in sediments obtained from hypersaline lakes in Western Australia. Reductive dechlorination of CF to dichloromethane (DCM) was observed in enrichment cultures derived from sediments of Lake Strawbridge which has been reported as a natural source of CF. The lack of CF removal in the abiotic control cultures without artificial electron donors indicated that the observed CF removal is a biotic process. Experiments with ^{13}C labelled CF in the sediment-free enrichment cultures (pH 8.5, salinity 5%) showed that increasing the vitamin B_{12} concentration from 0.04 to 4 µM enhanced CF removal, reduced DCM formation, and increased $^{13}CO_2$ production which is likely a product of CF oxidation. Known organohalide-respiring bacteria were not detected using 16S rRNA gene-based quantitative PCR or bacterial community analysis. Rather, members of the genus *Clostridium* known to include acetogenic species capable of co-metabolic transformation of CF to DCM and CO_2 were detected in the enrichment cultures, and the genes encoding enzymes involved in acetogenesis were identified by metagenome analysis of the enrichment cultures. This study indicates that microbiota may act as a filter to reduce CF emission from hypersaline lakes to the atmosphere.

Introduction

Until the 1970s, halogenated organic compounds, organohalogens, were believed to originate exclusively from anthropogenic sources (Cicerone *et al.* 1974). This long-held view was changed following the discovery of diverse organohalogens from natural environments and (micro)organisms. To date, over 5000 naturally occurring organohalogens have been identified (Gribble 2010). A remarkable example is chloroform (trichloromethane, CF) which is a known environmental contaminant and a potential carcinogen that is accumulative and harmful for living organisms (Rosenthal 1987). CF is synthetically produced in chemical industries as an anesthetic, as an intermediate for the production of refrigerants, and as a degreasing agent and fumigant (ATSDR 1997). However, anthropogenic sources were estimated to contribute to less than 10% of the annual 700,000–820,000 tons global CF production (Field 2016). Natural CF emissions have been reported from numerous terrestrial and aquatic environments such as forest soils (Albers *et al.* 2010, Breider *et al.* 2013, Haselmann *et al.* 2002, Osswald *et al.* 2016), rice fields (Khalil *et al.* 1998), groundwater (Hunkeler *et al.* 2012), oceans (Nightingale 1991), and hypersaline lakes (Ruecker *et al.* 2014, Weissflog *et al.* 2005). Biotic and abiotic processes like burning of vegetation, chemical production by reactive Fe species, and enzymatic halogenation can lead to natural production of CF (Laturnus *et al.* 2002). Similar to other low molecular weight volatile organohalogens (VOX), CF release into the atmosphere can cause ozone depletion and impact climate change (Read *et al.* 2008).

CF is persistent in the environment and is hardly degraded under oxic conditions due to the three chlorine substitutes (Cappelletti *et al.* 2012, Janssen *et al.* 2005). In contrast, CF transformation is often observed using anaerobic microbial consortia under anoxic conditions (Grostern *et al.* 2010, Guerrero-Barajas and Field 2005, Justicia-Leon *et al.* 2014, Rodríguez-Fernández *et al.* 2018b, Shan *et al.* 2010). Anaerobic CF transformation has been reported to be mediated by acetogens like *Acetobacterium woodii* (Egli *et al.* 1988) and *Clostridium* sp. strain TCAIIB (Gälli and McCARTY 1989), and methanogenic *Methanosarcina* spp. (Baeseman and Novak 2001, Bagley and Gossett 1995, Mikesell and Boyd 1990), producing dichloromethane (DCM), carbon monoxide (CO) and/or carbon dioxide (CO_2). This is a co-metabolic process likely mediated by enzymes involved in acetogenesis (acetyl-CoA pathway) and methanogenesis (Egli *et al.* 1988, Holliger *et al.* 1992). Moreover, transition-metal co-factors, e.g. cob(I)/cob(II)alamins and F_{430} (nickel(I)-porphinoid), that facilitate key enzymes of acetogenesis (5-methyltetrahydrofolate corrinoid/iron-sulfur protein methyltransferase) and methanogenesis (methyl-coenzyme M reductase) can act as reductants and nucleophilic reagents catalyzing nonspecific reductive dechlorination of chloromethanes (Gantzer and Wackett 1991, Krone *et al.* 1989a, Krone *et al.* 1989b).

Another group of anaerobes known as organohalide-respiring bacteria (OHRB) can use CF as a terminal electron acceptor, and couple CF reductive dechlorination to energy conservation (Fincker and Spormann 2017, Schubert *et al.* 2018). For instance, CF respiration to DCM has been reported using *Desulfitobacterium* sp. strain PR (Ding *et al.* 2014), *Desulfitobacterium hafniense* TCE1 (Gerritse *et al.* 1999), *Dehalobacter* sp. strain UNSWDHB (Lee *et al.* 2012, Wong *et al.* 2016) and a mixed culture containing *Dehalobacter* (Justicia-Leon *et al.* 2014). The enzymes responsible for reductive dehalogenation in OHRB are corrinoid cofactor dependent reductive dehalogenases (RDases) such as a CF RDase (CfrA) identified from *Dehalobacter*-containing microbial consortia (Tang and Edwards 2013). CF can also be abiotically dechlorinated under anoxic conditions via hydrogenolysis to DCM, or reductive elimination to CH_4 (He *et al.* 2015, Rodríguez-Fernández *et al.* 2018a, Torrentó *et al.* 2017).

Previous studies have shown the presence of organohalogen-metabolizing microbes in environments where natural organohalogens have been shown or suspected to be present (Atashgahi *et al.* 2018a, Krzmarzick *et al.* 2012). Hypersaline lakes and marshes are natural sources of VOX emissions to the atmosphere (Rhew *et al.* 2000, Ruecker *et al.* 2014, Weissflog *et al.* 2005) where NaCl might promote high rates of organic matter halogenation (Oren 2001). However, knowledge about the microbial metabolism of VOX in such extreme environments is lacking. This information is necessary to understand whether microbes can act as a filter for VOX in hypersaline environments that at least partly prevent their emission to the atmosphere. In this study, we prepared microcosms from the sediments of hypersaline Lake Strawbridge and Lake Whurr in Western Australia. Lake Strawbridge has been reported as a natural source of chloromethane (CM) and CF (Ruecker *et al.* 2014). The CF transformation process and responsible microbes were studied by a combination of anaerobic cultivation, stable isotope labelling, and chemical and molecular analyses.

Materials and Methods

Sampling site

Duplicate sediment cores of approximately 24 cm length and 4 cm internal diameter were collected from Lake Strawbridge (LS, 32.84°S, 119.40°E) and Lake Whurr (LW, 33.04°S, 119.01°E) in Western Australia (Fig. S4.1). Sediment cores were taken by pushing a polypropylene tube into the sediment. The top and the bottom of the tube were immediately closed with rubber stoppers after pulling the core from the sediment. The sediment samples were transported at 8°C to the Laboratory of Microbiology, Wageningen University & Research, The Netherlands.

Physical-chemical analysis

The sediment cores were cut into a top (0–12 cm) and a bottom (12–24 cm) layer in an anoxic chamber filled with an atmosphere of N_2/H_2 (96 : 4%). Subsamples from each sediment layer were homogenized and subsequently used for physical-chemical analysis and as inocula for enrichment set up. The remaining sediments were kept in -80°C for molecular analysis. Water content was determined by the percentage of weight loss observed after drying the samples in a desiccator at 105°C overnight with a subsequent cooling down to room temperature. pH was measured immediately and again after two hours using a pH meter (ProLine B210, Oosterhout, The Netherlands) with air-dried sediments suspended in 0.01 M $CaCl_2$ solution. Sediment total organic carbon (TOC) was measured using the Kurmies method (Mebius 1960). Low crystalline “bioavailable” iron was extracted from 0.5 g wet sediment for one hour in the dark using 25 ml of 0.5 M anoxic HCl (Amstaetter *et al.* 2012), and concentrations of dissolved Fe(II) and Fe(III) were quantified using the spectrophotometric Ferrozine assay (Stookey 1970). Major anions including Cl^-, SO_4^{2-}, NO_3^- and ClO_3^- were analysed using a Thermo Scientific Dionex™ ICS-2100 Ion Chromatography System (Dionex ICS-2100). Major cations including Ca^{2+}, K^+, Mg^{2+} and Na^+ were measured using inductively coupled plasma-optical emission spectroscopy (ICP-OES, Varian, The Netherlands). Salinity was calculated based on the NaCl concentration (weight/volume) as described before (Weigold *et al.* 2016).

Microcosm preparation

Due to dominant presence of halophilic microbes in hypersaline environments (Amoozegar *et al.* 2017), and in an attempt to find halophilic microbes capable of CF metabolism, two media were used for halophilic bacteria and archaea enrichment: modified growth medium (MGM) and DBCM2 medium (DBC) (Dyall-Smith 2008). The media were boiled and flushed with nitrogen to remove oxygen. $Na_2S{\cdot}9H_2O$ (0.48 g/L) was added as the reducing reagent and resazurin (0.005 g/L) was added as redox indicator. Tris-base (10 mM) and acetic acid (10 mM) were used as the buffer for MGM and DBC media, respectively. The salinity (5–20%) and pH (4.6–8.5) of the media were adjusted to the corresponding values measured in the sediments used as inocula (Table 4.1, Table S4.1).

Initial sediment enrichment cultures were prepared in 50 ml serum bottles with 2.5 g wet sediment of either the top or bottom layer of lake sediments and 25 ml of either MGM or DBCM2 medium. The bottles were sealed with Teflon lined butyl rubber stoppers, and the headspace was exchanged with N_2 gas (140 kPa). CF was added to each bottle at a nominal concentration of 1.25 µmol/bottle. All cultures were set up in duplicate and incubated stationary in the dark at 37°C. Of all cultures, the sediment enrichments containing the bottom layer sediment of Lake Strawbridge in MGM medium with 5% salinity showed better CF

dechlorination, and were therefore used for all subsequent experiments. Sediment-free cultures were obtained by sequential transfers of this culture (10% (v/v)) in duplicate in 120 ml bottles containing 50 ml MGM medium except that peptone was decreased from 5 to 0.5 g/L and yeast extract was decreased from 1 to 0.5 g/L, and glycerol (10 mM) and CF (2.5 µmol/bottle) was added as a carbon source. The sediment-free cultures were used to test the influence of vitamin B_{12} (0.04, 0.4, 0.8, 1.6 and 4 µM) on CF (5 µmol/bottle) dechlorination. Abiotic controls for CF transformation were performed in the modified MGM medium with decreased amount of peptone (0.5 g/L) and yeast extract (0.5 g/L) and glycerol (10 mM), and amended with 4 µM vitamin B_{12} and 5 µmol/bottle CF, and the same inoculum that was autoclaved at 121°C for 30 min. In a subset of abiotic controls, titanium(III) citrate (Ti(III), 5 mM) or dithiothreitol (DTT, 100 mM) were used as artificial electron donors (Assaf-Anid *et al.* 1994, Chiu and Reinhard 1995). To test CO_2 production from CF, ^{13}C-labelled CF (99%, Cambridge Isotope Laboratories, Inc., Massachusetts, USA) was used for detecting production of $^{13}CO_2$. $^{13}CO_2$ formation in the cultures was monitored as outlined below. Cultures without ^{13}C-labelled CF were prepared in parallel by supplying 100% non-labelled CF and were used for measuring natural abundance of $^{13}CO_2$. The CF dechlorination rate was determined as the disappearance of CF (µmol) per day per liter enrichment culture (µmol/day/L) during the incubation period when dechlorination was stably observed.

GC analysis

Chloromethanes were quantified from 0.2 ml headspace samples using a gas chromatograph equipped with a flame ionization detector (GC-FID, Shimadzu 2010) and a Stabilwax column (Cat. 10655-126, Restek Corporation, USA). The column was operated isothermally at 35°C. Nitrogen was used as the carrier gas at a flow rate of 1 ml/min. Carbon monoxide (CO), Carbon dioxide (CO_2) and methane were analysed using a Compact GC 4.0 (Global Analyzer Solutions, Breda, The Netherlands) with a thermal conductivity detector (GC-TCD). CO and methane were measured using a molsieve 5A column operated at 100°C coupled to a Carboxen 1010 precolumn, and CO_2 was measured using a Rt-Q-BOND column operated at 80°C.

Isotope analysis

$^{13}CO_2$ was measured in sediment-free cultures contained 1.25 µmol/bollte ^{13}C-labelled CF, 3.75 µM non-labelled CF and 0.04/4 µM vitamin B_{12}, and control cultures contained 100 µM non-labelled CF and 0.04/4 µM vitamin B_{12}. The carbon isotope composition of CO_2 was determined using gas chromatography combustion isotope ratio mass spectrometry (GC/C-IRMS) consisting of a gas chromatograph (7890A Series, Agilent Technology, USA) coupled via Conflo IV interface (ThermoFinnigan, Germany) to a MAT 253 mass spectrometer

(ThermoFinnigan, Germany). Sample separation was done with a CP-PoraBOND Q column (50 m × 0.32 mm ID, 5 um film thickness; Agilent Technology, Netherlands) operated isothermally at 40°C using helium as a carrier gas at a flow rate of 2.0 ml/min. Sample aliquots of 0.1–0.5 ml were injected at split ratios ranging from 1:10 to 1:20. The carbon isotope signatures are reported in δ notation (per mill) relative to the Vienna Pee Dee Belemnite standard.

The amount of $^{13}CO_2$ produced from the ^{13}C-labelled CF was expressed according to:

$\delta^{13}C = (R_{sample}/R_{standard} - 1) \times 1000$

Where $\delta^{13}C$ is the ^{13}C isotopic composition (per mil, ‰), R_{sample} is the ^{13}C to ^{12}C ratio of the CO_2 in the sample, $R_{standard}$ is the international Vienna Pee Dee Belemnite standard (VPDB, $^{13}C/^{12}C$ = 0.0112372).

DNA extraction

The sediment aliquots collected during start-up of the microcosms were thawed and washed three times with 1.5 ml of 10 mM TE buffer (pH 7.0) to avoid interference of the high salinity with the DNA extraction. For each sample, wet sediment (0.5 g) and the washing buffer collected by filtration through a 0.22 µm membrane filter (Millipore, MP, USA) were used for DNA extraction. DNA loss during washing was anticipated, but washing was necessary to be able to extract enough DNA for further analysis (Weigold *et al.* 2016). DNA was extracted separately from the washed sediment and the biomass collected on the membrane filter using the PowerSoil DNA isolation kit (MO-BIO, USA) following the manufacturer's instructions. DNA extracts from the sediment and filters were combined for each sample and used for molecular analysis. DNA of the sediment-free enrichment cultures was extracted from 2 ml culture samples using the PowerSoil DNA isolation kit. For metagenome sequencing of the sediment-free cultures, 50 ml of culture was used for DNA extraction using the MasterPure™ Gram Positive DNA Purification Kit (Epicentre, WI, USA).

Quantitative PCR (qPCR)

The abundance of 16S rRNA genes of total bacteria and archaea, and OHRB including *Desulfitobacterium*, *Dehalobacter*, *Dehalococcoides*, *Sulfurospirillum* and *Geobacter* in sediments (Lake Strawbridge) and the sediment derived enrichment cultures were determined by qPCR. Assays were performed in triplicates on a CFX384 Real-Time system in C1000 Thermal Cycler (Bio-Rad Laboratories, USA) with iQ™ SYBR Green Supermix (Bio-Rad Laboratories, USA) as previously outlined (Atashgahi *et al.* 2013). The primers and qPCR programs used in this study are listed in Table S4.2.

Bacterial community analysis

16S rRNA gene based bacterial community analysis was performed on sediments of Lake Strawbridge and the sediment derived enrichment cultures. Sediments from Lake Whurr were not proceeded for bacterial community analysis because no CF dichlorination was observed in the enrichment cultures derived from the sediments of Lake Whurr. Bacterial community performed as following: a 2-step PCR was applied to generate barcoded amplicons from the V1–V2 region of the bacterial 16S rRNA genes, and the PCR products were purified and sequenced on an Illumina MiSeq platform (GATC-Biotech, Konstanz, Germany) as described previously (Atashgahi *et al.* 2017). Primers for PCR amplification of the 16S rRNA genes are listed in Table S4.2. Sequence analysis was performed using NG-Tax (Ramiro-Garcia *et al.* 2016). Operational taxonomic units (OTUs) were assigned using uclust (Edgar 2010) in an open reference approach against the SILVA 16S rRNA gene reference database (LTPs128_SSU, version 111) (Quast *et al.* 2012). Subsequently, a biological observation matrix (biom) file was generated and sequence data was further analyzed using Quantitative Insights Into Microbial Ecology (QIIME) v1.2 (Caporaso *et al.* 2010).

Metagenome

Metagenome sequencing of duplicate sediment-free cultures with and without 4 µM vitamin B_{12} was performed on an Illumina HiSeq platform (PE 150 mode). The reads were first filtered with Trimmomatic (v0.36) with parameters: PE-phred33\ ILUMINACLIP:TruSeq3-PE-2.fa:2:30:10 LEADING:3, TRAILING:3, SLIDINGWINDOW:4:15 MINLEN:36 (Bolger *et al.* 2014). The filtered reads were assembled with MEGAHIT (v1.1.2) with default parameters (Li *et al.* 2016). Gene prediction was performed on each assembly with Prodigal (v2.6.3) with parameters -meta, -c11 (Hyatt *et al.* 2010b).

Sequence deposition

Nucleotide sequences of 16S rRNA genes of bacteria were deposited in the European Nucleotide Archive (ENA) with accession number ERS1165096-ERS1165117 under study PRJEB14107. Raw metagenome sequences were deposited at ENA under study PRJEB32090.

Results

Physical-chemical characteristics of sediments

The top and bottom layer sediments of Lake Strawbridge were slightly alkaline with a pH ranging from 8.2 to 8.5 whereas those of Lake Whurr were acidic with a pH of 4.6–5.4 (Table 4.1). The salinity of the sediments, water content and total organic carbon (TOC) in both lakes Strawbridge and Whurr were higher in the top layer compared to the bottom layer (Table 4.1). Sodium (17.5–71.1 mg/g) and chloride (31.9–123.5 mg/g) were dominant among the cations and anions, respectively. Neither nitrate nor chlorate were detected in the top and bottom layer sediments of the lakes (Table 4.1).

Table 4.1 Geochemical properties of Lake Strawbridge and Lake Whurr sediments. Duplicate sediment cores from each hypersaline lake are labelled as as LS1&LS2 (Lake Strawbridge) and LW1&LW2 (Lake Whurr). TOP: top layer (0–12 cm depth), BOT: bottom layer (12–24 cm depth).

	Lake Strawbridge (LS)				Lake Whurr (LW)			
	LS1-TOP	LS2-TOP	LS1-BOT	LS2-BOT	LW1-TOP	LW2-TOP	LW1-BOT	LW2-BOT
pH [a]	8.2	8.3	8.5	8.5	5.4	5.4	4.5	4.6
Water content (%)	37.3	27.3	16.7	15.4	26.0	25.7	24.2	23.0
Salinity (%)	17	14	5	5	15	20	11	11
TOC (g/kg)	21	15	5	5	12	14	6	6
Na (mg/g)	57.0	48.5	17.5	18.1	55.0	71.1	35.0	35.8
Ca (mg/g)	0.7	0.8	0.1	0.2	6.8	4.2	0.3	0.3
K (mg/g)	2.0	2.0	1.0	0.9	1.7	1.8	1.1	1.2
Mg (mg/g)	2.8	2.9	1.1	1.1	4.5	4.6	3.5	3.4
Total Fe (mg/g)	6.5	6.3	2.2	1.9	1.5	3.2	0.3	0.6
Cl^- (mg/g)	101.3	84.7	31.9	33.1	93.1	123.5	64.8	64.0
SO_4^{2-} (mg/g)	3.9	3.6	1.5	1.8	19.6	14.8	4.3	4.4
NO_3^- (mg/g)	ND [b]	ND	ND	ND	ND	ND	ND	ND
ClO_3^- (mg/g)	ND	ND	ND	ND	ND	ND	ND	ND

[a] Measured in 0.01 M $CaCl_2$ after 2 h

[b] ND: not detected

CF dechlorination in enrichment cultures

No CF dechlorination was observed in the sediment enrichment cultures of Lake Whurr after 70 days of incubation (data not shown), whereas CF was reductively dechlorinated to DCM in the sediment enrichment cultures of Lake Strawbridge (Fig. 4.1A–D). CM and methane as the potential products of CF transformation were not detected (data not shown), despite evident lack of mass balance between CF disappearance and DCM production in sediment cultures and some transfer cultures (Fig. 4.1A–F). The lack of methane production also indicated supressed/absent methanogenesis. The fastest CF dechlorination rate (1.82 µmol/day/L) to DCM was observed in the enrichment cultures with the bottom layer sediments in the MGM medium (Fig. 4.1B). Therefore, these cultures were selected to obtain sediment-free cultures in subsequent transfers (Fig. 4.1E–G).

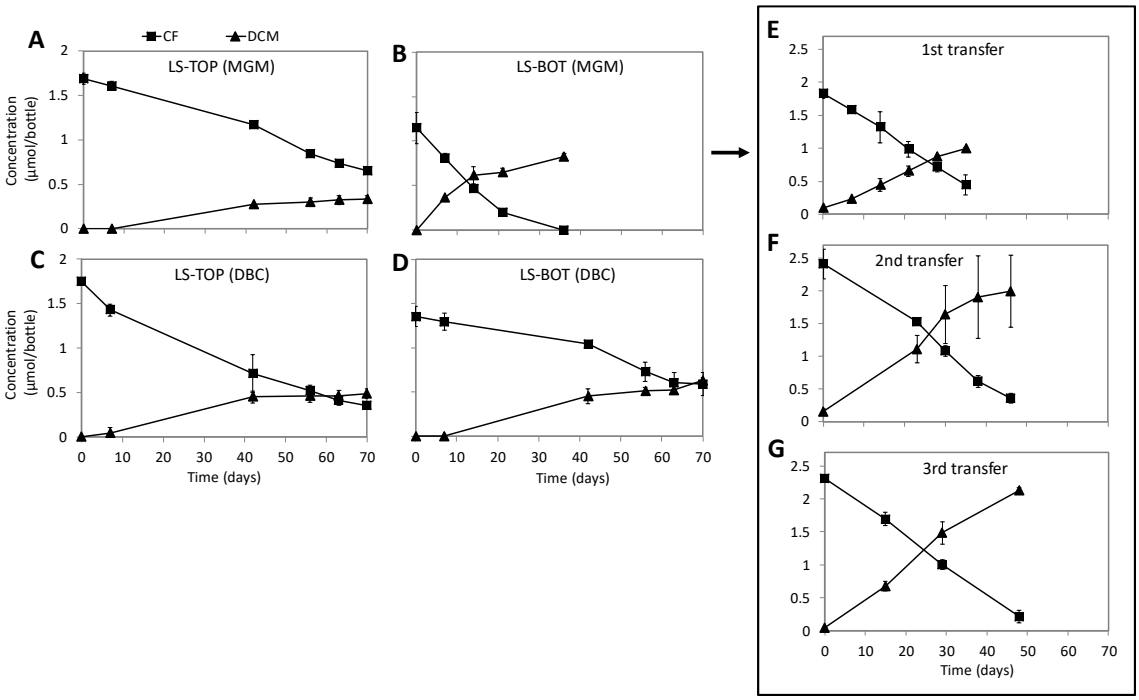

Fig. 4.1 CF transformation in the sediment enrichment cultures and subsequent transfer cultures. Dechlorination of CF in MGM medium with top layer (LS-TOP, A) and bottom layer sediments (LS-BOT, B) from Lake Strawbridge, and dechlorination of CF in DBC medium with top (C) and bottom layer (D) sediments from the same lake. Dechlorination of CF in subsequent transfer cultures of the bottom layer sediment enrichment cultures with MGM medium (E, F, G). Points and error bars represent the average and standard deviation of samples taken from duplicate cultures.

Adding vitamin B_{12} from 0.04 to 4 µM steadily increased CF dechlorination rates in the sediment-free cultures (Fig. 4.2). For instance, in the cultures amended with 4 µM vitamin B_{12}, the CF dechlorination rate reached 31.9 µmol/day/L (Fig. 4.2E), ~30 times higher than the dechlorination rate in the cultures without extra vitamin B_{12} supplementation (~0.9 µmol/day/L)

(Fig. 4.1E–G). In turn, increasing vitamin B_{12} concentration led to concurrent decrease of DCM accumulation. Accordingly, less than 30% of the CF was converted to DCM in the cultures amended with 4 µM vitamin B_{12} (Fig. 4.2E). No CF dechlorination was observed in the abiotic controls even in the presence of 4 µM vitamin B_{12} (data not shown). In contrast, CF dechlorination to DCM and (or) CM was observed in abiotic controls when either Ti(III) or DTT were used as an artificial electron donor together with 4 µM vitamin B_{12} (Fig. S4.2).

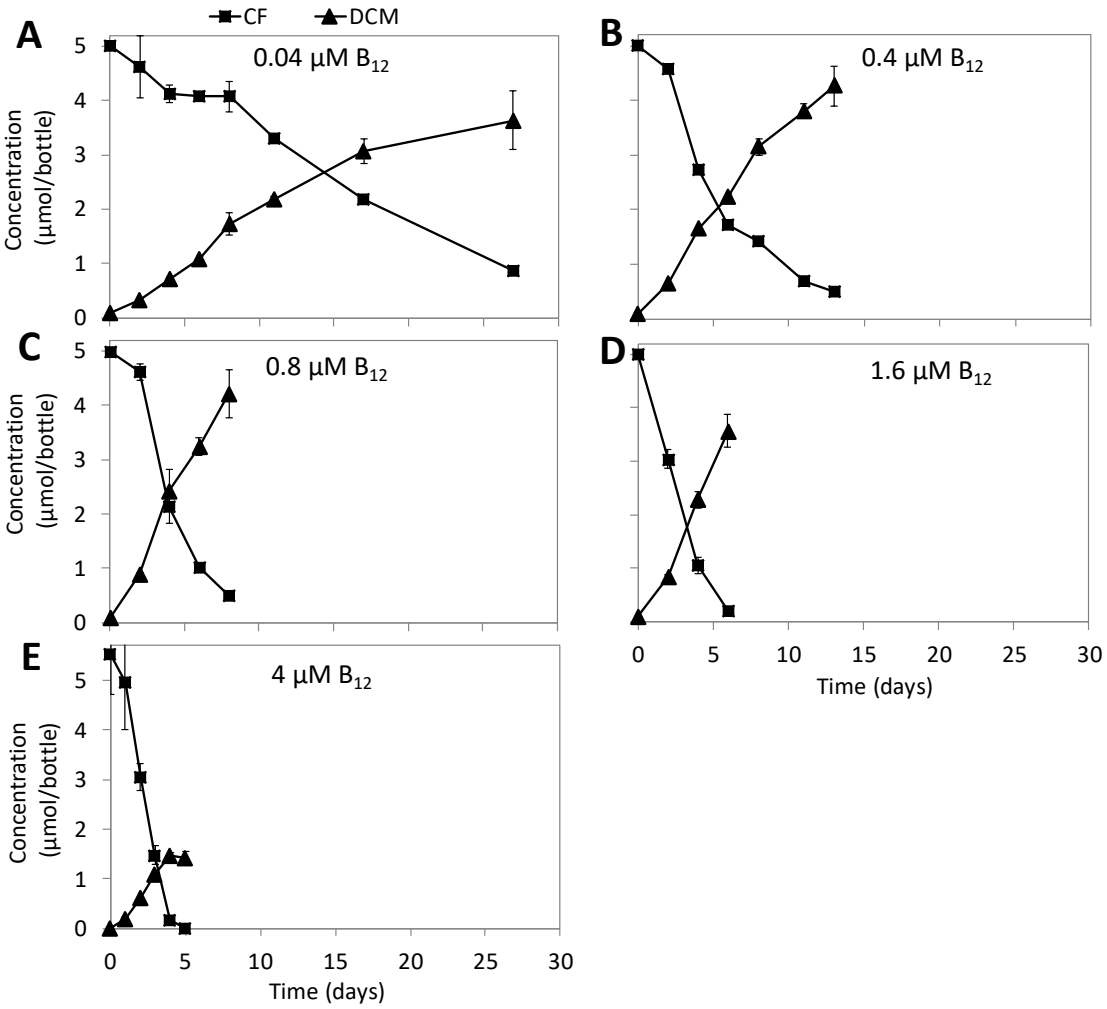

Fig. 4.2 CF transformation in sediment-free cultures amended with 0.04 (A), 0.4 (B), 0.8 (C), 1.6 (D), and 4 µM (E) vitamin B_{12}. Points and error bars represent the average and standard deviation of samples taken from duplicate cultures.

Analysis of $^{13}CO_2$ production from ^{13}CF

$^{13}CO_2$ production was detected in the cultures containing 1.25 µmol/bottle ^{13}C-labelled CF, 3.75 µmol/bottle non-labelled CF and 4 µM vitamin B_{12} during the incubation (Fig. 4.3A). At day 5, 0.84 µmol/bottle $^{13}CO_2$ and 1.7 µmol/bottle DCM were detected (Fig. 4.3A). Assuming that 25% of the DCM (0.43 µmol/bottle) originated from ^{13}C-labelled CF, the ^{13}C mass balance

would be: ^{13}C-labelled CF (1.25 µmol/bottle) = ^{13}C-DCM (0.43 µmol/bottle) + $^{13}CO_2$ (0.84 µmol/bottle). This will indicate a ca. 100% ^{13}C recovery and conversion of CF to CO_2 and DCM as the main products. The δ^{13}C value of $^{13}CO_2$ increased from -23.42‰ to 263.46‰ during the first four days of incubation whereas no significant change of the δ^{13}C value of CO_2 was observed in the cultures without ^{13}C-labelled CF (Fig. 4.3B).

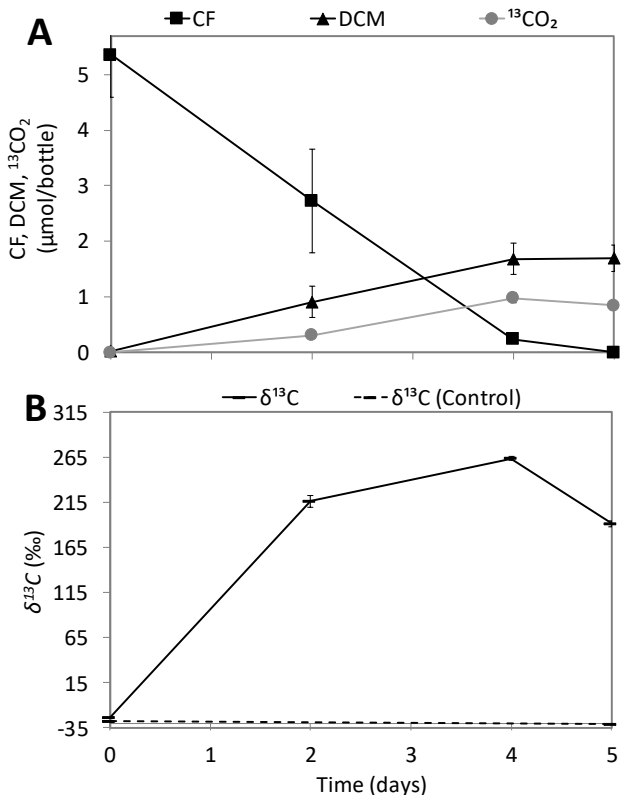

Fig. 4.3 $^{13}CO_2$ production from CF (A) and δ^{13}C values (B) in the sediment-free cultures amended with 1.25 µmol/bottle ^{13}C-labelled CF, 3.75 µmol/bottle non-labelled CF and 4 µM vitamin B_{12}. Control cultures contained the same concentrations of non-labelled CF and vitamin B_{12}. Points and error bars represent the average and standard deviation of samples taken from duplicate cultures.

qPCR and bacterial community analysis

Bacterial and archaeal 16S rRNA gene copies in the top sediment layers of Lake Whurr and Lake Strawbridge were at least one order of magnitude higher compared to the 16S rRNA gene copies in bottom layers of the same lakes (Fig. 4.4A). The top layer sediment from Lake Strawbridge had the highest number of 16S rRNA gene copies of bacteria (3.3×10^8 copies/g dry sediment) and archaea (8.6×10^7 copies/g dry sediment) among all the sediments from the two lakes (Fig. 4.4A). Sediment enrichment cultures and subsequent transfer cultures prepared from the bottom layer sediment of Lake Strawbridge, contained 10^6–10^7 bacterial 16S rRNA gene copies/ml culture (Fig. 4.4B). However, archaeal 16S rRNA gene copies decreased dramatically to 10^4 copies/ml in the sediment enrichment cultures, and to below 10^2 copies/ml

culture in the transfer cultures (Fig. 4.4B). OHRB including *Desulfitobacterium*, *Dehalobacter*, *Dehalococcoides*, *Geobacter* and *Sulfurospirillum* were not detected in the enrichment cultures (data not shown).

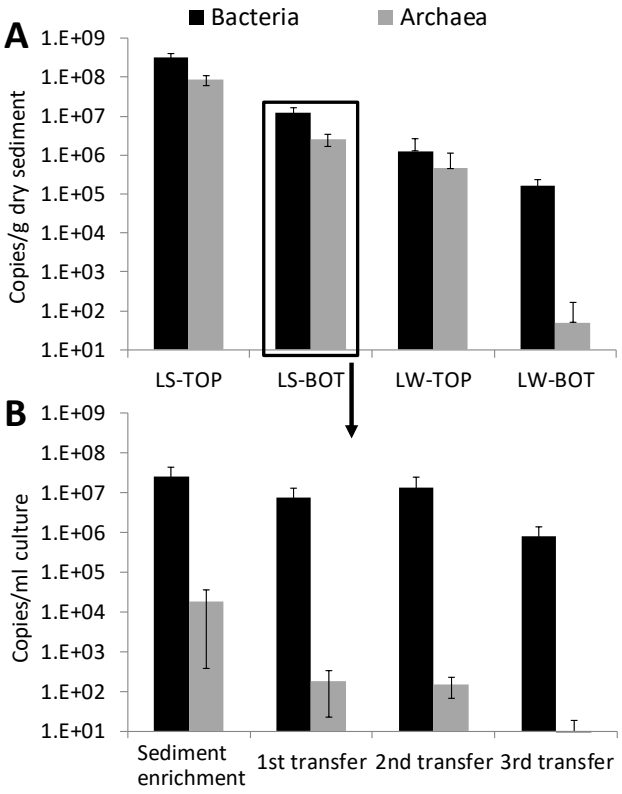

Fig. 4.4 Quantitative PCR (qPCR) targeting total bacterial and archaeal 16S rRNA genes in the top and bottom layer sediment of Lake Strawbridge and Lake Whurr (A), and sediment enrichment culture and subsequent transfer cultures derived from the bottom layer sediment microcosms of Lake Strawbridge (B). Abbreviation: LS, Lake Strawbridge; LW, Lake Whurr; TOP, top layer (0–12 cm depth); BOT, bottom layer (12–24 cm depth). Error bars represent standard deviations of two (for enrichment samples) or four (for sediment samples) independent DNA extractions, and triplicate qPCR reactions were conducted for each DNA sample (n = 2 (4) × 3).

Bacterial community analysis based on Illumina sequencing of barcoded 16S rRNA gene V1–V2 region amplicons showed that *Cyanobacteria*, *Chloroflexi*, *Proteobacteria* and *Firmicutes* were the most abundant phyla (cumulative relative abundance > 70%) in top and bottom layer sediments of Lake Strawbridge (Fig. 4.5). The relative abundance of *Firmicutes* increased from 25–34% in the bottom layer sediments to ~90% in the initial as well as the sediment-free enrichment cultures (Fig. 4.5). The relative abundance of *Clostridium* and *Desulfovibrio* in phyla *Firmicutes* and *Proteobacteria*, respectively, increased from less than 0.1% to 9–20% (*Clostridium*) and from less than 0.1% to 0.3–8% (*Desulfovibrio*) in the initial as well as the sediment-free enrichment cultures.

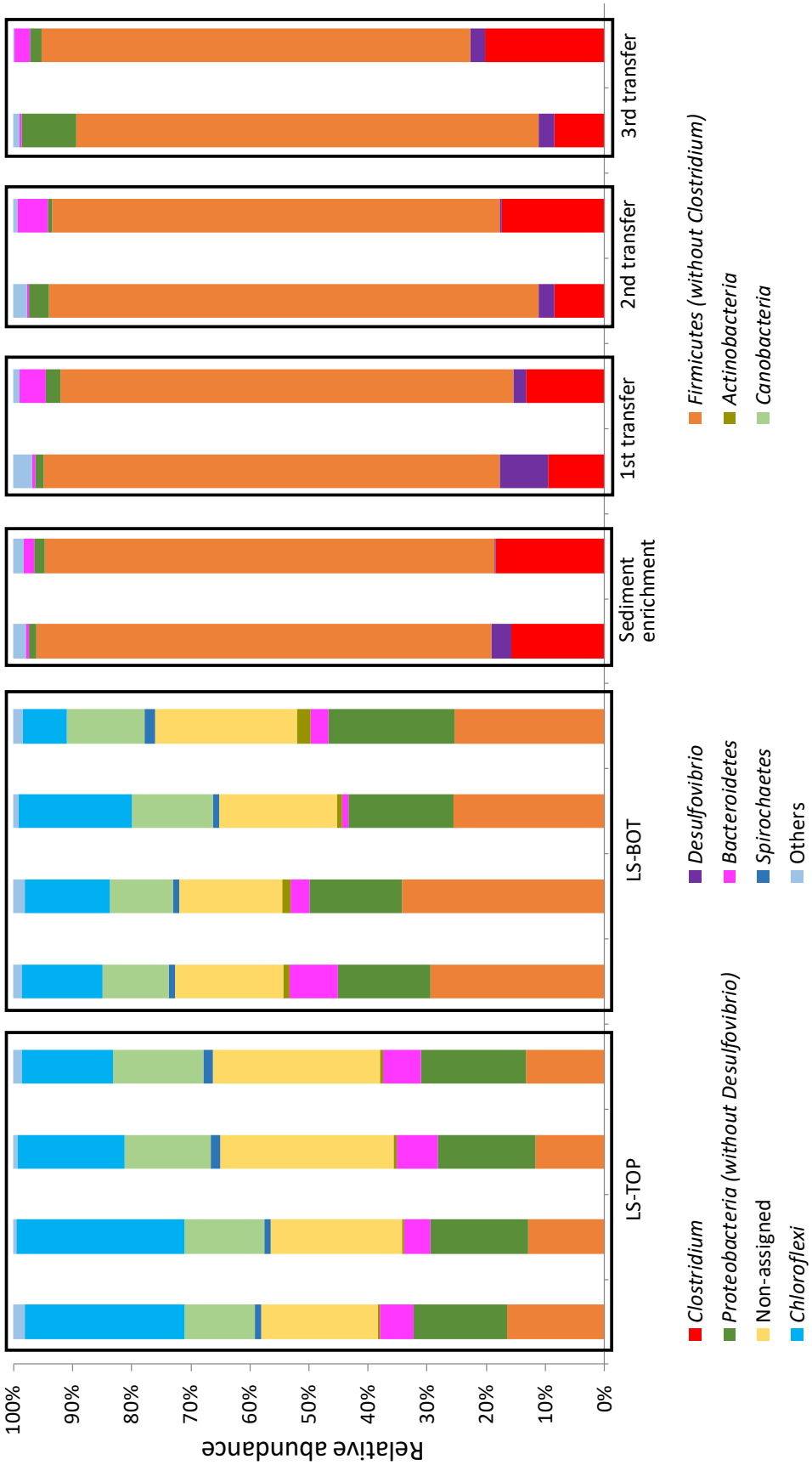

Fig. 4.5 16S rRNA gene based bacterial community analysis of the sediment of Lake Strawbridge and enrichment cultures. Abbreviation: LS, Lake Strawbridge; TOP, top layer (0–12 cm depth); BOT, bottom layer (12–24 cm depth). Data are shown at phylum level, except *Clostridium* and *Desulfovibrio* that are shown at genus level. Taxa that were observed at a relative abundance below 1% were summed up and categorized as 'Others'.

Preliminary metagenomic analysis

The overall assembly features of the four metagenomes were similar to each other (Table S4.3). As bacterial community analysis suggested the enrichment of potentially acetogenic *Clostridium* spp., the preliminary analysis of metagenomes presented here focused on a screening for genes encoding enzymes involved in the acetyl-CoA pathway (Drake *et al.* 2008), which possibly mediated CF transformation. Preliminary metagenome analysis showed presence of these genes in the sediment-free cultures with (4 µM) and without extra vitamin B_{12} amendment (Fig. 4.6).

Discussion

The present study showed CF dechlorination to DCM and CO_2 in microcosms prepared from the sediments of the hypersaline Lake Strawbridge in Western Australia which has previously been shown to be a natural source of CF and CM (Ruecker *et al.* 2014). The lack of CF removal in the abiotic control cultures without artificial electron donors (Ti(III) or DTT) indicated that the CF removal in the sediment and sediment-free enrichment cultures is a biotic process and at least needs cellular metabolism for electron donor generation. However, known CF-respiring bacteria such as *Desulfitobacterium* (Ding *et al.* 2014, Gerritse *et al.* 1999) and *Dehalobacter* (Wong *et al.* 2016) were neither detected in the sediment microcosms nor in the sediment-free cultures by qPCR (data not shown) or 16S rRNA gene-targeted bacterial community analysis (Fig. 4.4–4.5). In contrast, *Desulfovibrio* was found in the enrichment cultures (Fig. 6). *Desulfovibrio* sp. TBP-1 (Boyle *et al.* 1999) and *D. dechloracetivorans* SF3 (Sun *et al.* 2000), are known OHRB, but their ability for CF dechlorination has not been reported. Moreover, preliminary metagenome analysis showed no presence of known reductive dehalogenase genes (*rdhA*) in the sediment-free enrichment cultures (data not shown). Therefore, *Desulfovibrio* was likely not responsible for the observed CF dechlorination.

Compared to the sediment, the relative abundance of *Clostridium* was increased in the sediment-free enrichment cultures (Fig. 4.5). Acetogens belonging to *Clostridium* and *Acetobacterium* can mediate fortuitous CF dechlorination (Drake *et al.* 2008, Egli *et al.* 1988, Gälli and McCARTY 1989). For instance, *Clostridium* sp. strain TCAIIB was shown to dechlorinate CF to DCM and unidentified products (Gälli and McCARTY 1989), although underlying mechanisms remain unknown. One plausible explanation can be conversion of vitamin B_{12} (cob(III)alamin) to cob(I)/cob(II)alamins by *Clostridium* species (Walker *et al.* 1969, Weissbach *et al.* 1961) that can mediate CF dechlorination.

Addition of extra vitamin B_{12} shifted the dominant CF transformation pathway from reductive dechlorination to DCM, to oxidation to CO_2 (Fig. 4.2, Fig. S4.2) in line with former reports using fermentative (Shan *et al.* 2010) and methanogenic enrichment cultures (Becker and Freedman 1994, Guerrero-Barajas and Field 2005, Rodríguez-Fernández *et al.* 2018b). A

previous study suggested CF oxidation likely via net hydrolysis of CF to CO mediated by enzyme(s) involved in the acetyl-CoA pathway (Egli *et al.* 1988). Except for the acetyl-CoA synthase gene, we detected all genes encoding enzymes involved in the acetyl-CoA pathway in a preliminary metagenome analysis of the sediment-free enrichment cultures (Fig. 4.6). The CO produced from CF could be further oxidized to CO_2 by CO dehydrogenase (Becker and Freedman 1994). We did not detect CO in the enrichment cultures likely due to its rapid conversion to CO_2.

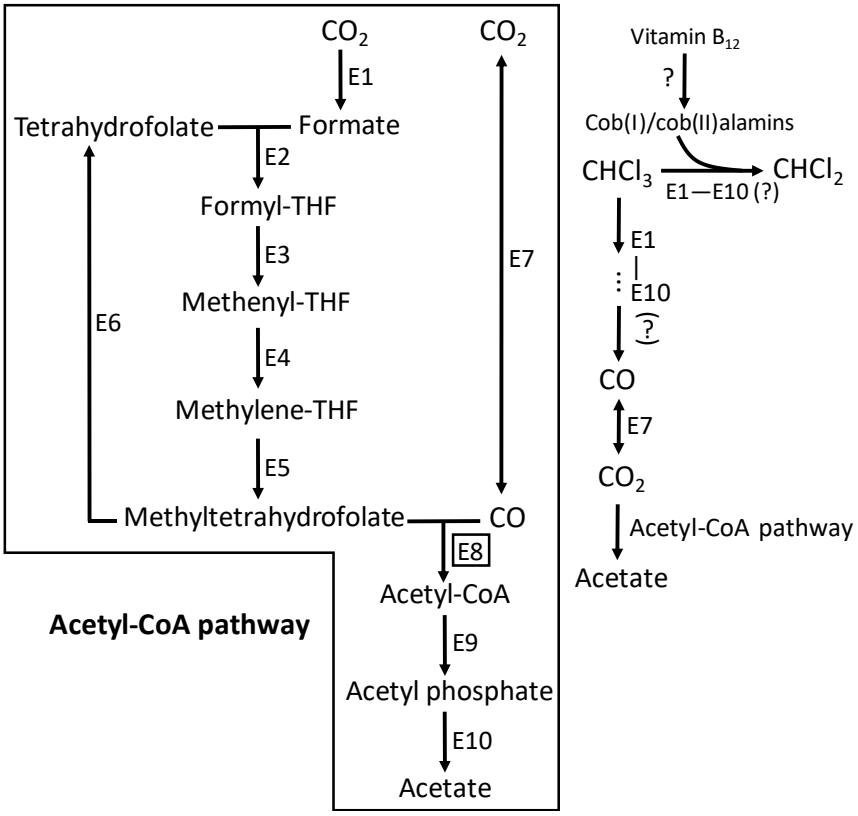

Fig. 4.6 Proposed CF transformation pathway that can be mediated by cob(I)/cob(II)alamins and enzymes involved in acetyl-CoA pathway. Genes encoding all enzymes (E1-E10) were detected in the metagenome sequences of the sediment-free cultures with and without 4 µM vitamin B_{12}, except for the gene encoding acetyl-CoA synthase (E8, enclosed in a square). Enzyme names: E1: formate dehydrogenase, E2: formate-tetrahydrofolate ligase, E3: methylenetetrahydrofolate dehydrogenase, E4: methenyltetrahydrofolate cyclohydrolase, E5: methylenetetrahydrofolate reductase, E6: 5-methyltetrahydrofolate corrinoid/iron sulfur protein methyltransferase, E7: carbon-monoxide dehydrogenase, E8: acetyl-CoA synthase, E9: phosphate acetyltransferase, E10: acetate kinase.

Hypersaline lakes are among the major sources for VOX emissions on Earth (Read *et al.* 2008). This study showed the potential of sediments from pristine hypersaline Lake Strawbridge for CF transformation in cultures with moderate salinity (5%) and alkaline condition (pH 8.5). One possibility is fortuitous CF transformation by enzymes and/or

cobalamin cofactors of acetogens that have been shown in *Acetobacterium woodii* (Hashsham and Freedman 1999) and *Clostridium* sp. (not known for its acetogenic potential) (Gälli and McCARTY 1989). Besides reducing CF toxicity, CF transformation products (DCM, CO, CO_2) can be growth substrates for other microbes, e.g. CO/CO_2 for acetogens (Drake *et al.* 2008), CO_2 for methanogens (Conrad 2007), and DCM for a variety of aerobic and anaerobic microbes that can use it as a carbon and energy source (Chen *et al.* 2018, Hermon *et al.* 2018, Janssen *et al.* 2005, Kleindienst *et al.* 2019, Kleindienst *et al.* 2017, Mägli *et al.* 1996). Therefore, microbial transformations may act as a filter to reduce CF emission from hypersaline lakes.

Acknowledgements

We thank Steffen Kümmel and Florian Tschernikl (UFZ) for their help with the GC/C-IRMS measurement and data analysis, Laura A. Hug and Pascal Weigold for technical assistance for sediment sampling, Mohammad Ali Amoozegar for advice on media selection for halophilic microbes, and the Chemical Biological Soil Laboratory (CBLB) of Wageningen University & Research for assistance with TOC measurement. We acknowledge the China Scholarship Council (CSC) for the support to PP and YL. SA, DS and HS received support by a grant of BE-Basic-FES funds from the Dutch Ministry of Economic Affairs. YL received funding from National Natural Science Foundation of China, project No.51709100. Andreas Kappler and Alexander Ruecker received funding from the research unit 763 “Natural Halogenation Processes in the Environment, Atmosphere and Soil” funded by the German Research Foundation (DFG).

Supplementary Information

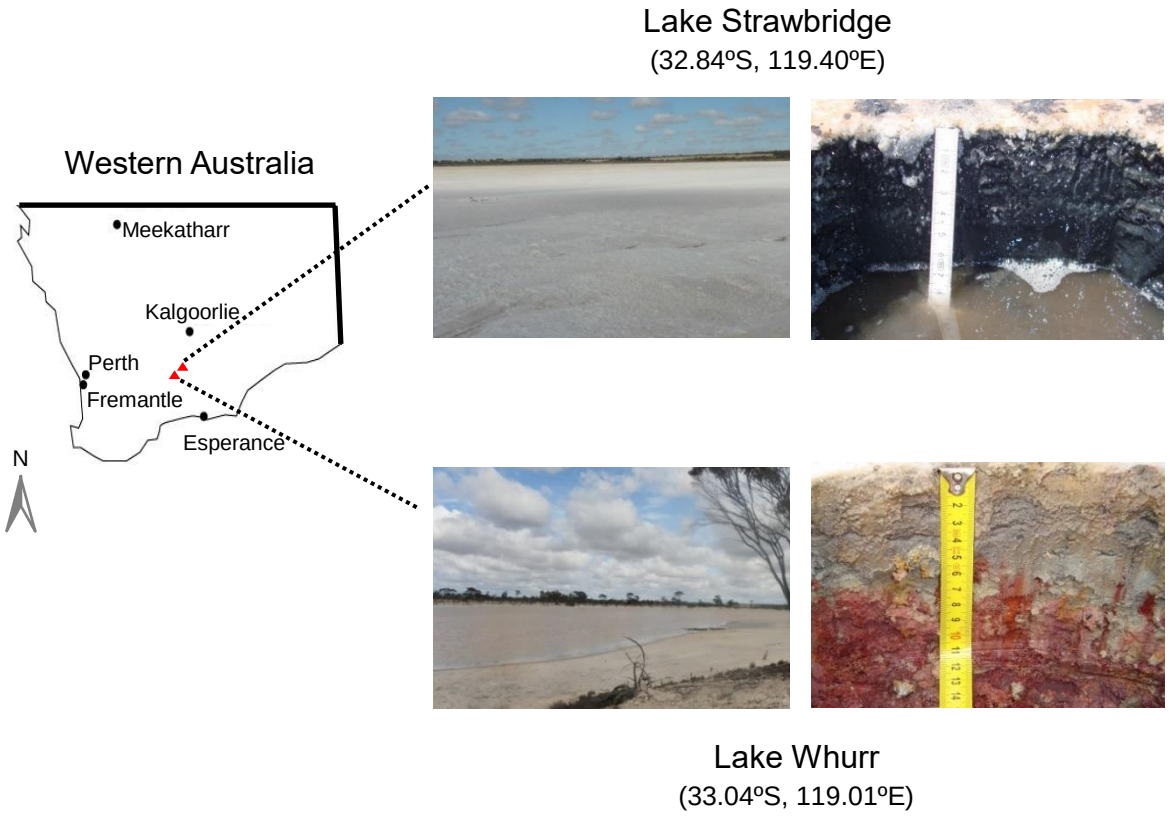

Fig. S4.1 Location and overview of Lake Strawbridge and Lake Whurr. The coordinates of the sampling points and the depth profile are shown in the photos. The photos are a courtesy of Christoph Tubbesing from the Department of Geosciences, Universität Heidelberg.

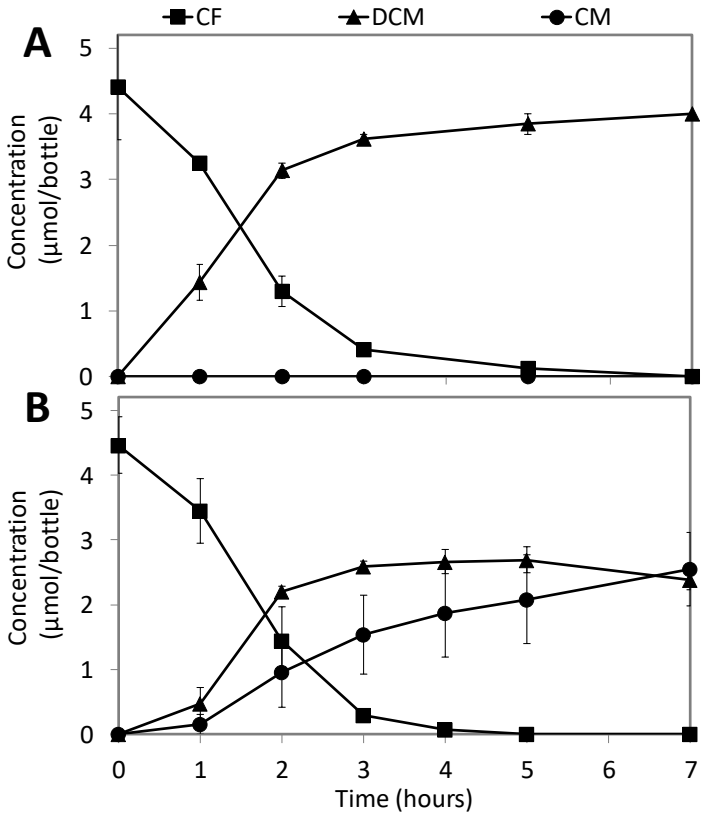

Fig. S4.2 CF transformation in the presence of vitamin B_{12} (4 µM) in MGM medium with dithiothreitol (100 mM) (A) or titanium(III) citrate (5 mM) (B) as the electron donor. Points and error bars represent the average and standard deviation of samples taken from duplicate cultures.

Table S4.1 Media components

Medium type (Salinity %)	pH [a]	Salt water [b] (ml/L)	Demi water (ml/L)	1 M Acetic acid (ml/L)	1 M Tris-base (ml/L)	NH_4Cl (g/L)	Pep-tone (g/L)	Yeast extract (g/L)	Pyru-vate (g/L)	Resa-zurin (g/L)	$Na_2S \cdot 9H_2O$ (g/L)	SL10 trace elements [b] (ml/L)	Vit10 vitamin solution [b] (ml/L)	Cultivated sediment
MGM (20%)	5.4	660	240	10	0	0	5	1	0	0.005	0.48	0	0	LW2 TOP
MGM (17%)	8.1	560	340	0	10	0	5	1	0	0.005	0.48	0	0	LS1 TOP
MGM (15%)	5.5	500	400	10	0	0	5	1	0	0.005	0.48	0	0	LW1 TOP
MGM (14%)	8.3	460	440	0	10	0	5	1	0	0.005	0.48	0	0	LS2 TOP
MGM (11%)	4.6	360	540	10	0	0	5	1	0	0.005	0.48	0	0	LW1&2 BOT
MGM (5%)	8.5	160	740	0	10	0	5 [c]	1 [c]	0	0.005	0.48	0	0	LS 1&2 BOT
DBC (20%)	5.4	660	240	10	0	0.5	0	0	1.1	0.005	0.48	1	3	LW2 TOP
DBC (17%)	8.1	560	340	0	10	0.5	0	0	1.1	0.005	0.48	1	3	LS1 TOP
DBC (15%)	5.5	500	400	10	0	0.5	0	0	1.1	0.005	0.48	1	3	LW1 TOP
DBC (14%)	8.3	460	440	0	10	0.5	0	0	1.1	0.005	0.48	1	3	LS2 TOP
DBC (11%)	4.6	360	540	10	0	0.5	0	0	1.1	0.005	0.48	1	3	LW 1&2 BOT
DBC (5%)	8.5	160	740	0	10	0.5	0	0	1.1	0.005	0.48	1	3	LS 1&2 BOT

Duplicates sediment cores from each hypersaline lake are labelled as as LS-1/2TOP/BOT for Lake Strawbridge and LW1/2-TOP/BOT for Lake Whurr. TOP: top layer, 0–12 cm depth. BOT: bottom layer, 12–24 cm depth

[a] pH was adjusted to the indicated values using 10% HCl or 5 M NaOH

[b] Salt water, SL10 trace elements and Vit10 vitamin solution were prepared as described by Dyall-Smith (Dyall-Smith 2008)

[c] Peptone was decreased from 5 to 0.5 g/L and yeast extract was decreased from 1 to 0.5 g/L in MGM (5%) medium, and glycerol (10 mM) was added as a carbon source in the subsequent sediment-free transfer cultures

Table S4.2 Primers used in this study. All primers target the 16S rRNA gene, except for Unitag primers.

Target	Name [a]	Sequence (5´–3´) [b]	Reference for primer	Reference for PCR/qPCR program
Total bacteria	27F-DegS	GTTYGATYMTGGCTCAG	(van den Bogert *et al.* 2011)	
	338R–I	GCWGCCTCCCGTAGGAGT	(Daims *et al.* 1999)	(Lu *et al.* 2017)
	338R–II	GCWGCCACCCGTAGGTGT		
	Unitag1	GAGCCGTAGCCAGTCTGC	(Tian *et al.* 2016)	(Lu *et al.* 2017)
	Unitag2	GCCGTGACCGTGACATCG		
Total bacteria	Eub341F	CCTACGGGAGGCAGCAG	(Muyzer *et al.* 1993)	(Atashgahi *et al.* 2013)
	Eub534R	ATTACCGCGGCTGCTGGC		
Total archaea	ARC787F	ATTAGATACCCSBGTAGTCC	(Yu *et al.* 2005b)	(Yu *et al.* 2005b)
	ARC1059R	GCCATGCACCWCCTCT		
Desulfitobacterium	Dsb406F	GTACGACGAAGGCCTTCGGGT	(Smits *et al.* 2004)	(Smits *et al.* 2004)
	Dsb619R	CCCAGGGTTGAGCCCTAGGT		
Dehalococcoides	Dco728F	AAGGCGGTTTTCTAGGTTGTCAC	(Smits *et al.* 2004)	(Atashgahi *et al.* 2013)
	Dco944R	CTTCATGCATGTCAAAT		
Dehalobacter	Dre441F	GTTAGGGAAGAACGGCATCTGT	(Smits *et al.* 2004)	(Atashgahi *et al.* 2013)
	Dre645R	CCTCTCCTGTCCTCAAGCCATA		
Geobacter	Geo196F	GAATATGCTCCTGATTC	(Amos *et al.* 2007)	(Azizian *et al.* 2010)
	Geo535R	TAAATCCGAACAACGCTT		
Sulfurospirillum	Sulfuro114F	GCTAACCTGCCCTTTAGTGG	(Sutton *et al.* 2015)	(Sutton *et al.* 2015)
	Sulfuro421R	GTTTACACACCGAAATGCGT		

[a] Primer names may not correspond to original publication

[b] M = A or C; R = A or G; W = A or T; Y = C or T

Table S4.3 Basic features of the assembled metagenomes of the sediment-free enrichment cultures

Sample	Contigs	Total_size (bp)	Contigs N50	Biggest scaffold	GC fraction	Proteins	Domains	ECs	INTERPRO
Sediment-free enrichment (R1)	3553	26037675	44247	333276	0.368	26864	20804	9146	20280
Sediment-free enrichment (R2)	2950	26222661	82451	461805	0.364	26443	21067	9303	20586
Sediment-free enrichment (with 4 µM B12, R1)	2934	25995639	77928	460766	0.366	26070	20838	9238	20371
Sediment-free enrichment (with 4 µM B12, R2)	3553	26000027	78567	460765	0.366	26210	20962	9276	20493

Chapter 5

Reductive dechlorination of 1,2-dichloroethane in the presence of chloroethenes and 1,2-dichloropropane as co-contaminants

Peng Peng [#], Uwe Schneidewind [#], Pieter Jan Haest, Tom N.P. Bosma, Anthony S. Danko, Hauke Smidt, Siavash Atashgahi

[#] equal contribution

Published in *Applied Microbiology and Biotechnology*

Abstract

1,2-dichloroethane (1,2-DCA) is one of the most abundant manmade chlorinated organic contaminants in the world. Reductive dechlorination of 1,2-DCA by organohalide-respiring bacteria (OHRB) can be impacted by other chlorinated contaminants such as chloroethenes and chloropropanes that can co-exist with 1,2-DCA at contaminated sites. The aim of this study was to evaluate the effect of chloroethenes and 1,2-dichloropropane (1,2-DCP) on 1,2-DCA dechlorination using sediment cultures enriched with 1,2-DCA as the sole chlorinated compound (EA culture) or with 1,2-DCA and tetrachloroethene (PCE) (EB culture), and to model dechlorination kinetics. Both cultures contained *Dehalococcoides* as most predominated OHRB, and *Dehalogenimonas* and *Geobacter* as other known OHRB. In sediment-free enrichments obtained from the EA and EB cultures, dechlorination of 1,2-DCA was inhibited in the presence of same concentrations of either PCE, vinyl chloride (VC) or 1,2-DCP, however, concurrent dechlorination of dual chlorinated compounds was achieved. In contrast, 1,2-DCA dechlorination completely ceased in the presence of *cis*-dichloroethene (cDCE) and only occurred after cDCE was fully dechlorinated. In turn, 1,2-DCA did not affect dechlorination of PCE, cDCE, VC and 1,2-DCP. In sediment-free enrichments obtained from the EA culture, *Dehalogenimonas* 16S rRNA gene copy numbers decreased 1–3 orders of magnitude likely due to an inhibitory effect of chloroethenes. Dechlorination with and without competitive inhibition fit Michaelis-Menten kinetics and confirmed the inhibitory effect of chloroethenes and 1,2-DCP on 1,2-DCA dechlorination. This study reinforces that the type of chlorinated substrate drives the selection of specific OHRB, and indicates that removal of chloroethenes and in particular cDCE might be necessary before effective removal of 1,2-DCA at sites contaminated with mixed chlorinated solvents.

Introduction

Understanding biodegradation bottlenecks has been a major objective in efforts to harness the metabolic potential of microorganisms for bioremediation of sites contaminated with organic pollutants (Atashgahi et al. 2018; Meckenstock et al. 2015; Vandermaesen et al. 2016). An important class of such contaminants comprises chlorinated solvents such as chloroethenes, chloroethanes and chloropropanes that have adverse effects on human and environmental health (EPA 2018; Weatherill et al. 2018). Organohalide respiration (OHR) is an example of a microbial metabolism that has been successfully harnessed for engineered remediation of sites contaminated with chlorinated solvents (Atashgahi et al. 2017; Edwards 2014; Ellis et al. 2000). This process is mediated by organohalide-respiring bacteria (OHRB) belonging to distinct genera within the phyla *Chloroflexi* (e.g. *Dehalococcoides* and *Dehalogenimonas*), *Firmicutes* (e.g. *Dehalobacter* and *Desulfitobacterium*) and *Proteobacteria* (e.g. *Sulfurospirillum* and *Geobacter*) (Atashgahi et al. 2016).

One of the challenges of bioremediation is the presence of mixtures of organohalogens at contaminated sites. During dechlorination of co-mingled organohalogens, bioattenuation of specific chlorinated solvents has been shown to be prone to inhibition due to the inhibitory effect of dechlorination intermediates on OHRB, their reductive dehalogenase enzymes, and their syntrophic partners (Chan et al. 2011; Dillehay et al. 2014; Grostern et al. 2009; Mayer-Blackwell et al. 2016). For instance, 1,1,1-trichloroethane (1,1,1-TCA) was shown to strongly inhibit chloroethene reductive dehalogenases of *Dehalococcoides* (Chan et al. 2011). Moreover, long-term exposure to 1,2-dichloroethane (1,2-DCA) was shown to shift the *Dehalococcoides* community within a microbial consortium from vinyl chloride (VC) reductive dehalogenase gene (*vcrA*)-containing *Dehalococcoides* to trichloroethene (TCE) reductive dehalogenase gene (*tceA*)-containing *Dehalococcoides*, leading to diminished VC transforming ability (Mayer-Blackwell et al. 2016). In turn, kinetic modelling using the same culture revealed that 1,2-DCA dechlorination was strongly inhibited by *cis*-dichloroethene (cDCE), and efficient 1,2-DCA dechlorination occurred only when cDCE was completely dechlorinated to VC (Mayer-Blackwell et al. 2016). In another study, presence of 1,1,2-trichloroethane (1,1,2-TCA) and 1,2-dichloropropane (1,2-DCP) inhibited 1,2-DCA dechlorination by *Dehalogenimonas lykanthroporepellens* BL-DC-9 and *D. alkenigignens* IP3-3 (Dillehay et al. 2014). An improved understanding of such inhibitory effects can aid in designing bioremediation approaches for sites contaminated with a mixture of chloroethenes, chloroethanes and/or chloropropanes (Dillehay et al. 2014; Field and Sierra-Alvarez 2004; Mayer-Blackwell et al. 2016).

Different modelling approaches of varying complexity have been developed to understand the reductive dechlorination of chloroethenes with and without competitive inhibition (Chambon et al. 2013). The description of the reaction kinetics varies from first-order

(Corapcioglu et al. 2004; Da Silva and Alvarez 2008) to the more elaborate Michaelis-Menten equations (Garant and Lynd 1998; Haston and McCarty 1999) or Monod kinetics if the responsible OHRB can be sufficiently quantified (Yu and Semprini 2004). The latter two kinetic modelling approaches have been applied at lab- and field-scales to study competitive inhibition (Christ and Abriola 2007; Lai and Becker 2013; Yu et al. 2005), self-inhibition (Haest et al. 2010a), electron donor limitation (Cupples et al. 2004), dechlorination in the presence of multiple bacterial species (Brovelli et al. 2012; Duhamel and Edwards 2006; Haest et al. 2010b), and dechlorination in conjunction with fermentation, sulfate reduction or methanogenesis (Kouznetsova et al. 2010; Malaguerra et al. 2011). The Michaelis-Menten and Monod kinetic modelling approaches can also be used to study the dechlorination of chloroethanes or chloropropanes, however, examples in literature are rare. Notable exceptions are Mayer-Blackwell et al. (2016) who studied concurrent dechlorination of 1,2-DCA and cDCE, and Colombani et al. (2014) who studied 1,2-DCA degradation under the influence of salt water intrusion.

The aim of this study was to evaluate the impact of chloroethenes and 1,2-DCP on 1,2-DCA dechlorination using enrichment cultures containing *Dehalococcoides*, *Geobacter* and *Dehalogenimonas* as the known OHRB. The prime focus was to obtain an improved understanding of 1,2-DCA dechlorination, which is the most abundant chlorinated organic contaminant worldwide (Field and Sierra-Alvarez 2004). 1,2-DCA can be dihaloeliminated to ethene by diverse OHRB including members of the genera *Dehalococcoides* (Maymó-Gatell et al. 1999; Parthasarathy et al. 2015; Wang and He 2013), *Geobacter* (Duhamel and Edwards 2006), *Dehalogenimonas* (Maness et al. 2012), *Desulfitobacterium* (Low et al. 2019; Marzorati et al. 2007) and *Dehalobacter* (Grostern and Edwards 2009). 1,2-DCA has been found to co-exist with chloroethenes and/or chloropropanes at many contaminated sites (Dillehay et al. 2014; Mayer-Blackwell et al. 2016). Despite some reports on suppression of 1,2-DCA dechlorination by co-occurring chloroethenes, chloroethanes and bromoethanes (Dillehay et al. 2014; Mayer-Blackwell et al. 2016; Yu et al. 2013), comprehensive studies on the interaction between 1,2-DCA, 1,2-DCP and chloroethenes with respect to their dechlorination in complex organohalide-respiring microbial consortia are limited.

In this study, in cultures amended with one or two chlorinated compounds (1,2-DCA with either tetrachloroethene (PCE), cDCE, VC or 1,2-DCP), the impact of co-contaminants on OHRB was investigated by quantifying 16S ribosomal RNA (rRNA) genes of known OHRB. The dechlorination reactions were approximated with Michaelis-Menten kinetics taking into account competitive inhibition. Parameter estimation was performed using AMALGAM (Vrugt and Robinson 2007), a multi-objective, multi-method (ensemble) evolutionary optimization procedure to account for the high correlation among the parameters describing dechlorination kinetics and the existence of multiple solutions. Results showed that all applied chlorinated

compounds inhibited 1,2-DCA dechlorination whereas 1,2-DCA had no pronounced inhibitory effect on the dechlorination of other chlorinated compounds.

Materials and Methods

Chemicals

1,2-DCA, chloroethenes, 1,2-DCP, ethene and propene were purchased from Sigma-Aldrich, and were used directly in the following experiments. Lactate stock solution (1 M) was prepared from 60% sodium DL-lactate solution (Sigma-Aldrich). Other organic and inorganic chemicals were of analytical grade and were used without further purification.

Sediment collection and enrichment set-up

Surface sediment samples (down to 15 cm below surface) were collected from a wetland in Estarreja, Portugal. This site has a long history of contamination with agrochemical and fine chemistry effluents (Carvalho *et al.* 2005). Sediment enrichment cultures were set up in 120 mL serum bottles using 10 g of wet sediment and 50 mL of an anoxic medium as described previously (Stams *et al.* 1993). Resazurin (0.005 g/L) and $Na_2S \cdot 9H_2O$ (0.48 g/L) were added as redox indicator and reducing reagent, respectively. The headspace of the bottles was exchanged with N_2 and CO_2 (80:20%, 140 kPa). Lactate (3 mM) was used as the carbon source and electron donor. The electron acceptors for the sediment cultures were PCE (10 µmol/bottle, designed EA culture) and PCE plus 1,2-DCA (10 µmol/bottle each, designed EB culture). The bottles were sealed with Teflon lined butyl rubber stoppers and aluminum crimp caps (GRACE, MD, USA) and incubated statically in the dark at 20°C. EA and EB cultures were spiked 21 times with their respective chlorinated electron acceptors during enrichment. After dechlorination of each spike of the chlorinated substrates to ethene, the headspace of the cultures was flushed with N_2 and CO_2 (80:20%) for three times (3 min for each run and 10 min rest in between each flushing cycle) before re-amendment of the respective chlorinated substrate(s). In the last three spikes, the concentration of each chlorinated substrate was increased stepwise from 10 µmol/bottle to 25 and 40 µmol/bottle. To avoid toxicity of the chlorinated compounds, each single chlorinated substrate was added at 25 µmol/bottle for all the following experiments unless otherwise stated.

Sediment-free cultures were obtained by transferring the EA and EB sediment cultures as following: a 5% slurry from the EA and EB sediment cultures was transferred into bottles containing fresh anoxic medium with lactate (5 mM) and single or double chlorinated substrate mixtures of 1,2-DCA with either PCE, cDCE or VC (Fig. 5.1A). Each transfer culture was amended with three spikes of the respective chlorinated substrate(s), and then diluted to duplicate cultures (50% inoculum, Fig. 5.1B) and amended with another three spikes of the respective chlorinated substrate(s). In parallel, 5% slurries from the EA and EB sediment

cultures were also transferred into bottles containing 1,2-DCP (10 µmol/bottle). Only the EA transfer culture showed 1,2-DCP dechlorination. Therefore only this culture was subsequently transferred (5% inoculum) to fresh anoxic medium with either 1,2-DCP, 1,2-DCA or a mixture of 1,2-DCP and 1,2-DCA (Fig. 5.1C). After depletion of three spikes of the respective chlorinated substrate, these cultures were then diluted to duplicate cultures (50% inoculum, Fig. 5.1D) and amended with another three spikes of the respective chlorinated substrate. The dechlorination pattern of the last (third) spike of chlorinated substrates(s) (Fig. 5.1B, D) was used for kinetic modelling. To study the relief of inhibition by different chlorinated compounds on 1,2-DCA dechlorination, the cultures containing mixture substrates were subsequently spiked with only 1,2-DCA.

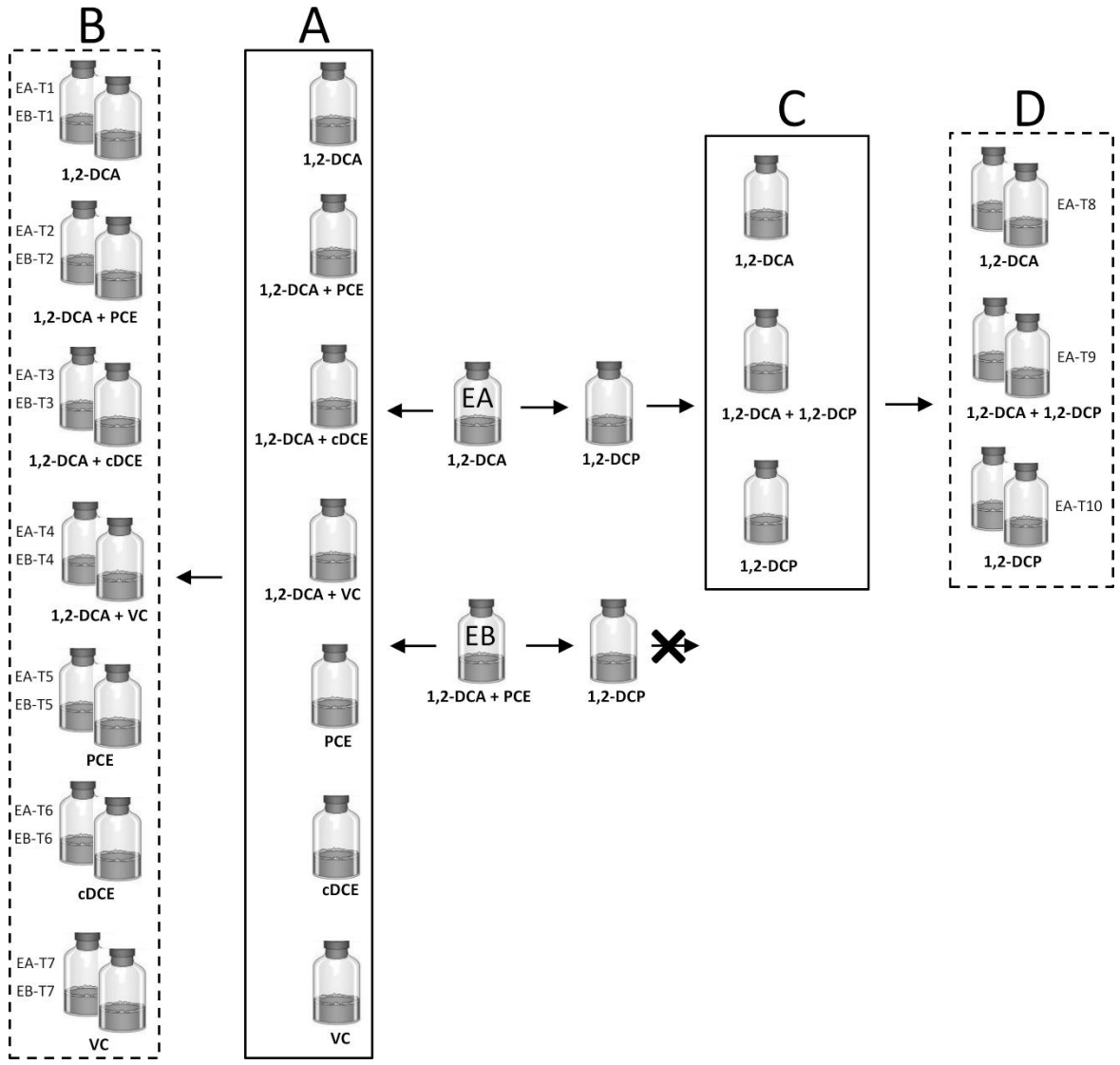

Fig. 5.1 Schematic representation of the experimental set up. Cultures in box A received inoculum from either EA or EB culture. Cultures in dashed boxes (B, D) were used for the kinetic study. The EB culture was not able to dechlorinate 1,2-DCP and hence it was not used for the kinetic study performed using cultures in box D.

DNA extraction and quantitative PCR

After dechlorination of each spike of the chlorinated compounds (respectively 10, 25, and 40 µmol/bottle each compound) in the EA and EB cultures (Fig. 5.1), 2 mL slurry samples were taken for DNA extraction. After dechlorination of the third spike of chlorinated compounds in the sediment-free transfer cultures that were used for kinetic modelling, 2 mL samples were also taken for DNA extraction. DNA was extracted using a DNeasy PowerSoil Kit (QIAGEN, Hilden, Germany) following the manufacturer's instructions. The copy numbers of 16S rRNA genes of total bacteria and OHRB including *Dehalococcoides*, *Geobacter*, *Dehalogenimonas*, *Dehalobacter*, *Desulfitobacterium* and *Sulfurospirillum* were determined by real-time quantitative PCR (qPCR). Assays were performed in triplicates using a CFX384 Real-Time system in a C1000 Thermal Cycler (Bio-Rad Laboratories, USA) with iQ™ SYBR Green Supermix (Bio-Rad Laboratories, USA). The primers and qPCR programs used in this study are listed in Table S5.1.

Analytical methods

Chloroethenes, 1,2-DCA, 1,2-DCP, ethene and propene were analyzed using a gas chromatograph-mass spectrometer (GC-MS) composed of a Trace GC Ultra (Thermo Fisher Scientific, Waltham, MA, USA) equipped with an Rt®-Q-BOND column (Retek, PA, USA) and a DSQ MS (Thermo Fisher Scientific). Helium was used as a carrier gas with a flow rate of 2 ml min^{-1}. The inlet temperature was 100°C. The split ratio was 30. The temperature program of the column was: 40°C hold for 1 min, followed by an increase at 40°C min^{-1} to 260°C and hold for 1.5 min.

Modelling and parameter estimation

Reductive dechlorination of the chloroethenes in cultures shown in Fig. 5.1B and 5.1D was modelled using a Michaelis-Menten model with competitive inhibition following Eq. (1)

$$r_n = \frac{k_{max,n} C_n}{C_n + K_{s,n}\left(1 + \sum_{i=1}^{x} \frac{C_{n+i}}{I_{n+i}}\right)} \quad (1)$$

Where r_n (µM d^{-1}) is the dechlorination rate that depends on the respective chlorinated compound, $k_{max,n}$ (µM d^{-1}) is the compound-specific maximum utilisation rate or degradation constant, $K_{s,n}$ (µM) is the compound-specific half velocity constant, I_n (µM) is the compound-specific competitive inhibition rate, and C_n (µM) is the aqueous concentration of the chlorinated compounds. The index i represents the number of parent compounds considered in the dechlorination during competitive inhibition that varied with enrichment set-up.

Dihaloelimination of 1,2-DCA to ethene and of 1,2-DCP to propene were also modelled using Eq. (1). In the enrichment cultures containing both chloroethenes/1,2-DCP and 1,2-DCA,

competitive inhibition between 1,2-DCA and the other compounds was also included in the models.

As the Michaelis-Menten parameters describing dechlorination are highly correlated, model calibration was performed using AMALGAM (Vrugt and Robinson 2007), a multi-objective, multi-method (ensemble) evolutionary optimization procedure executable in MATLAB. AMALGAM attempts to find for each culture a set of optimal solutions, i.e. an ensemble of optimized kinetics parameters. These solutions have to adhere to the Pareto-principle, which means that all objectives (here, concentrations of the individual dechlorination products) must be met with equal efficiency. The number of Pareto-efficient solutions depends on model complexity, the size of the parameter space as well as the number of model runs and varies for each culture. As such we chose to provide in the results section ranges based on the 50 best parameter combinations of each culture. These were ranked according to their Euclidean distance to the zero-objective-point of our n-dimensional space, where n is the number of culture-specific objectives. Using a compromise solution (Werisch *et al.* 2014, Wöhling *et al.* 2008), the parameter set representing the solution with the smallest Euclidean distance on the Pareto front to the zero-objective point was then utilized to create graphical representations as previously outlined (Schneidewind *et al.* 2014).

All cultures were modelled individually, and models were calibrated on the data obtained from the third spike, during which steady dechlorination patterns were noted. Initially, the cultures with the simplest dechlorination sequences (i.e. VC to ethene or 1,2-DCA to ethene) were modelled, and subsequently model complexity was gradually increased by including additional dechlorination reactions (i.e. cDCE to VC to ethene, etc.). Following this procedure, additional prior information could be used for more complex models to decrease the parameter space (defined by user-set upper and lower boundaries) from which AMALGAM retrieves optimal solutions. Initial boundary values were based on literature (Garant and Lynd 1998, Haest *et al.* 2010a, Haston and McCarty 1999, Mayer-Blackwell *et al.* 2016, Schaefer *et al.* 2009, Schneidewind *et al.* 2014, Yu and Semprini 2004) for chloroethenes and 1,2-DCA. For 1,2-DCP, boundary conditions were derived from simple Lineweaver-Burk plots (Lineweaver and Burk 1934). Dimensionless, species dependent Henry coefficients at 20°C were used to account for volatilisation of the chlorinated compounds in the cultures (PCE = 0.711, trichloroethene (TCE) = 0.419, cDCE = 0.182, VC = 1.075, 1,2-DCA = 0.054, 1,2-DCP = 0.123, ethene = 7.108, propene = 8.923) (Mackay and Shiu 1981, Sander 2015, Staudinger and Roberts 2001).

Results

Reductive dechlorination and dynamics of OHRB in the original sediment cultures

1,2-DCA (10–40 µmol/bottle) was stoichiometrically converted to ethene in the original EA and EB sediment enrichment cultures without production of any chlorinated intermediates indicating 1,2-DCA dihaloelimination (Fig. 5.2A). Besides 1,2-DCA, each spike of PCE (10–40 µmol/bottle) in the EB culture was concurrently dechlorinated to ethene (Fig. 5.2C). *Dehalococcoides* (10^7–10^8 16S rRNA gene copies/mL), *Geobacter* (~10^8 16S rRNA gene copies/mL), and *Dehalogenimonas* (10^6–10^7 16S rRNA gene copies/mL) were the predominant OHRB in the EA culture (Fig. 5.2B). In contrast, *Dehalococcoides* (10^8–10^9 16S rRNA gene copies/mL) was the predominant OHRB in the EB culture, and *Geobacter* and *Dehalogenimonas* numbers were ~10^7 and 10^4 16S rRNA gene copies/mL, respectively (Fig. 5.2D). The 16S rRNA gene numbers of *Dehalobacter*, *Desulfitobacterium* and *Sulfurospirillum* in both EA and EB cultures were below 10^6 copies/mL, representing less than 0.1% of the total bacterial 16S rRNA gene number (Fig. 5.2B, D). The 16S rRNA gene copy numbers of OHRB were rather stable during the three spikes of chlorinated compound(s) (Fig 5.2B, D). Hence for the subsequent sediment-free transfer cultures, qPCR analysis was performed only at the end of the last (third) spike of chlorinated compound(s).

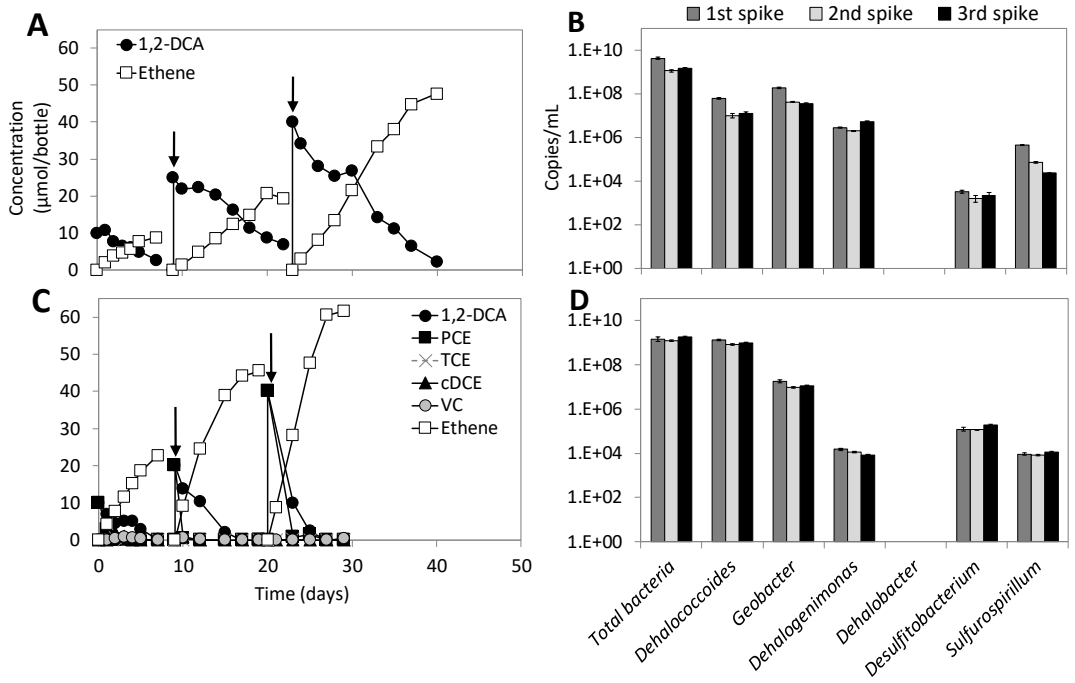

Fig. 5.2 Reductive dechlorination of 1,2-DCA and PCE by the sediment cultures EA (A) and EB (C), and 16S rRNA gene copy numbers of total bacteria, *Dehalococcoides*, *Geobacter*, *Dehalogenimonas*, *Dehalobacter*, *Desulfitobacterium*, *Sulfurospirillum* at the end of each spike (B, D). The arrows in panel A and C indicate re-spike of the chlorinated substrates. Error bars of the qPCR values indicate standard deviations of triplicate qPCRs performed on one sample of each culture.

Dechlorination and co-contaminant effect of 1,2-DCA and chloroethenes

1,2-DCA dechlorination was maintained in the EA and EB sediment-free transfer cultures (cultures EA-T1 and EB-T1, Fig. 5.3A, 5.4A). Moreover, PCE, cDCE and VC were completely dechlorinated to ethene in both EA and EB transfer cultures (EA-T5–T7, Fig. 5.3E–G and EB-T5–T7 cultures, Fig. 5.4E–G), although PCE was not amended in the original EA culture. In EA and EB transfer cultures amended with the same amounts (25 µmol/bottle each spike) of 1,2-DCA and either PCE, cDCE, or VC, dechlorination of 1,2-DCA was delayed (decreased dechlorination rate) by the chloroethenes (EA-T2–T4 cultures, Fig. 5.3B–D and EB-T2–T4 cultures, Fig. 5.4B–D), especially when cDCE was present as co-contaminant, where 1,2-DCA dechlorination did not start until cDCE was depleted (EA-T3 cultures Fig. 5.3C and EB-T3 cultures, Fig. 5.4C). During dechlorination of the third spike, the time to complete dechlorination of 1,2-DCA increased from around three days (Fig. S5.3–S5.4) to 7–14 days (Fig. S5.5–S5.10) in EA transfer cultures in the presence of chloroethenes, and from around three (Fig. S5.23–S5.24) days to 6–8 days (Fig. S5.25–S5.30) in EB transfer cultures. After the third spike, when the cultures with co-contaminants (Fig. 5.3B–D, Fig. 5.4B–D) were amended with only 1,2-DCA, its dechlorination was completed in 2–5 days in both EA and EB transfer cultures (Fig. S5.2A–F), whereas the same amount of 1,2-DCA was dechlorinated in 6–14 days in the presence of chloroethenes. In contrast, no pronounced inhibitory effect of 1,2-DCA on chloroethene dechlorination was observed. Dechlorination of chloroethenes was comparable between cultures where chloroethenes were amended as a single compound (EA-T5–T7 cultures, Fig. 5.3E–G, S5.11–S5.16 and EB-T5–T7 cultures, Fig. 5.4E–G, S5.31–S5.36) and cultures where they were added together with 1,2-DCA (EA-T2–T4 cultures, Fig. 5.3B–D, S5.5–S5.10 and EB-T2–T4 cultures, Fig. 5.4B–D, S5.25–S5.30).

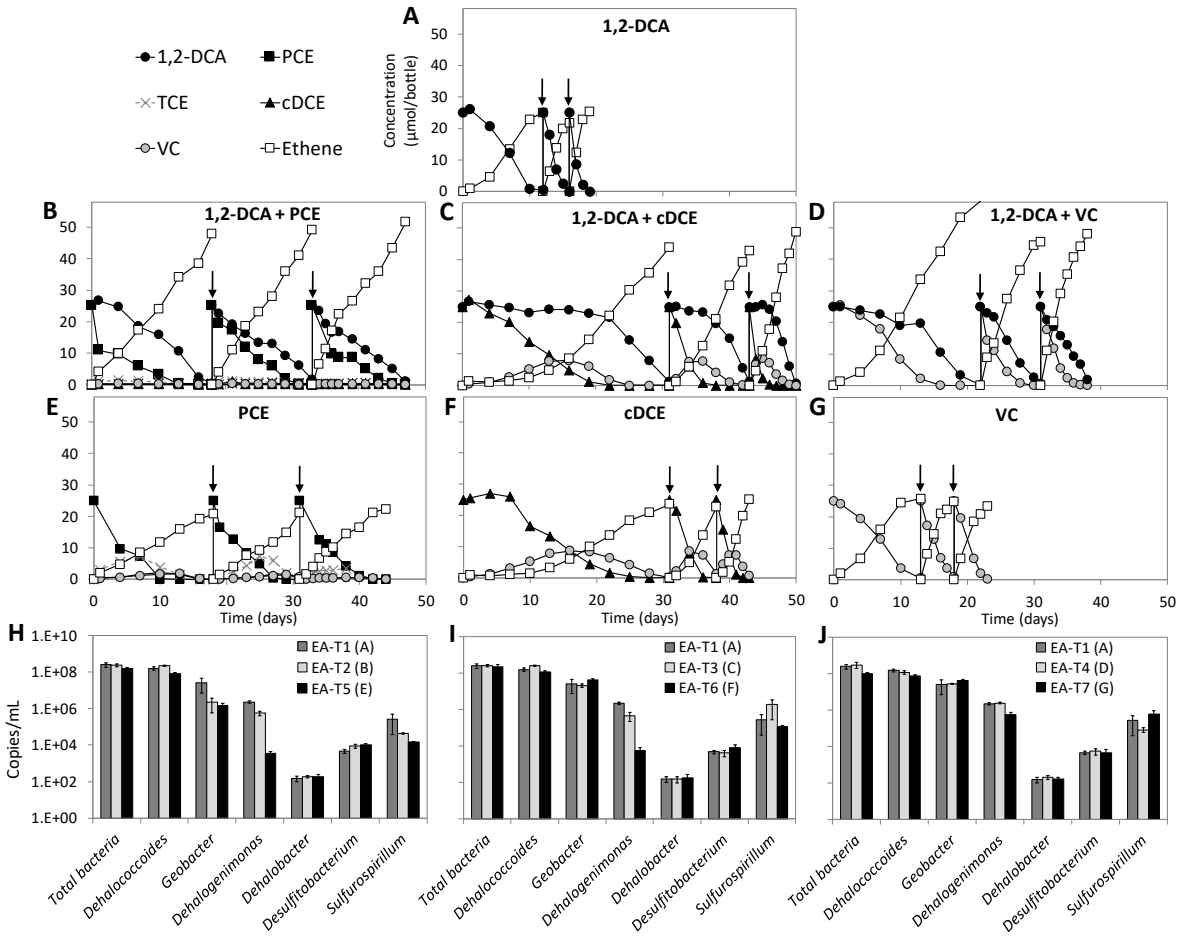

Fig. 5.3 Reductive dechlorination of 1,2-DCA (EA-T1, A), 1,2-DCA plus PCE (EA-T2, B), 1,2-DCA plus cDCE (EA-T3, C), 1,2-DCA plus VC (EA-T4, D), PCE (EA-T5, E), cDCE (EA-T6, F), VC (EA-T7, G) in the sediment-free enrichment cultures obtained from EA sediment culture, and 16S rRNA gene copy numbers of total bacteria, *Dehalococcoides*, *Geobacter*, *Dehalogenimonas*, *Dehalobacter*, *Desulfitobacterium*, *Sulfurospirillum* at the end of the third spike in these cultures (H, I, J). Each concentration value represents the average measured from duplicate cultures. The arrows in panel A–G indicate re-spike of the chlorinated substrates. Error bars were not included in panels A–G for clarity. Error bars of the qPCR values indicate standard deviations of triplicate qPCRs performed on one sample of each of the duplicate cultures (n = 2 × 3).

The 16S rRNA gene copy number of *Dehalococcoides* in EA transfer cultures (~10^8 copies/mL, Fig. 5.3H–J) was about one order of magnitude higher than in the original EA sediment culture (Fig. 5.2B), whereas the 16S rRNA gene copy numbers of *Dehalococcoides* in the EB culture (10^8–10^9 copies/mL, Fig. 5.2D) and its transfer cultures (Fig. 5.4H–J) were similar. In EA transfer cultures, *Dehalogenimonas* 16S rRNA gene copy numbers were 1–3 orders of magnitude higher in the cultures fed 1,2-DCA, VC or 1,2-DCA plus chloroethenes (PCE, cDCE, VC) than in the cultures fed only PCE or cDCE (Fig. 5.3H–J). The 16S rRNA gene copy numbers of *Dehalogenimonas* were below 10^3 in the EB transfer cultures (Fig.

5.4H–J), in line with the pattern in the EB sediment culture (Fig. 5.2D). The 16S rRNA gene copy numbers of *Geobacter* in the EA and EB transfer cultures were 10^7–10^8 copies/mL (Fig. 5.3H–J, 5.4H–J).

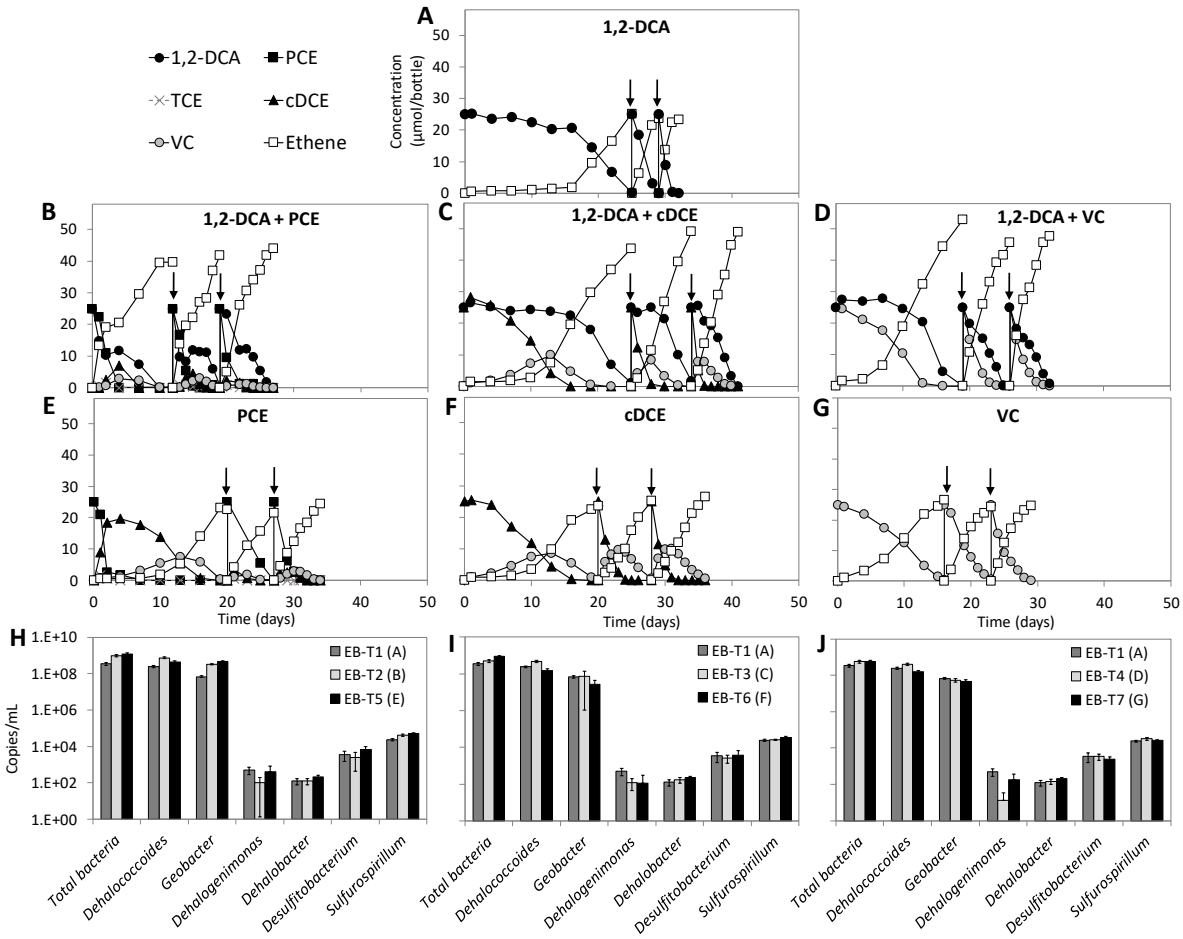

Fig. 5.4 Reductive dechlorination of 1,2-DCA (EB-T1, A), 1,2-DCA plus PCE (EB-T2, B), 1,2-DCA plus cDCE (EB-T3, C), 1,2-DCA plus VC (EB-T4, D), PCE (EB-T5, E), cDCE (EB-T6, F), VC (EB-T7, G) in the sediment-free enrichment cultures obtained from EB sediment culture, and 16S rRNA gene copy numbers of total bacteria, *Dehalococcoides*, *Geobacter*, *Dehalogenimonas*, *Dehalobacter*, *Desulfitobacterium*, *Sulfurospirillum* at the end of the third spike in these cultures (H, I, J). Each concentration value represents the average measured from duplicate cultures. The arrows in panel A–G indicate re-spike of the chlorinated substrates. Error bars were not included in panels A–G for clarity. Error bars of the qPCR values indicate standard deviations of triplicate qPCRs performed on one sample of each of the duplicate cultures (n = 2 × 3).

Dechlorination and co-contaminant effect of 1,2-DCA and 1,2-DCP

The original EA and EB sediment cultures had not been amended with 1,2-DCP. To study the co-contaminant effect between 1,2-DCA and 1,2-DCP, EA and EB cultures were first transferred (5% inoculum) to fresh media containing only 1,2-DCP (10 µmol/bottle). During 70

days of incubation, more than 90% of the 1,2-DCP in the EA transfer culture was dechlorinated to propene (Fig. S5.1), whereas no 1,2-DCP dechlorination was observed in the EB transfer culture (data not shown). Therefore, the EA transfer culture fed 1,2-DCP was used to study the co-contaminant effect (Fig. 5.1D). In the subsequent transfer cultures, 1,2-DCP dechlorination was stably maintained (cultures EA-T10, Fig. 5.5C), while 1,2-DCA was also dechlorinated (cultures EA-T8, Fig. 5.5A). Similar to the co-contaminant effect between 1,2-DCA and chloroethenes, 1,2-DCA dechlorination was inhibited in the transfer cultures concurrently amended with 1,2-DCP, whereas no obvious inhibitory effect of 1,2-DCA on 1,2-DCP dechlorination was observed (cultures EA-T9, Fig. 5.5B). Specifically, the time to complete dechlorination of 1,2-DCA was increased from around three days (Fig. S5.17–S5.18) to nine days in the presence of 1,2-DCP (Fig. S5.19–S5.20), while 1,2-DCP dechlorination was not inhibited (Fig. S19–S22). When these cultures were amended only with 1,2-DCA, its dechlorination was completed in two days (Fig. S5.2G), which was strongly enhanced compared to its dechlorination in the presence of 1,2-DCP (same amount of 1,2-DCA was dechlorinated in nine days) (Fig. 5.5B). *Dehalococcoides* (~10^8 16S rRNA gene copies/mL), *Geobacter* (~10^7 16S rRNA gene copies/mL) and *Dehalogenimonas* (10^6–10^7 16S rRNA gene copies/mL) were the predominant known OHRB in these transfer cultures, similar to EA transfer cultures amended with 1,2-DCA and chloroethenes (Fig. 5.3H–G, Fig. 5.5D).

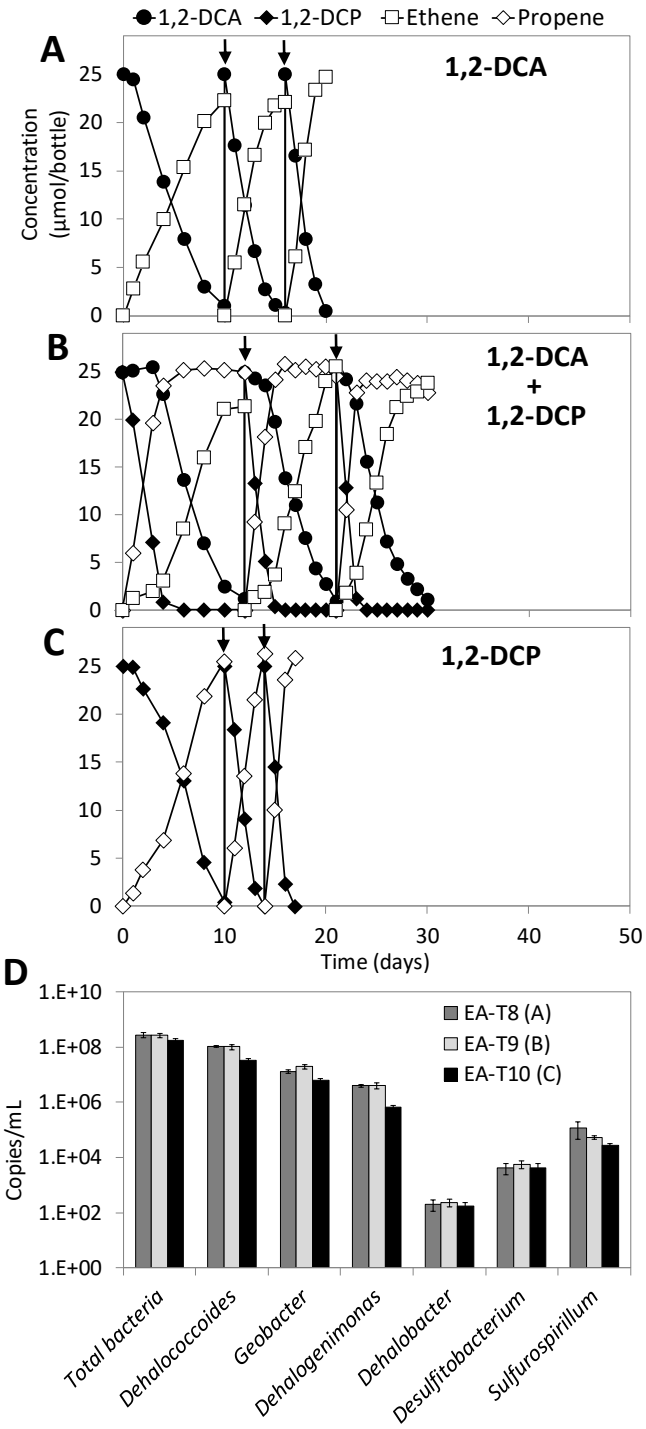

Fig. 5.5 Reductive dechlorination of 1,2-DCA (EA-T8, A), 1,2-DCA plus 1,2-DCP (EA-T9, B), 1,2-DCP (EA-T10, C) in sediment-free cultures derived from the EA transfer culture amended with 1,2-DCP, and 16S rRNA gene copy numbers of total bacteria, *Dehalococcoides*, *Geobacter*, *Dehalogenimonas*, *Dehalobacter*, *Desulfitobacterium*, *Sulfurospirillum* at the end of the third spike in these cultures (D). Each concentration value represents the average measured from duplicate cultures. The arrows in panel A–C indicate re-spike of the chlorinated substrates. Error bars were not included in panels A–C for clarity. Error bars of the qPCR values indicate standard deviations of triplicate qPCRs performed on one sample of each of the duplicate cultures (n = 2 × 3).

Dechlorination kinetics

Table 5.1 provides a summary of parameter ranges for all compounds as compared to values from previous studies. Those parameter ranges were obtained by modelling dechlorination after the third spike only. Maximum and minimum values of the 50 best parameter combinations for individual cultures are shown in Table S5.2. K_s and I values of the chloroethenes are in the same range as in the previous studies listed in Table 5.1. A comparison of values of k_{max} is less straight forward as many studies provide k_{max} in units related to the bacterial cell or protein mass. k_{max} estimates for PCE and TCE obtained here are similar to those in Haston and McCarty (1999) and Schneidewind *et al.* (2014) whereas k_{max} estimates for cDCE and VC in this study were about one order of magnitude higher.

A comparison of parameter estimates for 1,2-DCP dechlorination was not possible due to the lack of kinetic models in literature. Parameter estimates of 1,2-DCA were comparable to those found by Mayer-Blackwell et al. (2016). However, in our study they span a rather wide range, defined by cultures EA-T9, where concurrent dechlorination of 1,2-DCA and 1,2-DCP occurred (see Fig. S5.19 and S5.20 and Table S5.2), as further discussed below.

In general, modelled and observed results showed a good fit for cultures amended with a single chlorinated compound (e.g., EA-T1, EA-T7, Figs. S5.3–S5.4, S5.15–S5.16) indicated by low root-mean-square errors (RMSE, data not shown). Model fits decreased (higher RMSE) for the cultures with more complex reaction networks (e.g., EB-T2, Fig. S5.25–S5.26). Duplicate batches showed comparable parameter ranges, and parameters differed by less than one order of magnitude. A notable exception is experiment EA-T9 (Fig. S5.19, S5.20) where one of the replicate cultures (culture A) showed relatively narrow parameter ranges for 1,2-DCA whereas parameter ranges for culture B for 1,2-DCA varied by several orders of magnitude.

Table 5.1 Range of parameter estimates obtained from modelling using a Michaelis-Menten kinetics approach in comparison to previous studies.

Parameter	Unit	This work	Garant and Lynd (1998) [a]	Haston and McCarty (1999) [b]	Yu and Semprini (2004) [c]	Schneidewind et al. (2014) [d]	Mayer-Blackwell et al. (2016) [e]
$k_{max,PCE}$	[µM d^{-1}]	38.7—443.4	15550 [f]	77	12.4 / 13.3 [g]		
$K_{s,PCE}$	[µM]	≤ 1.0	70.7	0.1	1.6 / 3.9		
I_{PCE}	[µM]	3.7—370	70.7		1.6 / 3.9		
$k_{max,\ TCE}$	[µM d^{-1}]	39.5—1000	9380 [f]	59	124 / 125 [g]	2.6—12	
$K_{s,TCE}$	[µM]	0.1—14	17.4	1.4	1.8 / 2.8	2.1—42	
I_{TCE}	[µM]	3.7—370	17.4		1.8 / 2.8	3.7—37	
$k_{max,cDCE}$	[µM d^{-1}]	139.7—245.2	5880 [f]	14	13.8 / 22 [g]	0.9—94.4	2688
$K_{s,cDCE}$	[µM]	< 0.1—50.8	11.9	3.3	1.8 / 1.9	3.8—37.8	8.5
I_{cDCE}	[µM]	3.7—370	11.9		1.8 / 1.9	3.7—370	9
$k_{max,\ VC}$	[µM d^{-1}]	127.4—161	6670 [f]	13	2.4 / 8.1 [g]	0.4—14.4	
$K_{s,VC}$	[µM]	17.7—26.3	383	2.6	62.6 / 60.2	3.8—37.8	
I_{VC}	[µM]	3.7—370			62.6 / 60.2		
$k_{max,DCA}$	[µM d^{-1}]	< 0.1—7535.8 [h]					960
$K_{s,DCA}$	[µM]	< 0.1—1032.5 [i]					127
I_{DCA}	[µM]	< 0.1—370 [j]					45
$k_{max,DCP}$	[µM d^{-1}]	220.5—243.1					
$K_{s,DCP}$	[µM]	≤ 1.1					
I_{DCP}	[µM]	1.2—370					

[a] from Table II of the reference (competitive case);
[b] from Table 2 of the reference;
[c] from Table II of the reference, first number EV, second number PM;
[d] from Table 2 of the reference;
[e] from Table 3 of the reference;
[f] [µmol/d and g cells];
[g] [µmol/d and mg protein];
[h,i,j] for 1,2-DCA in batches without 1,2-DCP: 157.9 ≤ $k_{max,DCA}$ ≤ 1428.9, 2.9 ≤ $K_{s,DCA}$ ≤ 1032.5, 2.5 ≤ I_{DCA} ≤ 250

Discussion

The present study revealed inhibition of 1,2-DCA dechlorination in the presence of chloroethenes and 1,2-DCP using organohalide-respiring microbial consortia obtained from a wetland contaminated with agrochemical products. Among the tested chlorinated substrates, cDCE showed the strongest inhibitory effect on 1,2-DCA dechlorination. Dechlorination of 1,2-DCA started only when cDCE was completely depleted (culture EA-T3, Fig. 5.3C and culture EB-T3, Fig. 5.4C). This is consistent with previous findings showing that cDCE strongly inhibited 1,2-DCA dechlorination using a continuous enrichment culture containing *Dehalococcoides* (Mayer-Blackwell *et al.* 2016). We also noted inhibition of 1,2-DCA dechlorination in the presence of PCE, VC and 1,2-DCP, further supported by the decreased $k_{max,DCA}$ and increased $K_{s,DCA}$ values compared to the cultures amended with 1,2-DCA only. Notably, the inhibitory pattern of PCE, VC and 1,2-DCP on 1,2-DCA dechlorination was different from that of cDCE. In cultures containing 1,2-DCA with either PCE, VC or 1,2-DCP as the co-contaminants, the cultures concurrently dechlorinated both amended chlorinated compounds. However, delayed dechlorination of 1,2-DCA due to decreased dechlorination rate was observed during concurrent dechlorination of 1,2-DCA and PCE (culture EA-T2, Fig. 5.3B and culture EB-T2, Fig. 5.4B), probably because of transient cDCE production from PCE.

The observed inhibitory impact of VC on 1,2-DCA dechlorination is in contrast to what was reported by Mayer-Blackwell et al. (2016) using a continuous enrichment culture containing *Dehalococcoides* where VC had a negligible inhibitory effect on 1,2-DCA dechlorination. Interestingly, Mayer-Blackwell et al. (2016) found that long-term exposure of the continuous culture to 1,2-DCA shifted the *Dehalococcoides* population, leading to diminished VC dechlorinating ability. In contrast, we found no inhibitory effect of 1,2-DCA on the dechlorination of chloroethenes and 1,2-DCP in batch cultures.

Based on the data presented here, it is likely that the original sediments in EA and EB cultures contained at least two different *Dehalococcoides* populations. The 1,2-DCP dechlorinating population was maintained during enrichment in the presence of 1,2-DCA (EA culture) but likely lost during incubation in the presence of 1,2-DCA plus PCE (EB culture). This suggests that 1,2-DCA but not PCE was also a growth substrate for the 1,2-DCP dechlorinating *Dehalococcoides* population, whereas PCE was likely a substrate for the other *Dehalococcoides* population. The EA transfer cultures were also able to dechlorinate PCE (Fig. 5.3B, E). This indicates that feeding 1,2-DCA alone in the EA sediment culture also maintained the *Dehalococcoides* population capable of PCE dechlorination, and therefore 1,2-DCA was also a growth substrate for the PCE-dechlorinating *Dehalococcoides* population. Feeding 1,2-DCA plus PCE likely promoted selective growth of the 1,2-DCA/PCE dechlorinating *Dehalococcoides* over the 1,2-DCA/1,2-DCP dechlorinating *Dehalococcoides*. This is also likely the reason for the loss of *Dehalogenimonas* in the EB culture, as

Dehalogenimonas is known to dechlorinate 1,2-DCA and 1,2-DCP via dihaloelimination but does not dechlorinate PCE (Bowman *et al.* 2013, Moe *et al.* 2009). Accordingly, *Dehalogenimonas* was only maintained in the EA transfer cultures amended with substrates known to support *Dehalogenimonas* growth (e.g. 1,2-DCA or 1,2-DCA plus VC or 1,2-DCA plus 1,2-DCP) (Maness *et al.* 2012, Martín-González *et al.* 2015, Moe *et al.* 2016, Yang *et al.* 2017) (Fig. 5.3H–J). Notably, feeding solely PCE or cDCE that are not known growth substrates for *Dehalogenimonas* decreased *Dehalogenimonas* 16S rRNA gene copy numbers by 1–3 orders of magnitude (Fig. 5.3H, I), whereas feeding solely VC or 1,2-DCP that are known substrates to support *Dehalogenimonas* growth (Bowman *et al.* 2013, Moe *et al.* 2009, Yang *et al.* 2017) did not strongly reduce its 16S rRNA gene copy numbers (Fig. 5.3J, 5.4D). *Geobacter*, which is known to dechlorinate PCE/TCE (Sung *et al.* 2006), and 1,2-DCA (Duhamel and Edwards 2007), was stably maintained in both EA (Fig. 5.3H–J) and EB (Fig. 5.4H–J) transfer cultures. Our results indicate that the type of chlorinated substrate drives the selection of OHRB. Likewise, a recent study showed that a *Dehalococcoides* population shift was driven by different chlorinated electron acceptors in enrichment cultures containing *Dehalococcoides* and at a contaminated site (Pérez-de-Mora *et al.* 2018).

Michaelis-Menten kinetics could be successfully used to model dechlorination after the third spike where near steady-state conditions were observed. Parameter estimates obtained here compare well with those obtained in previous studies (see Table 5.1). Different kinetic models could be better suited to model dechlorination after the first and the second spikes. Especially dechlorination after the first spike might be modelled more successfully using Monod kinetics (see also Schneidewind et al., 2014) to better account for an apparent lag phase before the onset of dechlorination. However, Monod modelling was not used in this study due to limited information on microbial interactions (growth and decay patterns).

An interpretation of competitive inhibition is not straightforward from the obtained inhibition constants *I* (Table S5.2). For example, cDCE seems to have a pronounced effect on 1,2-DCA dechlorination only at starting concentrations of cDCE (~I_{cDCE}). As soon as cDCE concentrations drop by a factor ≥10, inhibition of 1,2-DCA dechlorination by cDCE becomes much less important. The calibrated inhibition constants suggest that VC is a stronger inhibitor on 1,2-DCA dechlorination than cDCE in all cultures except EB-T2 (I_{vc} is substantially below I_{cDCE}). However, I_{VC} is largest in cultures EA-T4 and EB-T4 where no higher chlorinated compounds were present. A higher competitive inhibition constant indicates a smaller inhibitive effect. The parameter for VC probably lumps inhibition effects from higher chlorinated parent products when present, resulting in a higher simulated inhibition effect of VC in mixed compound tests.

In addition, interpreting parameter estimates (especially inhibition constants) obtained from cultures with multiple chlorinated compounds proved challenging, as strong cross-

correlation exists among the parameters of the Michaelis-Menten kinetics. For example, we observed comparable K_s and k_{max} values for chloroethenes and 1,2-DCP in cultures with and without 1,2-DCA. In contrast, $k_{max,DCA}$ values decreased and $K_{s,DCA}$ values increased in multi-compound cultures compared to the cultures amended with 1,2-DCA only. This hints towards an effect of the chloroethenes and 1,2-DCP on 1,2-DCA dechlorination. However, the best parameter combination did not put this effect in the inhibition constants, but rather in the degradation constants of 1,2-DCA itself. Another example is the EA-T9 culture: a small K_s of 1,2-DCA is counteracted by a small inhibition constant of 1,2-DCP in the duplicate cultures. In other words, the obtained parameters suggest that dechlorination of 1,2-DCA could occur at a maximal rate at low substrate concentration, but would then be more inhibited by 1,2-DCP; or in contrast, the maximal dechlorination rate of 1,2-DCA is not attained under the current experimental conditions but its dechlorination would be less inhibited by 1,2-DCP. However, both parameter combinations would yield a proper fit of the experimental observations, proving the non-uniqueness of the solution (Beven 2001).

The use of results from less complex culture set-ups in the refinement of the parameter space, from which AMALGAM choses viable solutions for more complex set-ups (e.g., EA-T1, EA-T4 and EA-T6 for EA-T2) allowed us to reduce the uncertainty on the parameter estimates. However, the problem of non-uniqueness still remains, i.e., the existence of multiple parameter combinations producing an equally good fit. Uncertainty on the parameter estimates arises due to incomplete or insufficient information on the dechlorination processes in the individual cultures (e.g. information on microbial interactions or on necessary micro-nutrients).

In conclusion, the identified inhibitory effect of chloroethenes and 1,2-DCP on 1,2-DCA dechlorination in this study has important implications for understanding the persistence of 1,2-DCA at contaminated sites. For effective bioremediation of such contaminated sites, it will be necessary to first remove potential inhibitors such as cDCE as well as its parent compounds PCE and TCE, which can inhibit 1,2-DCA dechlorination and even cause loss of 1,2-DCA/1,2-DCP dechlorinating *Dehalococcoides* and *Dehalogenimonas* populations. Further studies are needed to better understand the inhibitory mechanisms. Possible experimental approaches include identification of the genes and enzymes involved in 1,2-DCA dichlorination, study the transcriptional regulation of these genes, and competitive inhibition of the enzymes. Theoretical modelling experiments that more rigorously look into the effect of the size of the parameter space or the use of different estimation algorithms could further improve our understanding of parameter/model uncertainty.

Acknowledgements

This study was supported by the BE-BASIC funds (grant F08.004.01) from the Dutch Ministry of Economic Affairs, and the Gravitation grant (project 024.002.002) of the

Netherlands Ministry of Education, Culture and Science and the Netherlands Science Foundation (NWO). PP was supported by the China Scholarship Council (CSC). The assistance of Rita Lopes and Olga Nunes (FEUP), and Nora B. Sutton (Wageningen University & Research) is greatly appreciated.

Supplenmentary Information

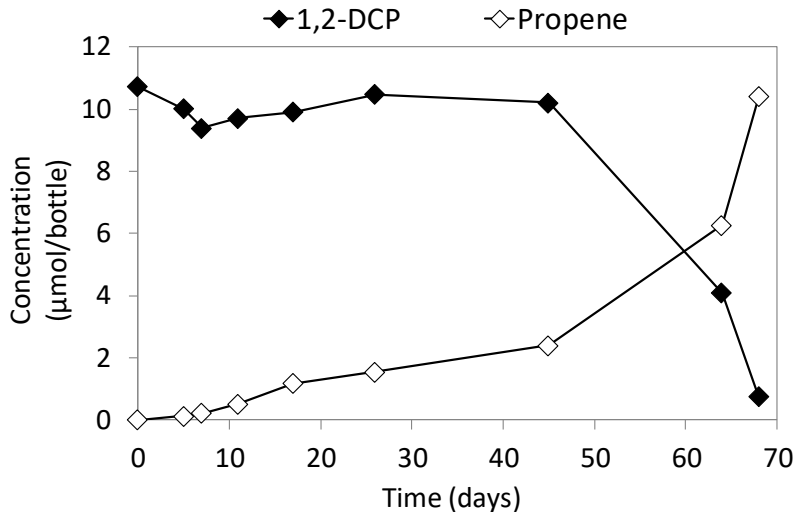

Fig. S5.1 Reductive dechlorination of 1,2-DCP in EA transfer culture.

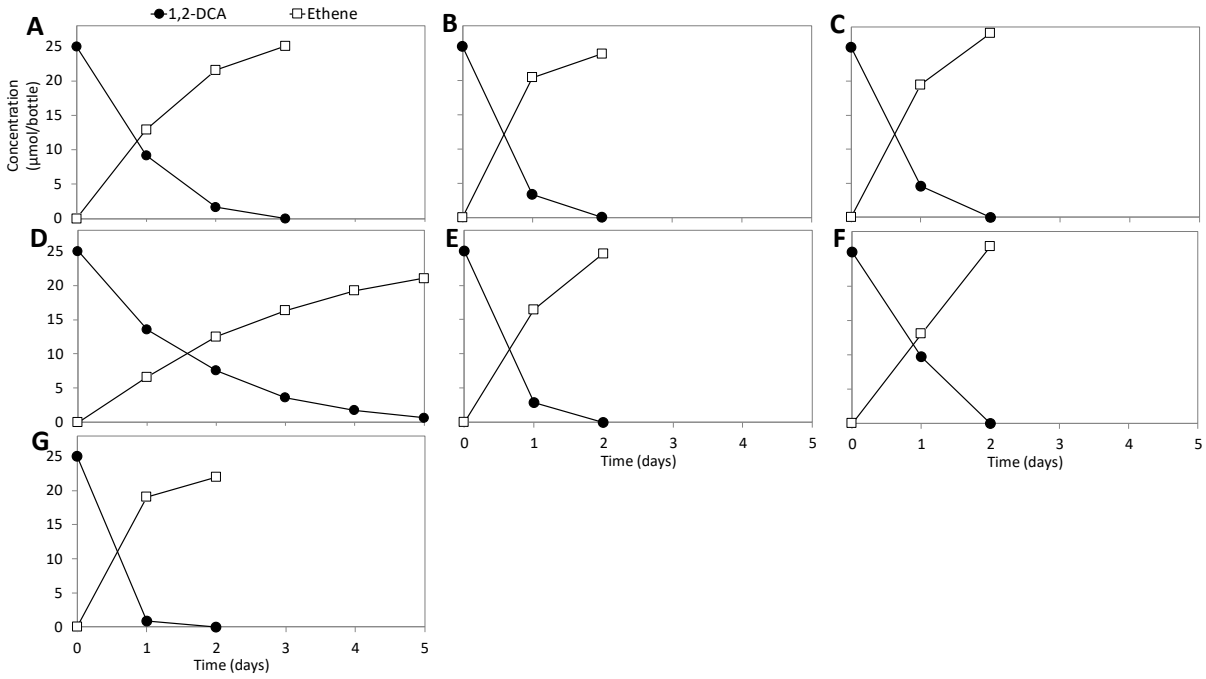

Fig. S5.2 Reductive dechlorination of 1,2-DCA alone in EA and EB transfer cultures previously amended with 1,2-DCA plus PCE (cultures EA-T2 and EB-T2) (A, D); 1,2-DCA plus cDCE (cultures EA-T3 and EB-T3) (B, E); 1,2-DCA plus VC (cultures EA-T4 and EB-T4) (C, F); 1,2-DCA plus 1,2-DCP (cultures EA-T9) (G). Each concentration value represents the average measured from duplicate cultures.

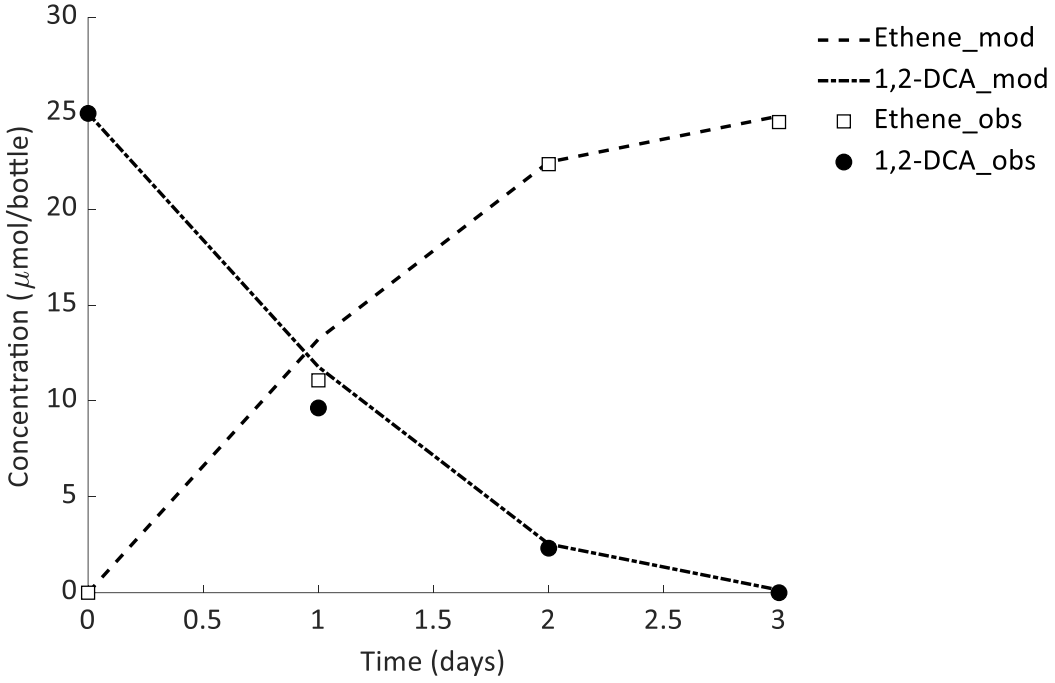

Fig. S5.3 Modeled (mod) and observed (obs) concentrations in culture EA-T1_A.

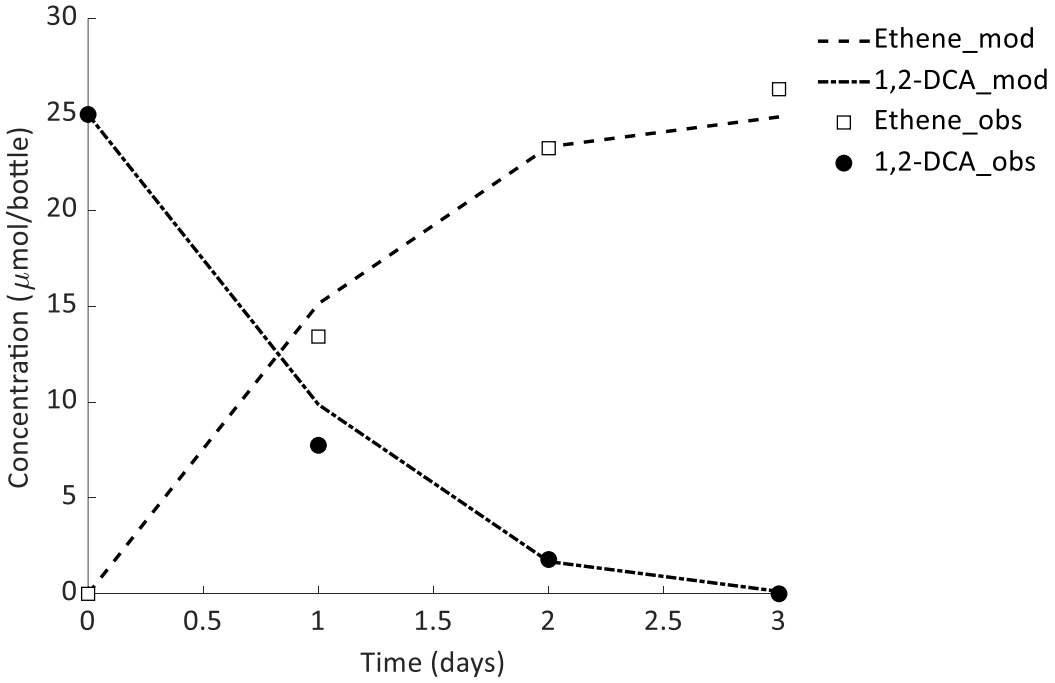

Fig. S5.4 Modeled (mod) and observed (obs) concentrations in culture EA-T1_B.

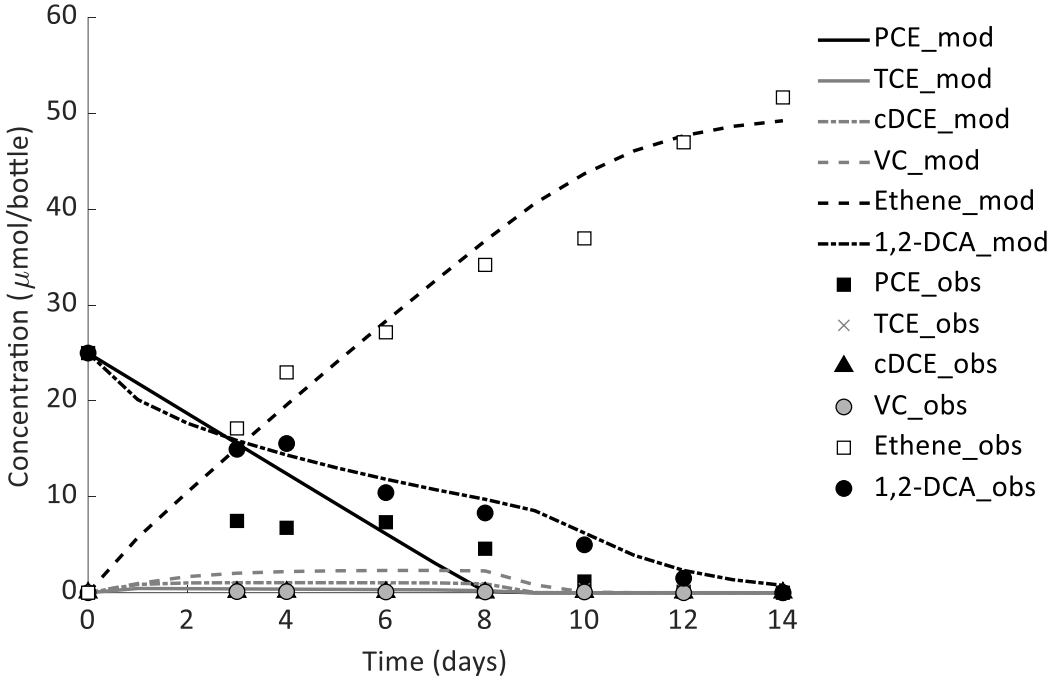

Fig. S5.5 Modeled (mod) and observed (obs) concentrations in culture EA-T2_A.

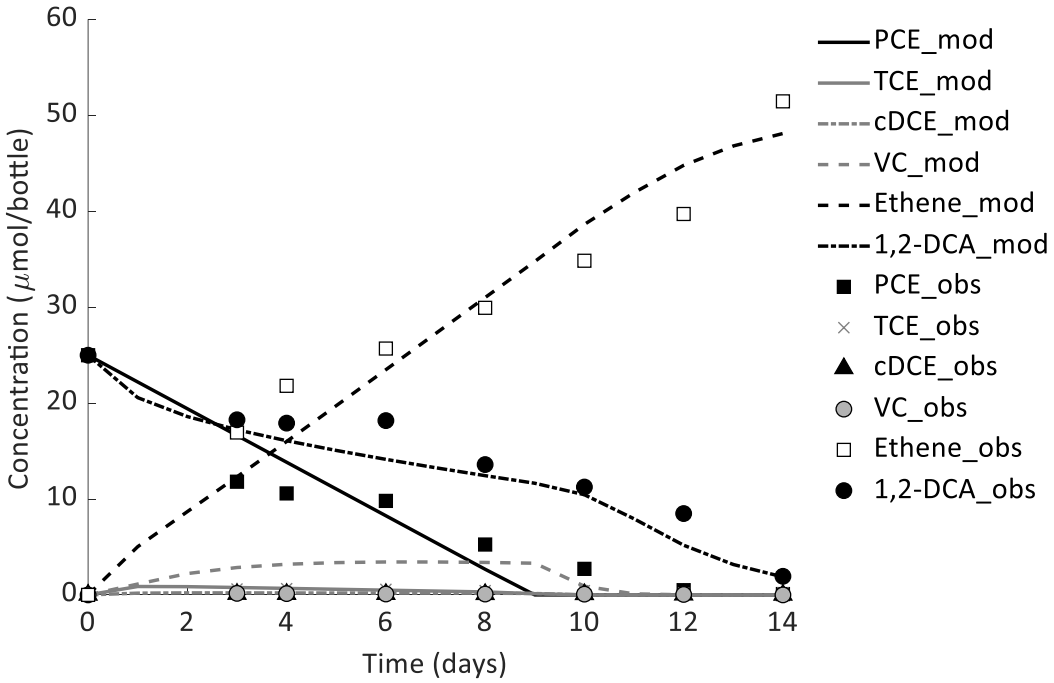

Fig. S5.6 Modeled (mod) and observed (obs) concentrations in culture EA-T2_B.

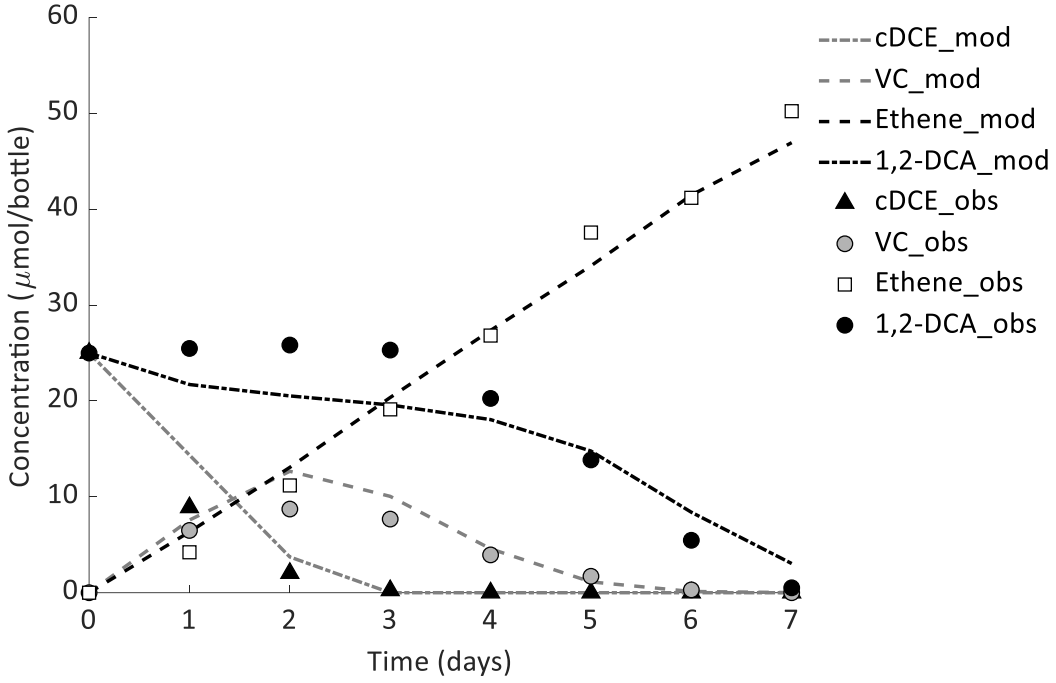

Fig. S5.7 Modeled (mod) and observed (obs) concentrations in culture EA-T3_A.

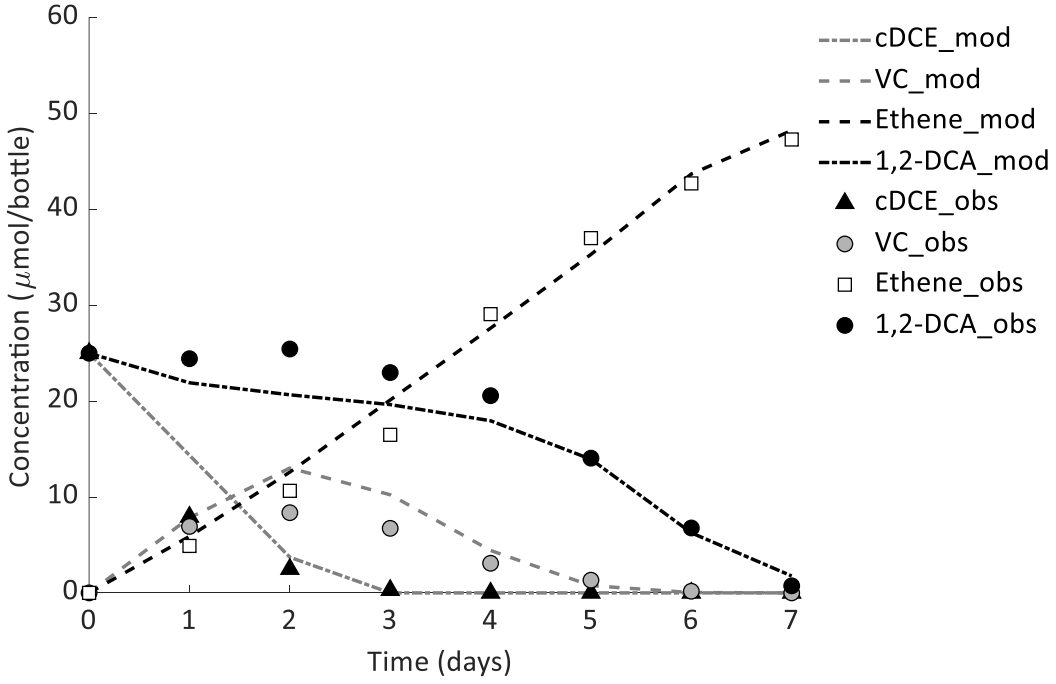

Fig. S5.8 Modeled (mod) and observed (obs) concentrations in culture EA-T3_B.

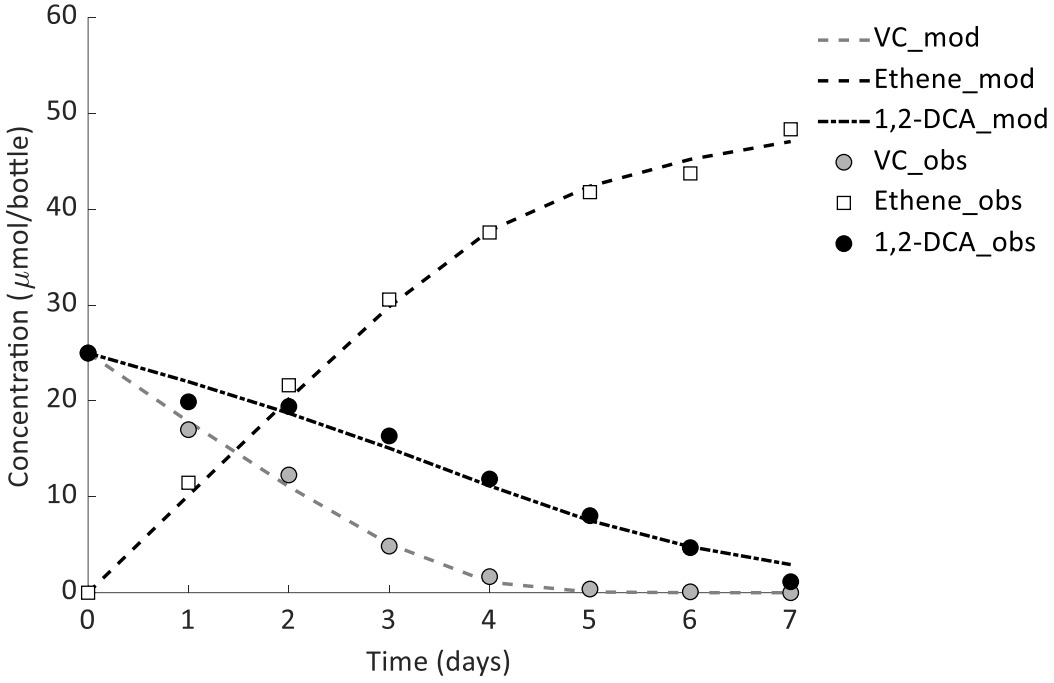

Fig. S5.9 Modeled (mod) and observed (obs) concentrations in culture EA-T4_A.

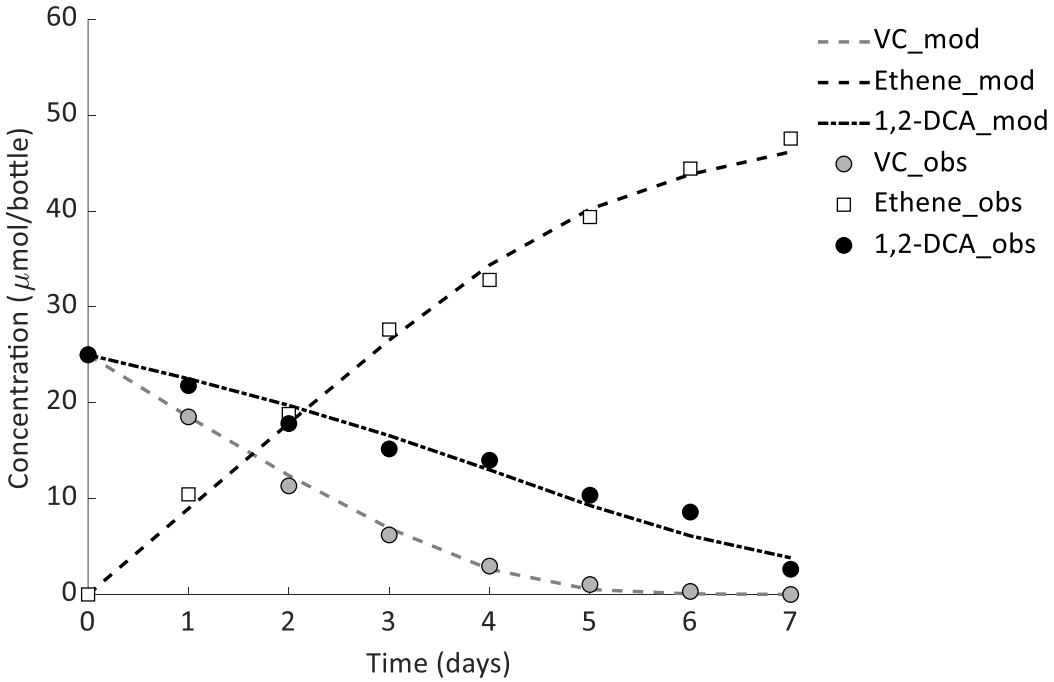

Fig. S5.10 Modeled (mod) and observed (obs) concentrations in culture EA-T4_B.

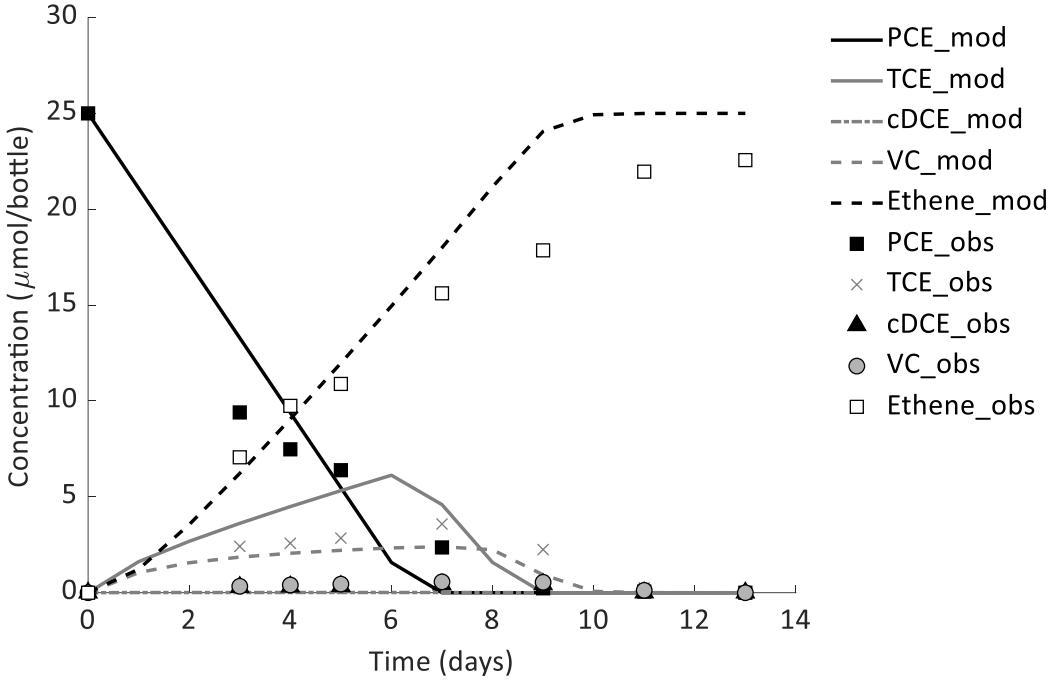

Fig. S5.11 Modeled (mod) and observed (obs) concentrations in culture EAT5_A.

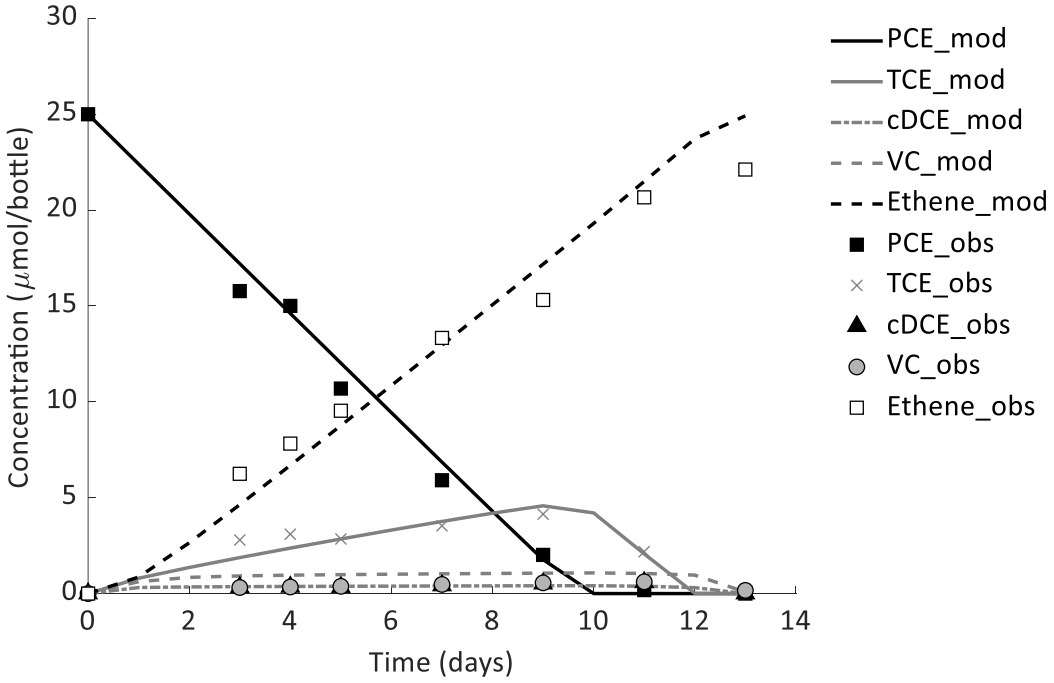

Fig. S5.12 Modeled (mod) and observed (obs) concentrations in culture EAT5_B.

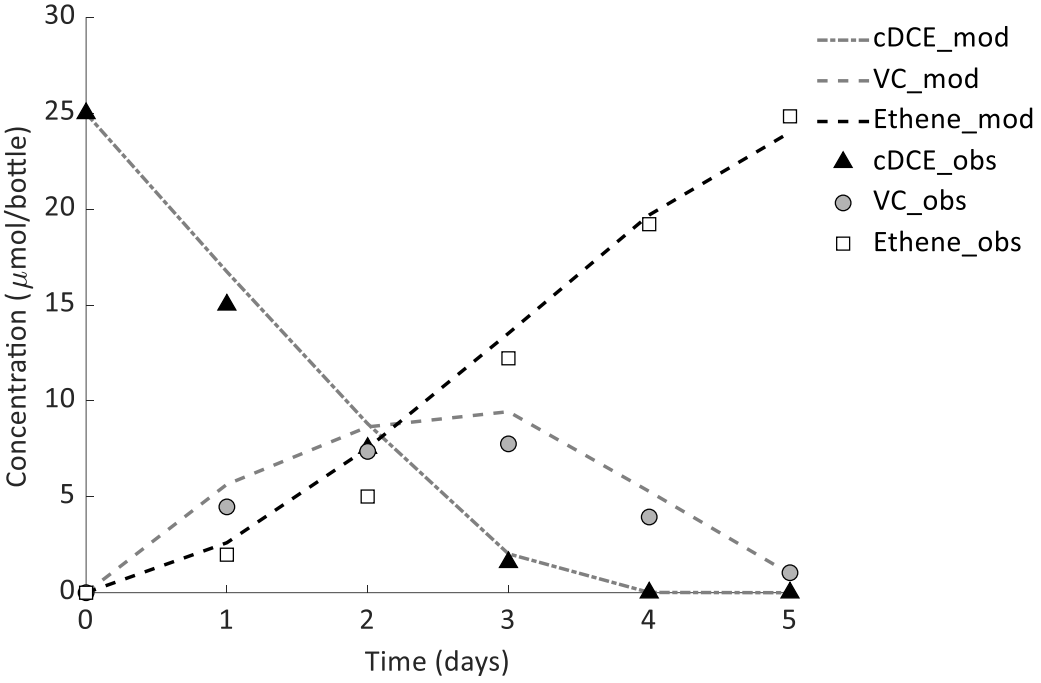

Fig. S5.13 Modeled (mod) and observed (obs) concentrations in culture EA-T6_A.

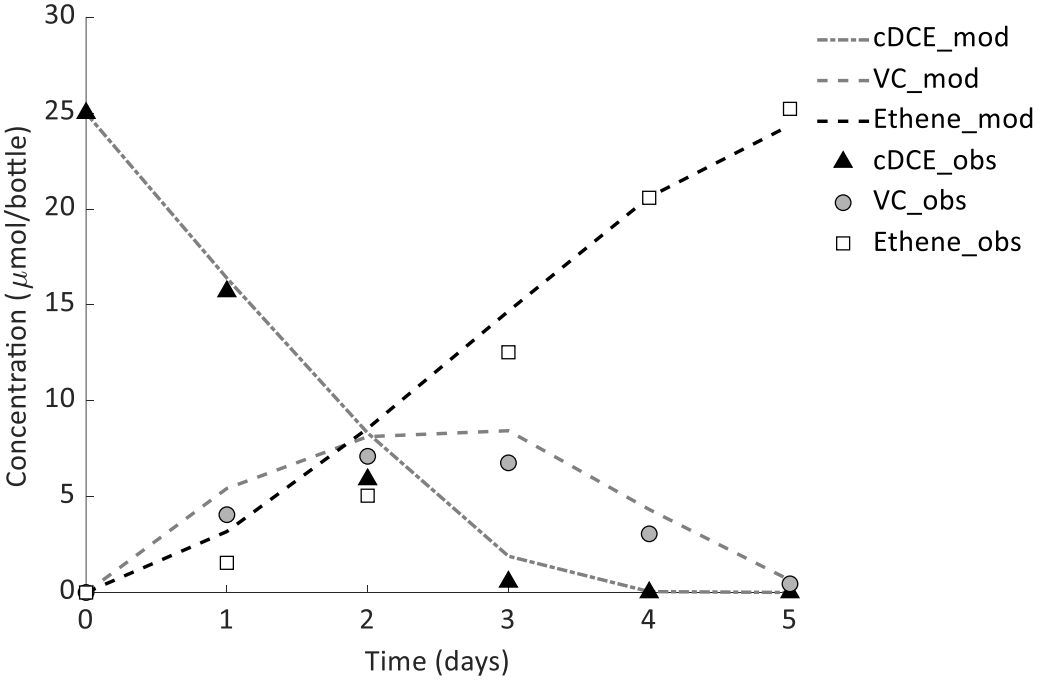

Fig. S5.14 Modeled (mod) and observed (obs) concentrations in culture EA-T6_B.

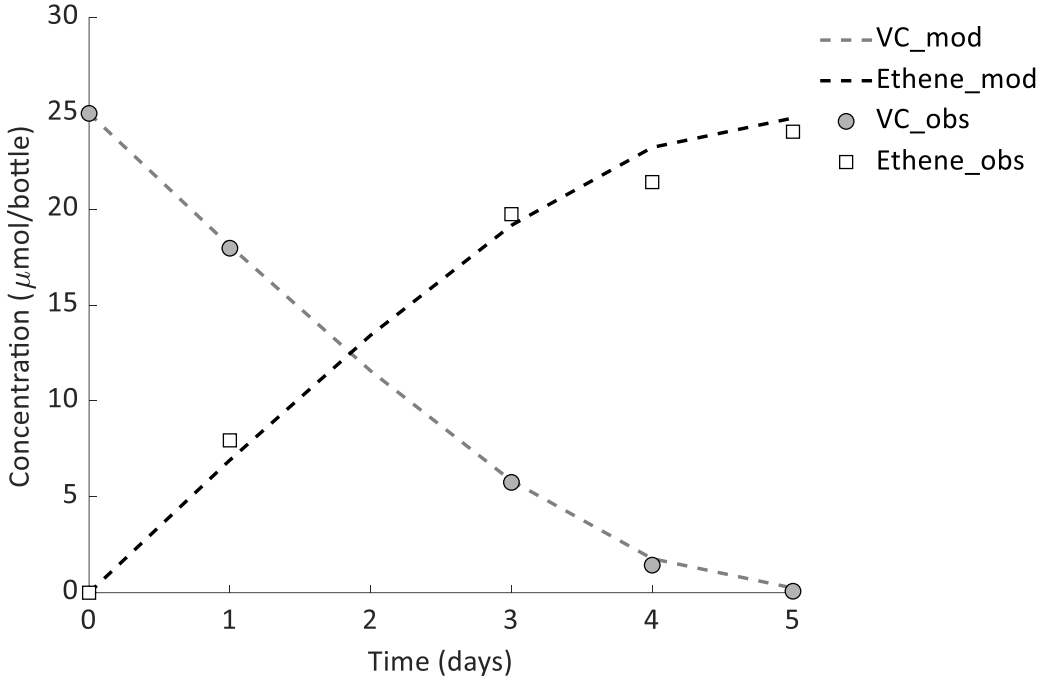

Fig. S5.15 Modeled (mod) and observed (obs) concentrations in culture EA-T7_A.

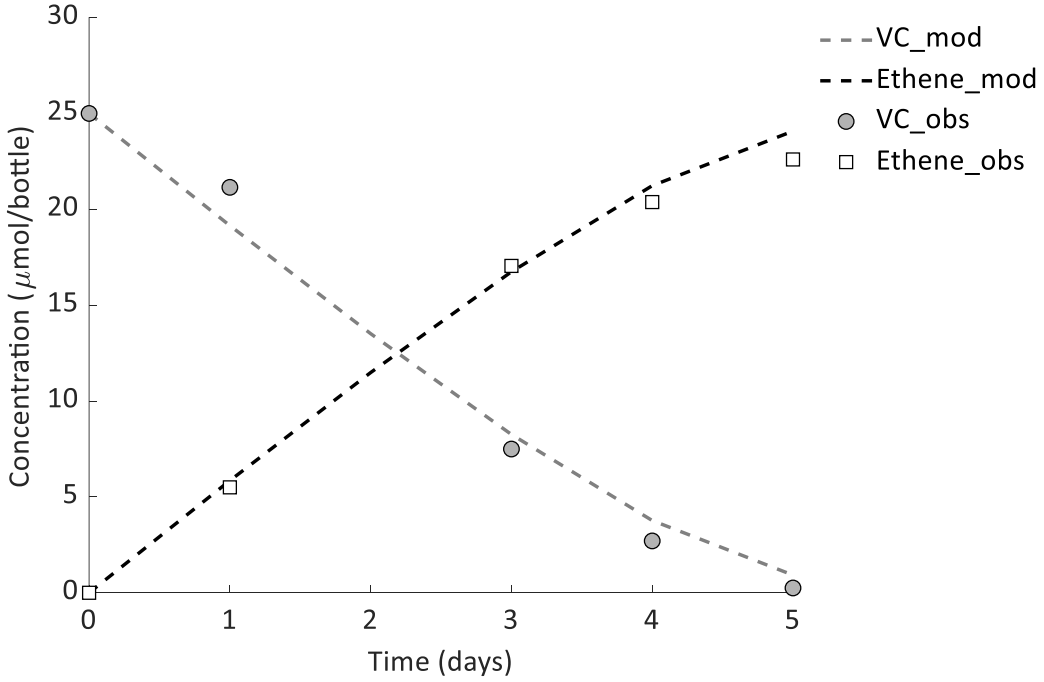

Fig. S5.16 Modeled (mod) and observed (obs) concentrations in culture EA-T7_B.

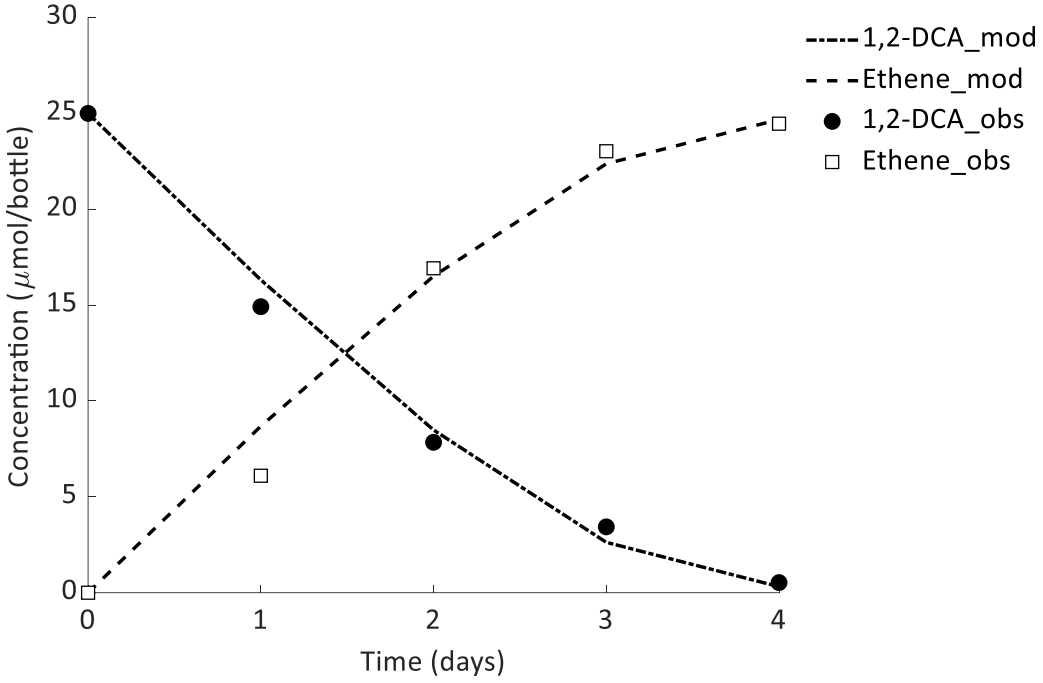

Fig. S5.17 Modeled (mod) and observed (obs) concentrations in culture EA-T8_A.

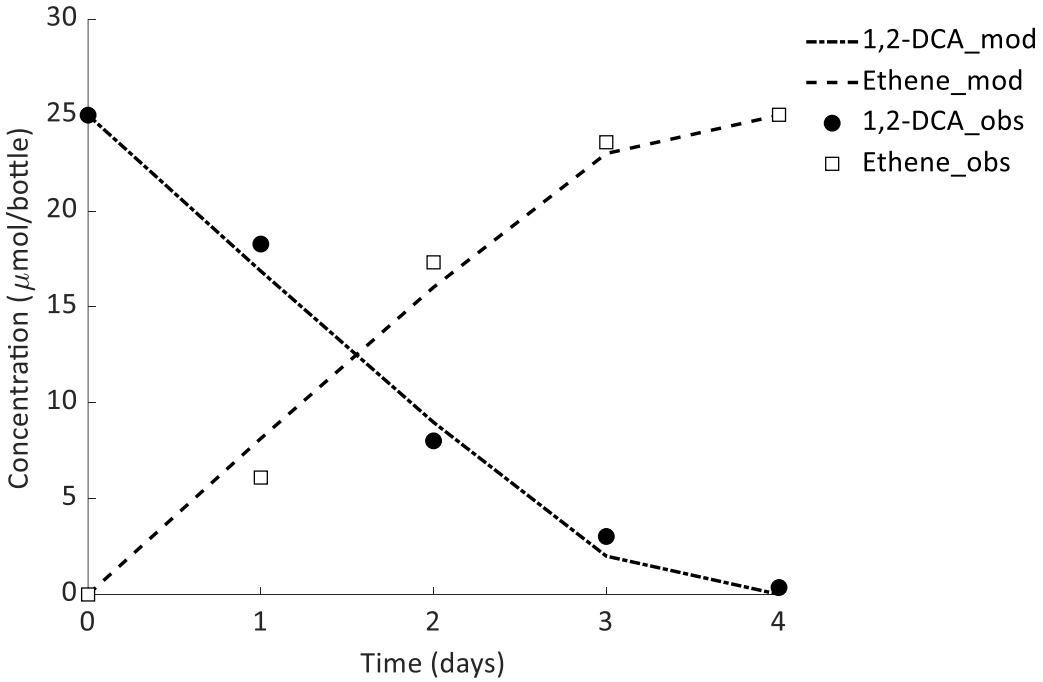

Fig. S5.18 Modeled (mod) and observed (obs) concentrations in culture EA-T8_B.

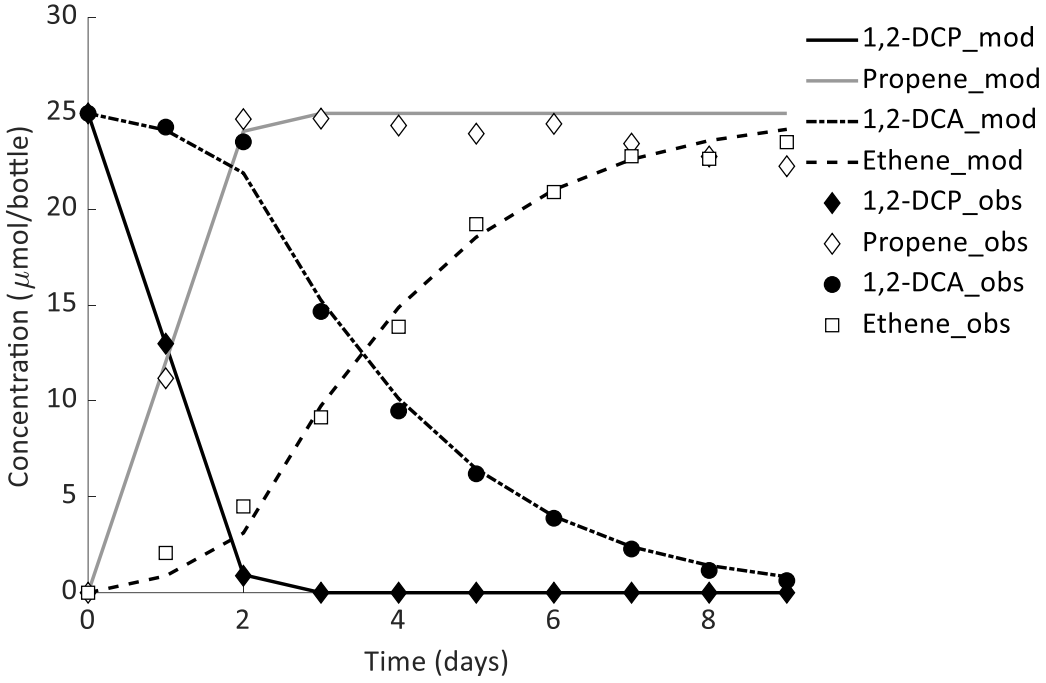

Fig. S5.19 Modeled (mod) and observed (obs) concentrations in culture EA-T9_A.

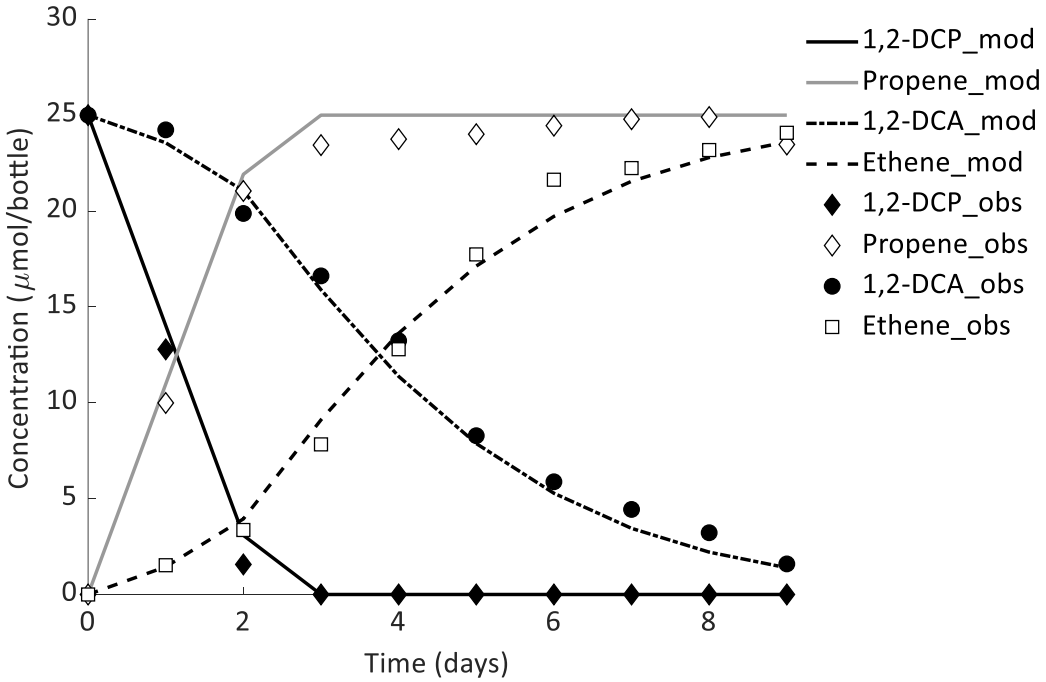

Fig. S5.20 Modeled (mod) and observed (obs) concentrations in culture EA-T9_B.

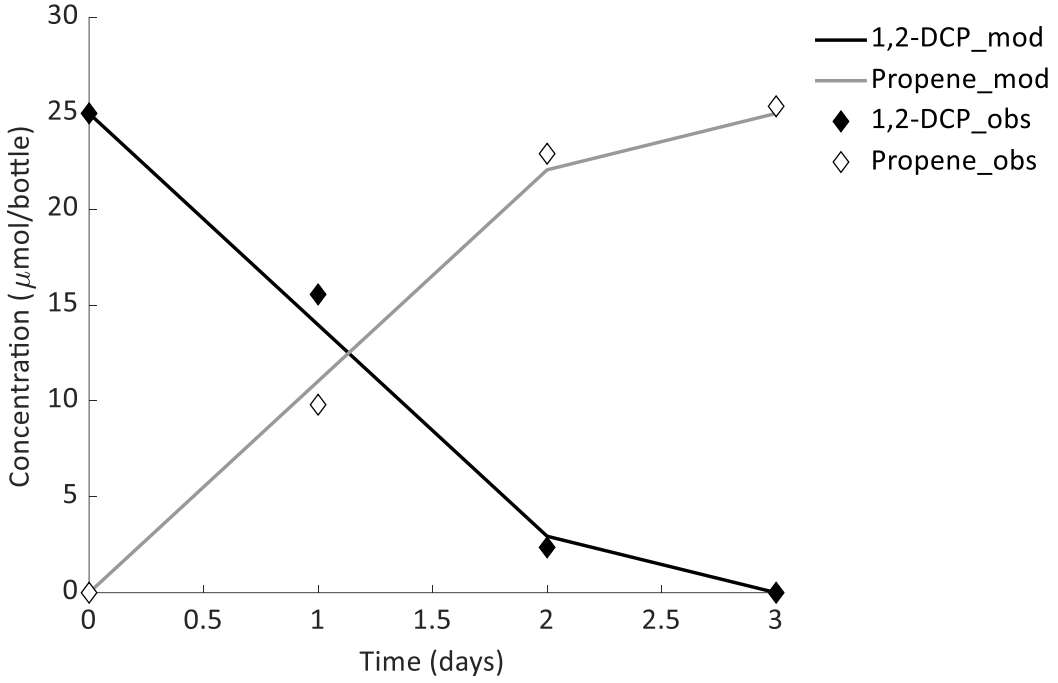

Fig. S5.21 Modeled (mod) and observed (obs) concentrations in culture EA-T10_A.

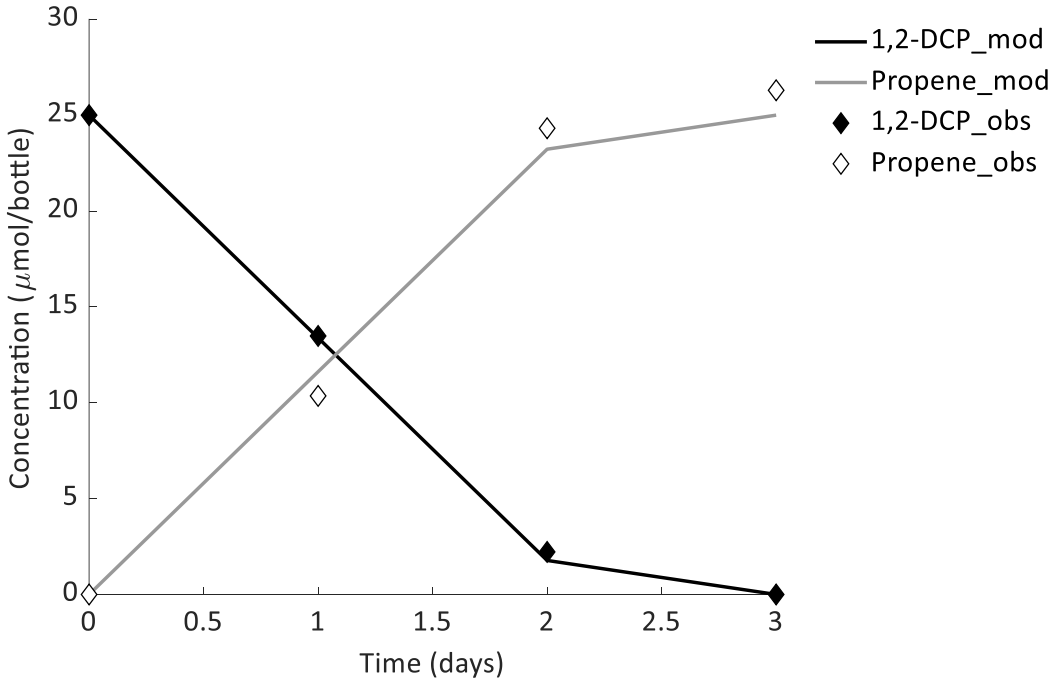

Fig. S5.22 Modeled (mod) and observed (obs) concentrations in culture EA-T10_B.

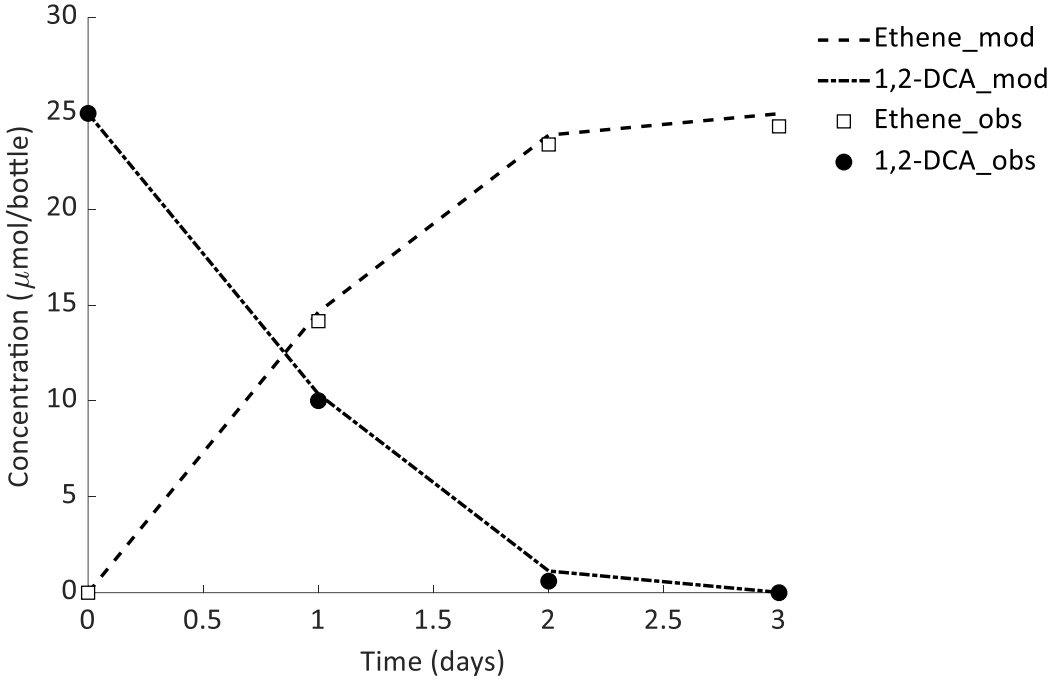

Fig. S5.23 Modeled (mod) and observed (obs) concentrations in culture EB-T1_A.

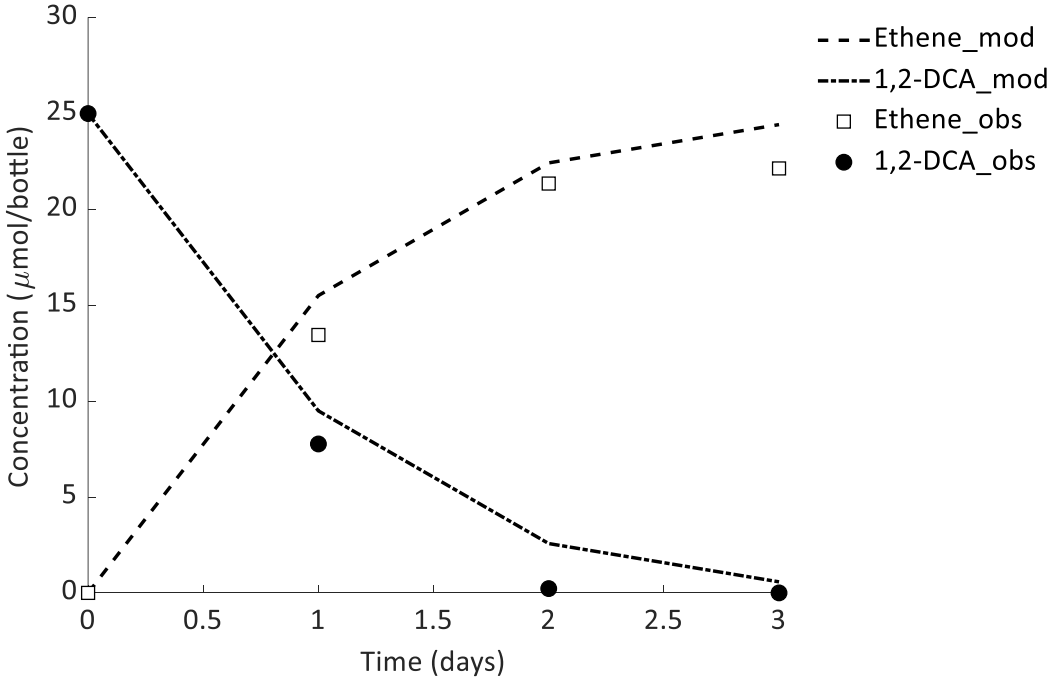

Fig. S5.24 Modeled (mod) and observed (obs) concentrations in culture EB-T1_B.

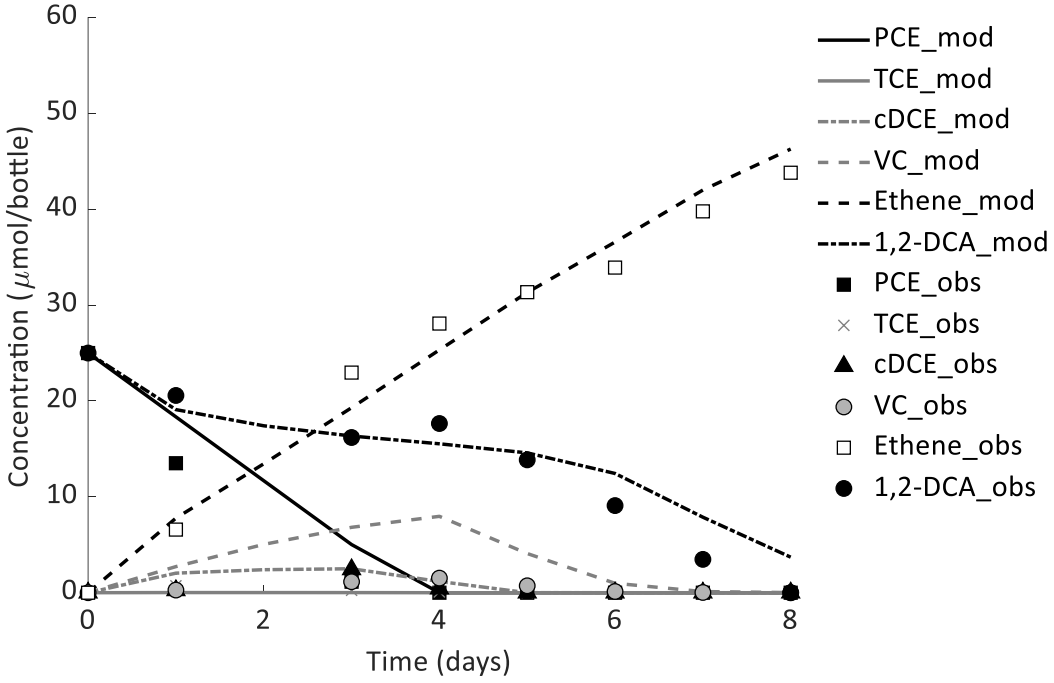

Fig. S5.25 Modeled (mod) and observed (obs) concentrations in culture EB-T2_A.

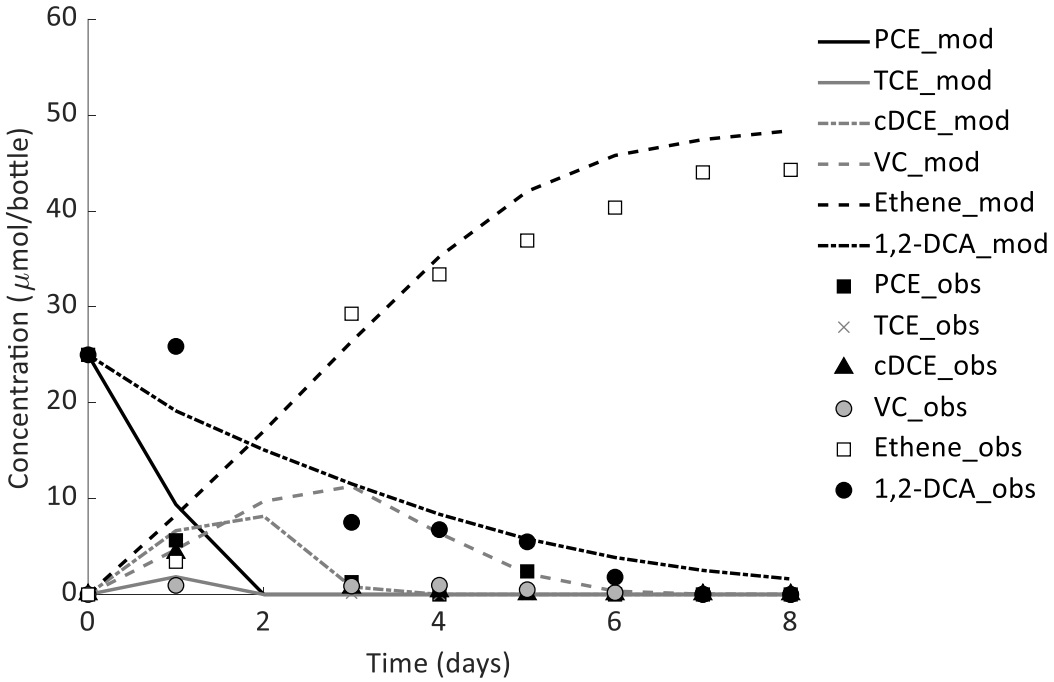

Fig. S5.26 Modeled (mod) and observed (obs) concentrations in culture EB-T2_B.

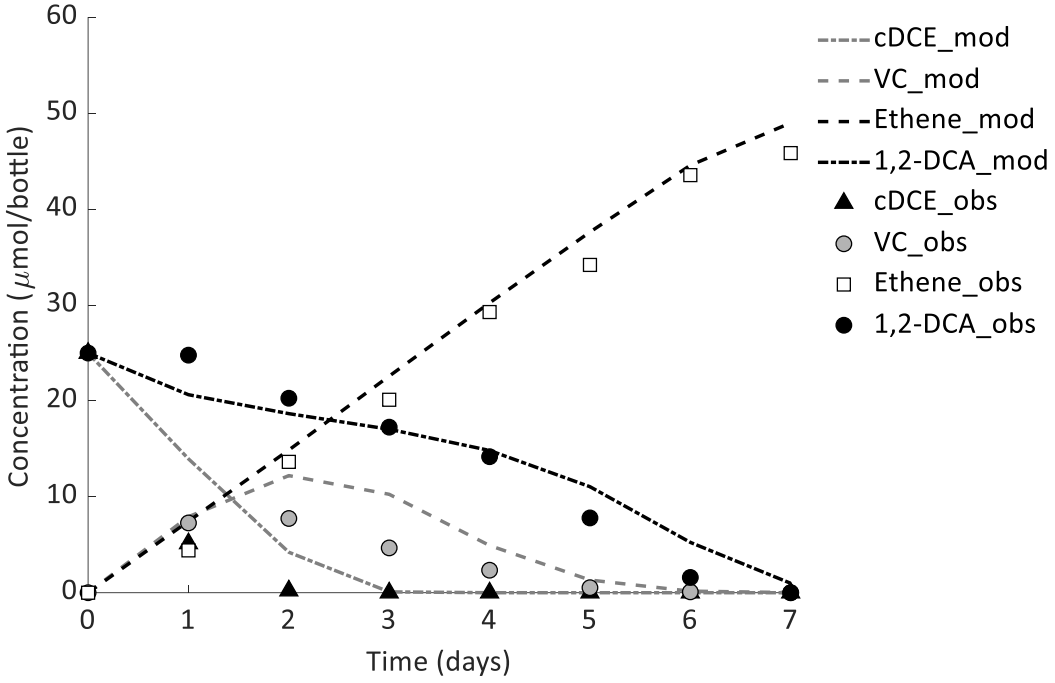

Fig. S5.27 Modeled (mod) and observed (obs) concentrations in culture EB-T3_A.

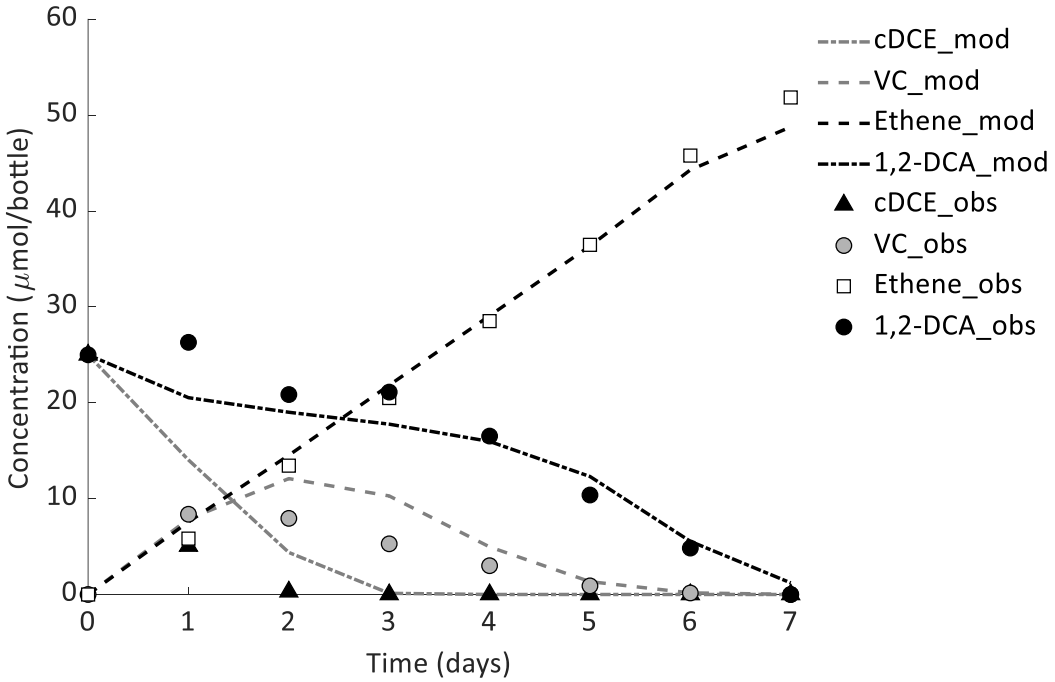

Fig. S5.28 Modeled (mod) and observed (obs) concentrations in culture EB-T3_B.

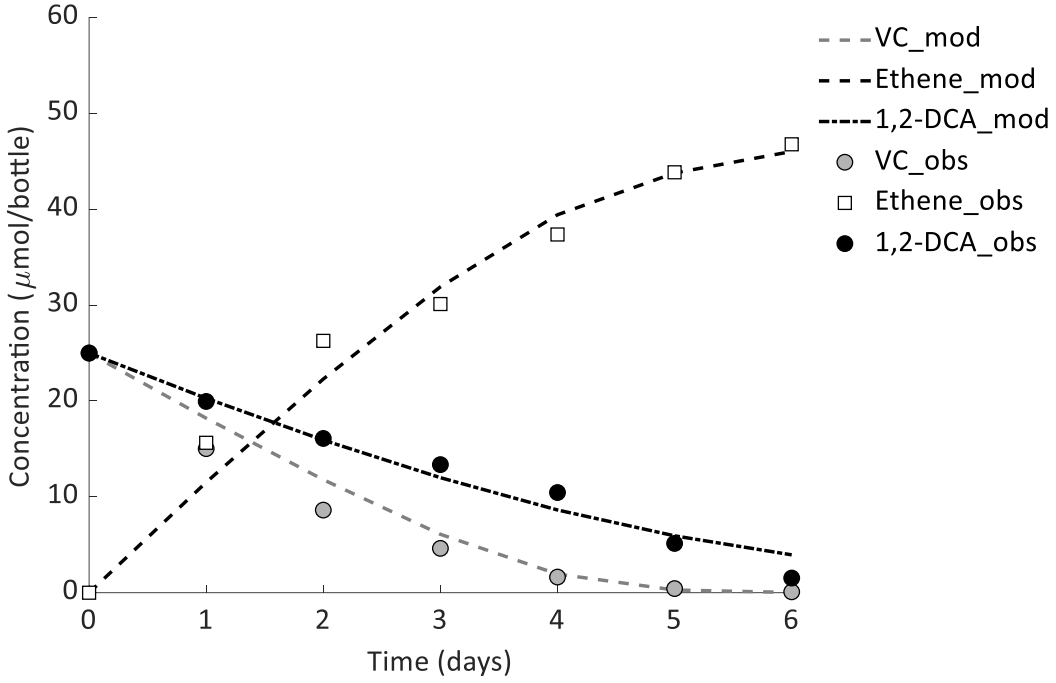

Fig. S5.29 Modeled (mod) and observed (obs) concentrations in culture EB-T4_A.

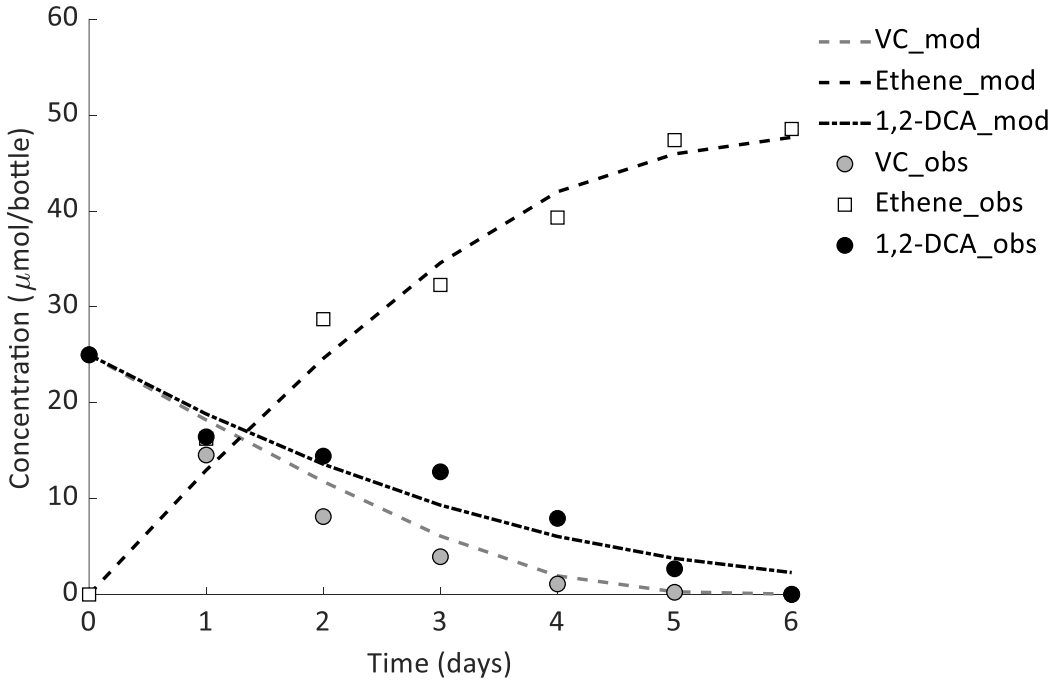

Fig. S5.30 Modeled (mod) and observed (obs) concentrations in culture EB-T4_B.

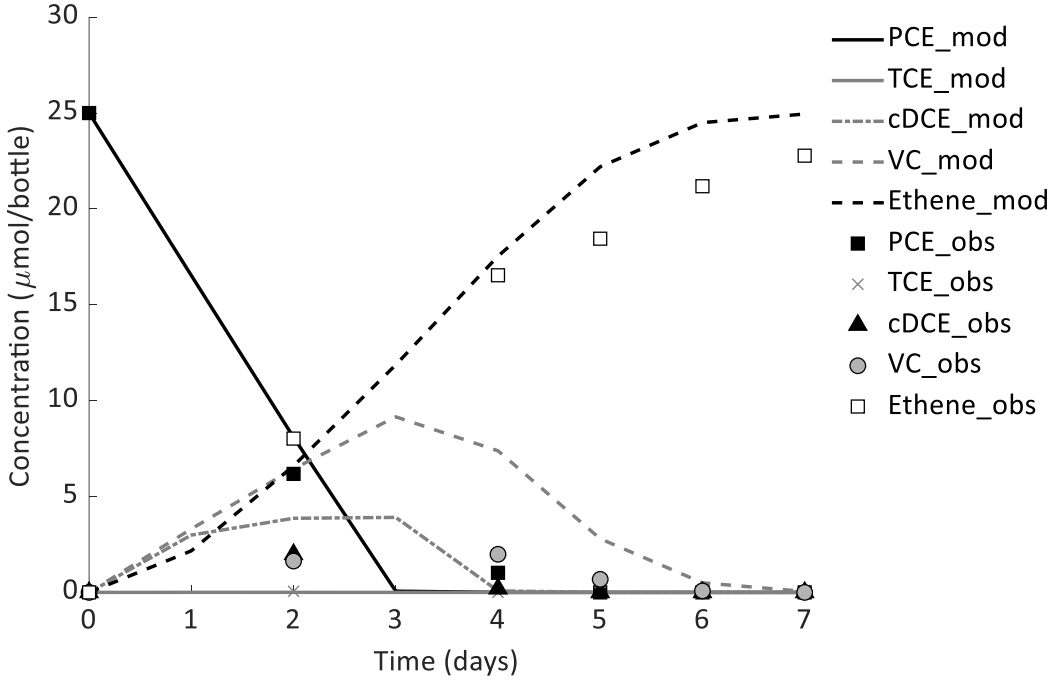

Fig. S5.31 Modeled (mod) and observed (obs) concentrations in culture EB-T5_A.

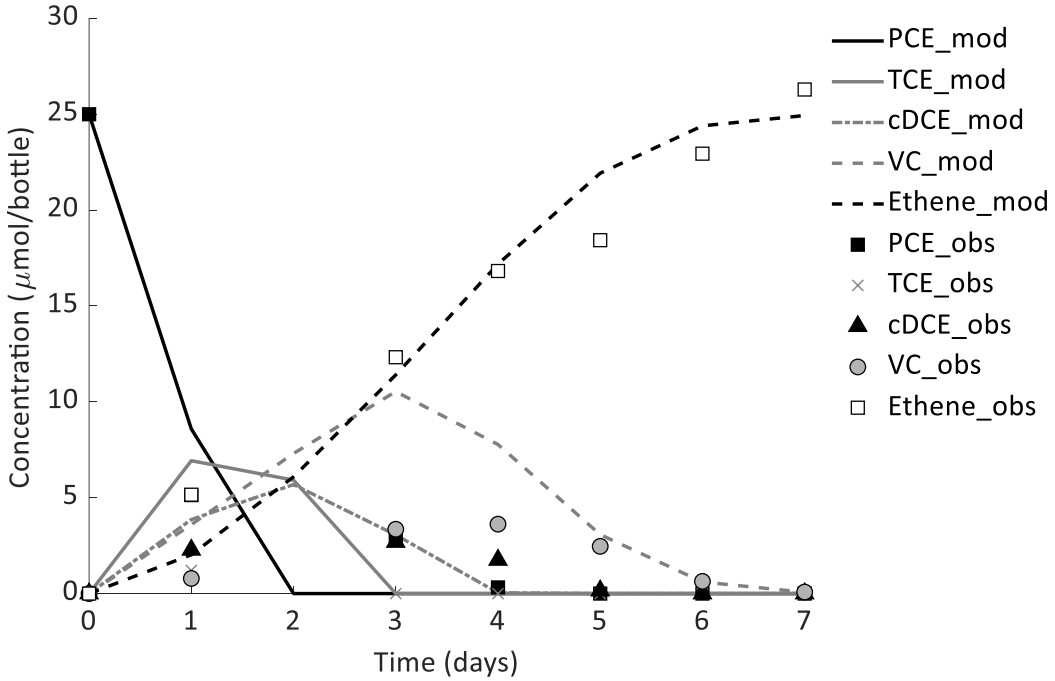

Fig. S5.32 Modeled (mod) and observed (obs) concentrations in culture EB-T5_B.

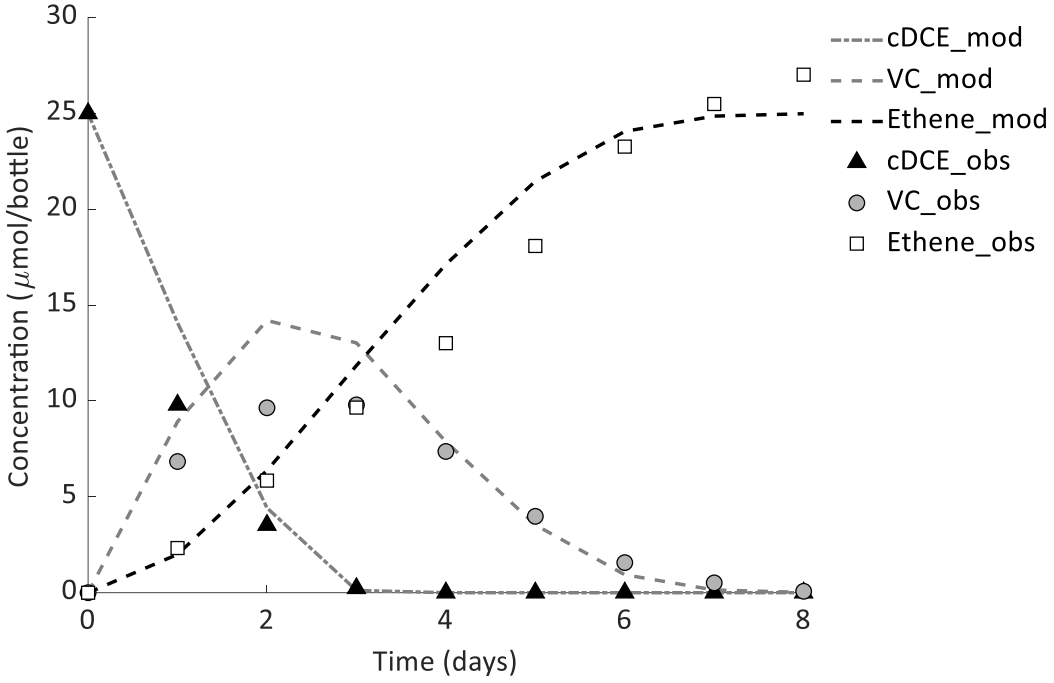

Fig. S5.33 Modeled (mod) and observed (obs) concentrations in culture EB-T6_A.

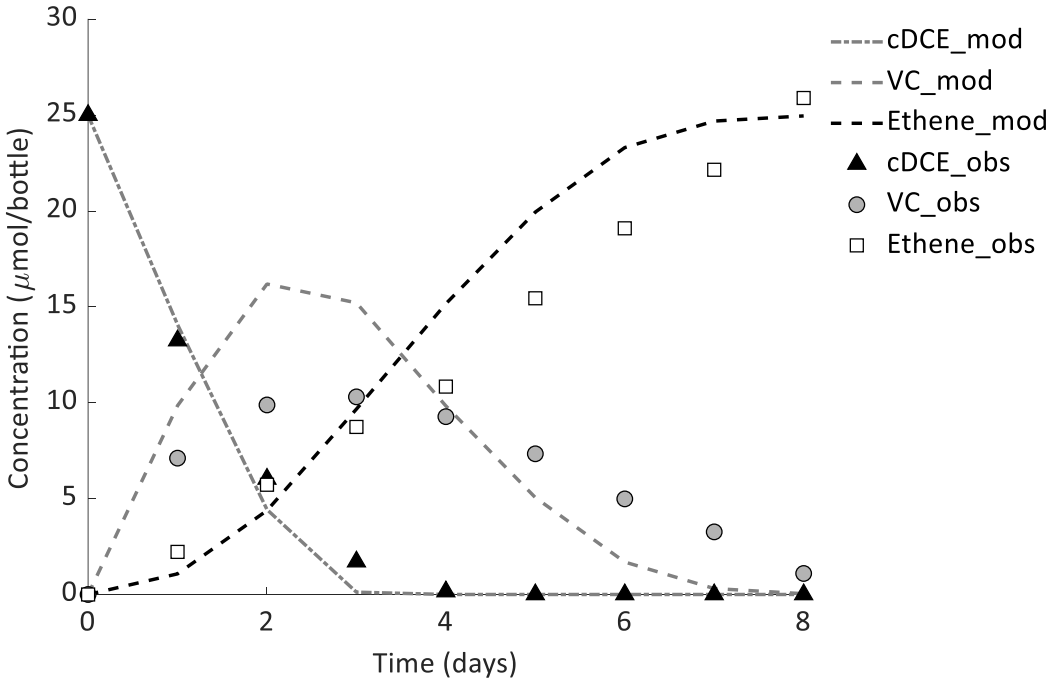

Fig. S5.34 Modeled (mod) and observed (obs) concentrations in culture EB-T6_B.

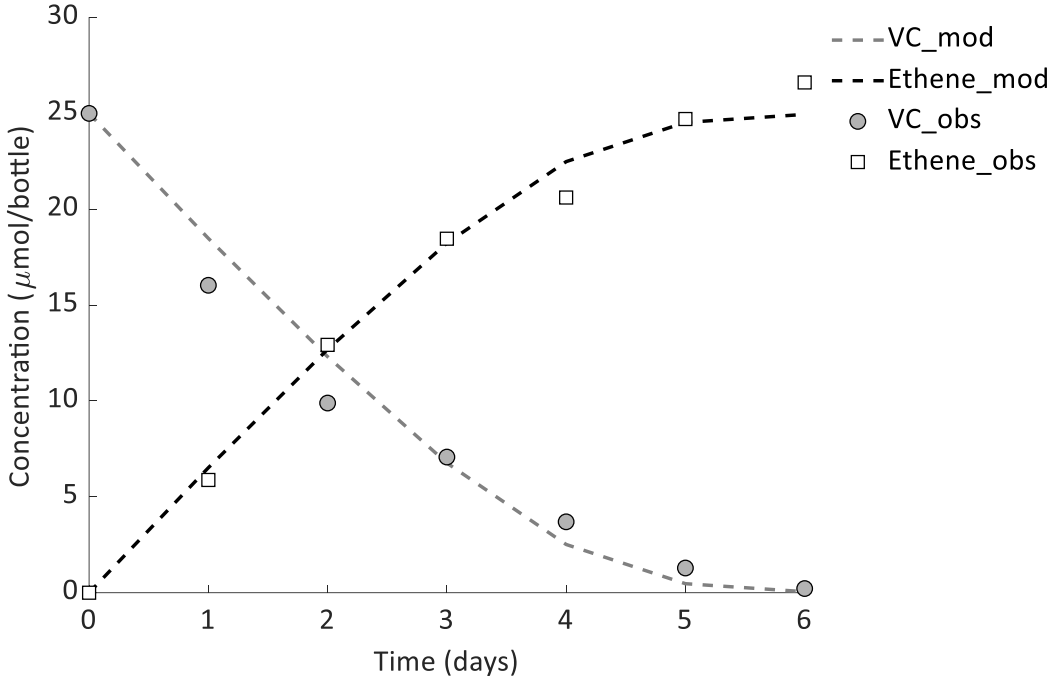

Fig. S5.35 Modeled (mod) and observed (obs) concentrations in culture EB-T7_A.

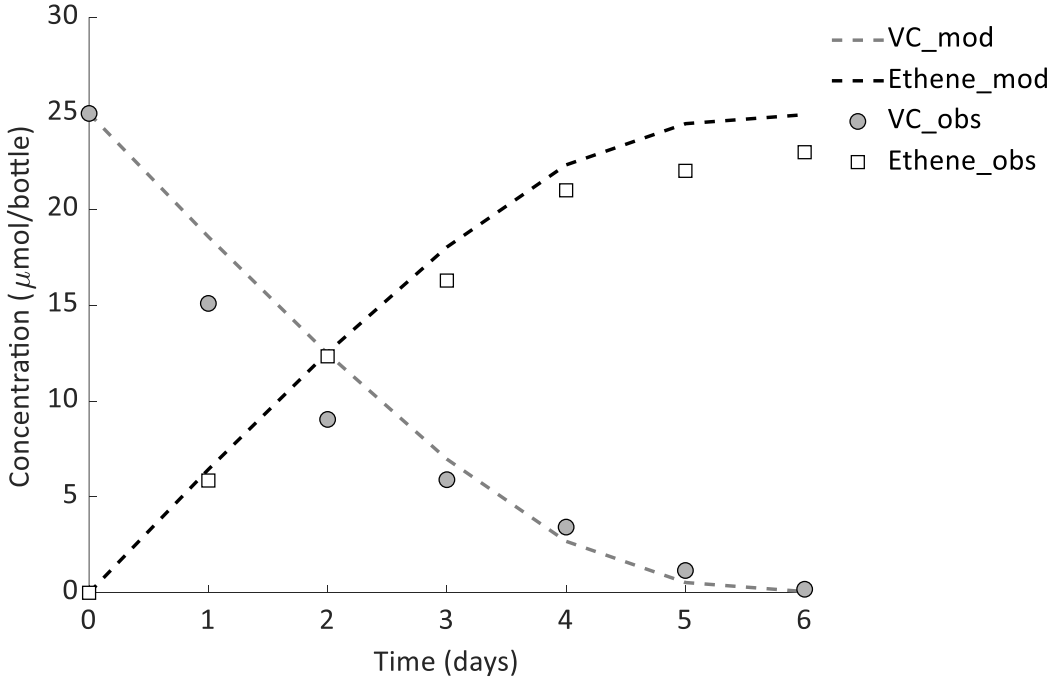

Fig. S5.36 Modeled (mod) and observed (obs) concentrations in culture EB-T7_B.

Table S5.1 Primers and amplification programs used for qPCR in this study

Target	Name [a]	Sequence (5´–3´)	Reference for primer	Reference for qPCR program
Total bacteria	Eub341F	CCTACGGGAGGCAGCAG	(Muyzer *et al.* 1993)	(Atashgahi *et al.* 2013)
	Eub534R	ATTACCGCGGCTGCTGGC		
Dehalogenimonas	BL-DC-1243F	GGYACAATGGGTTGCCACCGG	(Chen *et al.* 2014a)	(Chen *et al.* 2014a) [b]
	BL-DC-1351R	AACGCGCTATGCTGACACGCGT		
Desulfitobacterium	Dsb406F	GTACGACGAAGGCCTTCGGGT	(Smits *et al.* 2004)	(Smits *et al.* 2004)
	Dsb619R	CCCAGGGTTGAGCCCTAGGT		
Dehalococcoides	Dco728F	AAGGCGGTTTTCTAGGTTGTCAC	(Smits *et al.* 2004)	(Atashgahi *et al.* 2013)
	Dco944R	CTTCATGCATGTCAAAT		
Dehalobacter	Dre441F	GTTAGGGAAGAACGGCATCTGT	(Smits *et al.* 2004)	(Atashgahi *et al.* 2013)
	Dre645R	CCTCTCCTGTCCTCAAGCCATA		
Geobacter	Geo196F	GAATATGCTCCTGATTC	(Amos *et al.* 2007)	(Azizian *et al.* 2010)
	Geo535R	TAAATCCGAACAACGCTT		
Sulfurospirillum	Sulfuro114F	GCTAACCTGCCCTTTAGTGG	(Sutton *et al.* 2015)	(Sutton *et al.* 2015)
	Sulfuro421R	GTTTACACACCGAAATGCGT		

[a] Primer names may not correspond to original publication

[b] The qPCR program was modified as 98°C for 5 min, followed by 40 cycles of 98°C for 15 s, 68.2°C for 45 s. Melting curves were included from 55°C to 95°C with increments of 0.5°C and 10 s at each step

Table S5.2 can be found at: https://github.com/mibwurrepo/Peng-et-al-2019

Chapter 6

General discussion

Organic and inorganic halogen compounds originating from anthropogenic and natural sources are found in a broad range of different environments (Ali *et al.* 2016, Gribble 2010). Microbes capable of transforming these compounds play an important role in bioremediation applications as well as in the halogen cycling in a range of polluted and pristine environments. Research described in this thesis focused on the physiology, genetics, and ecology of microorganisms derived from different contaminated and pristine environments and that were able to transform various organic and inorganic halogen compounds. Furthermore, potential bottlenecks for their application in bioremediation were addressed (Table 6.1).

The aim of this thesis was to further expand our knowledge on these microbes transforming organic and inorganic halogen compounds, through i) revealing novel metabolic features (**Chapter 2**), ii) enriching and isolating new microbes capable of organohalogen transformation from pristine environments (**Chapters 3, 4**), and iii) understanding biodegradation bottlenecks at contaminated sites where mixtures of chlorinated solvents occur, providing possible ways for effective bioremediation (**Chapter 5**).

Table 6.1 Overview of pure and mixed cultures applied/studied in this thesis

	Pseudomonas chloritidismutans AW-1^T (**Chapter 2**)	*Desulfoluna* spp. strains DBB, AA1^T, MSL71^T (**Chapter 3**)	Enrichment culture void of the known OHRB but containing acetogenic *Clostridium* (**Chapter 4**)	Enrichment culture containing *Dehalococcoides*, *Dehalogenimonas*, *Geobacter* (**Chapter 5**)
Original habitat	Wastewater containing bioreactor [1]	Marine intertidal sediments [2]	Hypersaline lakes [2]	Wetland [3]
Substrate	Haloalkanoates, chlorate	1,4-dibromobenzene, halophenols	Chloroform	1,2-dichloroethane, chloroethenes, 1,2-dichloropropane
Substrate utilization type	Carbon source and electron donor (haloalkanoates), Electron acceptor (chlorate)	Electron acceptor	Co-metabolic transformation	Electron acceptor
Transformation product	hydroxyl alkanoates, chloride, oxygen	Bromobenzene, phenol	Dichloromethane, CO_2	Ethene, propane

[1] Inoculated with chlorate and bromate polluted wastewater (Wolterink *et al.* 2002)
[2] Pristine environment
[3] Long history of contamination with agrochemical and fine chemistry effluents

Genome-guided physiology of microbes capable of transforming organic and/or inorganic halogen compounds

Recent advances in genomic and allied technologies have enabled gaining detailed insights into the genetics and potential metabolism of previously isolated/characterized microbes capable of transforming organic/inorganic halogen compounds. A notable example was genomic analysis of the chlorate-reducing bacterium *Pseudomonas chloritidismutans* AW-1^T that showed presence of two haloacid dehalogenase genes, indicating its potential for concurrent haloalkanoates dehalogenation and chlorate reduction (**Chapter 2**). Likewise, genome sequencing of the previously described sulfate-reducing bacterium *Desulfoluna butyratoxydans* MSL71^T revealed presence of three reductive dehalogenase genes (*rdh*) (**Chapter 3**), indicating potential of this bacterium for organohalide respiration (OHR), a trait that had not previously been reported. Physiological experiments indeed confirmed the potential metabolism of strain AW-1^T for concurrent dehalogenation of haloalkanoates and chlorate reduction (**Chapter 2**), and OHR potential for strain MSL71^T (**Chapter 3**). The newly found/verified metabolic feature of strain AW-1^T is important for bioremediation of sites contaminated with multiple halogen compounds such as organic haloalkanoates and inorganic chlorate that could co-occur in environments as herbicides and disinfection by-products (Ali *et al.* 2016, Atashgahi *et al.* 2018d, Bodnár *et al.* 1990, Righi *et al.* 2014). Strain AW-1^T can also use nitrate as another oxo compound for acetate utilization (Mehboob *et al.* 2015). One avenue of future research would be testing degradation of haloalkanoates under denitrifying condition and whether oxygen can be produced from denitrification for hydrocarbon degradation as previously reported for the denitrifying bacterium *Candidatus* Methylomirabilis oxyfera (Ettwig *et al.* 2010). Additionally, **chapter 2** identified 25 bacterial genomes that harbor genes involved in haloalkanoates dehalogenation and chlorate reduction. Another interesting avenue of research would be experimental verification of their metabolic potential for concurrent haloalkanoates degradation and chlorate reduction. Similar genome-guided physiological explorations will continue to identify novel metabolic features that further propel the boundaries of science and application.

Dissemination of dehalogenase genes

The two haloacid dehalogenase genes (halocarboxylic acid dehydrogenase gene (*dehI*) and L-2-haloacid dehalogenase (L-DEX) gene) in strain AW-1^T are carried by transposons (Fig. 6.1), similar to many *Pseudomonas* degradative genes carried by transmissible plasmids and/or transposons, allowing their dissemination to other microorganisms by horizontal gene transfer (HGT) (Clark *et al.* 2013, Ma *et al.* 2006, Urata *et al.* 2004). In the *dehI* gene cluster of strain AW-1^T, an insertion element (IS) that shares 100% identity to IS30 family transposase was found upstream of the *dehI* (Fig. 6.1A). The genetic organization of *dehI* is similar to that

of *dhlB* in the mutant strain *X. autotrophicus* GJ10M50, in which an IS (IS*1247*) was inserted upstream of *dhlB*. Compared to the wild type *X. autotrophicus* GJ10, the insertion of IS*1247* caused overexpression of *dhlB* and enabled transposition of *dhlB* to transmissible plasmids (Van der Ploeg *et al.* 1995). The L-DEX gene of strain AW-1^T is carried by a Tn*402/5090* like transposon (Fig. 6.1B). Tn*402/5090* transposons belong to class I integrons that are frequently carry antibiotic resistance genes and are major contributors to spreading antibiotic-resistant genes among pathogens (Hall and Collis 1998). Moreover, a genetic study of chlorate-reducing *Pseudomonas* species including strain AW-1^T showed their chlorite dismutase gene (*cld*) and chlorate reduction gene (*clrABDC*) were separated and flanked by different types of ISs, resulting in formation of chlorate reduction composite transposons (Clark *et al.* 2013). These genetic characteristics of the halogen compound degradation genes of strain AW-1^T suggest their acquisition/dissemination by HGT, enabling AW-1^T as a single bacterium to concurrently transform organic and inorganic halogenated compounds. However, future experiments will be needed to confirm this hypothesis.

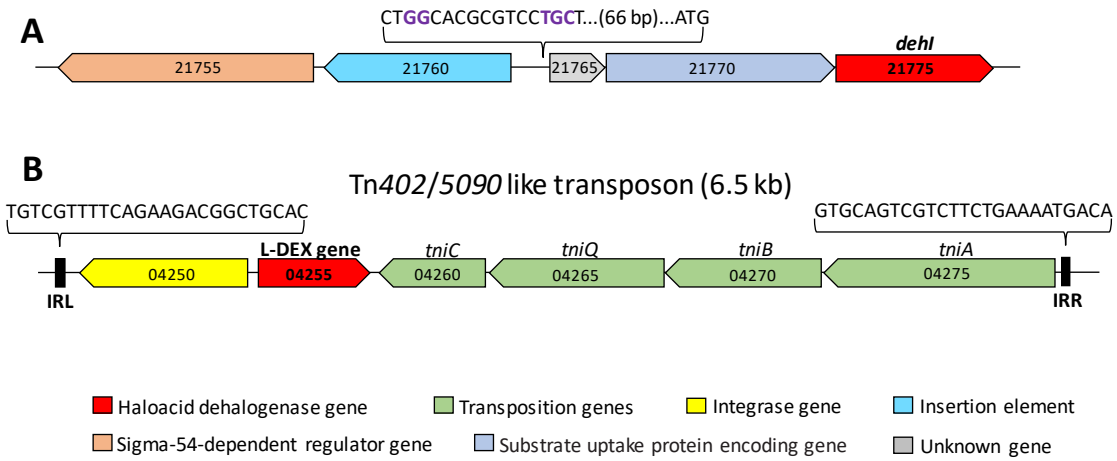

Fig. 6.1 Genetic organization of the halocarboxylic acid dehydrogenase gene (*dehI*, A) and L-2-haloacid dehalogenase (L-DEX, B) gene of *P. chloritidismutans* AW-1^T. The sequence of sigma factor 54 binding site in the *dehI* cluster is indicated with the –24 (GG) and –12 (TGC) promoter elements marked in purple. The sequence of left and right inverted repeats (IRL and IRR) of the Tn*402*/*5090* like transposon is indicated. Numbers indicate the locus tags of the respective genes in the genome of *P. chloritidismutans* AW-1^T.

HGT as well as vertical evolution have also been suggested to play an important role in distribution and evolution of *rdh* genes in OHRB. For example, most *rdh* genes in *Dehalococcoides mccartyi* are located in high plasticity regions of their genomes containing mobile genetic elements and genomic islands (Hug 2016). Active circularization of an integrated genomic island containing the vinyl chloride (VC) reductive dehalogenase gene

(*vcrABC*) was observed in *D. mccartyi*. Prophage-mediated HGT of *rdh* genes has also been suggested for *Sulfurospirillum multivorans* (Goris *et al.* 2014). In contrast, no evidence was found for a similar HGT of the *rdh* genes in *Desulfoluna* strains (**Chapter 3**). The *rdh* genes were not localized in any genomic islands in the *Desulfoluna* genomes, or flanked by any mobile genetic elements such as transposons. This may suggest vertical inheritance of *rdh* genes in *Desulfoluna*.

Regulation of dehalogenase genes

Like most of the known dehalogenase genes, the *dehI* gene of *P. chloritidismutans* AW-1^T (**Chapter 2**), and the three *rdh* genes of *D. spongiiphila* strain DBB (**Chapter 3**) are inductively expressed, indicating existence of functional regulatory systems for these genes. The *dehI* of strain AW-1^T is located next to a symporter-encoding gene (locus tag: 21770, Fig. 6.1A) that was suggested to encode a substrate uptake protein (van der Ploeg and Janssen 1995). A sigma factor 54 dependent transcriptional activator gene (21755) and a –24/–12 promoter sequence (sigma factor 54 binding site) are also located upstream of this symporter gene and *dehI* (Fig. 6.1A). This suggests that the expression of the symporter gene and *dehI* might be controlled by the sigma factor 54 dependent transcriptional activator, similar to the regulatory system that controls expression of the haloalkanoic acid dehalogenase gene (*dhlB*) in *Xanthobacter autotrophicus* GJ10 (van der Ploeg and Janssen 1995). Interestingly, such a sigma factor 54 dependent regulatory system was also found upstream of the *rdh* gene clusters (*rdhA1* and *rdhA3*) of *Desulfoluna* strains (**Chapter 3**), indicating widespread occurrence of this type of regulatory systems. In contrast to the *dehI* and *rdh* genes of strains AW-1^T and DBB, respectively, the L-DEX gene (04255) of strain AW-1^T that resides on a gene cassette in a Tn*402/5090* like transposon (Fig. 6.1B) was constitutively expressed (**Chapter 2**). The constitutive expression of the L-DEX gene is likely controlled by an unknown promotor of this integron (Bennett 1999).

Future perspectives

Considering mounting genomic evidence for OHR in marine *Deltaproteobacteria* (Liu and Häggblom 2018), future research is expected to reveal additional diversity of organohalide-respiring *Deltaproteobacteria* and to further provide new insights of their metabolism. Apart from environmental samples, a wide range of dehalogenation genes were recently identified in the genomes and metagenomes obtained from human and animal gastrointestinal tracts (Atashgahi *et al.* 2018d). Can halogenated compounds be transformed by gut microbiota? Can we find novel microbes/biochemistries from gut microbiota? There has been lack of cross-disciplinary collaboration between environmental microbiologists, gut microbiologists and toxicologists in thinking outside the box and addressing such questions.

Chapter 3 left some open questions for future investigations. The proteins proposed to play a role in electron transport during OHR and respiratory sulfate reduction await functional verification, for example, by genetic construction of *Desulfoluna* mutant strains that lack genes potentially involved in the electron transport chain. Similar genetic approaches were applied in the phylogenetically related *Desulfovibrio* species for functional verification of electron transport proteins involved in sulfate reduction (Keller and Wall 2011). Moreover, transcriptomic and proteomic analysis of *Desulfoluna* spp. grown in the presence of oxygen can contribute to identifying the enzymes involved in oxygen defence.

Chapter 5 revealed decreased dechlorination rates or complete disruption of 1,2-dichloroethane in the presence of structurally similar chloroethenes and 1,2-dichloropropane. The subsurface is a complex environment where OHRB can not only be challenged by co-occurring organohalogen mixtures, but other organic and inorganic co-contaminants such as heavy metals (e.g. Pb, Cd, Cr, Zn, Cu, Ni) (Bunge *et al.* 2007, Costa and Jesus-Rydin 2001, Olaniran *et al.* 2009, Subramanian *et al.* 2015), (per)chlorate (Wen *et al.* 2017), nitrous oxide (Yin *et al.* 2019) and BTEX (benzene, toluene, ethylbenzene, xylenes) (Chen *et al.* 2014b, Richmond *et al.* 2001). Such co-contaminants normally not considered in studies focusing on dehalogenation may exert inhibitory/toxic effects on reductive dehalogenase (RDase) enzymes (e.g. nitrous oxide) (Yin *et al.* 2019) and/or growth of OHRB and their syntrophic partners (e.g. heavy metals) (Fu and Wang 2011, Paulo *et al.* 2015). Moreover, additive toxic and/or inhibitory effects of a mixture of co-occurring (in)organic compounds on OHRB has not been investigated, representing big cavities on the roadmaps towards effective bioremediation using OHRB.

Finally, research on microbes with novel dehalogenating metabolic routes can extend our current knowledge on dehalogenation. For example, recent (meta)genomic studies identified a novel type of *rdh* genes in pure cultures and uncultured members of *Bacteriodetes* and *Deltaproteobacteria* (Atashgahi 2019). Unlike the well-known *rdhA* genes from OHRB, the newly found *rdhA* genes were not accompanied by a *rdhB*, but rather encode transmembrane helixes at the N-terminus. It is likely that the encoded RDases are a hybrid of RdhA and RdhB that can directly connect to the cell membrane with its transmembrane helixes (Atashgahi 2019). The function and regulation of this novel group of *rdh* genes remain unknown. Additionally, biochemical studies, especially those focusing on enzymology and structure-function relationships of known RDases is limited. So far only two structures of RDases have been resolved (Bommer *et al.* 2014, Payne *et al.* 2015). Further structure investigation of RDases is needed to better understand the dehalogenation mechanism and provide possibilities to create modified enzymes with desired catalytic properties for environmental applications.

References

Achenbach LA, Michaelidou U, Bruce RA, Fryman J, Coates JD. *Dechloromonas agitata* gen. nov., sp. nov. and *Dechlorosoma suillum* gen. nov., sp. nov., two novel environmentally dominant (per) chlorate-reducing bacteria and their phylogenetic position. *Int J Syst Evol Microbiol* 2001;**51**: 527-533.

Adrian L, Hansen SK, Fung JM, Görisch H, Zinder SH. Growth of *Dehalococcoides* strains with chlorophenols as electron acceptors. *Environ Sci Technol* 2007;**41**: 2318-2323.

Agarwal V, Miles ZD, Winter JM, Eustáquio AS, El Gamal AA, Moore BS. Enzymatic halogenation and dehalogenation reactions: pervasive and mechanistically diverse. *Chem Rev* 2017;**117**: 5619-5674.

Ahn Y-B, Kerkhof LJ, Häggblom MM. *Desulfoluna spongiiphila* sp. nov., a dehalogenating bacterium in the *Desulfobacteraceae* from the marine sponge *Aplysina aerophoba*. *Int J Syst Evol Microbiol* 2009;**59**: 2133-2139.

Ahn Y-B, Rhee S-K, Fennell DE, Kerkhof LJ, Hentschel U, Häggblom MM. Reductive dehalogenation of brominated phenolic compounds by microorganisms associated with the marine sponge *Aplysina aerophoba*. *Appl Environ Microbiol* 2003;**69**: 4159-4166.

Albers CN, Hansen PE, Jacobsen OS. Trichloromethyl compounds—Natural background concentrations and fates within and below coniferous forests. *Sci Total Environ* 2010;**408**: 6223-6234.

Ali SN, Ahmad MK, Mahmood R. Sodium chlorate, a herbicide and major water disinfectant byproduct, generates reactive oxygen species and induces oxidative damage in human erythrocytes. *Environ Sci Pollut Res* 2016;**24**: 1898-1909.

Amoozegar MA, Siroosi M, Atashgahi S, Smidt H, Ventosa A. Systematics of haloarchaea and biotechnological potential of their hydrolytic enzymes. *Microbiology* 2017;**163**: 623-645.

Amos BK, Sung Y, Fletcher KE, Gentry TJ, Wu W-M, Criddle CS, Zhou J, Löffler FE. Detection and quantification of *Geobacter lovleyi* strain SZ: implications for bioremediation at tetrachloroethene-and uranium-impacted sites. *Appl Environ Microbiol* 2007;**73**: 6898-6904.

Amstaetter K, Borch T, Kappler A. Influence of humic acid imposed changes of ferrihydrite aggregation on microbial Fe(III) reduction. *Geochim Cosmochim Acta* 2012;**85**: 326-341.

Assaf-Anid N, Hayes KF, Vogel TM. Reduction dechlorination of carbon tetrachloride by cobalamin(II) in the presence of dithiothreitol: mechanistic study, effect of redox potential and pH. *Environ Sci Technol* 1994;**28**: 246-252.

Atashgahi S. Discovered by genomics: putative reductive dehalogenases with N-terminus transmembrane helixes. *FEMS Microbiol Ecol* 2019;**95**: fiz048.

Atashgahi S, Häggblom MM, Smidt H. Organohalide respiration in pristine environments: implications for the natural halogen cycle. *Environ Microbiol* 2018a;**20**: 934-948.

Atashgahi S, Liebensteiner MG, Janssen DB, Smidt H, Stams A, Sipkema D. Microbial synthesis and transformation of inorganic and organic chlorine compounds. *Front Microbiol* 2018b;**9**: 3079.

Atashgahi S, Lu Y, Smidt H. Overview of known organohalide-respiring bacteria—phylogenetic diversity and environmental distribution. In: Adrian L, Löffler FE (eds.) *Organohalide-Respiring Bacteria*. Berlin, Germany: Springer, 2016, 63-105.

Atashgahi S, Lu Y, Zheng Y, Saccenti E, Suarez-Diez M, Ramiro-Garcia J, Eisenmann H, Elsner M, Stams AJM, Springael D, Dejonghe W, Smidt H. Geochemical and microbial community determinants of reductive dechlorination at a site biostimulated with glycerol. *Environ Microbiol* 2017;**19**: 968-981.

Atashgahi S, Maphosa F, Doğan E, Smidt H, Springael D, Dejonghe W. Small-scale oxygen distribution determines the vinyl chloride biodegradation pathway in surficial sediments of riverbed hyporheic zones. *FEMS Microbiol Ecol* 2013;**84**: 133-142.

Atashgahi S, Sanchez-Andrea I, Heipieper HJ, van der Meer JR, Stams AJM, Smidt H. Prospects for harnessing biocide resistance for bioremediation and detoxification. *Science* 2018c;**360**: 743-746.

Atashgahi S, Shetty SA, Smidt H, De Vos WM. Flux, impact and fate of halogenated xenobiotic compounds in the gut. *Front Physiol* 2018d;**9**: 888.

ATSDR. Toxicological Profile for Chloroform. U.S. Department of Health and Human Services, Atlanta, Georgia, 1997.

Azizian MF, Marshall IP, Behrens S, Spormann AM, Semprini L. Comparison of lactate, formate, and propionate as hydrogen donors for the reductive dehalogenation of trichloroethene in a continuous-flow column. *J Contam Hydrol* 2010;**113**: 77-92.

Baeseman JL, Novak PJ. Effects of various environmental conditions on the transformation of chlorinated solvents by *Methanosarcina thermophila* cell exudates. *Biotechnol Bioeng* 2001;**75**: 634-641.

Bagherbaigi S, Gicana RG, Lamis RJ, Nemati M, Huyop F. Characterisation of *Arthrobacter* sp. S1 that can degrade α and β-haloalkanoic acids isolated from contaminated soil. *Ann Microbiol* 2013;**63**: 1363−1369.

Bagley DM, Gossett JM. Chloroform degradation in methanogenic methanol enrichment cultures and by *Methanosarcina barkeri* 227. *Appl Environ Microbiol* 1995;**61**: 3195-3201.

Balk M, van Gelder T, Weelink SA, Stams AJ. (Per)chlorate reduction by the thermophilic bacterium *Moorella perchloratireducens* sp. nov., isolated from underground gas storage. *Appl Environ Microbiol* 2008;**74**: 403-409.

Bankevich A, Nurk S, Antipov D, Gurevich AA, Dvorkin M, Kulikov AS, Lesin VM, Nikolenko SI, Pham S, Prjibelski AD. SPAdes: a new genome assembly algorithm and its applications to single-cell sequencing. *J Comput Biol* 2012;**19**: 455-477.

Barth PT, Bolton L, Thomson JC. Cloning and partial sequencing of an operon encoding two *Pseudomonas putida* haloalkanoate dehalogenases of opposite stereospecificity. *J Bacteriol* 1992;**174**: 2612−2619.

Bayer K, Scheuermayer M, Fieseler L, Hentschel U. Genomic mining for novel FADH2-dependent halogenases in marine sponge-associated microbial consortia. *Mar Biotechnol* 2013;**15**: 63-72.

Becker JG, Freedman DL. Use of cyanocobalamin to enhance anaerobic biodegradation of chloroform. *Environ Sci Technol* 1994;**28**: 1942-1949.

Bennett PM. Integrons and gene cassettes: a genetic construction kit for bacteria. *J Antimicrob Chemother* 1999;**43**: 1-4.

Beven K. How far can we go in distributed hydrological modelling? *Hydrol Earth Syst Sci* 2001;**5**: 1-12.

Bisaillon A, Beaudet R, Lépine F, Villemur R. Quantitative analysis of the relative transcript levels of four chlorophenol reductive dehalogenase genes in *Desulfitobacterium hafniense* PCP-1 exposed to chlorophenols. *Appl Environ Microbiol* 2011;**77**: 6261-6264.

Bodnár J, Gubicza L, Szabó L-P. Enantiomeric separation of 2-chloropropionic acid by enzymatic esterification in organic solvents. *J Mol Catal* 1990;**61**: 353−361.

Bolger AM, Lohse M, Usadel B. Trimmomatic: a flexible trimmer for Illumina sequence data. *Bioinformatics* 2014;**30**: 2114-2120.

Bommer M, Kunze C, Fesseler J, Schubert T, Diekert G, Dobbek H. Structural basis for organohalide respiration. *Science* 2014: 1258118.

Bowman KS, Nobre MF, da Costa MS, Rainey FA, Moe WM. *Dehalogenimonas alkenigignens* sp. nov., a chlorinated-alkane-dehalogenating bacterium isolated from groundwater. *Int J Syst Evol Microbiol* 2013;**63**: 1492-1498.

Boyle AW, Phelps CD, Young L. Isolation from estuarine sediments of a *Desulfovibrio* strain which can grow on lactate coupled to the reductive dehalogenation of 2,4,6-tribromophenol. *Appl Environ Microbiol* 1999;**65**: 1133−1140.

Bradford MM. A rapid and sensitive method for the quantitation of microgram quantities of protein utilizing the principle of protein-dye binding. *Anal Biochem* 1976;**72**: 248-254.

Breider F, Albers CN, Hunkeler D. Assessing the role of trichloroacetyl-containing compounds in the natural formation of chloroform using stable carbon isotopes analysis. *Chemosphere* 2013;**90**: 441-448.

Brovelli A, Barry DA, Robinson C, Gerhard JI. Analysis of acidity production during enhanced reductive dechlorination using a simplified reactive transport model. *Adv Water Resour* 2012;**43**: 14-27.

Bui TPN, de Vos WM, Plugge CM. *Anaerostipes rhamnosivorans* sp. nov., a human intestinal, butyrate-forming bacterium. *Int J Syst Evol Microbiol* 2014;**64**: 787-793.

Bunge M, K hk nen MA, R misch W, Opel M, Vogler S, Walkow F, Salkinoja-Salonen M, Lechner U. Biological activity in a heavily organohalogen-contaminated river sediment. *Environ Sci Pollut Res* 2007;**14**: 3-10.

Burns JL, DiChristina TJ. Anaerobic respiration of elemental sulfur and thiosulfate by *Shewanella oneidensis* MR-1 requires *psrA*, a homolog of the *phsA* gene of *Salmonella enterica* serovar typhimurium LT2. *Appl Environ Microbiol* 2009;**75**: 5209-5217.

Burrichter A, Denger K, Franchini P, Huhn T, Müller N, Spiteller D, Schleheck D. Anaerobic degradation of the plant sugar sulfoquinovose concomitant with H_2S production: *Escherichia coli* K-12 and *Desulfovibrio* sp. strain DF1 as co-culture model. *Front Microbiol* 2018;**9**: 2792.

Buttet GF, Willemin MS, Hamelin R, Rupakula A, Maillard J. The membrane-bound C subunit of reductive dehalogenases: topology analysis and reconstitution of the FMN-binding domain of PceC. *Front Microbiol* 2018;**9**: 755.

Caffrey SM, Voordouw G. Effect of sulfide on growth physiology and gene expression of *Desulfovibrio vulgaris* Hildenborough. *Antonie Van Leeuwenhoek* 2010;**97**: 11-20.

Camacho C, Coulouris G, Avagyan V, Ma N, Papadopoulos J, Bealer K, Madden TL. BLAST+: architecture and applications. *BMC Bioinformatics* 2009;**10**: 421.

Caporaso JG, Kuczynski J, Stombaugh J, Bittinger K, Bushman FD, Costello EK, Fierer N, Peña AG, Goodrich JK, Gordon JI. QIIME allows analysis of high-throughput community sequencing data. *Nat Methods* 2010;**7**: 335-336.

Cappelletti M, Frascari D, Zannoni D, Fedi S. Microbial degradation of chloroform. *Appl Microbiol Biotechnol* 2012;**96**: 1395-1409.

Carlström CI, Loutey D, Bauer S, Clark IC, Rohde RA, Iavarone AT, Lucas L, Coates JD. (Per)Chlorate-reducing bacteria can utilize aerobic and anaerobic pathways of aromatic degradation with (per)chlorate as an electron acceptor. *mBio* 2015;**6**: e02287−02214.

Carlström CI, Wang O, Melnyk RA, Bauer S, Lee J, Engelbrektson A, Coates JD. Physiological and genetic description of dissimilatory perchlorate reduction by the novel marine bacterium *Arcobacter* sp. strain CAB. *MBio* 2013;**4**: e00217-00213.

Carvalho M, Ferreira Jorge R, Pacheco C, De Marco P, Castro P. Isolation and properties of a pure bacterial strain capable of fluorobenzene degradation as sole carbon and energy source. *Environ Microbiol* 2005;**7**: 294-298.

Chakraborty M, Baldwin-Brown JG, Long AD, Emerson J. Contiguous and accurate de novo assembly of metazoan genomes with modest long read coverage. *Nucleic Acids Res* 2016;**44**: e147.

Chambon JC, Bjerg PL, Scheutz C, Bælum J, Jakobsen R, Binning PJ. Review of reactive kinetic models describing reductive dechlorination of chlorinated ethenes in soil and groundwater. *Biotechnol Bioeng* 2013;**110**: 1-23.

Chan WW, Grostern A, Löffler FE, Edwards EA. Quantifying the effects of 1,1,1-trichloroethane and 1,1-dichloroethane on chlorinated ethene reductive dehalogenases. *Environ Sci Technol* 2011;**45**: 9693-9702.

Chen G, Shouakar-Stash O, Phillips E, Justicia-Leon SD, Gilevska T, Sherwood Lollar B, Mack EE, Seger ES, Löffler FE. Dual carbon-chlorine isotope analysis indicates distinct anaerobic dichloromethane degradation pathways in two members of the *Peptococcaceae*. *Environ Sci Technol* 2018;**52**: 8607-8616.

Chen J, Bowman KS, Rainey FA, Moe WM. Reassessment of PCR primers targeting 16S rRNA genes of the organohalide-respiring genus *Dehalogenimonas*. *Biodegradation* 2014a;**25**: 747-756.

Chen L, Liu Y, Liu F, Jin S. Treatment of co-mingled benzene, toluene and TCE in groundwater. *J Hazard Mater* 2014b;**275**: 116-120.

Chikhi R, Medvedev P. Informed and automated k-mer size selection for genome assembly. *Bioinformatics* 2013;**30**: 31-37.

Chiu P-C, Reinhard M. Metallocoenzyme-mediated reductive transformation of carbon tetrachloride in titanium(III) citrate aqueous solution. *Environ Sci Technol* 1995;**29**: 595-603.

Christ JA, Abriola LM. Modeling metabolic reductive dechlorination in dense non-aqueous phase liquid source-zones. *Adv Water Resour* 2007;**30**: 1547-1561.

Cicerone RJ, Stolarski RS, Walters S. Stratospheric ozone destruction by man-made chlorofluoromethanes. *Science* 1974;**185**: 1165-1167.

Clark IC, Melnyk RA, Engelbrektson A, Coates JD. Structure and evolution of chlorate reduction composite transposons. *Mbio* 2013;**4**: e00379-00313.

Cline JD. Spectrophotometric determination of hydrogen sulfide in natural waters. *Limnol Oceanogr* 1969;**14**: 454-458.

Colombani N, Pantano A, Mastrocicco M, Petitta M. Reactive modelling of 1,2-DCA and DOC near the shoreline. *J Contam Hydrol* 2014;**169**: 100-111.

Conrad R. Microbial ecology of methanogens and methanotrophs. *Adv Agron* 2007;**96**: 1-63.

Corapcioglu MY, Sung K, Kim J. Parameter determination of sequential reductive dehalogenation reactions of chlorinated hydrocarbons. *Transport Porous Med* 2004;**55**: 169-182.

Costa C, Jesus-Rydin C. Site investigation on heavy metals contaminated ground in Estarreja—Portugal. *Eng Geol* 2001;**60**: 39-47.

Crawford RL, Jung CM, Strap JL. The recent evolution of pentachlorophenol (PCP)-4-monooxygenase (PcpB) and associated pathways for bacterial degradation of PCP. *Biodegradation* 2007;**18**: 525-539.

Cupples AM, Spormann AM, McCarty PL. Vinyl chloride and *cis*-dichloroethene dechlorination kinetics and microorganism growth under substrate limiting conditions. *Environ Sci Technol* 2004;**38**: 1102-1107.

Da Silva ML, Alvarez P. Exploring the correlation between halorespirer biomarker concentrations and TCE dechlorination rates. *J Environ Eng* 2008;**134**: 895-901.

Daims H, Brühl A, Amann R, Schleifer K-H, Wagner M. The domain-specific probe EUB338 is insufficient for the detection of all Bacteria: development and evaluation of a more comprehensive probe set. *Syst Appl Microbiol* 1999;**22**: 434-444.

Damsté JSS, Rijpstra WIC, Hopmans EC, Weijers JW, Foesel BU, Overmann J, Dedysh SN. 13,16-Dimethyl octacosanedioic acid (*iso*-diabolic acid): A common membrane-spanning lipid of *Acidobacteria* subdivisions 1 and 3. *Appl Environ Microbiol* 2011;**77**: 4147-4154.

Darling AE, Mau B, Perna NT. progressiveMauve: multiple genome alignment with gene gain, loss and rearrangement. *PLoS One* 2010;**5**: e11147.

DeWeerd KA, Mandelco L, Tanner RS, Woese CR, Suflita JM. *Desulfomonile tiedjei* gen. nov. and sp. nov., a novel anaerobic, dehalogenating, sulfate-reducing bacterium. *Arch Microbiol* 1990;**154**: 23-30.

DeWeerd KA, Suflita JM. Anaerobic aryl reductive dehalogenation of halobenzoates by cell extracts of "*Desulfomonile tiedjei*". *Appl Environ Microbiol* 1990;**56**: 2999-3005.

Dillehay JL, Bowman KS, Yan J, Rainey FA, Moe WM. Substrate interactions in dehalogenation of 1,2-dichloroethane, 1,2-dichloropropane, and 1,1,2-trichloroethane mixtures by *Dehalogenimonas* spp. *Biodegradation* 2014;**25**: 301-312.

Ding C, Zhao S, He J. A *Desulfitobacterium* sp. strain PR reductively dechlorinates both 1,1,1-trichloroethane and chloroform. *Environ Microbiol* 2014;**16**: 3387-3397.

Dobson L, Reményi I, Tusnády GE. CCTOP: a Consensus Constrained TOPology prediction web server. *Nucleic Acids Res* 2015;**43**: W408-W412.

Dolfing J, Janssen DB. Estimates of Gibbs free energies of formation of chlorinated aliphatic compounds. *Biodegradation* 1994;**5**: 21−28.

Dolla A, Fournier M, Dermoun Z. Oxygen defense in sulfate-reducing bacteria. *J Biotechnol* 2006;**126**: 87-100.

Dos Santos PC, Fang Z, Mason SW, Setubal JC, Dixon R. Distribution of nitrogen fixation and nitrogenase-like sequences amongst microbial genomes. *BMC Genomics* 2012;**13**: 162.

Drake HL, Gößner AS, Daniel SL. Old acetogens, new light. *Ann N Y Acad Sci* 2008;**1125**: 100-128.

Duarte AG, Catarino T, White GF, Lousa D, Neukirchen S, Soares CM, Sousa FL, Clarke TA, Pereira IA. An electrogenic redox loop in sulfate reduction reveals a likely widespread mechanism of energy conservation. *Nat Commun* 2018;**9**: 5448.

Duhamel M, Edwards EA. Microbial composition of chlorinated ethene-degrading cultures dominated by *Dehalococcoides*. *FEMS Microbiol Ecol* 2006;**58**: 538-549.

Duhamel M, Edwards EA. Growth and yields of dechlorinators, acetogens, and methanogens during reductive dechlorination of chlorinated ethenes and dihaloelimination of 1,2-dichloroethane. *Environ Sci Technol* 2007;**41**: 2303-2310.

Dyall-Smith M. *The Halohandbook: protocols for haloarchaeal genetics* volume 14. Haloarchaeal Genetics Laboratory, Melbourne, 2008.

Edgar RC. Search and clustering orders of magnitude faster than BLAST. *Bioinformatics* 2010;**26**: 2460-2461.

Edgren T, Nordlund S. The *fixABCX* genes in *Rhodospirillum rubrum* encode a putative membrane complex participating in electron transfer to nitrogenase. *J Bacteriol* 2004;**186**: 2052-2060.

Edwards EA. Breathing the unbreathable. *Science* 2014;**346**: 424-425.

Egert M, De Graaf AA, Maathuis A, De Waard P, Plugge CM, Smidt H, Deutz NEP, Dijkema C, De Vos WM, Venema K. Identification of glucose-fermenting bacteria present in an in vitro model of the human intestine by RNA-stable isotope probing. *FEMS Microbiol Ecol* 2007;**60**: 126−135.

Egli C, Tschan T, Scholtz R, Cook AM, Leisinger T. Transformation of tetrachloromethane to dichloromethane and carbon dioxide by *Acetobacterium woodii*. *Appl Environ Microbiol* 1988;**54**: 2819-2824.

Eliopoulos G, Wennersten C. Antimicrobial activity of quinupristin-dalfopristin combined with other antibiotics against vancomycin-resistant enterococci. *Antimicrob Agents Chemother* 2002;**46**: 1319-1324.

Ellis DE, Lutz EJ, Odom JM, Buchanan RJ, Bartlett CL, Lee MD, Harkness MR, DeWeerd KA. Bioaugmentation for accelerated in situ anaerobic bioremediation. *Environ Sci Technol* 2000;**34**: 2254-2260.

EPA. 2018 Edition of the Drinking Water Standards and Health Advisories Tables. Washington, DC: US Environmental Protection Agency, 2018, 20.

Ettwig KF, Butler MK, Le Paslier D, Pelletier E, Mangenot S, Kuypers MM, Schreiber F, Dutilh BE, Zedelius J, De Beer D. Nitrite-driven anaerobic methane oxidation by oxygenic bacteria. *Nature* 2010;**464**: 543-548.

Fetzner S, Müller R, Lingens F. Purification and some properties of 2-halobenzoate 1, 2-dioxygenase, a two-component enzyme system from *Pseudomonas cepacia* 2CBS. *J Bacteriol* 1992;**174**: 279-290.

Field JA. Natural production of organohalide compounds in the environment. In: Adrian L, Löffler FE (eds.) *Organohalide-Respiring Bacteria*. Berlin Heidelberg: Springer, 2016, 7-29.

Field JA, Sierra-Alvarez R. Biodegradability of chlorinated solvents and related chlorinated aliphatic compounds. *Rev Environ Sci Bio* 2004;**3**: 185-254.

Field JA, Sierra-Alvarez R. Microbial degradation of chlorinated benzenes. *Biodegradation* 2008;**19**: 463-480.

Fincker M, Spormann AM. Biochemistry of catabolic reductive dehalogenation. *Annu Rev Biochem* 2017;**86**: 357-386.

Finneran KT, Forbush HM, VanPraagh CVG, Lovley DR. *Desulfitobacterium metallireducens* sp. nov., an anaerobic bacterium that couples growth to the reduction of metals and humic acids as well as chlorinated compounds. *Int J Syst Evol Microbiol* 2002;**52**: 1929-1935.

Flowers JJ, Richards MA, Baliga N, Meyer B, Stahl DA. Constraint-based modelling captures the metabolic versatility of *Desulfovibrio vulgaris*. *Environ Microbiol Rep* 2018;**10**: 190-201.

Fournier M, Zhang Y, Wildschut JD, Dolla A, Voordouw JK, Schriemer DC, Voordouw G. Function of oxygen resistance proteins in the anaerobic, sulfate-reducing bacterium *Desulfovibrio vulgaris* Hildenborough. *J Bacteriol* 2003;**185**: 71-79.

Fu F, Wang Q. Removal of heavy metal ions from wastewaters: a review. *J Environ Manage* 2011;**92**: 407-418.

Futagami T, Goto M, Furukawa K. Genetic system of organohalide-respiring bacteria. In: Nojiri H, Tsuda M, Fukuda M, Kamagata Y (eds.) *Biodegradative Bacteria*. Japan: Springer, 2014, 59-81.

Futagami T, Morono Y, Terada T, Kaksonen AH, Inagaki F. Dehalogenation activities and distribution of reductive dehalogenase homologous genes in marine subsurface sediments. *Appl Environ Microbiol* 2009;**75**: 6905-6909.

Gábor K, Veríssimo CS, Cyran BC, ter Horst P, Meijer NP, Smidt H, de Vos WM, van der Oost J. Characterization of CprK1, a CRP/FNR-type transcriptional regulator of halorespiration from Desulfitobacterium hafniense. *J Bacteriol* 2006;**188**: 2604-2613.

Gadkari J, Goris T, Schiffmann CL, Rubick R, Adrian L, Schubert T, Diekert G. Reductive tetrachloroethene dehalogenation in the presence of oxygen by *Sulfurospirillum multivorans*: physiological studies and proteome analysis. *FEMS Microbiol Ecol* 2018;**94**: fix176.

Gälli R, McCARTY PL. Biotransformation of 1,1,1-trichloroethane, trichloromethane, and tetrachloromethane by a *Clostridium* sp. *Appl Environ Microbiol* 1989;**55**: 837-844.

Gantzer CJ, Wackett LP. Reductive dechlorination catalyzed by bacterial transition-metal coenzymes. *Environ Sci Technol* 1991;**25**: 715-722.

Garant H, Lynd L. Applicability of competitive and noncompetitive kinetics to the reductive dechlorination of chlorinated ethenes. *Biotechnol Bioeng* 1998;**57**: 751-755.

Gerritse J, Drzyzga O, Kloetstra G, Keijmel M, Wiersum LP, Hutson R, Collins MD, Gottschal JC. Influence of different electron donors and acceptors on dehalorespiration of tetrachloroethene by *Desulfitobacterium frappieri* TCE1. *Appl Environ Microbiol* 1999;**65**: 5212-5221.

Goris T, Schiffmann CL, Gadkari J, Schubert T, Seifert J, Jehmlich N, Von Bergen M, Diekert G. Proteomics of the organohalide-respiring Epsilonproteobacterium *Sulfurospirillum multivorans* adapted to tetrachloroethene and other energy substrates. *Sci Rep* 2015;**5**: 13794.

Goris T, Schubert T, Gadkari J, Wubet T, Tarkka M, Buscot F, Adrian L, Diekert G. Insights into organohalide respiration and the versatile catabolism of *Sulfurospirillum multivorans* gained from comparative genomics and physiological studies. *Environ Microbiol* 2014;**16**: 3562-3580.

Gribble GW. Naturally occurring organohalogen compounds. *Acc Chem Res* 1998;**31**: 141-152.

Gribble GW. The natural production of organobromine compounds. *Environ Sci Pollut Res* 2000;**7**: 37−49.

Gribble GW. The diversity of naturally produced organohalogens. *Chemosphere* 2003;**52**: 289−297.

Gribble GW. *Naturally occurring organohalogen compounds—a comprehensive update* volume 91: Springer, Vienna, 2010.

Gribble GW. A recent survey of naturally occurring organohalogen compounds. *Environ Chem* 2015;**12**: 396-405.

Grostern A, Chan WW, Edwards EA. 1,1,1-Trichloroethane and 1,1-dichloroethane reductive dechlorination kinetics and co-contaminant effects in a *Dehalobacter*-containing mixed culture. *Environ Sci Technol* 2009;**43**: 6799-6807.

Grostern A, Duhamel M, Dworatzek S, Edwards EA. Chloroform respiration to dichloromethane by a *Dehalobacter* population. *Environ Microbiol* 2010;**12**: 1053-1060.

Grostern A, Edwards EA. Characterization of a *Dehalobacter* coculture that dechlorinates 1,2-dichloroethane to ethene and identification of the putative reductive dehalogenase gene. *Appl Environ Microbiol* 2009;**75**: 2684-2693.

Guerrero-Barajas C, Field JA. Riboflavin- and cobalamin-mediated biodegradation of chloroform in a methanogenic consortium. *Biotechnol Bioeng* 2005;**89**: 539-550.

Haest PJ, Springael D, Smolders E. Dechlorination kinetics of TCE at toxic TCE concentrations: Assessment of different models. *Water Res* 2010a;**44**: 331-339.

Haest PJ, Springael D, Smolders E. Modelling reactive CAH transport using batch experiment degradation kinetics. *Water Res* 2010b;**44**: 2981-2989.

Hage JC, Hartmans S. Monooxygenase-mediated 1, 2-dichloroethane degradation by *Pseudomonas* sp. strain DCA1. *Appl Environ Microbiol* 1999;**65**: 2466-2470.

Hall RM, Collis CM. Antibiotic resistance in gram-negative bacteria: the role of gene cassettes and integrons. *Drug resistance UPDATES* 1998;**1**: 109-119.

Harper DB. The global chloromethane cycle: biosynthesis, biodegradation and metabolic role. *Nat Prod Rep* 2000;**17**: 337-348.

Hasan AQ, Takada H, Koshikawa H, Liu J-Q, Kurihara T, Esaki N, Soda K. Two kinds of 2-haloacid dehalogenases from *Pseudomonas* sp. YL induced by 2-chloroacrylate and 2-chloropropionate. *Biosci Biotechnol Biochem* 1994;**58**: 1599−1602.

Haselmann KF, Laturnus F, Grøn C. Formation of chloroform in soil. A year-round study at a Danish spruce forest site. *Water Air Soil Pollut* 2002;**139**: 35-41.

Hashsham SA, Freedman DL. Enhanced biotransformation of carbon tetrachloride by *Acetobacterium woodii* upon addition of hydroxocobalamin and fructose. *Appl Environ Microbiol* 1999;**65**: 4537-4542.

Haston ZC, McCarty PL. Chlorinated ethene half-velocity coefficients (Ks) for reductive dehalogenation. *Environ Sci Technol* 1999;**33**: 223-226.

He J, Sung Y, Krajmalnik-Brown R, Ritalahti KM, Löffler FE. Isolation and characterization of *Dehalococcoides* sp. strain FL2, a trichloroethene (TCE)-and 1,2-dichloroethene-respiring anaerobe. *Environ Microbiol* 2005;**7**: 1442-1450.

He Y, Wilson J, Su C, Wilkin R. Review of abiotic degradation of chlorinated solvents by reactive iron minerals in aquifers. *Ground Water Monit Remediat* 2015;**35**: 57-75.

Hermon L, Denonfoux J, Hellal J, Joulian C, Ferreira S, Vuilleumier S, Imfeld G. Dichloromethane biodegradation in multi-contaminated groundwater: Insights from biomolecular and compound-specific isotope analyses. *Water Res* 2018;**142**: 217-226.

Hill KE, Marchesi JR, Weightman AJ. Investigation of two evolutionarily unrelated halocarboxylic acid dehalogenase gene families. *J Bacteriol* 1999;**181**: 2535−2547.

Hisano T, Hata Y, Fujii T, Liu J-Q, Kurihara T, Esaki N, Soda K. Crystal structure of L-2-haloacid dehalogenase from *Pseudomonas* sp. YL. *J Biol Chem* 1996a;**271**: 20322−20330.

Hisano T, Hata Y, Fujii T, Liu J-Q, Kurihara T, Esaki N, Soda K. Crystal Structure of L-2-Haloacid Dehalogenase from Pseudomonas sp. YL. An α/β hydrolase structure that is different from the α/β hydrolase fold. *J Biol Chem* 1996b;**271**: 20322-20330.

Holliger C, Schraa G, Stams AJM, Zehnder AJB. A highly purified enrichment culture couples the reductive dechlorination of tetrachloroethene to growth. *Appl Environ Microbiol* 1993;**59**: 2991−2997.

Holliger C, Schraa G, Stupperich E, Stams A, Zehnder A. Evidence for the involvement of corrinoids and factor F_{430} in the reductive dechlorination of 1,2-dichloroethane by Methanosarcina barkeri. *J Bacteriol* 1992;**174**: 4427-4434.

Hug LA. Diversity, evolution, and environmental distribution of reductive dehalogenase genes. In: Adrian L, Löffler FE (eds.) *Organohalide-Respiring Bacteria*. Berlin Heidelberg: Springer, 2016, 377-393.

Hug LA, Maphosa F, Leys D, Löffler FE, Smidt H, Edwards EA, Adrian L. Overview of organohalide-respiring bacteria and a proposal for a classification system for reductive dehalogenases. *Phil Trans R Soc B* 2013;**368**: 20120322.

Hunkeler D, Laier T, Breider F, Jacobsen OS. Demonstrating a natural origin of chloroform in groundwater using stable carbon isotopes. *Environ Sci Technol* 2012;**46**: 6096-6101.

Hyatt D, Chen G-L, LoCascio PF, Land ML, Larimer FW, Hauser LJ. Prodigal: prokaryotic gene recognition and translation initiation site identification. *BMC Bioinformatics* 2010a;**11**: 119−130.

Hyatt D, Chen G-L, LoCascio PF, Land ML, Larimer FW, Hauser LJ. Prodigal: prokaryotic gene recognition and translation initiation site identification. *BMC Bioinformatics* 2010b;**11**: 119.

Janssen DB, Dinkla IJ, Poelarends GJ, Terpstra P. Bacterial degradation of xenobiotic compounds: evolution and distribution of novel enzyme activities. *Environ Microbiol* 2005;**7**: 1868-1882.

Janssen DB, Oppentocht JE, Poelarends GJ. Microbial dehalogenation. *Curr Opin Biotechnol* 2001;**12**: 254−258.

Janssen DB, Pries F, van der Ploeg JR. Genetics and biochemistry of dehalogenating enzymes. *Annu Rev Microbiol* 1994;**48**: 163-191.

Janssen DB, Scheper A, Dijkhuizen L, Witholt B. Degradation of halogenated aliphatic compounds by *Xanthobacter autotrophicus* GJ10. *Appl Environ Microbiol* 1985;**49**: 673-677.

Jochum LM, Schreiber L, Marshall IP, Jørgensen BB, Schramm A, Kjeldsen KU. Single-cell genomics reveals a diverse metabolic potential of uncultivated *Desulfatiglans*-related Deltaproteobacteria widely distributed in marine sediment. *Front Microbiol* 2018;**9**: 2038.

Jones DH, Barth PT, Byrom D, Thomas CM. Nucleotide sequence of the structural gene encoding a 2-haloalkanoic acid dehalogenase of *Pseudomonas putida* strain AJ1 and purification of the encoded protein. *Microbiology* 1992;**138**: 675−683.

Justicia-Leon SD, Higgins S, Mack EE, Griffiths DR, Tang S, Edwards EA, Löffler FE. Bioaugmentation with distinct *Dehalobacter* strains achieves chloroform detoxification in microcosms. *Environ Sci Technol* 2014;**48**: 1851-1858.

Kang N, Jackson WA, Dasgupta PK, Anderson TA. Perchlorate production by ozone oxidation of chloride in aqueous and dry systems. *Sci Total Environ* 2008;**405**: 301-309.

Kawasaki H, Toyama T, Maeda T, Nishino H, Tonomura K. Cloning and sequence analysis of a plasmid-encoded 2-haloacid dehalogenase gene from *Pseudomonas putida* no. 109. *Biosci Biotechnol Biochem* 1994;**58**: 160−163.

Keller KL, Wall JD. Genetics and molecular biology of the electron flow for sulfate respiration in *Desulfovibrio*. *Front Microbiol* 2011;**2**: 135.

Kemp LR, Dunstan MS, Fisher K, Warwicker J, Leys D. The transcriptional regulator CprK detects chlorination by combining direct and indirect readout mechanisms. *Phil Trans R Soc B* 2013;**368**: 1-8.

Kennish MJ. *Practical handbook of estuarine and marine pollution*: CRC press, 2017.

Kettlitz B, Kemendi G, Thorgrimsson N, Cattoor N, Verzegnassi L, Le Bail-Collet Y, Maphosa F, Perrichet A, Christall B, Stadler RH. Why chlorate occurs in potable water and processed foods: a critical assessment and challenges faced by the food industry. *Food Addit Contam Part A* 2016;**33**: 968-982.

Khalil M, Rasmussen R, Shearer M, Chen ZL, Yao H, Yang J. Emissions of methane, nitrous oxide, and other trace gases from rice fields in China. *J Geophys Res Atmos* 1998;**103**: 25241-25250.

Kirk DG, Palonen E, Korkeala H, Lindström M. Evaluation of normalization reference genes for RT-qPCR analysis of *spo0A* and four sporulation sigma factor genes in *Clostridium botulinum* group I strain ATCC 3502. *Anaerobe* 2014;**26**: 14-19.

Kleindienst S, Chourey K, Chen G, Murdoch RW, Higgins SA, Iyer R, Campagna SR, Mack EE, Seger ES, Hettich RL. Proteogenomics reveals novel reductive dehalogenases and methyltransferases expressed during anaerobic dichloromethane metabolism. *Appl Environ Microbiol* 2019;**85**: e02768-02718.

Kleindienst S, Higgins SA, Tsementzi D, Chen G, Konstantinidis KT, Mack EE, Löffler FE. 'Candidatus *Dichloromethanomonas elyunquensis*' gen. nov., sp. nov., a dichloromethane-degrading anaerobe of the *Peptococcaceae* family. *Syst Appl Microbiol* 2017;**40**: 150-159.

Koehorst JJ, Saccenti E, Schaap PJ, dos Santos VAPM, Suarez-Diez M. Protein domain architectures provide a fast, efficient and scalable alternative to sequence-based methods for comparative functional genomics. *F1000Res* 2016a;**5:1987**.

Koehorst JJ, van Dam JCJ, van Heck RGA, Saccenti E, dos Santos VAPM, Suarez-Diez M, Schaap PJ. Comparison of 432 *Pseudomonas* strains through integration of genomic, functional, metabolic and expression data. *Sci Rep* 2016b;**6:38699**

Kouznetsova I, Mao X, Robinson C, Barry DA, Gerhard JI, McCarty PL. Biological reduction of chlorinated solvents: Batch-scale geochemical modeling. *Adv Water Resour* 2010;**33**: 969-986.

Krone UE, Laufer K, Thauer RK, Hogenkamp HP. Coenzyme F_{430} as a possible catalyst for the reductive dehalogenation of chlorinated C1 hydrocarbons in methanogenic bacteria. *Biochemistry* 1989a;**28**: 10061-10065.

Krone UE, Thauer RK, Hogenkamp HP. Reductive dehalogenation of chlorinated C1-hydrocarbons mediated by corrinoids. *Biochemistry* 1989b;**28**: 4908-4914.

Kruse T, Goris T, Maillard J, Woyke T, Lechner U, de Vos W, Smidt H. Comparative genomics of the genus *Desulfitobacterium*. *FEMS Microbiol Ecol* 2017;**93**: fix135.

Kruse T, Smidt H, Lechner U. Comparative genomics and transcriptomics of organohalide-respiring bacteria and regulation of rdh gene transcription. In: Adrian L, Löffler FE (eds.) *Organohalide-Respiring Bacteria*. Berlin Heidelberg: Springer, 2016, 345-376.

Kruse T, van de Pas BA, Atteia A, Krab K, Hagen WR, Goodwin L, Chain P, Boeren S, Maphosa F, Schraa G. Genomic, proteomic, and biochemical analysis of the organohalide respiratory pathway in *Desulfitobacterium dehalogenans*. *J Bacteriol* 2015;**197**: 893-904.

Krzmarzick MJ, Crary BB, Harding JJ, Oyerinde OO, Leri AC, Myneni SC, Novak PJ. Natural niche for organohalide-respiring *Chloroflexi*. *Appl Environ Microbiol* 2012;**78**: 393-401.

Kublik A, Deobald D, Hartwig S, Schiffmann CL, Andrades A, von Bergen M, Sawers RG, Adrian L. Identification of a multi-protein reductive dehalogenase complex in *Dehalococcoides mccartyi* strain CBDB 1 suggests a protein-dependent respiratory electron transport chain obviating quinone involvement. *Environ Microbiol* 2016;**18**: 3044-3056.

Kuever J. The family *DesulfobacteraceaeThe Prokaryotes*: Springer, 2014, 45-73.

Kunze C, Bommer M, Hagen WR, Uksa M, Dobbek H, Schubert T, Diekert G. Cobamide-mediated enzymatic reductive dehalogenation via long-range electron transfer. *Nat Commun* 2017;**8**: 15858.

Kurihara T, Esaki N, Soda K. Bacterial 2-haloacid dehalogenases: structures and reaction mechanisms. *J Mol Catal B Enzym* 2000;**10**: 57−65.

Lai Y, Becker JG. Compounded effects of chlorinated ethene inhibition on ecological interactions and population abundance in a *Dehalococcoides-Dehalobacter* coculture. *Environ Sci Technol* 2013;**47**: 1518-1525.

Langford NJ. Carbon dioxide poisoning. *Toxicol Rev* 2005;**24**: 229-235.

Langmead B, Salzberg SL. Fast gapped-read alignment with Bowtie 2. *Nature methods* 2012;**9**: 357-359.

Laturnus F, Haselmann KF, Borch T, Grøn C. Terrestrial natural sources of trichloromethane (chloroform, CHCl 3)–an overview. *Biogeochemistry* 2002;**60**: 121-139.

Lavric ED, Konnov AA, De Ruyck J. Dioxin levels in wood combustion—a review. *Biomass Bioenergy* 2004;**26**: 115-145.

Ledbetter RN, Garcia Costas AM, Lubner CE, Mulder DW, Tokmina-Lukaszewska M, Artz JH, Patterson A, Magnuson TS, Jay ZJ, Duan HD. The electron bifurcating FixABCX protein complex from *Azotobacter vinelandii*: generation of low-potential reducing equivalents for nitrogenase catalysis. *Biochemistry* 2017;**56**: 4177-4190.

Lee M, Low A, Zemb O, Koenig J, Michaelsen A, Manefield M. Complete chloroform dechlorination by organochlorine respiration and fermentation. *Environ Microbiol* 2012;**14**: 883-894.

Leri AC, Mayer LM, Thornton KR, Northrup PA, Dunigan MR, Ness KJ, Gellis AB. A marine sink for chlorine in natural organic matter. *Nat Geosci* 2015;**8**: 620-624.

Letunic I, Bork P. Interactive Tree Of Life v2: online annotation and display of phylogenetic trees made easy. *Nucleic Acids Res* 2011;**39**: W475-W478.

Lewis TA, Morra MJ, Brown PD. Comparative product analysis of carbon tetrachloride dehalogenation catalyzed by cobalt corrins in the presence of thiol or titanium (III) reducing agents. *Environ Sci Technol* 1995;**30**: 292-300.

Li D, Luo R, Liu C-M, Leung C-M, Ting H-F, Sadakane K, Yamashita H, Lam T-W. MEGAHIT v1. 0: a fast and scalable metagenome assembler driven by advanced methodologies and community practices. *Methods* 2016;**102**: 3-11.

Li H, Handsaker B, Wysoker A, Fennell T, Ruan J, Homer N, Marth G, Abecasis G, Durbin R. The sequence alignment/map format and SAMtools. *Bioinformatics* 2009;**25**: 2078-2079.

Li Y-F, Hata Y, Fujii T, Hisano T, Nishihara M, Kurihara T, Esaki N. Crystal structures of reaction intermediates of L-2-haloacid dehalogenase and implications for the reaction mechanism. *J Biol Chem* 1998a;**273**: 15035−15044.

Li Y-F, Hata Y, Fujii T, Hisano T, Nishihara M, Kurihara T, Esaki N. Crystal Structures of Reaction Intermediates ofL-2-Haloacid Dehalogenase and Implications for the Reaction Mechanism. *J Biol Chem* 1998b;**273**: 15035-15044.

Lin C, Yang L, Xu G, Wu J. Biodegradation and metabolic pathway of β-chlorinated aliphatic acid in *Bacillus* sp. CGMCC no. 4196. *Appl Microbiol Biotechnol* 2011;**90**: 689−696.

Lineweaver H, Burk D. The determination of enzyme dissociation constants. *J Am Chem Soc* 1934;**56**: 658-666.

Liu J, Häggblom MM. Genome-guided identification of organohalide-respiring *Deltaproteobacteria* from the marine environment. *mBio* 2018;**9**: e02471-02418.

Liu J, Lopez N, Ahn YB, Goldberg T, Bromberg Y, Kerkhof LJ, Häggblom MM. Novel reductive dehalogenases from the marine sponge associated bacterium *Desulfoluna spongiiphila*. *Environ Microbiol Rep* 2017;**9**: 537-549.

Low A, Zhao S, Rogers MJ, Zemb O, Lee M, He J, Manefield M. Isolation, characterization and bioaugmentation of an acidotolerant 1, 2-dichloroethane respiring *Desulfitobacterium* species from a low pH aquifer. *FEMS Microbiol Ecol* 2019;**95**: fiz055.

Lu Y, Atashgahi S, Hug LA, Smidt H. Primers that target functional genes of organohalide-respiring bacteria. In: McGenity TJ, Timmis KN, Nogales B (eds.) *Hydrocarbon and Lipid Microbiology Protocols*. Berlin, Heidelberg: Springer, 2015, 177-205.

Lu Y, Ramiro-Garcia J, Vandermeeren P, Herrmann S, Cichocka D, Springael D, Atashgahi S, Smidt H. Dechlorination of three tetrachlorobenzene isomers by contaminated harbor sludge-derived enrichment cultures follows thermodynamically favorable reactions. *Appl Microbiol Biotechnol* 2017;**101**: 2589-2601.

Ma Y, Wang L, Shao Z. *Pseudomonas*, the dominant polycyclic aromatic hydrocarbon-degrading bacteria isolated from Antarctic soils and the role of large plasmids in horizontal gene transfer. *Environ Microbiol* 2006;**8**: 455-465.

Mackay D, Shiu WY. A critical review of Henry's law constants for chemicals of environmental interest. *J Phys Chem Ref Data* 1981;**10**: 1175-1199.

Mägli A, Wendt M, Leisinger T. Isolation and characterization of *Dehalobacterium formicoaceticum* gen. nov. sp. nov., a strictly anaerobic bacterium utilizing dichloromethane as source of carbon and energy. *Arch Microbiol* 1996;**166**: 101-108.

Malaguerra F, Chambon JC, Bjerg PL, Scheutz C, Binning PJ. Development and sensitivity analysis of a fully kinetic model of sequential reductive dechlorination in groundwater. *Environ Sci Technol* 2011;**45**: 8395-8402.

Maness AD, Bowman KS, Yan J, Rainey FA, Moe WM. *Dehalogenimonas* spp. can reductively dehalogenate high concentrations of 1,2-dichloroethane, 1,2-dichloropropane, and 1,1,2-trichloroethane. *AMB Express* 2012;**2**: 54.

Mao X, Polasko A, Alvarez-Cohen L. The effects of sulfate reduction on trichloroethene dechlorination by *Dehalococcoides*-containing microbial communities. *Appl Environ Microbiol* 2017;**83**: e03384-03316.

Martín-González L, Hatijah Mortan S, Rosell M, Parladé E, Martínez-Alonso M, Gaju N, Caminal G, Adrian L, Marco-Urrea E. Stable carbon isotope fractionation during 1,2-dichloropropane-to-propene transformation by an enrichment culture containing *Dehalogenimonas* strains and a *dcpA* gene. *Environ Sci Technol* 2015;**49**: 8666-8674.

Marzorati M, De Ferra F, Van Raemdonck H, Borin S, Allifranchini E, Carpani G, Serbolisca L, Verstraete W, Boon N, Daffonchio D. A novel reductive dehalogenase, identified in a contaminated groundwater enrichment culture and in *Desulfitobacterium dichloroeliminans* strain DCA1, is linked to dehalogenation of 1,2-dichloroethane. *Appl Environ Microbiol* 2007;**73**: 2990-2999.

May HD, Miller GS, Kjellerup BV, Sowers KR. Dehalorespiration with polychlorinated biphenyls by an anaerobic ultramicrobacterium. *Appl Environ Microbiol* 2008;**74**: 2089-2094.

Mayer-Blackwell K, Fincker M, Molenda O, Callahan B, Sewell H, Holmes S, Edwards EA, Spormann AM. 1,2-Dichloroethane exposure alters the population structure, metabolism, and kinetics of a trichloroethene-dechlorinating dehalococcoides mccartyi consortium. *Environ Sci Technol* 2016;**50**: 12187-12196.

Maymó-Gatell X, Anguish T, Zinder SH. Reductive dechlorination of chlorinated ethenes and 1,2-dichloroethane by "*Dehalococcoides ethenogenes*" 195. *Appl Environ Microbiol* 1999;**65**: 3108-3113.

Mebius LJ. A rapid method for the determination of organic carbon in soil. *Anal Chim Acta* 1960;**22**: 120-124.

Meckenstock RU, Elsner M, Griebler C, Lueders T, Stumpp C, Aamand J, Agathos SN, Albrechtsen H-J, Bastiaens L, Bjerg PL. Biodegradation: updating the concepts of control for microbial cleanup in contaminated aquifers. *Environ Sci Technol* 2015;**49**: 7073-7081.

Mehboob F, Junca H, Schraa G, Stams AJM. Growth of *Pseudomonas chloritidismutans* AW-1^T on *n*-alkanes with chlorate as electron acceptor. *Appl Microbiol Biotechnol* 2009a;**83**: 739−747.

Mehboob F, Oosterkamp MJ, Koehorst JJ, Farrakh S, Veuskens T, Plugge CM, Boeren S, de Vos WM, Schraa G, Stams AJM, Schaap PJ. Genome and proteome analysis of *Pseudomonas chloritidismutans* AW-1^T that grows on *n*-decane with chlorate or oxygen as electron acceptor. *Environ Microbiol* 2015;**18**: 3247−3257.

Mehboob F, Wolterink AFM, Vermeulen AJ, Jiang B, Hagedoorn P-L, Stams AJM, Kengen SWM. Purification and characterization of a chlorite dismutase from *Pseudomonas chloritidismutans*. *FEMS Microbiol Lett* 2009b;**293**: 115−121.

Méndez-Díaz JD, Shimabuku KK, Ma J, Enumah ZO, Pignatello JJ, Mitch WA, Dodd MC. Sunlight-driven photochemical halogenation of dissolved organic matter in seawater: a natural abiotic source of organobromine and organoiodine. *Environ Sci Technol* 2014;**48**: 7418-7427.

Mesri S, Wahab RA, Huyop F. Degradation of 3-chloropropionic acid (3CP) by *Pseudomonas* sp. B6P isolated from a rice paddy field. *Ann Microbiol* 2009;**59**: 447−451.

Meyer B, Kuehl J, Deutschbauer AM, Price MN, Arkin AP, Stahl DA. Variation among *Desulfovibrio* species in electron transfer systems used for syntrophic growth. *J Bacteriol* 2013;**195**: 990-1004.

Mikesell MD, Boyd SA. Dechlorination of chloroform by *Methanosarcina* strains. *Appl Environ Microbiol* 1990;**56**: 1198-1201.

Mitchell A, Chang H-Y, Daugherty L, Fraser M, Hunter S, Lopez R, McAnulla C, McMenamin C, Nuka G, Pesseat S, Sangrador-Vegas A, Scheremetjew M, Rato C, Yong S-Y, Bateman A, Punta M, Attwood TK, Sigrist CJA, Redaschi N, Rivoire C, Xenarios I, Kahn D, Guyot D, Bork P, Letunic I, Gough J, Oates M, Haft D, Huang H, Natale DA, Wu CH, Orengo C, Sillitoe I, Huaiyu M, Thomas PD, Finn RD. The InterPro protein families database: the classification resource after 15 years. *Nucleic Acids Res* 2014;**43**: D213−D221.

Moe WM, Rainey FA, Yan J. The Genus *Dehalogenimonas*. In: Adrian L, Löffler FE (eds.) *Organohalide-Respiring Bacteria*. Berlin Heidelberg: Springer, 2016, 137-151.

Moe WM, Yan J, Nobre MF, da Costa MS, Rainey FA. *Dehalogenimonas lykanthroporepellens* gen. nov., sp. nov., a reductively dehalogenating bacterium isolated from chlorinated solvent-contaminated groundwater. *Int J Syst Evol Microbiol* 2009;**59**: 2692-2697.

Mohn WW, Tiedje JM. Microbial reductive dehalogenation. *Microbiol Rev* 1992;**56**: 482-507.

Monserrate E, Häggblom M. Dehalogenation and biodegradation of brominated phenols and benzoic acids under iron-reducing, sulfidogenic, and methanogenic conditions. *Appl Environ Microbiol* 1997;**63**: 3911-3915.

Moore SJ, Warren MJ. The anaerobic biosynthesis of vitamin B_{12}. *Biochem Soc Trans* 2012;**40**: 581-586.

Motosugi K, Esaki N, Soda K. Bacterial assimilation of D-and L-2-chloropropionates and occurrence of a new dehalogenase. *Arch Microbiol* 1982a;**131**: 179−183.

Motosugi K, Esaki N, Soda K. Purification and properties of 2-halo acid dehalogenase from *Pseudomonas putida*. *Agric Biol Chem* 1982b;**46**: 837−838.

Muyzer G, De Waal EC, Uitterlinden AG. Profiling of complex microbial populations by denaturing gradient gel electrophoresis analysis of polymerase chain reaction-amplified genes coding for 16S rRNA. *Appl Environ Microbiol* 1993;**59**: 695-700.

Nardi-Dei V, Kurihara T, Okamura T, Liu J-Q, Koshikawa H, Ozaki H, Terashima Y, Esaki N, Soda K. Comparative studies of genes encoding thermostable L-2-halo acid dehalogenase from *Pseudomonas* sp. strain YL, other dehalogenases, and two related hypothetical proteins from *Escherichia coli*. *Appl Environ Microbiol* 1994;**60**: 3375−3380.

Nardi-Dei V, Kurihara T, Park C, Esaki N, Soda K. Bacterial DL-2-haloacid dehalogenase from Pseudomonas sp. strain 113: gene cloning and structural comparison with D-and L-2-haloacid dehalogenases. *J Bacteriol* 1997;**179**: 4232-4238.

Nardi-Dei V, Kurihara T, Park C, Miyagi M, Tsunasawa S, Soda K, Esaki N. DL-2-haloacid dehalogenase from *Pseudomonas* sp. 113 is a new class of dehalogenase catalyzing hydrolytic dehalogenation not involving enzyme-substrate ester intermediate. *J Biol Chem* 1999;**274**: 20977−20981.

Neumann A, Wohlfarth G, Diekert G. Tetrachloroethene dehalogenase from Dehalospirillum multivorans: cloning, sequencing of the encoding genes, and expression of the pceA gene in *Escherichia coli*. *J Bacteriol* 1998;**180**: 4140-4145.

Ni HG, Zeng H, Tao S, Zeng EY. Environmental and human exposure to persistent halogenated compounds derived from e-waste in China. *Environ Toxicol Chem* 2010;**29**: 1237-1247.

Nightingale PD. Low molecular weight halocarbons in seawater volume Doctoral: University of East Anglia, 1991.

Nikel PI, Pérez-Pantoja D, de Lorenzo V. Why are chlorinated pollutants so difficult to degrade aerobically? Redox stress limits 1, 3-dichloprop-1-ene metabolism by Pseudomonas pavonaceae. *Phil Trans R Soc B* 2013;**368**: 20120377.

Oelkers EH, Helgeson HC, Shock EL, Sverjensky DA, Johnson JW, Pokrovskii VA. Summary of the apparent standard partial molal Gibbs free energies of formation of aqueous species, minerals,

and gases at pressures 1 to 5000 bars and temperatures 25 to 1000 °C. *J Phys Chem Ref Data* 1995;**24**: 1401−1560.

Olaniran AO, Balgobind A, Pillay B. Impacts of heavy metals on 1,2-dichloroethane biodegradation in co-contaminated soil. *J Environ Sci* 2009;**21**: 661-666.

Omi R, Jitsumori K, Yamauchi T, Ichiyama S, Kurihara T, Esaki N, Kamiya N, Hirotsu K, Miyahara I. Expression, purification and preliminary X-ray characterization of DL-2-haloacid dehalogenase from *Methylobacterium* sp. CPA1. *Acta Crystallogr Sect F Struct Biol Cryst Commun* 2007;**63**: 586−589.

Oren A. The bioenergetic basis for the decrease in metabolic diversity at increasing salt concentrations: implications for the functioning of salt lake ecosystems*Saline Lakes*. Dordrecht: Springer, 2001, 61-72.

Orris G, Harvey G, Tsui D, Eldrige J. *Preliminary analyses for perchlorate in selected natural materials and their derivative products*: US Department of the Interior, US Geological Survey, 2003.

Orser CS, Lange C, Xun L, Zahrt T, Schneider B. Cloning, sequence analysis, and expression of the Flavobacterium pentachlorophenol-4-monooxygenase gene in Escherichia coli. *J Bacteriol* 1993;**175**: 411-416.

Osswald A, Poszwa A, Bueno M, Arnaudguilhem C, Billet D, Thiry Y, Leyval C. Contribution of microbial activity to formation of organically bound chlorine during batch incubation of forest soil using ^{37}Cl as a tracer. *Soil Biology and Biochemistry* 2016;**100**: 210-217.

Parthasarathy A, Stich TA, Lohner ST, Lesnefsky A, Britt RD, Spormann AM. Biochemical and EPR-spectroscopic investigation into heterologously expressed vinyl chloride reductive dehalogenase (VcrA) from *Dehalococcoides* mccartyi strain VS. *J Am Chem Soc* 2015;**137**: 3525-3532.

Paulo LM, Stams AJ, Sousa DZ. Methanogens, sulphate and heavy metals: a complex system. *Rev Environ Sci Bio* 2015;**14**: 537-553.

Payne KA, Quezada CP, Fisher K, Dunstan MS, Collins FA, Sjuts H, Levy C, Hay S, Rigby SE, Leys D. Reductive dehalogenase structure suggests a mechanism for B12-dependent dehalogenation. *Nature* 2015;**517**: 513-516.

Peng P, Zheng Y, Koehorst JJ, Schaap PJ, Stams AJ, Smidt H, Atashgahi S. Concurrent haloalkanoate degradation and chlorate reduction by *Pseudomonas chloritidismutans* AW-1^T. *Appl Environ Microbiol* 2017;**83**: 00325-00317.

Pereira IA, Ramos AR, Grein F, Marques MC, Da Silva SM, Venceslau SS. A comparative genomic analysis of energy metabolism in sulfate reducing bacteria and archaea. *Front Microbiol* 2011;**2**: 69.

Pérez-de-Mora A, Lacourt A, McMaster ML, Liang X, Dworatzek SM, Edwards EA. Chlorinated electron acceptor abundance drives selection of *Dehalococcoides mccartyi* (*D. mccartyi*) strains in dechlorinating enrichment cultures and groundwater environments. *Front Microbiol* 2018;**9**: 812.

Pfaffl MW. A new mathematical model for relative quantification in real-time RT-PCR. *Nucleic Acids Res* 2001;**29**: 2002−2007.

Piontek A, Bisz E, Szostak M. Iron-catalyzed cross-coupling in the synthesis of pharmaceuticals: in pursuit of sustainability. *Angew Chem Int Ed* 2018;**57**: 11116-11128.

Plewa MJ, Simmons JE, Richardson SD, Wagner ED. Mammalian cell cytotoxicity and genotoxicity of the haloacetic acids, a major class of drinking water disinfection by-products. *Environ Mol Mutagen* 2010;**51**: 871−878.

Pop SM, Kolarik RJ, Ragsdale SW. Regulation of anaerobic dehalorespiration by the transcriptional activator CprK. *J Biol Chem* 2004;**279**: 49910-49918.

Prat L, Maillard J, Grimaud R, Holliger C. Physiological adaptation of *Desulfitobacterium hafniense* strain TCE1 to tetrachloroethene respiration. *Appl Environ Microbiol* 2011;**77**: 3853-3859.

Prince LA. Determination of Chloride, Hypochlorite, Chlorite, Chlorate, Perchlorate, and Chlorine Dioxide in Composite Mixtures. *Anal Chem* 1964;**36**: 613-616.

Quast C, Pruesse E, Yilmaz P, Gerken J, Schweer T, Yarza P, Peplies J, Glöckner FO. The SILVA ribosomal RNA gene database project: improved data processing and web-based tools. *Nucleic Acids Res* 2012;**41**: D590-D596.

Rajagopalan S, Anderson T, Cox S, Harvey G, Cheng Q, Jackson WA. Perchlorate in wet deposition across North America. *Environ Sci Technol* 2008;**43**: 616−622.

Ramiro-Garcia J, Hermes GD, Giatsis C, Sipkema D, Zoetendal EG, Schaap PJ, Smidt H. NG-Tax, a highly accurate and validated pipeline for analysis of 16S rRNA amplicons from complex biomes. *F1000Research* 2016;**5**.

Rao B, Anderson TA, Orris GJ, Rainwater KA, Rajagopalan S, Sandvig RM, Scanlon BR, Stonestrom DA, Walvoord MA, Jackson WA. Widespread natural perchlorate in unsaturated zones of the southwest United States. *Environ Sci Technol* 2007;**41**: 4522-4528.

Rao B, Hatzinger PB, Böhlke JK, Sturchio NC, Andraski BJ, Eckardt FD, Jackson WA. Natural chlorate in the environment: application of a new IC-ESI/MS/MS method with a Cl18O3-internal standard. *Environ Sci Technol* 2010;**44**: 8429−8434.

Ravot G, Casalot L, Ollivier B, Loison G, Magot M. *rdlA*, a new gene encoding a rhodanese-like protein in Halanaerobium congolense and other thiosulfate-reducing anaerobes. *Res Microbiol* 2005;**156**: 1031-1038.

Read KA, Mahajan AS, Carpenter LJ, Evans MJ, Faria BV, Heard DE, Hopkins JR, Lee JD, Moller SJ, Lewis AC. Extensive halogen-mediated ozone destruction over the tropical Atlantic Ocean. *Nature* 2008;**453**: 1232-1235.

Reinhold A, Westermann M, Seifert J, von Bergen M, Schubert T, Diekert G. Impact of vitamin B12 on formation of the tetrachloroethene reductive dehalogenase in *Desulfitobacterium hafniense* strain Y51. *Appl Environ Microbiol* 2012;**78**: 8025-8032.

Rhew RC, Miller BR, Weiss RF. Natural methyl bromide and methyl chloride emissions from coastal salt marshes. *Nature* 2000;**403**: 292-295.

Richmond SA, Lindstrom JE, Braddock JF. Assessment of natural attenuation of chlorinated aliphatics and BTEX in subarctic groundwater. *Environ Sci Technol* 2001;**35**: 4038-4045.

Richter M, Rosselló-Móra R. Shifting the genomic gold standard for the prokaryotic species definition. *Proc Natl Acad Sci USA* 2009;**106**: 19126-19131.

Righi E, Fantuzzi G, Predieri G, Aggazzotti G. Bromate, chlorite, chlorate, haloacetic acids, and trihalomethanes occurrence in indoor swimming pool waters in Italy. *Microchem J* 2014;**113**: 23−29.

Rikken GB, Kroon AGM, Van Ginkel CG. Transformation of (per)chlorate into chloride by a newly isolated bacterium: reduction and dismutation. *Appl Microbiol Biotechnol* 1996;**45**: 420−426.

Rodríguez-Fernández D, Heckel B, Torrentó C, Meyer A, Elsner M, Hunkeler D, Soler A, Rosell M, Domènech C. Dual element (CCl) isotope approach to distinguish abiotic reactions of chlorinated methanes by Fe(0) and by Fe (II) on iron minerals at neutral and alkaline pH. *Chemosphere* 2018a;**206**: 447-456.

Rodríguez-Fernández D, Torrentó C, Guivernau M, Viñas M, Hunkeler D, Soler A, Domènech C, Rosell M. Vitamin B_{12} effects on chlorinated methanes-degrading microcosms: Dual isotope and metabolically active microbial populations assessment. *Sci Total Environ* 2018b;**621**: 1615-1625.

Rosenthal SL. A review of the mutagenicity of chloroform. *Environ Mol Mutagen* 1987;**10**: 211-226.

Ruecker A, Weigold P, Behrens S, Jochmann M, Laaks J, Kappler A. Predominance of biotic over abiotic formation of halogenated hydrocarbons in hypersaline sediments in Western Australia. *Environ Sci Technol* 2014;**48**: 9170-9178.

Safe S. Polychlorinated biphenyls (PCBs), dibenzo-p-dioxins (PCDDs), dibenzofurans (PCDFs), and related compounds: environmental and mechanistic considerations which support the development of toxic equivalency factors (TEFs). *Crit Rev Toxicol* 1990;**21**: 51-88.

Sander R. Compilation of Henry's law constants (version 4.0) for water as solvent. *Atmos Chem Phys* 2015;**15**: 4399-4981.

Sanford RA, Chowdhary J, Löffler FE. Organohalide-Respiring *Deltaproteobacteria*. In: Adrian L, Löffler FE (eds.) *Organohalide-Respiring Bacteria*. Berlin Heidelberg: Springer, 2016, 235-258.

Santos AA, Venceslau SS, Grein F, Leavitt WD, Dahl C, Johnston DT, Pereira IA. A protein trisulfide couples dissimilatory sulfate reduction to energy conservation. *Science* 2015;**350**: 1541-1545.

Schaefer CE, Condee CW, Vainberg S, Steffan RJ. Bioaugmentation for chlorinated ethenes using *Dehalococcoides* sp.: Comparison between batch and column experiments. *Chemosphere* 2009;**75**: 141-148.

Schmidberger JW, Wilce JA, Weightman AJ, Whisstock JC, Wilce MC. The crystal structure of DehI reveals a new α-haloacid dehalogenase fold and active-site mechanism. *J Mol Biol* 2008;**378**: 284−294.

Schneidewind U, Haest PJ, Atashgahi S, Maphosa F, Hamonts K, Maesen M, Calderer M, Seuntjens P, Smidt H, Springael D. Kinetics of dechlorination by *Dehalococcoides* mccartyi using different carbon sources. *J Contam Hydrol* 2014;**157**: 25-36.

Schubert T, Adrian L, Sawers RG, Diekert G. Organohalide respiratory chains: composition, topology and key enzymes. *FEMS Microbiol Ecol* 2018;**94**: fiy035.

Senior E, Bull A, Slater J. Enzyme evolution in a microbial community growing on the herbicide Dalapon. *Nature* 1976;**263**: 476−479.

Shan H, Kurtz HD, Mykytczuk N, Trevors JT, Freedman DL. Anaerobic biotransformation of high concentrations of chloroform by an enrichment culture and two bacterial isolates. *Appl Environ Microbiol* 2010;**76**: 6463-6469.

Silver S, Walderhaug M. Gene regulation of plasmid-and chromosome-determined inorganic ion transport in bacteria. *Microbiol Mol Biol Rev* 1992;**56**: 195-228.

Smidt H, de Vos WM. Anaerobic microbial dehalogenation. *Annu Rev Microbiol* 2004;**58**: 43-73.

Smidt H, van Leest M, van der Oost J, de Vos WM. Transcriptional regulation of the *cpr* gene cluster inortho-chlorophenol-respiring *Desulfitobacterium dehalogenans*. *J Bacteriol* 2000;**182**: 5683-5691.

Smits TH, Devenoges C, Szynalski K, Maillard J, Holliger C. Development of a real-time PCR method for quantification of the three genera *Dehalobacter, Dehalococcoides*, and *Desulfitobacterium* in microbial communities. *J Microbiol Methods* 2004;**57**: 369-378.

Stams AJ, Van Dijk JB, Dijkema C, Plugge CM. Growth of syntrophic propionate-oxidizing bacteria with fumarate in the absence of methanogenic bacteria. *Appl Environ Microbiol* 1993;**59**: 1114-1119.

Staudinger J, Roberts PV. A critical compilation of Henry's law constant temperature dependence relations for organic compounds in dilute aqueous solutions. *Chemosphere* 2001;**44**: 561-576.

Stenklo K, Thorell HD, Bergius H, Aasa R, Nilsson T. Chlorite dismutase from *Ideonella dechloratans*. *J Biol Inorg Chem* 2001;**6**: 601−607.

Stookey LL. Ferrozine—a new spectrophotometric reagent for iron. *Anal Chem* 1970;**42**: 779-781.

Stringer R, Johnston P. *Chlorine and the environment: an overview of the chlorine industry*: Springer Science & Business Media, 2001.

Subramanian A, Kunisue T, Tanabe S. Recent status of organohalogens, heavy metals and PAHs pollution in specific locations in India. *Chemosphere* 2015;**137**: 122-134.

Sun B, Cole JR, Sanford RA, Tiedje JM. Isolation and characterization of *Desulfovibrio dechloracetivorans* sp. nov., a marine dechlorinating bacterium growing by coupling the oxidation of acetate to the reductive dechlorination of 2-chlorophenol. *Appl Environ Microbiol* 2000;**66**: 2408-2413.

Sung Y, Fletcher KE, Ritalahti KM, Apkarian RP, Ramos-Hernández N, Sanford RA, Mesbah NM, Löffler FE. *Geobacter lovleyi* sp. nov. strain SZ, a novel metal-reducing and tetrachloroethene-dechlorinating bacterium. *Appl Environ Microbiol* 2006;**72**: 2775-2782.

Sutton NB, Atashgahi S, Saccenti E, Grotenhuis T, Smidt H, Rijnaarts HH. Microbial community response of an organohalide respiring enrichment culture to permanganate oxidation. *PLoS One* 2015;**10**: e0134615.

Suzuki D, Ueki A, Amaishi A, Ueki K. *Desulfoluna butyratoxydans* gen. nov., sp. nov., a novel Gram-negative, butyrate-oxidizing, sulfate-reducing bacterium isolated from an estuarine sediment in Japan. *Int J Syst Evol Microbiol* 2008;**58**: 826-832.

Takagi K, Iwasaki A, Kamei I, Satsuma K, Yoshioka Y, Harada N. Aerobic mineralization of hexachlorobenzene by newly isolated pentachloronitrobenzene-degrading *Nocardioides* sp. strain PD653. *Appl Environ Microbiol* 2009;**75**: 4452-4458.

Tandoi V, DiStefano TD, Bowser PA, Gossett JM, Zinder SH. Reductive dehalogenation of chlorinated ethenes and halogenated ethanes by a high-rate anaerobic enrichment culture. *Environ Sci Technol* 1994;**28**: 973-979.

Tang S, Edwards EA. Identification of *Dehalobacter* reductive dehalogenases that catalyse dechlorination of chloroform, 1,1,1-trichloroethane and 1,1-dichloroethane. *Phil Trans R Soc B* 2013;**368**: 20120318.

Thrash JC, Ahmadi S, Torok T, Coates JD. *Magnetospirillum bellicus* sp. nov., a novel dissimilatory perchlorate-reducing alphaproteobacterium isolated from a bioelectrical reactor. *Appl Environ Microbiol* 2010;**76**: 4730-4737.

Tian L, Scholte J, Borewicz K, Bogert B, Smidt H, Scheurink AJ, Gruppen H, Schols HA. Effects of pectin supplementation on the fermentation patterns of different structural carbohydrates in rats. *Mol Nutr Food Res* 2016;**60**: 2256-2266.

Tobler M, Passow CN, Greenway R, Kelley JL, Shaw JH. The evolutionary ecology of animals inhabiting hydrogen sulfide–rich environments. *Annu Rev Ecol Evol Syst* 2016;**47**: 239-262.

Torrentó C, Palau J, Rodríguez-Fernández D, Heckel B, Meyer A, Domènech C, Rosell Mn, Soler A, Elsner M, Hunkeler D. Carbon and chlorine isotope fractionation patterns associated with different engineered chloroform transformation reactions. *Environ Sci Technol* 2017;**51**: 6174-6184.

Townsend GT, Suflita JM. Influence of sulfur oxyanions on reductive dehalogenation activities in *Desulfomonile tiedjei*. *Appl Environ Microbiol* 1997;**63**: 3594-3599.

Türkowsky D, Jehmlich N, Diekert G, Adrian L, von Bergen M, Goris T. An integrative overview of genomic, transcriptomic and proteomic analyses in organohalide respiration research. *FEMS Microbiol Ecol* 2018;**94**: fiy013.

Turon X, Becerro MA, Uriz MJ. Distribution of brominated compounds within the sponge Aplysina aerophoba: coupling of X-ray microanalysis with cryofixation techniques. *Cell Tissue Res* 2000;**301**: 311-322.

Urata M, Miyakoshi M, Kai S, Maeda K, Habe H, Omori T, Yamane H, Nojiri H. Transcriptional regulation of the ant operon, encoding two-component anthranilate 1,2-dioxygenase, on the carbazole-degradative plasmid pCAR1 of *Pseudomonas resinovorans* strain CA10. *J Bacteriol* 2004;**186**: 6815-6823.

van den Bogert B, de Vos WM, Zoetendal EG, Kleerebezem M. Microarray analysis and barcoded pyrosequencing provide consistent microbial profiles depending on the source of human intestinal samples. *Appl Environ Microbiol* 2011;**77**: 2071-2080.

van der Ploeg J, Janssen DB. Sequence analysis of the upstream region of *dhlB*, the gene encoding haloalkanoic acid dehalogenase of *Xanthobacter autotrophicus* GJ10. *Biodegradation* 1995;**6**: 257-263.

Van der Ploeg J, Van Hall G, Janssen DB. Characterization of the haloacid dehalogenase from *Xanthobacter autotrophicus* GJ10 and sequencing of the *dhlB* gene. *J Bacteriol* 1991;**173**: 7925−7933.

Van der Ploeg J, Willemsen M, Van Hall G, Janssen DB. Adaptation of *Xanthobacter autotrophicus* GJ10 to bromoacetate due to activation and mobilization of the haloacetate dehalogenase gene by insertion element IS*1247*. *J Bacteriol* 1995;**177**: 1348-1356.

Van Ginkel C, Rikken G, Kroon A, Kengen S. Purification and characterization of chlorite dismutase: a novel oxygen-generating enzyme. *Arch Microbiol* 1996;**166**: 321-326.

Vandermaesen J, Horemans B, Bers K, Vandermeeren P, Herrmann S, Sekhar A, Seuntjens P, Springael D. Application of biodegradation in mitigating and remediating pesticide contamination of freshwater resources: state of the art and challenges for optimization. *Appl Microbiol Biotechnol* 2016;**100**: 7361-7376.

Venceslau SS, Lino RR, Pereira IA. The Qrc membrane complex, related to the alternative complex III, is a menaquinone reductase involved in sulfate respiration. *J Biol Chem* 2010;**285**: 22774-22783.

Vita N, Valette O, Brasseur G, Lignon S, Denis Y, Ansaldi M, Dolla A, Pieulle L. The primary pathway for lactate oxidation in *Desulfovibrio vulgaris*. *Front Microbiol* 2015;**6**: 606.

Vrugt JA, Robinson BA. Improved evolutionary optimization from genetically adaptive multimethod search. *Proc Natl Acad Sci* 2007;**104**: 708-711.

Wagner A, Cooper M, Ferdi S, Seifert J, Adrian L. Growth of *Dehalococcoides mccartyi* strain CBDB1 by reductive dehalogenation of brominated benzenes to benzene. *Environ Sci Technol* 2012;**46**: 8960-8968.

Wagner A, Segler L, Kleinsteuber S, Sawers G, Smidt H, Lechner U. Regulation of reductive dehalogenase gene transcription in *Dehalococcoides mccartyi*. *Philos Trans R Soc Lond B Biol Sci* 2013;**368**: 1-10.

Walker BJ, Abeel T, Shea T, Priest M, Abouelliel A, Sakthikumar S, Cuomo CA, Zeng Q, Wortman J, Young SK. Pilon: an integrated tool for comprehensive microbial variant detection and genome assembly improvement. *PLoS One* 2014;**9**: e112963.

Walker G, Murphy S, Huennekens F. Enzymatic conversion of vitamin B_{12a} to adenosyl-B_{12}: evidence for the existence of two separate reducing systems. *Arch Biochem Biophys* 1969;**134**: 95-102.

Wang S, He J. Dechlorination of commercial PCBs and other multiple halogenated compounds by a sediment-free culture containing *Dehalococcoides* and *Dehalobacter*. *Environ Sci Technol* 2013;**47**: 10526-10534.

Wasmund K, Mußmann M, Loy A. The life sulfuric: microbial ecology of sulfur cycling in marine sediments. *Environ Microbiol Rep* 2017;**9**: 323-344.

Watanabe T, Tsuru T. Water plasma generation under atmospheric pressure for HFC destruction. *Thin Solid Films* 2008;**516**: 4391-4396.

Weatherill JJ, Atashgahi S, Schneidewind U, Krause S, Ullah S, Cassidy N, Rivett MO. Natural attenuation of chlorinated ethenes in hyporheic zones: a review of key biogeochemical processes and in-situ transformation potential. *Water Res* 2018;**128**: 362-382.

Weightman AJ, Topping AW, Hill KE, Lee LL, Sakai K, Slater JH, Thomas AW. Transposition of DEH, a broad-host-range transposon flanked by ISPpu12, in *Pseudomonas putida* is associated with genomic rearrangements and dehalogenase gene silencing. *J Bacteriol* 2002;**184**: 6581−6591.

Weigold P, Ruecker A, Loesekann-Behrens T, Kappler A, Behrens S. Ribosomal tag pyrosequencing of DNA and RNA reveals “rare” taxa with high protein synthesis potential in the sediment of a hypersaline lake in Western Australia. *Geomicrobiol J* 2016;**33**: 426-440.

Weisburger EK. Carcinogenicity studies on halogenated hydrocarbons. *Environ Health Perspect* 1977;**21**: 7.

Weiss B, Ebel R, Elbrächter M, Kirchner M, Proksch P. Defense metabolites from the marine sponge *Verongia aerophoba*. *Biochem Syst Ecol* 1996;**24**: 1−12.

Weissbach H, Redfield B, Peterkofsky A. Conversion of vitamin B_{12} to coenzyme B_{12} in cell-free extracts of *Clostridium tetanomorphum*. *J Biol Chem* 1961;**236**: PC40-PC42.

Weissflog L, Lange CA, Pfennigsdorff A, Kotte K, Elansky N, Lisitzyna L, Putz E, Krueger G. Sediments of salt lakes as a new source of volatile highly chlorinated C1/C2 hydrocarbons. *Geophys Res Lett* 2005;**32**: 1-4.

Wen L-L, Zhang Y, Chen J-X, Zhang Z-X, Yi Y-Y, Tang Y, Rittmann BE, Zhao H-P. The dechlorination of TCE by a perchlorate reducing consortium. *Chem Eng J* 2017;**313**: 1215-1221.

Werisch S, Grundmann J, Al-Dhuhli H, Algharibi E, Lennartz F. Multiobjective parameter estimation of hydraulic properties for a sandy soil in Oman. *Environ Earth Sci* 2014;**72**: 4935-4956.

Wieczorek S, Combes F, Lazar C, Giai Gianetto Q, Gatto L, Dorffer A, Hesse A-M, Coute Y, Ferro M, Bruley C. DAPAR & ProStaR: software to perform statistical analyses in quantitative discovery proteomics. *Bioinformatics* 2017;**33**: 135-136.

Wöhling T, Vrugt JA, Barkle GF. Comparison of three multiobjective optimization algorithms for inverse modeling of vadose zone hydraulic properties. *Soil Sci Soc Am J* 2008;**72**: 305-319.

Wolterink A, Jonker A, Kengen S, Stams AJM. *Pseudomonas chloritidismutans* sp. nov., a non-denitrifying, chlorate-reducing bacterium. *Int J Syst Evol Microbiol* 2002b;**52**: 2183−2190.

Wong YK, Holland SI, Ertan H, Manefield M, Lee M. Isolation and characterization of *Dehalobacter* sp. strain UNSWDHB capable of chloroform and chlorinated ethane respiration. *Environ Microbiol* 2016;**18**: 3092-3105.

Yang Y, Higgins SA, Yan J, Şimşir B, Chourey K, Iyer R, Hettich RL, Baldwin B, Ogles DM, Löffler FE. Grape pomace compost harbors organohalide-respiring *Dehalogenimonas* species with novel reductive dehalogenase genes. *ISME J* 2017;**11**: 2767-2780.

Yin Y, Yan J, Chen G, Murdoch FK, Pfisterer N, Löffler FE. Nitrous oxide is a potent inhibitor of bacterial reductive dechlorination. *Environ Sci Technol* 2019;**53**: 692-701.

Youngblut MD, Wang O, Barnum TP, Coates JD. (Per)chlorate in biology on earth and beyond. *Annu Rev Microbiol* 2016;**70**: 435−457.

Yu R, Peethambaram HS, Falta RW, Verce MF, Henderson JK, Bagwell CE, Brigmon RL, Freedman DL. Kinetics of 1,2-dichloroethane and 1,2-dibromoethane biodegradation in anaerobic enrichment cultures. *Appl Environ Microbiol* 2013;**79**: 1359-1367.

Yu S, Dolan ME, Semprini L. Kinetics and inhibition of reductive dechlorination of chlorinated ethylenes by two different mixed cultures. *Environ Sci Technol* 2005a;**39**: 195-205.

Yu S, Semprini L. Kinetics and modeling of reductive dechlorination at high PCE and TCE concentrations. *Biotechnol Bioeng* 2004;**88**: 451-464.

Yu Y, Lee C, Kim J, Hwang S. Group-specific primer and probe sets to detect methanogenic communities using quantitative real-time polymerase chain reaction. *Biotechnol Bioeng* 2005b;**89**: 670-679.

Zanaroli G, Negroni A, Häggblom MM, Fava F. Microbial dehalogenation of organohalides in marine and estuarine environments. *Curr Opin Biotechnol* 2015;**33**: 287-295.

Zane GM, Yen H-cB, Wall JD. Effect of the deletion of qmoABC and the promoter-distal gene encoding a hypothetical protein on sulfate reduction in *Desulfovibrio vulgaris* Hildenborough. *Appl Environ Microbiol* 2010;**76**: 5500-5509.

Appendices

Summary

Acknowledgements

Co-author affiliations

About the author

List of publications

SENSE Diploma

Summary

Halogenated organic compounds, organohalogens, and inorganic chlorate are largely produced and used for a wide range of applications in industry and agriculture. Besides their anthropogenic origin, these compounds are also naturally produced in various environments including, for example, forest soils, deserts, marine environments and hypersaline lakes. Halogen compounds are often toxic and have adverse effects on human, animal and environmental health, and hence microbes capable of their transformation are important for bioremediation of polluted sites and for natural halogen cycling. Research described in this thesis set out to characterize ecophysiology, genetics and potential applications of microbes obtained from pristine and polluted environments that can (co)metabolically transform organohalogens and chlorate.

Chapter 1 provides an overview of different microbial pathways for organohalogen dehalogenation and chlorate reduction and the responsible microbes, genes and enzymes.

Many contaminated sites contain mixtures of organic and/or inorganic halogen compounds. Microbes that can concurrently degrade different halogen compounds are of particular interest. **Chapter 2** reported concurrent transformation of haloalkanoates and chlorate by *P. chloritidismutans* AW-1^T, a facultative anaerobic chlorate-reducing bacterium isolated from an anaerobic chlorate-reducing bioreactor. Analysis of the genome of strain AW-1^T showed co-existence of chlorate reduction genes (*clrABDC*, *cld*) and D/L-2-haloacid dehalogenase genes (*dehI* and L-DEX gene). This study, for the first time, verified concurrent transformation of haloalkanoates and chlorate by a single bacterium using combined physiological, biochemical and molecular techniques.

Organohalogens have a long history on earth e.g. in marine environments where dehalogenating microbes could evolve, most probably triggered by the natural production of organohalogens. **Chapter 3** described isolation and characterization of a new sulfate-reducing organohalide-respiring bacterium, *Desulfoluna spongiiphila* strain DBB, from pristine marine intertidal sediment samples. Furthermore, physiological and genomic properties of strain DBB were compared to those of two *Desulfoluna* species previously isolated from marine environments. Genomic analysis revealed similar potential for organohalide respiration, corrinoid biosynthesis, and resistance to oxygen among the three strains, and physiological experiments showed their specific preference for brominated/iodinated compounds rather than chlorinated compounds, and stimulation of OHR during concurrent sulfate reduction.

Chapter 4 reported microbial chloroform (CF) transformation in sediment samples obtained from the hypersaline lake Strawbridge in Western Australia that was previously shown to be a natural source of CF. In the sediment- and sediment-free enrichment cultures, CF was transformed to dichloromethane and CO_2. Known organohalide-respiring bacteria

(OHRB) and corresponding reductive dehalogenase encoding *rdhA* genes were not present in the sediment-free enrichment cultures. Rather, *Clostridium* spp. carrying genes involved in acetogenesis were enriched that likely mediated fortuitous transformation of CF to CO_2. This study indicated that microbiota may act as a filter to reduce CF emission from hypersaline lakes to the atmosphere.

The co-existence of different organohalogens such as multiple chlorinated solvents in contaminated sites often hampers reductive dechlorination due to inhibitory effects of one or more organohalogens on dehalogenation of another organohalogen. **Chapter 5** investigated kinetics of 1,2-dichloroethane (1,2-DCA) reductive dechlorination in the presence of chloroethenes and 1,2-dichloropropane as co-contaminants as well as the population dynamics of known OHRB. Dechlorination rates of 1,2-DCA were strongly decreased in the presence of a single chlorinated co-contaminant in enrichment cultures, and the type of chlorinated substrate drove the selection of specific OHRB. This study contributed to a better understanding of the mechanisms underlying the often observed 1,2-DCA persistence in environments in relation to specific 1,2-DCA dechlorinating microbial populations.

Finally, a discussion of the results described in this thesis, remaining knowledge gaps and perspectives for future studies were provided in **Chapter 6**. In conclusion, this thesis contributes to extend our understanding of physiology, genomics and ecology of different dehalogenating microbes in contaminated as well as pristine environments.

Acknowledgements

As it is coming to the end of this thesis, my thoughts return to all good memories of the past five years PhD journey in Microbiology. The completion of this thesis would not have been possible without help from many people. Here I would like to take this opportunity to thank all great people I have met during my PhD.

First, I would like to thank **Hauke** for giving me the opportunity to do a PhD in your group. It was a great experience and I have learned a lot. You are a very knowledgeable and experienced scientist. Thank you for all your support, encouragement and patience on my PhD work. And thanks for the inspiring discussion in our meetings and feedbacks on the manuscripts.

Siavash, thank you for being my supervisor. I have learned a lot from you on how to work as a PhD student and how to organize my time and staffs to work effectively and efficiently. You always push me forward and keep me on the right direction, and encourage me to go deep into my work, which I was trying to avoid at the beginning. But it proved at last that it was worth doing these and the thesis is getting solid with these extensive and in-depth research. And thanks for your fast reading and commenting on the countless versions of manuscripts (chapters) of this thesis.

Thanks all the co-authors and external collaborators for your contribution to this thesis. **Uwe** and **Pieter Jan**, thank you for spending so much time on the model construction and writing the corresponding part of the co-contamination manuscript. **Tobias**, thanks for your help in genomics and proteomics analyses, and your input and comments on the *Desulfoluna* manuscript. **Bart** and **Jasper**, thanks for your bioinformatics assistance that helped to build up three chapters of this thesis. **Tom** and **Ivonne**, thanks for your help in GC-MS and Isotope measurements, and the discussions for the data analysis. **David** and **Anna**, thanks for your protocol and assistance in preparation and analysing the proteome samples. **Yue**, **Aleksandr**, **Javier** and **Alexander** thanks for all your previous work on the hypersaline paper. All other co-authors' input and comments on chapters of this thesis are greatly appreciated.

It is great to be a member of MolEco group and also a member of Dehalo-team. **Ying**, thanks for all your help when I first came to the lab. I hope you can soon finish your thesis. **Yue**, thanks for teaching me the tips to work with anaerobes and use of GC-FID, and thanks for your work and collaboration in the hypersaline paper. **Tom**, thanks for all the discussion in the co-contamination work and your help in GC-MS. **Thomas** and **Tian**, it was nice to be with you as an officemate during my first year PhD. Thank you for all the nice sharing and discussion. **Chen**, it was nice to talk to you and work with you on some of your experiments. Success for your PhD project. **Nora**, thanks for your suggestions on the co-contamination experiment design. **Marjet**, it was nice work with you on the benzene and toluene degradation

work. I hope you will finish and publish the papers soon. **Johanna**, thanks for sampling the marine sediment from which we isolated a *Desulfoluna* strain, and that was the main focus of chapter 3. **Detmer**, thanks for your input and comments on the *Desulfoluna* and hypersaline manuscripts.

I would like to thank all MicFys people as I did most of the anaerobic work, GCs and HPLCs in MicFys lab. **Fons**, thanks for letting me work in your lab, and thank you for your suggestions and comments on the *Pseudomonas* and *Desulfoluna* manuscripts. **Ton**, thanks for your tips on anaerobic medium preparation, and assistance in GCs and HPLCs. **Monika**, thanks for your introduction on using of the anaerobic tent, and your help in SEM sample preparation and observation. **Anna**, thanks for your help in sulfide measurement. **Susakul**, thanks for all the nice talks and friendship**. Irene**, thanks for your help and arrangement in cellular fatty acids analysis of our *Desulfoluna* strains.

And thanks **Steven, Ineke, Hans** and **Tom** for taking care of my orders and samples for sequencing and all the technical assistance. **Wim** and **Sjon**, thanks for the PC assistance and installing of software. **Philippe**, thanks for giving the introductory lab tour when I first came to the lab. **Anja**, thanks for your help in all the paper works before and during my staying in Wageningen.

And thanks all my officemates during these years. **Thomas**, **Tian**, **Dennis**, **Indra**, **Gerben**, **Catarina**, **Patrick**, **Prokopis**, **Ioannis**, **Lennart** and **Romy**, thanks for making such a good working environment.

The PhD trip to California in 2015 was fantastic. Thanks all the committee members **Anna**, **Yue**, **Nico**, **Maarten**, **Kees**, **Jasper Sloothaak**, **Alex** and **Ruben** for organizing this trip. Thank **Detmer** for being the team leader. Thanks **Kees** and **Marcelle** for being the driver of our car.

Jie Lian, **Yifan Zhu**, **LooWee, Taojun Wang**, **Yuan Feng**, **Chen**, **Ying Liu**, **Zhuang Liu**, **Yangwenshan Ou**, **Zhan Huang**, **Ying Zhou**, thank you for organising all the nice lunch/dinner parties and the interesting talks and games afterwards. Thanks **Tian** and your mother for inviting me to have meals with all kinds of delicious food cooked by your mother.

And thanks **Chen** and **Martha** for being the paranymphs at my defence. Thanks **YingJung Chen** for designing the cover of this thesis.

Also thanks my Chinese friends in Groningen and Amsterdam. **Xiangfeng Meng**, **Yuxiang Bai**, **Yinxing Jin**, **Jinfeng Shao** and **Muhe Diao**, thanks for your friendship and help when I first came to the Netherlands. I wish you all the best in your science careers in China, Europe and USA.

And a special and big thanks to the International Christian Fellowship (ICF) in Wageningen and the Wednesday/Thursday bible study group, and the Chinese Fellowship in Wageningen. It has been wonderful to be part of you in the Sunday service, bible study and

prayer meetings. I learned and benefited a lot from your sharing and testimonies. You have played an important role in making my life here special and fulfil. Here I cannot mention all your names but I wish you all the blessings from our Lord in fellowship with Him!

Last but not least, thanks my parents and family for your support and encouragement in the past years. 感谢父母一直以来的言传身教，感谢所有家人们的鼓励和支持！

Co-author affiliations

Aleksandr Umanetc [1]
Alexander Ruecker [2, 3]
Alfons J.M. Stams [1, 4]
Andreas Kappler [3]
Anna Burrichter [5, 6]
Anthony S. Danko [7]
Bart Nijsse [8]
David Schleheck [5, 6]
Detmer Sipkema [1]
Hauke Smidt [1]
Ivonne Nijenhuis [9]
Jaap S. Sinninghe Damste [10, 11]
Jasper J. Koehorst [8]
Javier Ramiro-Garcia [1, 8]
Jie Liu [12]
Max M. Häggblom [1, 2]
Peter J. Schaap [8]
Pieter Jan Haest [13, 14]
Siavash Atashgahi [1]
Tobias Goris [15]
Tom N.P. Bosma [1]
Uwe Schneidewind [16]
Ying Zheng [1]
Yue Lu [17]

[1] Laboratory of Microbiology, Wageningen University & Research, Wageningen, The Netherlands
[2] Department of Biogeochemical Processes, Max Planck Institute for Biogeochemistry, Jena, Germany
[3] Geomicrobiology, Centre for Applied Geosciences, University of Tuebingen, Tuebingen, Germany
[4] Centre of Biological Engineering, University of Minho, Braga, Portugal
[5] Department of Biology, University of Konstanz, Konstanz, Germany
[6] The Konstanz Research School Chemical Biology, University of Konstanz, Konstanz, Germany

[7] Centre for Natural Resources and the Environment (CERENA), Department of Mining Engineering, University of Porto (FEUP), Porto, Portugal
[8] Laboratory of Systems and Synthetic Biology, Wageningen University & Research, Wageningen, The Netherlands
[9] Helmholtz Centre for Environmental Research-UFZ, Department of Isotope Biogeochemistry, Leipzig, Germany
[10] Department of Marine Microbiology and Biogeochemistry, NIOZ Royal Netherlands Institute for Sea Research, Den Burg, The Netherlands
[11] Department of Earth Sciences, Faculty of Geosciences, Utrecht University, Utrecht, The Netherlands
[12] Department of Biochemistry and Microbiology, Rutgers University, New Brunswick, USA
[13] Advanced Groundwater Techniques (AGT), Aartselaar, Belgium
[14] Division of Geology, Department of Earth and Environmental Sciences, KU Leuven, Heverlee, Belgium
[15] Department of Applied and Ecological Microbiology, Institute of Microbiology, Friedrich Schiller University, Jena, Germany
[16] Department of Civil and Environmental Engineering, Western University, London, ON, Canada
[17] College of Environmental Science and Engineering, Hunan University, Changsha, China

About the author

Peng Peng was born on 29 October 1986 in Jinan, Shandong province, China. In 2009, he obtained his BSc degree in Water Supply and Sewage Engineering from School of Municipal and Environmental Engineering, Shandong Jianzhu University. In the same year, he started his MSc study at School of Environmental Science and Engineering, Shandong University, under the supervision of Prof. Dr Li Li. The research topic of his MSc thesis was microbial degradation of polycyclic aromatic hydrocarbons (PAHs) and dioxins. He received his MSc degree in 2012, and after that he obtained a scholarship from the China Scholarship Council (CSC) to do a PhD in the Netherlands. He worked for six months at Microbial Physiology group of Groningen Biomolecular Sciences and Biotechnology Institute (GBB), University of Groningen, under the supervision of Prof. Dr Lubbert Dijkhuizen. During that time, his research focused on heterologous expression and biochemical analysis of enzymes responsible for microbial estrogens degradation. In February 2014, he moved to Wageningen and started a new PhD project (described in this thesis) in Molecular Ecology group at Laboratory of Microbiology, Wageningen University, under the supervision of Prof. Dr Hauke Smidt and Dr Siavash Atashgahi.

List of publications

Peng P, Goris T, Lu Y, Nijsse B, Burrichter A, Schleheck D, Koehorst JJ, Liu J, Sipkema D, Sinninghe-Damste JS, Stams AJM, Häggblom MM, Smidt H, Atashgahi S (2019). Organohalide-respiring *Desulfoluna* species isolated from marine environments. bioRxiv, 630186. *Under review in the ISME Journal*

Peng P, Lu Y, Bosma TNP, Nijenhuis I, Nijsse B, Ruecker A, Umanetc A, Ramiro-Garcia J, Kappler A, Sipkema D, Smidt H, Atashgahi S. Chloroform biotransformation in hypersaline sediments as natural sources of chloromethanes. *Manuscript in preparation*

Peng P, Schneidewind U, Haest PJ, Bosma TNP, Danko AS, Smidt H, Atashgahi S (2019). Reductive dechlorination of 1,2-dichloroethane in the presence of chloroethenes and 1,2-dichloropropane as co-contaminants. Applied Microbiology and Biotechnology, 103(16), 6837-6849.

Peng P, Zheng Y, Koehorst JJ, Schaap PJ, Stams AJM, Smidt H, Atashgahi S (2017). Concurrent haloalkanoate degradation and chlorate reduction by *Pseudomonas chloritidismutans* AW-1^{T}. Applied and Environmental Microbiology, 83(12), e00325-17.

Peng P, Yang H, Jia RB, Li L (2013). Biodegradation of dioxin by a newly isolated *Rhodococcus* sp. with the involvement of self-transmissible plasmids. Applied Microbiology and Biotechnology, 97(12), 5585-5595.

Atashgahi S, Lu Y, Ramiro-Garcia J, **Peng P**, Maphosa F, Sipkema D, Smidt H, Springael D (2017). Geochemical parameters and reductive dechlorination determine aerobic cometabolic vs aerobic metabolic vinyl chloride biodegradation at oxic/anoxic interface of hyporheic zones. Environmental Science & Technology, 51(3), 1626-1634.

Sun J, Qiu Y, Ding P, **Peng P**, Yang H, Li L (2017). Conjugative transfer of dioxin-catabolic megaplasmids and bioaugmentation prospects of a *Rhodococcus* sp. Environmental Science & Technology, 51(11), 6298-6307.

Wang MH, **Peng P**, Liu YM, Jia RB, Li L (2013). Algicidal activity of a dibenzofuran-degrader *Rhodococcus* sp. Journal of Microbiology and Biotechnology, 23(2), 260-266.

Netherlands Research School for the
Socio-Economic and Natural Sciences of the Environment

D I P L O M A

For specialised PhD training

The Netherlands Research School for the
Socio-Economic and Natural Sciences of the Environment
(SENSE) declares that

Peng Peng

born on 29 October 1986 in Jinan, China

has successfully fulfilled all requirements of the
Educational Programme of SENSE.

Wageningen, 6 September 2019

The Chairman of the SENSE board

Prof. dr. Martin Wassen

the SENSE Director of Education

Dr. Ad van Dommelen

The SENSE Research School has been accredited by the Royal Netherlands Academy of Arts and Sciences (KNAW)

KONINKLIJKE NEDERLANDSE
AKADEMIE VAN WETENSCHAPPEN

The SENSE Research School declares that **Peng Peng** has successfully fulfilled all requirements of the Educational PhD Programme of SENSE with a work load of 32.6 EC, including the following activities:

SENSE PhD Courses

- Environmental research in context (2014)
- Principles of ecological genomics (2014)
- Basic statistics (2014)
- Meta-analysis (2014)
- Research in context activity: 'Co-organizer and convener in the 5th Wageningen PhD Symposium on 'Bridging Science and Society: Unifying Knowledge' (Wageningen, 17 May 2018)'

Other PhD and Advanced MSc Courses

- The essentials of scientific writing and presenting, Wageningen Graduate Schools (2016)
- Project and time management, Wageningen Graduate Schools (2018)

Management and Didactic Skills Training

- Assisting practicals of the BSc course 'Microbial physiology' (2014-2016)
- Assisting practicals of the MSc course 'Microbial ecology' (2015-2017)
- Assisting practicals of the MSc course 'Advanced food microbiology' (2015)

Oral Presentations

- *Enrichment and isolation of organohalide-respiring bacteria (OHRB) using bromobenzenes as electron acceptors.* Stanford University and University of California, Los Angeles, 15-18 May 2015, Phd trip to the United States of America
- *Isolation and characterization of a bromobenzene debrominating Desulfoluna sp. from sea shore sand*. FOR 1530 PhD conference, 14 April 2016, Weimar, Germany

SENSE Coordinator PhD Education

Dr. ir. Peter Vermeulen

Research described in this thesis was performed at the Laboratory of Microbiology, Wageningen University, The Netherlands, and financially supported by a grant of BE-Basic-FES Funds from the Dutch Ministry of Economic Affairs. Peng Peng was sponsored by a fellowship from the China Scholarship Council (CSC).

Cover design: YingJung Chen
Thesis layout: Peng Peng
Printed by: Digiforce ProefschrifMaken

Financial support from the Laboratory of Microbiology, Wageningen University, for printing of this thesis is gratefully acknowledged.